Seismic Response of Nominally Symmetric Systems with Strength Uncertainty

by

S. Balopoulou and M. Grigoriu

NOTICE

Seismic Response of Nominally Symmetric Systems with Strength Uncertainty

by

S. Balopoulou[1] and M.Grigoriu[2]

1   Professor of Structural Engineering, School of Civil and Environmental Engineering, Cornell University
2   Ph.D. Graduate Student, School of Civil and Environmental Engineering, Cornell University

PREFACE

The National Center for Earthquake Engineering Research (NCEER) was established in 1986 to develop and disseminate new knowledge about earthquakes, earthquake-resistant design and seismic hazard mitigation procedures to minimize loss of life and property. The emphasis of the Center is on eastern and central United States *structures*, and *lifelines* throughout the country that may be exposed to any level of earthquake hazard.

NCEER's research is conducted under one of four Projects: the Building Project, the Nonstructural Components Project, and the Lifelines Project, all three of which are principally supported by the National Science Foundation, and the Highway Project which is primarily sponsored by the Federal Highway Administration.

The research and implementation plan in years six through ten (1991-1996) for the Building, Nonstructural Components, and Lifelines Projects comprises four interdependent elements, as shown in the figure below. Element I, Basic Research, is carried out to support projects in the Applied Research area. Element II, Applied Research, is the major focus of work for years six through ten for these three projects. Demonstration Projects under Element III have been planned to support the Applied Research projects and include individual case studies and regional studies. Element IV, Implementation, will result from activity in the Applied Research projects, and from Demonstration Projects.

ELEMENT I BASIC RESEARCH	ELEMENT II APPLIED RESEARCH	ELEMENT III DEMONSTRATION PROJECTS

• Seismic hazards and ground motion
 	
• Geotechnical engineering
 	
• Structures and systems
 	
• Risk and reliability
 	
• Intelligent and protective systems
 	
• Socioeconomic issues
	• The Building Project
	
	• The Nonstructural Components Project
	
	• The Lifelines Project
	
	• The Highway Project
		Case Studies
		  • Active and hybrid control
		  • Hospital and data processing facilities
		  • Short and medium span bridges
		  • Water supply systems in Memphis and San Francisco
		Regional Studies
		  • New York City
		  • Mississippi Valley
		  • San Francisco Bay Area
		  • City of Memphis and Shelby County, Tennessee

ELEMENT IV
IMPLEMENTATION
• Conferences/Workshops
• Education/Training courses
• Publications
• Public Awareness

Research in the **Building Project** focuses on the evaluation and retrofit of buildings in regions of moderate seismicity. Emphasis is on lightly reinforced concrete buildings, steel semi-rigid frames, and masonry walls or infills. The research involves small- and medium-scale shake table tests and full-scale component tests at several institutions. In a parallel effort, analytical models and computer programs are being developed to aid in the prediction of the response of these buildings to various types of ground motion.

Two of the short-term products of the **Building Project** will be a monograph on the evaluation of lightly reinforced concrete buildings and a state-of-the-art report on unreinforced masonry.

The **risk and reliability program** constitutes one of the important areas of research in the **Building Project**. The program is concerned with reducing the uncertainty in current models which characterize and predict seismically induced ground motion, and resulting structural damage and system unserviceability. The goal of the program is to provide analytical and empirical procedures to bridge the gap between traditional earthquake engineering and socioeconomic considerations for the most cost-effective seismic hazard mitigation. Among others, the following tasks are being carried out:

1. Study seismic damage and develop fragility curves for existing structures.
2. Develop retrofit and strengthening strategies.
3. Develop intelligent structures using high-tech and traditional sensors for on-line and real-time diagnoses of structural integrity under seismic excitation.
4. Improve and promote damage-control design for new structures.
5. Study critical code issues and assist code groups to upgrade seismic design code.
6. Investigate the integrity of nonstructural systems under seismic conditions.

The study described in this report focused on evaluating the effects of the seismic response and design of two aspects of system uncertainty: uncertainty in the functional form of the restoring force model of the lateral load resisting elements, and uncertainty in the parameters of this model. A simple one-storey structure and a realistic seven-storey structure, both designed according to the 1994 Uniform Building code provisions, were evaluated. The restoring force models used were the modified Clough and elastoplastic models. It was found that the UBC accidental eccentricity of 5% was inadequate to account for accidental torsion caused by strength uncertainty.

ABSTRACT

The two major sources of uncertainty in earthquake engineering are the input motion and the mathematical model of the structural system. The present study focuses on the effects on seismic response and design of two aspects of system uncertainty: uncertainty in the functional form of the restoring force model of the lateral load resisting elements and uncertainty in the parameters of this model.

The restoring force models selected for this study are the elastoplastic and the modified-Clough, the latter of which accounts for stiffness degradation. Of the model parameters, only the yield strength is treated as random variable following lognormal distribution. Input is deterministic, consisting of three earthquake records scaled to several peak ground accelerations.

Two system types are considered: a simple one-storey structure and a realistic seven-storey building. Both systems are designed according to the 1994 Uniform Building Code. They are nominally symmetric, i.e., they are symmetric in the elastic range but can experience torsional vibrations following yield, because of asymmetry in the element yield strengths caused by uncertainty. The one-storey system consists of a rigid slab supported by two lateral load resisting elements with random yield strengths. The seven-storey system is a regular seven- by three-span frame-shear wall structure. Each structural member is modeled by a set of inelastic springs. Yield strengths of springs modeling shear walls are treated as random variables. The study is based on Monte Carlo simulation.

Dissipated energy, interstorey displacement, and the maxima of displacement, ductility, and rotation are used to quantify the sensitivity of the response to strength uncertainty. The total energy dissipated by the system and the maximum rotation are found to be the least and most sensitive response measure, respectively. Torsion increases the mean of maximum displacements and ductilities.

The nondimensionalized ratio of the dynamic torsional moment to the design shear, called dynamic eccentricity, is used for code evaluation. The code accidental eccentricity appears inadequate to account for torsion caused by strength uncertainty, since it is significantly exceeded by the dynamic eccentricity for large fractions of the motion duration.

Finally, if the modified-Clough were the correct restoring force model, use of the elasto-plastic instead would not necessarily be conservative, since the latter may underestimate displacements and overestimate energy dissipation.

TABLE OF CONTENTS

TABLE OF CONTENTS (con't)

LIST OF ILLUSTRATIONS

LIST OF ILLUSTRATIONS (Cont'd)

LIST OF ILLUSTRATIONS (Cont'd)

LIST OF ILLUSTRATIONS (Cont'd)

LIST OF TABLES

SECTION 1

INTRODUCTION

Uncertainty in earthquake engineering has two sources: the input motion and the mathematical model of the structural system. The mathematical model includes the functional form of the restoring force model of the lateral-load-resisting elements and the parameters of this model. The present study focuses on the effects of these two aspects of system uncertainty on seismic response and design. To emphasize this focus, the input is considered deterministic and it consists of three ground acceleration records.

Inelastic time-history analysis may be used in seismic design, in which case a restoring force model has to be selected. The issue of appropriate restoring force model does not arise in the seismic design codes since inelastic response is considered only implicitly through reduction in the base shear. Since it is impossible to consider all restoring force models, a set of two, the elastoplastic and the modified-Clough, is selected. The elastoplastic model is the simplest inelastic model which makes it a popular choice. However, it is not a particularly realistic one since it fails to account for, among other behavior aspects, stiffness degradation with cycling. Reinforced concrete structures, for instance, will sustain stiffness degradation when subjected to seismic action strong enough to cause yield. The modified-Clough model does account for stiffness degradation at the expense of somewhat increased complexity. One of the issues addressed by this study is whether the use of the elastoplastic model instead of a more realistic one, such as the modified-Clough, is conservative.

Of the restoring force model parameters, the yield strength is considered uncertain. Strength uncertainty can introduce torsional vibrations to a nominally symmetric system. Such a system is symmetric in the elastic range but can become asymmetric following yield. The effects of these torsional vibrations on the seismic response are investigated in this study. The yield strength is treated as a random variable. Because of limited statistics, any physically admissible probabilistic model can be used for this variable. The lognormal distribution selected for this study is physically admissible, since it precludes unrealistic negative strength values.

Strength uncertainty is one possible source of accidental torsion in a structure. Seismic design provisions in codes such as the Uniform Building Code (UBC), the National Building Code of Canada, and the New Zealand Standard, to name a few, require that accidental

1

torsion be considered in design. The accidental torsional moment is commonly determined by assuming the mass is displaced from the calculated center of mass a distance equal to a certain percentage of the building dimension perpendicular to the direction of the input motion or the equivalent static force. This percentage varies from code to code but the most common values are 5% and 10%. This study investigates the adequacy of the accidental torsion provisions in the UBC to account for accidental torsion caused by strength uncertainty.

A review of the available literature on the seismic response of inelastic systems in torsion, presented in Section 2, shows the majority of available studies to be parametric investigations, with no probability model assumed for the system parameters.

The first part of the study involves a simple one-storey system consisting of a rigid slab supported by two lateral-load-resisting elements. A system with the same layout has been used by other investigators in the past. The difference is that in this case the element yield strengths are assumed to be random variables. Detailed information on this system and its design, as well as on the two restoring force models and the input motions considered, is found in Section 3. The same section includes numerical results from Monte Carlo simulation that illustrate the effects on the seismic response of uncertainty in the restoring force model and in the yield strength of this model.

The simplicity of the one-storey system selected for the first part of the study offers three advantages: (1) it allows for large numbers of samples to be considered in Monte Carlo simulation, (2) it makes possible to investigate multiple values of deterministic system parameters as well as scalings of the input motion, and (3) it facilitates interpretation of the observed response. However, it is evident that this system is just an idealization for research purposes, not a realistic structure. This raises the issue whether any observations made on the simple one-storey system would still be valid for a realistic multi-storey building. In an attempt to address this issue as well as to investigate the effects of system uncertainty on multi-storey systems, the second part of this study employs a realistic seven-storey building designed according to UBC specifications.

The seven-storey system is typical of what the UBC considers *regular structures*, i.e., structures with "no significant physical discontinuities in plan or vertical configuration or in their lateral-force-resisting systems". It has the same plan in all storeys and only minor variations of stiffness or mass from storey to storey. The description of this system and its design along with Monte Carlo simulation results are presented in Section 4.

2

To the writer's best knowledge this is the first study of the effects of system uncertainty on the seismic response of a realistic multi-storey building that extends beyond parametric investigations to treat yield strengths as random variables and to account for them by means of Monte Carlo simulation.

Evaluation of the accidental torsion provisions in the UBC drawing on numerical results from both one-storey and seven-storey systems is conducted in Section 5. The base of evaluation is comparison between the accidental torsional moment prescribed by the code and the dynamic torsional moment generated by strength uncertainty.

Each of the core sections in this work ends with conclusions pertaining to the specific section. These conclusions are collected and summarized in Section 6.

SECTION 2

LITERATURE REVIEW

The studies of the response of inelastic systems in torsion can be classified by the system types and the input motions considered, as shown in Figure 2-1. Each study involves a set of systems S_j, $j = 0, \ldots, q$, where S_0 denotes the symmetric system. The system S_j, $j = 0, \ldots, q$, depends on a set of parameters, θ_j, and is subjected to a set of input motions $a_i(t)$, $i = 1, \ldots, p$. The output is a response measure, μ_{ij}, for each combination of system type and input motion.

In the majority of studies there is no probability model for the system parameters θ. An exception is the study by Ayala and Escobar (1991) in which probability distributions are postulated for the system parameters.

Studies in which more than one input motions are considered fall into one of the following categories: (1) Studies where there is no probability structure on the input motions (Bozorgnia and Tso, 1986; Chopra and Goel, 1991; De Stefano et al., 1993; Goel and Chopra, 1990; Goel and Chopra, 1991; Rutenberg et al., 1992; Sadek and Tso, 1989; Tso and Sadek, 1985); (2) Studies where the input motions are artificially generated as realizations of a stochastic process (Shakib and Datta, 1993); and (3) Studies where it is *implicitly* assumed that the input motions are independent identically distributed (i.i.d.) realizations of a stochastic process (Bruneau and Mahin, 1987; Bruneau and Mahin, 1990; Bruneau and Mahin, 1991; Pekau and Guimond, 1990; Tso and Bozorgnia, 1986; Tso and

Input motions	System types						
	S_0	S_1	S_2	$\cdots$	S_j	$\cdots$	S_q
$a_1(t)$							
$a_2(t)$							
$\vdots$							
$a_i(t)$					μ_{ij}		
$\vdots$							
$a_p(t)$							

FIGURE 2-1 Schematic description of reviewed studies

5

Ying, 1990; Tso and Ying, 1992; Tso and Zhu, 1992; Zhu and Tso, 1992) . The term implicitly is used because the probability structure is not defined by the investigators. However, the presentation of the results in terms of response statistics can only be justified under the i.i.d. assumption for the input motions.

The input motions in a set are scaled so that they either (1) have the same peak ground acceleration (PGA) or (2) generate a target value of a response measure (e.g. ductility) in a reference structure. The first type of scaling is straightforward. In contrast, the second type involves a number of iterations where each iteration consists of a complete time-history analysis of the reference structure.

The reviewed studies are divided into two major groups: (1) studies of one-storey systems and (2) studies of multi-storey systems.

2.1 One-storey systems

One-storey systems are generally assumed to have a rigid slab supported by a number of lateral-load-resisting elements. The plan view of a typical one-storey system is shown in Figure 2-2. It has one axis of symmetry, denoted by x in the figure, and the input motion acts perpendicular to this axis. Consequently, only two of the three degrees-of-freedom of the system are active: translation in the y-direction and rotation.
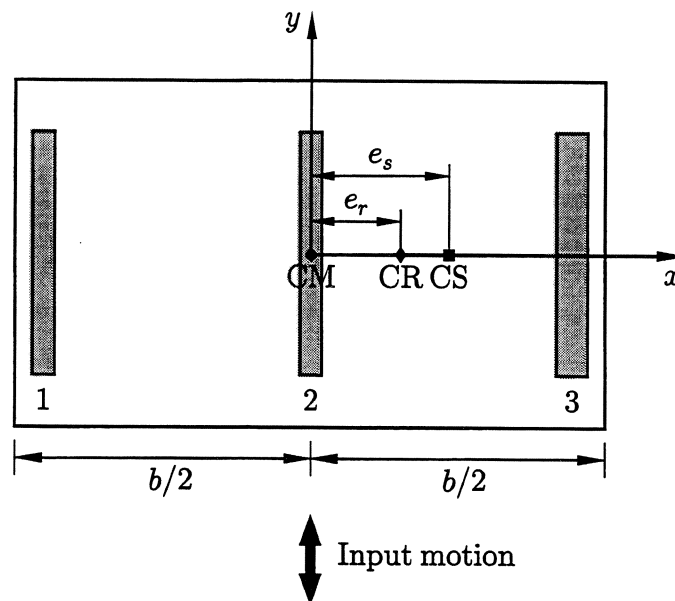
FIGURE 2-2 Plan view of a typical one-storey system

6

In most cases, the lateral-load-resisting elements, also referred to as 'elements', are walls aligned with the input motion. Systems with additional walls perpendicular on the input motion and systems with columns have also been investigated, but not as extensively. With few exceptions, the input motion is one of the two horizontal components of an earthquake record.

The center of stiffness (CS) is a point at a distance e_s from the center of mass (CM). The distance e_s is called stiffness eccentricity and is determined from the expression

$$e_s = \frac{1}{K} \sum_i x_i k_i$$

where x_i is the distance of the ith element from the CM, k_i is the initial stiffness of this element, and $K = \sum k_i$. An *elastic* system is *symmetric* when $e_s = 0$. A symmetric system sustains no torsional deformation. An elastic *stiffness eccentric* system has $e_s \neq 0$. It is created from the symmetric system by modifying the relative stiffness and/or the location of the elements. Alternatively, $e_s \neq 0$ can be obtained by changing the distribution of mass on the slab, which results in an elastic *mass eccentric* system. It is also possible to have an elastic eccentric system that is a mixture of the two types, when both the distributions of stiffness and mass are modified. As a matter of fact, only the value of the stiffness eccentricity affects the response of an elastic system. The way this eccentricity is achieved is irrelevant.

For *inelastic* systems, the elastic response of the ith element is bounded by its yield strength, f_{yi}. The center of resistance (CR) is a point at a distance e_r from the center of mass. The distance e_r is called strength or resistance eccentricity, and is determined from the expression

$$e_r = \frac{1}{F_y} \sum_i x_i f_{yi}$$

where $F_y = \sum f_{yi}$. The inelastic behavior of each element is fully described by its restoring force model. An inelastic system is *symmetric* when $e_s = e_r = 0$ and all its elements follow the same restoring force model. When $e_s = 0$ but $e_r \neq 0$, the system behaves as symmetric while in the elastic range but becomes eccentric following first yield. The same applies to systems with $e_s = e_r = 0$, the elements of which have different post-yield hysteretic behavior.

Quite often the response of the actual system is normalized by the response of an associated *reference* system. However, there is no consensus on the definition of the associated reference system. The definition starts with the elastic properties of the system and is

completed with the specification of yield strength(s) or yield displacement(s). Two major definitions are identified.

In the first and most commonly used definition, the reference system is derived from the actual system by first eliminating the stiffness eccentricity. The elimination is achieved either by changing the distribution of mass on the slab so that the CM is moved to the CS, as in (Chandler and Duan, 1991; Chopra and Goel, 1991; Goel and Chopra, 1990; Goel and Chopra, 1991; Tso and Zhu, 1992), or by modifying the relative stiffness of the elements so that the CS coincides with the CM, as in (Bozorgnia and Tso, 1986; Tso and Ying, 1990; Tso and Ying, 1992). The elastic behavior of this system is that of a single-degree-of-freedom (SDOF) system with period equal to the uncoupled lateral period, T, of the actual system. Generally, the symmetry of the reference system is preserved in the inelastic range by arranging that the relative yield strengths of the elements result in $e_r = e_s = 0$. The only exception to that is found in (Goel and Chopra, 1990), where the consideration of the accidental eccentricity code provision in the determination of the relative yield strengths of the elements leads to $e_r \neq 0$. Consequently, this latter associated reference system experiences torsion when excited into the inelastic range.

According to the second definition in (Bruneau and Mahin, 1990), the associated reference system is a SDOF system with period equal to the period of the predominantly translational mode of the actual coupled system. In this study the elements of the actual system share the same yield displacement, which is also assigned to the associated SDOF system.

The studies of one-storey systems are divided into three categories: (1) studies in which the input consists of a set of records and the response is reported on a per record basis (Section 2.1.1), (2) studies in which the input also consists of a set of records but response statistics across records are reported instead (Section 2.1.2), and (3) studies in which one or more system parameters are considered random and the response is presented in terms of statistics (Section 2.1.3). Finally, the review of one-storey systems is summarized in tabular form in Section 2.1.4.

2.1.1 Set of records. Response per record

Studies in this category make no explicit or implicit assumptions on the probability structure of the system variations and the input motion(s). The values of the response measures are presented separately for each system type and input motion combination considered.

The basis of the paper by *Chandler and Duan* (Chandler and Duan, 1991) is the evaluation of the torsional provisions in the 1976 and 1987 editions of the Mexico City building code. The investigators use site records to assess the validity of code provisions for a particular location. Therefore, the E-W component of the record obtained at the SCT building in Mexico City during the 1985 earthquake is used as input throughout this study.

Another issue raised by Chandler and Duan refers to the use of the accidental eccentricity, e_a, in the calculation of the element yield strengths, in the context of an evaluation of code provisions. Generally the accidental eccentricity is meant to account for uncertainties in the stiffnesses and yield strengths and/or rotational components of ground motion. Therefore, Chandler and Duan argue, it is inconsistent to include accidental eccentricity in the design when uncertainties and torsional components are ignored in the analysis. Moreover, they claim that the inclusion of accidental eccentricity can give misleading results. To prove this last point, the response of three-element systems with $e_s = 0.2b$ and $e_a = 0.0$, $0.05b$ and $0.1b$ is compared. Systems with uncoupled lateral periods from 0.1 to 2.0 sec are examined. The results show that the additional ductility demand on the element at the stiff edge decreases significantly as the accidental eccentricity increases, leading to very different conclusions on the adequacy of the code provisions. Hence, they base their code evaluation on results obtained for $e_a = 0$, T ranging from 0.1 to 2.0 sec, and $e_{sb} = 0.1$, 0.2 and 0.3.

Chandler and Duan find the 1976 Mexico City code provisions inadequate for failing to limit the additional ductility demand due to torsion on the element at the stiff edge of the structure. The changes in the 1987 edition of the code correct this problem by increasing the yield strength of the element in question. However, because of the resulting large increase in the total yield strength, the investigators deem them overconservative. They recommend as most appropriate expressions for the design eccentricity the ones included in the current Canadian code. Their conclusion on the superiority of the Canadian code provisions in controlling ductility demands concurs with the conclusion reached by Tso and Ying in (Tso and Ying, 1992) and Tso and Zhu in (Tso and Zhu, 1992).

In their study *Rutenberg et al.* (Rutenberg et al., 1992) compare the response of three model structures designed by two codes, the 1985 National Building Code of Canada (NBCC) and the 1978 Applied Technology Council (ATC) code. The three-element model structures are designed to have identical elastic behavior, while one is mass eccentric and the other two are stiffness eccentric with the middle element coinciding with the CM in

one case, and with the CS in the other. Four values of T, 0.25, 0.50, 0.75, and 1.00 sec, and three values of Ω, 0.8, 1.0, and 1.25 are considered. The seismic factor $C_s = F_y/W$, where F_y is the total yield strength and W is the total weight of the system, is actually different in the two codes. However, in this study it is taken as equal to make the code comparison meaningful, and it ranges between 5 and 25%. The input consists of four earthquake records with very different characteristics, selected to represent the extremes of possible ground motions. Rutenberg et al. conclude that design by the Canadian code results in lower values for the largest element ductility. They also observe that the element at the flexible edge experiences the largest displacement, while the largest ductility is usually found in the element at the rigid edge or in the central element.

The study by *De Stefano et al.* (De Stefano et al., 1993) involves a system with three elastoplastic elements in the direction of the ground motion and two elastic elements perpendicular to the motion. The input, consisting of two earthquake records from Italy, is particular to this study. The first period of the coupled system T_1 varies from 0.3 to 0.8 sec, the normalized stiffness radius of gyration ρ_{sb} takes values between 0.35 and 0.40, and the normalized stiffness eccentricity e_{sb} is set equal to either -0.1 or -0.2. In the first part of the study, the strength distribution among the three elements in the direction of the motion is controlled by modifying the normalized strength eccentricity e_{rb} and the normalized strength radius of gyration ρ_{rb}. The response measure is an element damage index $D_i = [\mu_i + \beta(E_{\text{dis},i}/(f_{yi}d_{yi})]/\mu_m$, where μ_i is the ductility, $E_{\text{dis},i}$ is the dissipated energy, f_{yi} is the yield strength, and d_{yi} is the yield displacement of element i. The coefficient β is taken as 0.15 and μ_m represents the available monotonic ductility set to 4. For given period, stiffness distribution and total yield strength, similar values of D_i for all elements can be obtained by selecting appropriate values for e_{rb} and ρ_{rb}. De Stefano et al. observe that e_{rb} is the most influential of the two parameters and that $D_{\max} = \max\{D_i\}$ is minimized for $0 \le e_{rb} \le e_{sb}$ and often close to $e_{sb}/2$.

In the second part of the same study the strength distribution is determined based on the torsional provisions in the 1990 NBCC, the 1997 and 1987 editions of the Mexico City code, the 1988 UBC, and the 1988 edition of the Eurocode. However, accidental eccentricity is ignored and any overstrength is eliminated. It is found, as in the first part of the study, that systems with e_{rb} close to $e_{sb}/2$ usually result in smaller values for $D_{\max}$. The Canadian code which leads to strength distributions satisfying this criterion is judged as the most adequate.

10

Evaluation of torsional code provisions is part of the investigation by *Goel and Chopra* (Chopra and Goel, 1991; Goel and Chopra, 1990). A system with two elements in the direction of the input motion, idealized as elastoplastic, and two more elements perpendicular on the input motion, taken as elastic, is selected. The uncoupled lateral period, T, varies between 0.1 and 20 sec and the strength reduction factor $R = 1, 4$. A value of $R = 1$ implies that the strength of the associated symmetric system is just enough for it to remain elastic during the input motion. However, the response of the code designed asymmetric building may become inelastic, because of the increased displacements due to torsion and the reduction in the yield strength of the element at the stiff edge allowed by codes. The codes considered are the 1985 NBCC, the 1984 New Zealand code, both the 1988 UBC and the 1978 ATC, as well as the 1976 and 1987 editions of the Mexico City code. The input consists of the N-S component of the 1940 El Centro record.

The significant increase in the ductility of the element at the stiff edge due to the asymmetry is once more observed. The Canadian code fares better than most, keeping this ductility close to its associated symmetric system value. The 1987 Mexico City code is judged rather overconservative. The additional displacement of the element at the flexible edge is also significant. Similar conclusions are reached by Tso and Ying (Tso and Ying, 1992), Tso and Zhu (Tso and Zhu, 1992), Chandler and Duan (Chandler and Duan, 1991), and Rutenberg et al. (Rutenberg et al., 1992). Goel and Chopra suggest that the additional ductility due to the asymmetry can be limited by precluding any reduction of the element yield strengths below their values in the associated symmetric system.

Goel and Chopra conducted also parametric studies independent of any actual code provisions (Goel and Chopra, 1990; Goel and Chopra, 1990; Goel and Chopra, 1991). In those they consider systems with two, three or four elements in the direction of the input motion and with none or two elements in the perpendicular direction. They also study the response of stiffness eccentric versus mass eccentric systems. In the first stages of their investigation, an artificial motion consisting of a half-cycle displacement pulse is used as input. Later, the N-S component of the 1940 El Centro record is added. The range of the uncoupled lateral period, T, is different for each of the two records. For the first, T takes values between $0.1t_1$ and $10t_1$, where t_1 is the half-duration of the displacement pulse. For the second, it ranges between 0.1 and 20 sec. Moreover, four values of Ω, 0.8, 1.0, 1.25, and 2.0, three values of e_{sr}, 0.05, 0.2, and 0.5, and four values of e_{rr}/e_{sr}, 0.0, 0.25, 0.5, and 1.0, are considered. A new parameter used in this study is the overstrength factor, O_s, defined as the ratio of the total strengths of the asymmetric system and the associated

symmetric reference system. Four values of O_s, 1.0, 1.1, 1.2, and 1.3, are considered.

Goel and Chopra conclude that the presence of elements perpendicular on the input motion reduces the effect of torsion, especially in systems with short uncoupled lateral periods. However, they find the response to be rather insensitive to the number of elements in the direction of the input motion, except for the maximum ductility of systems with strength eccentricity much smaller than stiffness eccentricity. They also point out the significant differences in the inelastic response of mass versus stiffness eccentric systems having identical elastic response and caution against using those two types of system interchangeably. Overstrength is found to reduce the effect of torsion on systems with short uncoupled lateral periods, while systems with longer periods remain unaffected. Finally, the effect of torsion on stiffness eccentric systems is generally smaller when e_r is close to zero.

Syamal and Pekau (Syamal and Pekau, 1985) studied a two-element system subjected to a sinusoidal input motion, $\ddot{u}_g(t) = U \cos \omega_g t$. In this study, Ω varies from 0.5 to 1.5 and e_{sr} from 0.0 to 0.4. The two elements share the same yield displacement, d_y, which results in $e_r = e_s$. Variations in both the frequency and the amplitude of the sinusoidal input are also considered. The ratio of the input frequency, ω_g, to the uncoupled lateral frequency, ω, is denoted by Ω_g, and takes values from 0.0 to 2.0. The values of the amplitude of the input motion, U, are determined through the parameter G_a, where $G_a = U/(d_y \omega^2)$, and G_a ranges from 0.0 to 4.0. The equations of motion are solved by the method of averaging and the response measures in Table 2-1 are, in fact, the amplitudes of the steady state average response of the system.

Syamal and Pekau observe that the response of inelastic systems does not exhibit the very large peaks characterizing the response of elastic systems, for ω_g close to one of the natural frequencies. They also find that the ductility demand on the element at the flexible edge increases rapidly with increase in eccentricity, while the ductility demand on the other element decreases, but rather slowly. Based on that last observation, they comment that the codes should not allow for reductions in the yield strength of elements at the stiff edge of structures, with increasing eccentricity.

Bozorgnia and Tso (Bozorgnia and Tso, 1986) study a three-element system with T varying between 0.1 and 2.0 sec, $\Omega = 0.8$, 1.0, and 1.2, $e_{sr} = 0.0$ and 0.25, and $R = $ 1, 3, and 5. All elements share the same yield displacement, which results in $e_r = e_s$. The total yield strength of the system is determined by means of a typical 'design'

spectrum, i.e., a spectrum constant for periods smaller than a specified value and varying inversely to the period for larger periods. For a specified value of the uncoupled lateral period of the system, a characteristic acceleration, a^*, is obtained from the spectrum, and $F_y = Ma^*/R$, where M is the mass of the system. The input consists of four records, two of which represent ground motions with elastic acceleration spectra similar in shape with the 'design' spectrum. The other two records represent motions showing a few pronounced acceleration pulses and having elastic acceleration spectra dissimilar to the 'design' spectrum.

For the system in this study, the element furthest away from the CS, being critical for the displacements, is critical for the ductilities as well, since the yield displacement is the same for all elements. It is concluded that the effect of torsion is most pronounced for systems with short uncoupled lateral periods, designed with large values of R. The ductility of such systems can be up to three times that of the associated symmetric system. Also, it is recommended to avoid the use of large values for the strength reduction factor, R, if ground motions of the second type considered are anticipated.

The study by *Tso and Sadek* presented in (Tso and Sadek, 1985) is one of very few — one other being the study by Pekau and Guimond (Pekau and Guimond, 1990) — that consider a restoring force model that accounts for stiffness degradation. The model considered in this case, in addition to the commonly used bilinear, is the Clough model. T ranges from 0.25 to 2.5 sec, $\Omega = 0.8$, 1.0, and 1.4, $e_{sb} = 0.0$, 0.05, 0.15, and 0.25, and R varies from 1 to 8. All three elements have the same yield displacement and, therefore, $e_r = e_s$. Two earthquake records with similar characteristics are used as input. The two restoring force models are compared by means of the ductility of the element furthest away from the CS. Tso and Sadek judge the results from the two models as similar, reporting that the use of the Clough model results in ductility values from 0.69 to 1.34 of the values obtained with the bilinear model.

Chandler et al. use the Ramberg-Osgood restoring force model in their work reported in (Chandler et al., 1991). They consider eight structural configurations with two or three elements in the direction of the input motion and none or two elements perpendicular to the motion. The input motion in all cases is the E-W component of the SCT record of the 1985 Mexico City earthquake. T takes values in the range 0.1–5.0 sec, Ω is equal to 0.7, 1.0, or 1.3, e_{sr} is either 0.0 or 0.2, and $e_{rr} = 0.0$, 0.1, and 0.2. The strength reduction factor R is varied between 1 and 6 for one structural configuration whereas it is kept

constant and equal to 2 for all others. Chandler et al. find that the maximum ductility increases with R, decreases with T for $T < 2$ sec, and is rather insensitive to period for $T > 2$ sec. They also conclude that the effect of torsion on the maximum displacement at the edge of the deck depends more on the strength than on the stiffness eccentricity.

Another study by *Tso and Sadek* (Sadek and Tso, 1989) is set apart by the type of system as well as the input motions considered. The system consists of a rigid square deck of plan dimension D, supported by four columns. It has one axis of symmetry, which means that the columns are identical in pairs. Each column has the same stiffness and yield strength along its two principal directions. The system is subjected to the two orthogonal horizontal components of two earthquake records with similar characteristics. The response is described in terms of two translational displacements and the rotation about the CM. The interaction effect on yielding of the columns due to the biaxial shear is neglected. T varies from 0.1 to 2.2 sec. Two types of system configuration are considered. For the first, e_s is fixed at $0.2D$ while $e_r = 0.0, 0.1D$, and $0.2D$. The second configuration is the inverse of the first, with fixed $e_r = 0.2D$ and varying $e_s = 0.0, 0.1D$, and $0.2D$.

Using as response measures the maximum rotation and the ductility of one of the two columns furthest away from the CS, Tso and Sadek conclude that the response of a system excited well into the inelastic range is sensitive to variations in strength eccentricity, while it is rather insensitive to similar variations in stiffness eccentricity. They find the sensitivity to be more pronounced for systems with short lateral periods.

2.1.2   Set of records. Response statistics

Studies in this category use as input a set of records to which a probability structure is explicitly or implicitly assigned. The response is presented in terms of estimates of mean and standard deviation, and extreme values of several response measures.

Bruneau and Mahin (Bruneau and Mahin, 1987; Bruneau and Mahin, 1990; Bruneau and Mahin, 1991) studied the response of two-element systems divided into two groups. The elements of the systems in the first group have unequal initial stiffnesses resulting in $e_s \neq 0$, but the same yield displacement, d_y, which leads to $e_r = e_s$. The systems in the second group are elastically symmetric ($e_s = 0$) but have different yield strengths, which lead to torsional deformation following first yield. For both groups, the uncoupled lateral period varies from 0.1 to 2.0 sec, while the uncoupled torsional to lateral frequency ratio, Ω, ranges between 0.4 and 2.0. For the first group e_{sr} is set equal to 0.1 and 0.3. For the

14

second group four element yield strength combinations are considered: 0.8 and $1.0F_{y0}$, 1.0 and $1.2F_{y0}$, 1.0 and $1.5F_{y0}$, 1.0 and $2.0F_{y0}$, where F_{y0} denotes the yield strength of the associated SDOF system.

The input consists of five earthquake records scaled according to the following procedure: (1) Given a system type, its associated SDOF system is defined as a system with period equal to the period of the predominantly translational mode of the actual system. For systems with $e_s \neq 0$, the associated SDOF system is assigned the common yield displacement of the elements, while for systems with $e_s = 0$, its yield strength is specified as F_{y0}. (2) Each record is scaled so that it generates a specified target ductility, μ_t, in the associated SDOF system. The determination of the appropriate scaling factor requires a number of iterations. This procedure is referred to in Table 2-1 as 'target ductility' method. Two values of μ_t, 4 and 8 are used in the study.

The element ductilities μ_i, $i = 1, 2$, of the actual system, are compared with the ductility of the associated SDOF system, μ_0. It is concluded that a conservative estimate for the maximum mean value of the ratio μ_i/μ_0 is 1.5. The maximum value for the mean-plus-one standard-deviation of the same ratio is estimated at about 2.0.

The study by *Pekau and Guimond* (Pekau and Guimond, 1990) focuses on two-element systems that are elastically symmetric but have asymmetry introduced during inelastic response due to a difference either in the element yield strengths or in the element restoring force models. Both types of asymmetry are among the unforeseen factors that the accidental eccentricity provisions in the codes are intended to account for. For the first type of asymmetry, it is assumed that both elements are elastoplastic, have identical elastic stiffnesses but the ratio of their yield strengths, f_{y2}/f_{y1}, ranges between 0.6 and 1.0. For the second type, the elements are assumed to have identical elastic stiffnesses and yield strengths but while one is elastoplastic the other follows the Takeda model, which accounts for stiffness degradation with cycling. In both cases, T takes values between 0.25 and 2.0 sec while Ω is set equal to 0.5, 1.0, and 1.5. A set of three earthquake records is used as input.

Pekau and Guimond conclude that both cases of asymmetry can result in increased displacements by a factor of up to approximately two, compared with the displacements of the associated symmetric reference system. They also find that the extreme values of d_{max} exceed by as much as 50% the respective values of a system designed with the accidental eccentricity provisions in the 1985 National Building Code of Canada (NBCC).

Tso and Bozorgnia (Tso and Bozorgnia, 1986) studied three-element systems. In a preliminary study they compare three models of such systems: (1) mass eccentric, (2) stiffness eccentric with $e_r = e_s$, and (3) stiffness eccentric with $e_r = 0$. The three models are designed to have the same elastic response. T varies from 0.1 to 2.0 sec, e_{sr} takes values of 0.3 and 0.6, and the strength reduction factor, R, is set equal to 3 and 5. The strength reduction factor can be defined as $R = F_{y0,\text{el}}/F_{y0}$, where F_{y0} is the yield strength of the associated symmetric system and $F_{y0,\text{el}}$ is the yield strength required for that same system to remain elastic during strong ground motion. The inelastic response of all three models to two earthquake records is studied. The second model generally results in larger edge displacements and hence, is selected for the subsequent more detailed investigation, outlined in Table 2-1.

Two values of T, 0.2 and 1.0 sec, three values of Ω, 0.8, 1.0, and 1.2, and two values of R, 3 and 5 are considered, while e_{sr} varies from 0.0 to 1.0. The six earthquake records used as input are scaled to a common peak acceleration. Based on the results of this study, Tso and Bozorgnia advocate the use of the 'effective eccentricity' concept in estimating the maximum edge displacement of the type of system covered in the study. Details on the effective eccentricity concept can be found in (Tso and Bozorgnia, 1986).

In a subsequent study (Tso and Ying, 1990), *Tso and Ying* expand the investigation of the three-element system used by Tso and Bozorgnia (Tso and Bozorgnia, 1986). In addition to strength distributions that result either in $e_r = e_s$ or in $e_r = 0$, they consider distributions that would result from the application of the torsional provisions in a number of codes. The eight earthquake records selected by the investigators have similar frequency contents and are scaled to the same peak acceleration. Consequently, the implicit assumption of i.i.d. can be considered reasonable for this set of records. Moreover, the frequency content of the records is such that the shapes of their elastic acceleration spectra are similar to the shape of the commonly used 'design' spectrum, i.e., a spectrum constant for periods smaller than a specified value and varying inversely to the period for larger periods.

A preliminary study with T fixed at 0.5 sec and $e_{sb} = 0.1$, 0.2 and 0.3, shows that the element at the flexible edge of the structure, i.e., the edge element furthest away from the CS, can undergo displacements up to two to three times those of the reference symmetric system, *independent* of the strength distribution. However, the ductility of this same element does not exceed the ductility of the symmetric system, except for the model with

$e_r = e_s$. When $e_r = e_s$, all elements have the same yield displacement and this yield displacement is independent of the stiffness eccentricity. In this case, any increase in the maximum element displacement leads to identical increase in the element ductility. For all the other designs considered in (Tso and Ying, 1990), the element at the flexible edge has lower stiffness and higher yield strength in the asymmetric system than in the associated symmetric system. Therefore, the increase in the yield displacement of this element offsets the increase in its maximum displacement and no increase in ductility is observed. On the other hand, the ductility of the element at the stiff edge of the structure, i.e., the edge element closest to the CS, is in some cases higher than the ductility of the associated symmetric system, despite of its maximum displacement never exceeding that of the symmetric system. This is due to the fact that, with the exception of the model with $e_r = e_s$, the element at the stiff edge has not only higher stiffness but also lower yield strength in the asymmetric than in the symmetric system. The consequent decrease in the yield strength of this element in some cases overcomes the decrease in its maximum displacement, and that shows up as an increase in ductility. Despite the observed increases in the ductility of the element at the stiff edge, Tso and Ying identify the element at the flexible edge as 'critical' for both displacements and ductilities, a conclusion disputed also by Chandler and Duan in (Chandler and Duan, 1991).

In the remainder of (Tso and Ying, 1990) additional results are presented for e_{sb} fixed at 0.3, R equal to 3 and 5, and T varying from 0.1 and 2.0 sec, but only the response measures of the 'critical' element are considered. The extended results support the conclusions of the preliminary study on the additional displacements due to torsion. Tso and Ying observe that strength distributions based on the 1985 NBCC, the 1984 New Zealand code, the 1976 Mexico City code, and the 1988 Uniform Building Code (UBC) of the United States, result in $e_r \simeq 0$. In systems designed by all these codes, the ductility of the element at the flexible edge does not exceed the ductility of the associated symmetric system.

A more recent study by *Tso and Ying* (Tso and Ying, 1992) considers both mass eccentric and stiffness eccentric three-element systems, with stiffness eccentricity, e_s, ranging from 0.0 to 0.3, and strength eccentricity, $e_r = e_s$ or $e_r = 0$. The input consists of the N-S component of the 1940 El Centro record. The response shows that to avoid exceptionally large ductilities due to torsion in a stiffness eccentric system the yield strengths should be distributed so that $e_r = 0$. Quite the opposite applies to mass eccentric systems, where the distribution with $e_r = e_s$ results in better control of the ductility due to torsion. Therefore, Tso and Ying conclude that use of the strength eccentricity alone is

not sufficient to properly specify strength distribution for all types of eccentric systems.

In the second part of (Tso and Ying, 1992), results of a study similar to the one in (Tso and Ying, 1990) are reported. The strength distributions considered correspond to the recommendations in the 1984 New Zealand code and in the 1990 NBCC, as applied to stiffness eccentric or mass eccentric systems. Four values of T, 0.2, 0.5, 1.0, and 2.0 sec are used, while e_{sb} varies between 0.0 and 0.3. The input consists of the same set of records used in (Tso and Ying, 1990). For mass eccentric systems, the edge opposite to the CS in respect to the CM is considered the flexible edge. The edge on the same side with the CS is considered the stiff edge. Based on averages of the response measures it is concluded that the expressions for the design eccentricity in the Canadian code lead to better control of the additional ductility due to torsion on the elements at both edges of the structure. Specifically, the mean ductility of the element at the stiff edge does not exceed 1.2 times the mean ductility of the symmetric reference system while the mean ductility of the element at the flexible edge is even lower. For comparison, the design by the New Zealand code results in mean ductility up to 2.0 times the mean ductility of the symmetric reference system. In agreement with the results in (Tso and Ying, 1990), the amplification of the flexible edge displacement appears to be relatively insensitive to the strength distribution and can be significant, more so for stiffness than for mass eccentric systems.

Tso and Zhu (Tso and Zhu, 1992; Zhu and Tso, 1992) studied a three-element model with the two edge elements at equal distance of $b/2$ from the central element. The stiffness distribution is defined by the distance of the CS from the central element, x_{CS}, and by the normalized radius of gyration of stiffness about the CS, $\rho_{sb} = (1/b)\sqrt{K_{\theta s}/K}$, where $K_{\theta s}$ is the torsional stiffness of the system about the CS. The larger the value of ρ_{sb}, the more torsionally stiff the system. Three values for each of x_{CS} and ρ_{sb} are considered. The resulting nine configurations range form torsionally stiff systems with centrally located CS to torsionally flexible systems with eccentrically located CS. The location of the CM is specified through the stiffness eccentricity, which ranges from 0.0 to $(0.5 + x_{CS}/b)$. Yield strength distributions follow the provisions in the 1990 NBCC, the 1984 New Zealand code, and the 1988 UBC of the United States. Fifteen earthquake records scaled to common peak acceleration of $1g$ are used as input. As in (Tso and Ying, 1990) and (Tso and Ying, 1992) the choice of records is based on their frequency content and the shape of their elastic acceleration spectra.

Tso and Zhu reach conclusions mostly similar to the ones reported by Tso and Ying in (Tso and Ying, 1990) and (Tso and Ying, 1992). They find that, independent of the adopted provisions, torsion increases the displacement at the flexible edge of the structure. The amount of the increase, as expected, depends on the stiffness eccentricity, the torsional stiffness, and the distance of that edge from the CS. Also, they conclude that all three codes adequately control the additional ductility demand due to torsion on the element at the flexible edge of the structure. However, systems designed based on either the New Zealand code or the UBC may experience significant additional ductility demand on the element at the stiff edge. This last observation applies to either torsionally flexible systems or to torsionally moderately stiff systems with stiffness eccentricity $e_s > 0.1b$. On the other hand, the Canadian code provisions avoid this problem. This is attributed to the limited reduction in the yield strength of the stiff edge element — relative to the yield strength of the same element in the associated symmetric reference system — allowed by this code.

The last study in this section (Shakib and Datta, 1993) is the only one in the review in which the input motion is explicitly considered a random process. *Shakib and Datta* use 30 artificial acceleration records with two components each, generated from specified power spectral density (PSD) and modulating functions. The structural system consists of a square deck of dimension D supported by four columns that follow a circular yield curve for biaxial shear. The system is stiffness eccentric in both the x- and y-direction. The stiffness eccentricity in the y-direction varies between 0 and $0.3D$ and the ratio of the two eccentricities is 0.5, 1.0, or 1.5. The center of resistance coincides either with the center of mass or with the center of stiffness. T ranges from 0.3 to 2.0 sec and $\Omega = 0.75$, 1, 1.5, 2, 2.5, and 3. Response is measured in terms of maximum column ductility $\mu_{\max}$ and maximum torque. The mean and variance of these response measures are found to decrease with T. The mean of $\mu_{\max}$ is rather insensitive to the stiffness eccentricity for eccentricities in the y-direction below $0.2D$. The mean of both response measures is lower when there is only stiffness eccentricity than when there are both stiffness and strength eccentricity.

2.1.3 Random system parameters. Response statistics

Studies in this category explicitly consider one or more of the system parameters as random variables, following specified distributions. Under this assumption, the response measures are also random variables, but with unknown distributions. Simulation is used

by the investigators to provide partial information on the response measures, such as estimates of their mean, m, and standard deviation, σ.

The study by Ayala and Escobar (Ayala and Escobar, 1991; Escobar and Ayala, 1991) belongs in this category. Systems with two, three or four elastoplastic elements are considered. The yield strengths of the elements are assumed to be independent lognormally distributed with mean values corresponding to a specified value of e_{rb} between -0.3 and $+0.3$, and coefficient of variation (COV) equal to 20%. Variations in a number of other parameters are also considered but without any probability structure. Specifically, the uncoupled lateral period, T, varies between 0.5 and 1.5 sec, and e_{sb} ranges from -0.3 to 0.0. The input is the E-W component of the SCT record of the 1985 Mexico City earthquake. The results of the Monte Carlo simulation are estimates of the mean, m, and the standard deviation, σ, of the response measures listed in Table 2-1. A major conclusion is that structures appear to be less sensitive to torsion if e_r and e_s have similar values.

2.1.4 Summary of reviewed studies

All studies considered in the review are outlined in Table 2-1. The tabular format provides an overview and facilitates comparisons between different approaches. Only the system parameters varied during a given study are listed in the table under 'System description and parameters'. Any additional parameters required for full system description that remain constant are omitted. The definition of all symbols used in Table 2-1 can be found in the list of notations for the literature review section that follows.

Notations

b	= Plan dimension of the structure perpendicular to the direction of the input motion
$BL(\cdot)$	= Bilinear restoring force model, where $\cdot$ is the ratio of the post yield stiffness to the initial stiffness in percent
C_s	= Seismic factor. $C_s = F_y/W$, where W is the total weight of the system
CM	= Center of mass
COV	= Coefficient of variation
CR	= Center of resistance
CS	= Center of stiffness
D_i	= Element damage index accounting for both maximum displacement and

TABLE 2-1 Summary of studies of one-storey systems

Input	System description and parameters	Response measures	Refs.
Set of records. Response per record. (Section 2.1.1)			
SCT record	3 elements, BL(3%) T, e_{sb}, e_a, f_{yi}'s by codes	μ_i/μ_0	[7]
4 records	3 elements, BL(2%) T, Ω, C_s, f_{yi}'s by Codes	μ_i, μ_{max}, $\max\{d_{max,i}\}$	[23]
2 records from Italy	3 EP elements in direction of motion and 2 elastic elements perpendicular on motion T_1, ρ_{sb}, e_{sb}, (e_{rb}, ρ_{rb}) or $(f_{yi}$'s by codes)	D_i, $\max\{D_i\}$	[10]
El Centro	2 EP elements in direction of motion and 2 elastic elements perpendicular on motion T, R, f_{yi}'s by codes	μ_i/μ_0, $d_{max,i}/d_{max,0}$	[9] [16]
El Centro & half-cycle displacement pulse	2–4 EP elements in direction of motion and none or 2 elements perpendicular on motion T, Ω, e_{sr}, e_{rr}/e_{sr}, O_s	μ_{max}, max displacement of and rotation about CS, $\max\{d_{max,i}\}/d_{max,0}$, e_d/e_s	[16] [17] [18]
$\ddot{u}_g(t) = U\cos\omega_g t$	2 elems, EP or BL(5%) Ω, U, Ω_g, e_{sr}, $e_{rr} = e_{sr}$	μ_i, max displacement of and rotation about CM	[28]
2 or 4 records	3 elements, BL(3%) or Clough T, Ω, R, e_{sr} or e_{sb}, $e_r = e_s$	μ_f, $\max\{d_{max,i}\}/d_{max,0}$, $d_{max}/d_{max,0}$ at edge of deck	[2] [31]
SCT record	2 or 3 Ramberg-Osgood elements in direction of motion and 0 or 2 elements perpendicular on motion T, Ω, R, e_{sr}, e_{rr}	$d_{max}/d_{max,0}$ at edge of deck, μ_{max}	[8]
2 records with two components each	4 columns, 3 DOF, EP T, e_s, e_r	μ_f, max displacement of and rotation about CM	[24]

21

TABLE 2-1 (Continued)

Input	System description and parameters	Response measures	Refs.
Set of records. Response statistics $^{(\bullet)}$. (Section 2.1.2)			
5 records scaled by 'target ductility' method	2 elements, BL(0.5%) T, Ω, μ_t, (e_{sr} & $e_{rr} = e_{sr}$) or ($e_s = 0$ & f_{yi} combinations)	Estimates of m and σ of μ_i/μ_0	[3] [4] [5]
3 records	2 EP elements or one EP & one Takeda T, Ω, f_{y2}/f_{y1}	Estimates of m and σ, and extreme values of $d_{\max}$ at edge of deck	[21]
6 records scaled to same PGA$^{(\diamond)}$	3 elements, BL(3%) T, Ω, e_{sr}, $e_{rr} = e_{sr}$, R	Estimates of m and σ of $d_{\max}/d_{\max,0}$ of point at $e_s + \sqrt{3}\,r$ from CS	[30]
8 records with similar frequency content, scaled to same PGA$^{(\diamond)}$	3 elements, BL(3%) T, e_{sb}, R, f_{yi}'s by codes	Estimates of m of μ_i/μ_0, $d_{\max,i}/d_{\max,0}$	[32] [33]
15 records with similar frequency content, scaled to PGA = g	3 elements, BL(3%) x_{CS}, ρ_{sb}, e_{sb}, f_{yi}'s by codes	Estimates of m of μ_i/μ_0, $d_{\max,i}/d_{\max,0}$	[34] [36]
30 artificially generated records with two components each 2 shapes of PSD and modulating function	4 columns, 3 DOF, biaxial bending with circular yield curve T, Ω, e_{sb}, $e_{rb} = e_{sb}$ or $e_{rb} = 0$, ratio of e_s in two directions	Estimates of m and σ, and extreme values of $\mu_{\max}$ and max torque	[26]
Random system parameters. Response statistics. (Section 2.1.3)			
SCT record	2-4 elements, EP T, $f_{yi}^{(\star)}$, e_{sb}, e_{rb}	Estimates of m and σ of $\mu_{\max}/\mu_0$, $N_{exc}/N_{exc,0}$, $N_{exc}^s/N_{exc,0}^s$, $E_{dis}/E_{dis,0}$	[1] [14]

Note: ($\star$) The parameter is treated as random

($\bullet$) It is assumed implicitly that $\mathrm{Prob}(\alpha_i(t), S_j) = 1/(pq)$,
for all i, $i = 1, \ldots, p$ and j, $j = 1, \ldots, q$

($\diamond$) Not specified in the reference

dissipated energy (for definition see (De Stefano et al., 1993))
$d_{\max}$ = Maximum displacement at a specified point in the structure
$d_{\max,i}$ = Maximum displacement of element i

d_y = Yield displacement

DOF = Degrees-of-freedom

e_a = Accidental eccentricity, specified in codes as a percentage of b

e_d = Dynamic eccentricity ($e_d = (K_{\theta s} u_\theta / (K d_{0,\text{max}})$, where u_θ = peak torsional deformation)

E_{dis} = Dissipated energy

E_{el} = Elastic energy ($E_{\text{el}} = 0.5 F_y d_y$)

e_r = Strength (resistance) eccentricity, i.e., distance between CM and CR

e_{rb} = Strength eccentricity normalized by b

e_{rr} = Strength eccentricity normalized by r

e_s = Stiffness eccentricity, i.e., distance between CM and CS

e_{sb} = Stiffness eccentricity normalized by b

e_{sr} = Stiffness eccentricity normalized by r

EP   = Elastoplastic restoring force model

F_y = Total yield strength of system

f_{yi} = Yield strength of lateral-load-resisting element i

K = Total lateral stiffness

k_i = Stiffness of element i

$K_{\theta s}$ = Torsional stiffness about the CS

M = Mass of the system

m = Mean

N_{exc} = Number of inelastic excursions

N_{exc}^s = Number of successive inelastic excursions in opposite directions

O_s = Overstrength factor, i.e., ratio of the total strengths of the asymmetric system and the associated symmetric reference system

PSD = Power Spectral Density

R = Strength reduction factor, depending on the capacity of the system to safely undergo inelastic deformation during a strong ground motion

r = Radius of gyration about the CM

SDOF = Single-degree-of-freedom

T = Uncoupled lateral period, $T = 2\pi \sqrt{M/K}$

T_1 = First period of the coupled system

$\ddot{u}_g$ = Ground acceleration

x_{CS} = Distance between CS and geometric center of the deck

μ_f = Ductility of the element furthest away from the CS

μ_i = Ductility of element i

μ_{max} = Maximum of all element ductilities

μ_t = Target ductility, i.e., a specified value of ductility that must be attained by the equivalent symmetric system. It is accomplished by appropriate scaling of the input motion(s)

ρ_{sb} = Radius of gyration of stiffness about the CS, defined as $\rho_{sb} = \sqrt{K_{\theta s}/K}$, normalized by b

ρ_{rb} = Radius of gyration of strength about the CR normalized by b

σ = Standard deviation

ω = Uncoupled lateral frequency

Ω = ω_θ/ω, i.e., uncoupled torsional to lateral frequency ratio

Ω_g = ω_g/ω, i.e., input frequency to uncoupled lateral frequency ratio (for $\ddot{u}_g = U \cos \omega_g t$)

ω_θ = Uncoupled torsional frequency

$(\cdot)_0$ = Subscript 0 denotes a response measure of the associated reference system

2.2 Multi-storey systems

Studies of the inelastic response of multi-storey systems in torsion are far less numerous because of the increased computational requirements involved in the analysis of such systems and the larger number of parameters required for sensitivity studies.

Bruneau and Mahin extend their study of one-storey systems to some very simple two-storey systems (Bruneau and Mahin, 1987; Bruneau and Mahin, 1990). The N-S component of the 1940 El Centro record scaled to peak acceleration of $0.5g$ is used as input. Several systems with regular and one with irregular configuration are considered. All systems have one axis of symmetry perpendicular on the ground motion.

Systems with regular configuration have the same total mass and the same mass and stiffness distribution in the two storeys. The total storey stiffness varies so that the ratio of the second to the first storey stiffnesses is either 2/3 or 1/3. Each storey has two lateral-load-resisting elements in the direction of the ground motion. Bruneau and Mahin examine the possibility of using some simpler associated reference system to predict the response of the actual two-storey system. In systems with $e_s \neq 0$ and $e_r = 0$ this associated reference system is a SDOF system with period equal to the period of the first dominantly translational mode of the two-storey system and yield displacement equal to

the sum of the original system's interstorey yield displacements. In systems with $e_s = 0$ and e_r such that the elements at one edge have 1.5 times the yield strength of the elements at the other, the associated reference system is defined as a two-storey system with a single translational degree-of-freedom per storey. The second storey of the system with irregular configuration is set back and has half the area and mass of the first storey. Moreover, the stiffness distribution is severely non-uniform in both plan and elevation. Details on this system and on its associated reference SDOF system can be found in (Bruneau and Mahin, 1987) and (Bruneau and Mahin, 1990).

Bruneau and Mahin use interstorey and roof element ductilities as response measures. It is obvious that a SDOF associated reference system can offer no predictions for the interstorey ductilities. Furthermore, the predictions for the roof ductilities are not very satisfactory. This is to be expected when attempting to predict the response of elaborate structures by means of systems as elementary as a SDOF system.

The study by *Sedarat and Bertero* (Sedarat and Bertero, 1990) involves a seven-storey reinforced concrete building with two shear walls and six moment resisting frames in the direction of the input motion. In order to reduce computational cost, inelastic dynamic analysis is performed on a simplified model of the actual structure. Inelasticity in this model is localized in the two structural walls while the six frames are considered to remain elastic. Moreover, the three frames on each half of the structure are lumped into one elastic frame with sectional properties determined by the summation of the properties of the individual frames. The in-plan distribution of the lateral-load-resisting elements is symmetric at all times and stiffness eccentricity is created by the asymmetric distribution of mass on the slabs. In this study, the strength eccentricity is defined as the distance of the CR from the geometric center of the structure. Stiffness and strength eccentricities are uniform over the height of the building and take the following values: (1) $e_s = 0.00D$, $0.05D$, and $0.25D$ and $e_r = 0.0D$, where D is the maximum dimension of the building plan, (2) $e_s = 0.05D$ and $e_r = 0.04D$, and (3) $e_s = 0.25D$ and $e_r = 0.11D$. The input consists of the N21E component of the 1952 Taft record scaled to peak accelerations of $0.18g$, $0.40g$, and $0.60g$. The different scalings are intended to account for different intensity levels. Wall displacements and inter-storey drifts, shear forces on the walls and plastic rotation at their bases are used as response measures.

Sedarat and Bertero give the following general recommendations: (1) the center of resistance should be kept as close as possible to the center of mass of the structure at

each storey, (2) the stiffness eccentricity should not be allowed to exceed 20% of the maximum plan dimension, (3) excessively large reductions of the total yield strength compared with the linear elastic strength demand should be precluded, and (4) adequate torsional redundancy should be provided by using a large number of properly allocated lateral-load-resisting elements.

Dolce and Ludovici (Dolce and Ludovici, 1992) studied a three-storey reinforced concrete building with six frames in the direction of the input motion and four frames perpendicular to it. The centers of stiffness and mass of all storeys lie on two vertical lines. The center of stiffness in each storey coincides with the geometric center of the structure, whereas the mass distribution can be asymmetric about an axis parallel to the direction of the input motion. The values of e_{sb} considered are 0.00, 0.15, and 0.30. The design forces on beams and columns are determined through three-dimensional elastic time-history analysis. The input consists of two groups of ten artificially generated motions consistent with two types of spectrum in the 1988 Eurocode and scaled to a common peak acceleration of $0.35g$. Design forces from the ten analyses are averaged and beam and column reinforcements are calculated. The minimum column reinforcement ratio is a parameter of the design with values 0.3% and 1.0%. The adequacy of the design is evaluated by inelastic time-history analysis of the structure under the same sets of motions employed in the design process. Response is measured in terms of local rotational ductilities in columns and beams, frame rotational ductilities defined as a weighted average of the local ductilities, and maximum storey rotations.

Dolce and Ludovici find the rotational ductilities in the mass-eccentric systems designed by the above described method to be comparable (not more than 30% higher) and at times even lower than the ductilities in the associated symmetric systems. They also conclude that a higher minimum column reinforcement ratio helps reduce the rotational ductilities in the eccentric systems.

The multi-storey building model used by *Duan and Chandler* (Duan and Chandler, 1993) has three frames, all in the direction of the input motion. All floors have the same mass and plan dimensions. The floor CM coincides with the geometric center and all centers of mass lie on a vertical line. The stiffness distribution is uniform in height and symmetric about the x-axis. The building is designed so that the centers of stiffness of all storeys lie also on a vertical line. Therefore, the stiffness eccentricity e_s is constant over the height of the building. Moreover, the beams are assumed to be much stiffer than the columns,

26

so that each frame is treated as a 'shear beam' for computational purposes.

The buildings considered by Duan and Chandler are 3, 5, and 8 storeys in height with fundamental uncoupled lateral periods of 0.3, 0.5, and 1.0 sec, respectively. The two shorter buildings have a fixed $e_{sb} = 0.2$ whereas for the 8-storey building $e_{sb} = 0.1, 0.2$, and 0.3. The base shear is calculated from the Newmark-Hall inelastic design spectrum with a strength reduction factor $R = 4$. The vertical and horizontal distributions of the base shear are obtained according to the static force procedures in several codes, as well as by elastic modal analysis, a method suggested by all but one of the codes considered. Accidental torsion is omitted in design. The input consists of the S00E component of the 1940 El Centro record and a record from the 1971 San Fernando earthquake, representing records with strong acceleration pulses. Both records are scaled to PGA = 0.3g. Inelastic action is concentrated at hinges at the ends of beams and columns and the moment-curvature relationship is taken as bilinear. Axial force-moment interaction in columns is neglected.

Duan and Chandler evaluate the code provisions by comparing the storey ductilities of the edge element closest to the CS in the asymmetric system to those of the same element in the torsion-free associated reference system. Excessive additional ductilities due to torsion are considered undesirable. Static force procedures that either preclude or limit the reduction in the design load for this element below the level calculated for the symmetric system tend to avoid this problem. Duan and Chandler conclude that the modal analysis method may be unconservative especially when used for the design of highly asymmetric systems excited well into the inelastic range. They also find that the ductilities in the upper storeys increase significantly with the fundamental uncoupled lateral period and with the stiffness eccentricity. However, based on their results, the increase in ductilities can be controlled by the application of a concentrated force at the top of the building. They recommend the use of this force for all buildings and not just long-period ones, as suggested by, for instance, the 1988 Eurocode and the 1987 Mexico City code.

2.3 Conclusions

One-storey systems. The inelastic torsional response of one-storey systems has been studied quite extensively. Based on the reviewed studies, a number of conclusions can be drawn. These conclusions are subject to the limitations of the system and the input motions considered.

- A significant increase in displacements due to torsion is to be expected. Factors of up to 2 or 3 over the displacements of the associated symmetric reference systems were calculated. Therefore, adequate separation between buildings should be provided to avoid pounding effects.

- Elastically symmetric systems can sustain significant torsional effects in the inelastic range due to the presence of strength eccentricity or to differences in the post-yield hysteretic behavior of the lateral-load-resisting elements.

- There is no consensus on the appropriate value of strength eccentricity in order to limit torsional effects. Most investigators conclude that it should be kept as close to zero as possible, but some, (Escobar and Ayala, 1991), recommend a value similar to that of the stiffness eccentricity. As pointed out in (Tso and Ying, 1992), the appropriate value is very much system dependent.

- The increase in the displacement of the edge of the structure furthest away from the center of stiffness can lead to significant increase in the ductility demand for the element at this edge. This can be avoided if the yield strength and consequently the yield displacement of this element is increased.

- The studies focusing on the evaluation of the torsional provisions in different codes show that the significant reduction in the yield strength of the edge element closest to the center of stiffness below its value in the associated symmetric system, allowed by many codes, can result in increased ductility demand for this element, compared with its ductility demand in the associated symmetric system.

- In reference to the two previous items, all considered codes provide adequate increase in the yield strength of the edge element furthest away from the center of stiffness, for the ductility of this element not to exceed the ductility of the associated symmetric system. However, only the Canadian code limits the reduction in the yield strength of the edge element closest to the center of stiffness, resulting in ductility for this element not much higher than than of the associated symmetric system. The superiority of the Canadian code in this aspect is stressed in all comparative studies.

Multi-storey systems. The limited number of available studies and the study-specific nature of the systems considered do not allow for general conclusions to be drawn.

SECTION 3

ONE-STOREY SYSTEMS

Uncertainty in Earthquake Engineering has two sources: the input motion and the mathematical model of the structural system. The mathematical model includes the functional form of the restoring force model of the lateral-load-resisting elements and the parameters of this model.

This study focuses on the effects of system uncertainty in seismic design. Therefore, the input is deterministic and consists of three ground acceleration records. Since it is impossible to consider all restoring force models, a set of two commonly used models, the elastoplastic and the modified-Clough, is selected. Of the model parameters, the yield strength is treated as a random variable. Because of limited statistics, any physically admissible probabilistic model can be used for the yield strength. The lognormal distribution selected for this study is physically admissible, since it precludes unrealistic negative strength values.

The elastoplastic model is very popular because of its simplicity. However, it is not particularly realistic since it fails to account for stiffness and/or strength degradation. The modified-Clough model does account for stiffness degradation at the expense of somewhat increased complexity. A question addressed by the present study is whether the use of the elastoplastic model instead of the modified-Clough is conservative.

Uncertainty in the element yield strengths can introduce torsional vibrations to a nominally symmetric system. Such a system is symmetric in the elastic range but can become asymmetric following yield. The effects on seismic response of torsional vibrations caused by strength uncertainty are also investigated in this study.

3.1 Structural model

The structural model considered, shown in Figure 3-1, consists of a rigid rectangular slab supported by two lateral-load-resisting elements. The lateral-load-resisting elements, also referred to as 'elements' for brevity, are aligned with the input motion, which is acting in the y-direction. The mass of the slab is assumed to be uniformly distributed so that the structure does not have an eccentric mass. That places the center of mass at mid-distance between the two elements.
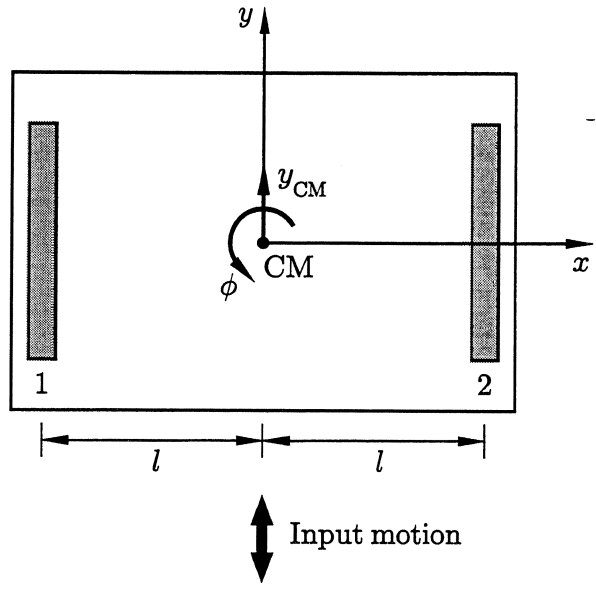
FIGURE 3-1 Structural model.

3.1.1 Restoring force models

The two lateral-load-resisting elements in Figure 3-1 follow the same restoring force model. The two models selected for this study, the elastoplastic and the modified-Clough, are shown in Figure 3-2. The elastoplastic model is attractively simple but cannot reflect stiffness and strength degradation. It is defined by only two parameters, the elastic stiffness k, and the yield strength f_y.

Elastoplastic model

Modified-Clough model
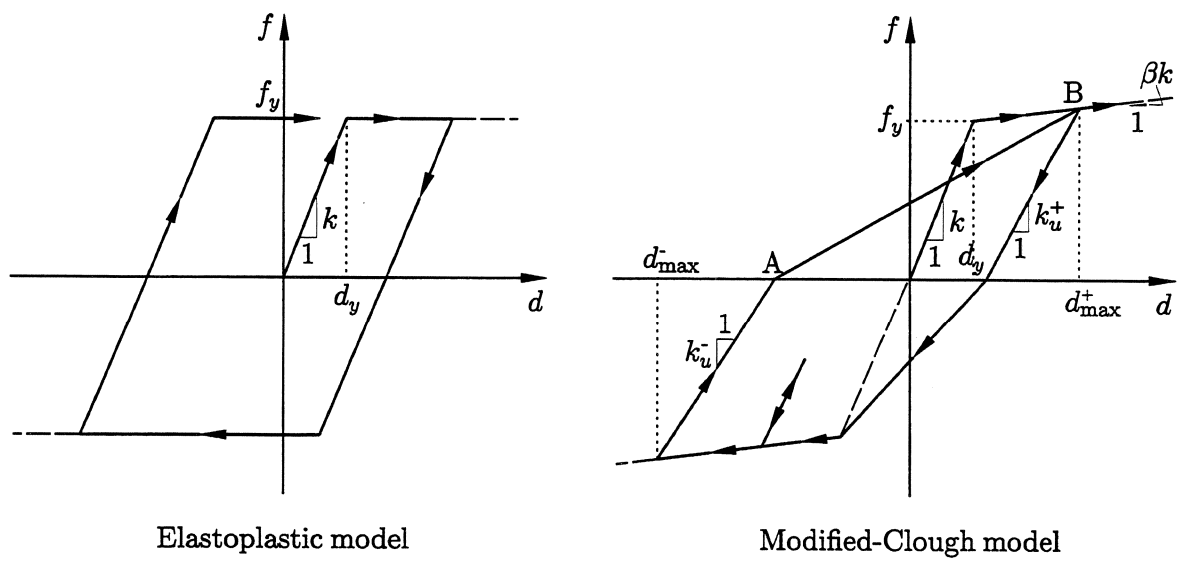
FIGURE 3-2 Restoring force models.

30

The modified-Clough is a more realistic model that can account for the stiffness degradation caused by repeated stress cycles. Moreover, the model is rather simple relative to, for example, the Takeda and other models. The modified-Clough model is based on a bilinear backbone curve and depends on four parameters (Otani, 1981). The backbone curve is defined by the elastic stiffness, the yield strength, and the ratio of post-yield stiffness to elastic stiffness β. Unloading after yield takes place according to stiffnesses

$$k_u^+ = k \left(\frac{d_y}{|d_{\max}^+|} \right)^\alpha \quad \text{and} \quad k_u^- = k \left(\frac{d_y}{|d_{\max}^-|} \right)^\alpha \qquad (3\text{-}1)$$

where k_u^+ and k_u^- are the unloading stiffnesses in the positive and negative restoring force regions, $d_{\max}^+$ and $d_{\max}^-$ are the maximum displacements attained in the same regions, d_y is the yield displacement, and α denotes the unloading stiffness degradation parameter. If the value of α is chosen to be zero there is no stiffness degradation during unloading so that $k_u^+ = k_u^- = k$. After the restoring force reverses sign the model follows the path defined by the line connecting the zero force point (e.g. point A in Figure 3-2) with the maximum yield excursion on the side entered after the reversal (point B). In this study both α and β are taken equal to zero. To have meaningful comparisons of the elastoplastic and the modified-Clough models the same values of parameters k and f_y are employed.

3.1.2 Random parameters of restoring force model

The elastic stiffnesses of the two resisting elements in Figure 3-1 are assumed to be deterministic and identical, $k_1 = k_2 = k$. The element yield strengths are the random variables F_{yi}, $i = 1, 2$, with means μ_i, variances σ_i^2, and correlation coefficient ρ. The vector $\boldsymbol{F}_y$ is modeled by a bivariate lognormal distribution with density function

$$f_{F_{y1},F_{y2}}(f_{y1}, f_{y2}) = \frac{1}{2\pi\tilde{\sigma}_1\tilde{\sigma}_2 f_{y1} f_{y2} (1 - \tilde{\rho}^2)^{1/2}}$$

$$\times \exp\left\{ -\frac{[(\tilde{f}_{y1} - \tilde{\mu}_1)/\tilde{\sigma}_1]^2 - 2\tilde{\rho}(\tilde{f}_{y1} - \tilde{\mu}_1)(\tilde{f}_{y2} - \tilde{\mu}_2)/(\tilde{\sigma}_1\tilde{\sigma}_2) + [(\tilde{f}_{y2} - \tilde{\mu}_2)/\tilde{\sigma}_2]^2}{2(1 - \tilde{\rho}^2)} \right\} \quad (3\text{-}2)$$

where $f_{yi} > 0$, $\tilde{f}_{yi} = \ln(f_{yi})$, and

$$\begin{bmatrix} \tilde{f}_{y1} \\ \tilde{f}_{y2} \end{bmatrix} \sim N\left(\begin{bmatrix} \tilde{\mu}_1 \\ \tilde{\mu}_2 \end{bmatrix}, \begin{bmatrix} \tilde{\sigma}_1^2 & \tilde{\rho}\tilde{\sigma}_1\tilde{\sigma}_2 \\ \tilde{\rho}\tilde{\sigma}_1\tilde{\sigma}_2 & \tilde{\sigma}_2^2 \end{bmatrix} \right). \qquad (3\text{-}3)$$

Let $\alpha_i = \sigma_i/\mu_i$. The relationships between the parameters of the lognormal distribution and those of the associated normal distribution are

$$\tilde{\mu}_i = \ln \frac{\mu_i}{\sqrt{1 + \alpha_i^2}} \qquad (3\text{-}4)$$

$$\tilde{\sigma}_i^2 = \ln(1 + \alpha_i^2) \tag{3-5}$$

$$\tilde{\rho} = \frac{\ln(1 + \rho\alpha_1\alpha_2)}{\tilde{\sigma}_1\tilde{\sigma}_2} \tag{3-6}$$

Two extreme levels of dependence between element yield strengths are considered: perfect correlation ($\rho = 1$) and independence ($\rho = 0$). If $\rho = 1$ the element yield strengths are identical and all realizations of the structure are symmetric in the inelastic as well as in the elastic range. On the other hand, if $\rho \neq 1$ the yield strengths of the two elements are usually different. In this case, the system is symmetric in the elastic range but becomes asymmetric following the first yield.

3.1.3 Equations of motion

The structure in Figure 3-1 has one axis of symmetry, denoted by x, while the input motion is aligned with the y-axis. Consequently, only two of the three degrees-of-freedom of the system are active: translation in the y-direction of the center of mass Y_{CM} and rotation about the center of mass Φ. The equations of motion relative to the center of mass (CM) are

$$\begin{aligned} m\,\ddot{Y}_{CM} + 2c\,\dot{Y}_{CM} + (F_1 + F_2) &= -m\ddot{y}_g \\ mr^2\ddot{\Phi} + 2cl^2\dot{\Phi} + (F_2 - F_1)l &= 0 \end{aligned} \tag{3-7}$$

where m = mass of the system, r = radius of gyration about the center of mass, c = element damping coefficient, assumed the same for both elements, l = distance of each element from the center of mass, F_i = restoring force from element i, $i = 1, 2$, and $\ddot{y}_g$ = ground acceleration acting in the y-direction.

When the element yield strengths are perfectly correlated ($\rho = 1$), $F_1 = F_2$ at all times and only the translational degree of freedom is active so that $\Phi(t) \equiv 0$, $t \geq 0$, and the second equation in (3-7) is satisfied identically.

3.2 Input motions

Three earthquake records from California are considered: (1) the S00E component of the El Centro record from the 1940 Imperial Valley earthquake (Figure 3-3(a)), (2) the N21E component of the Taft Lincoln School Tunnel record from the 1952 Kern county earthquake (Figure 3-4(a)), and (3) the N65E component of the Cholame Shandon record from the 1966 Parkfield earthquake (Figure 3-5(a)). The three input motions are referred to as 'El Centro', 'Taft', and 'Parkfield', respectively.
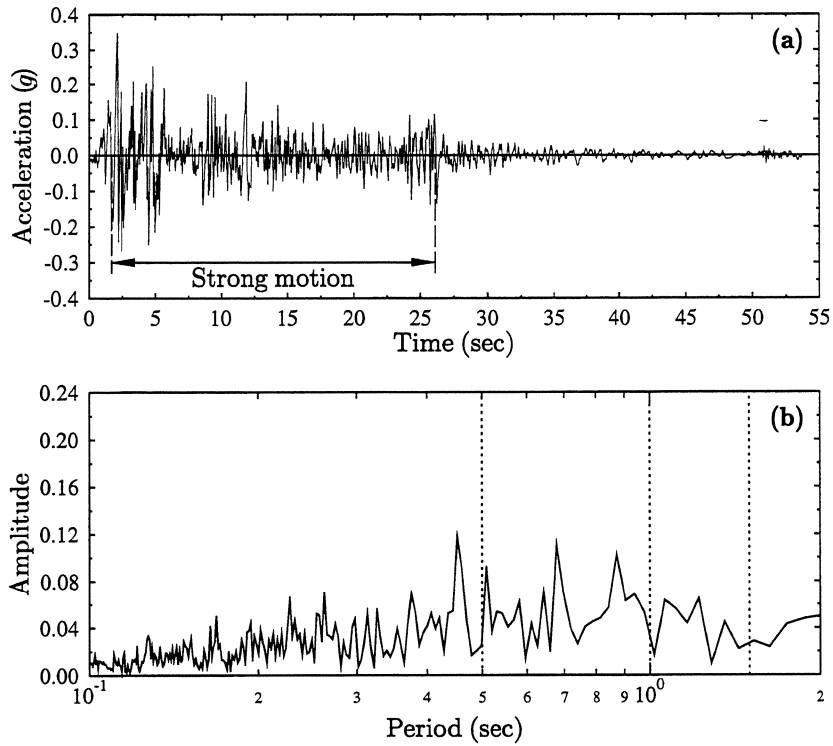
FIGURE 3-3 El Centro 1940, S00E component: (a) accelerogram and (b) Fourier transform of the strong motion portion.
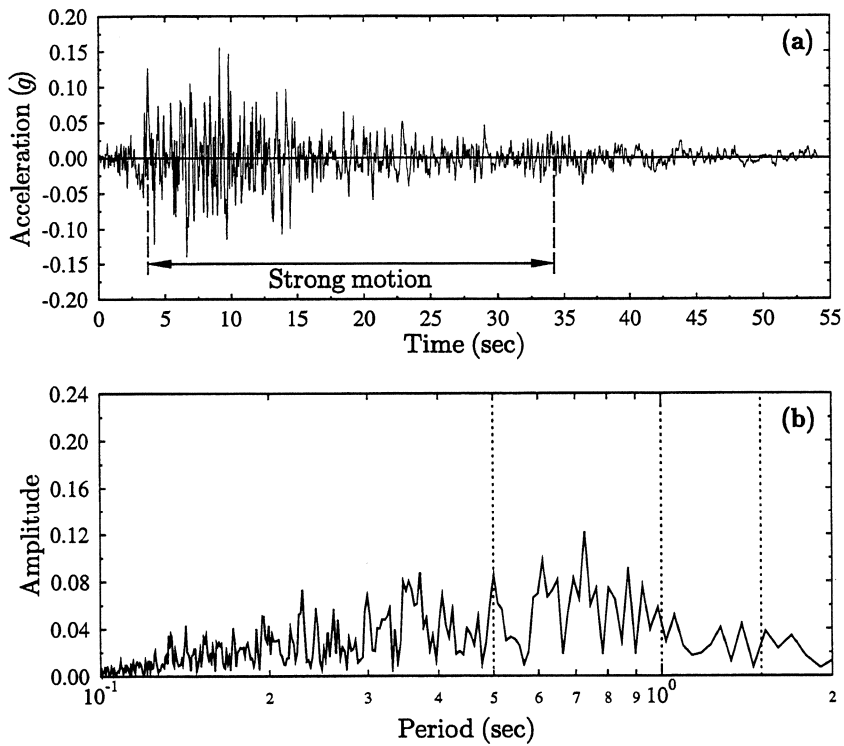
FIGURE 3-4 Taft 1952, N21E component: (a) accelerogram and (b) Fourier transform of the strong motion portion.
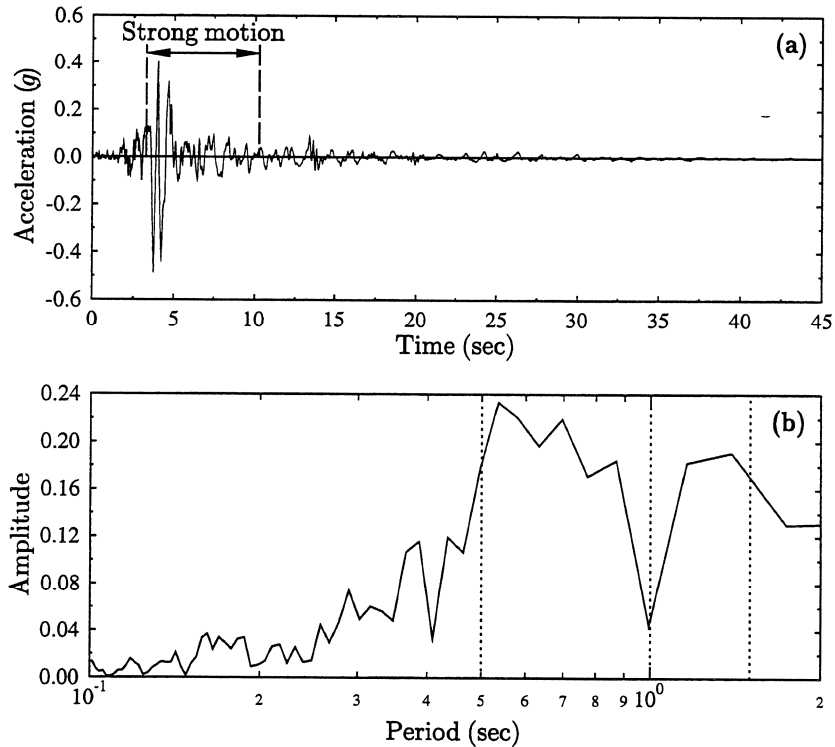
FIGURE 3-5 **Parkfield 1966, N65E component:** (a) **accelerogram and** (b) **Fourier transform of the strong motion portion.**

The El Centro record is the most widely used in earthquake response studies. El Centro and Taft belong in a category of ground motions characterized by irregular accelerograms and fairly uniform energy content over a wide band of frequencies, as indicated by the Fourier transforms in Figures 3-3(b) and 3-4(b). Parkfield is selected to represent a different type of ground motion with few pronounced acceleration pulses. Its Fourier transform, shown in Figure 3-5(b), is markedly different from those of the other two motions.

The actual input used in this study is the strong motion portion of the three records, as marked in Figures 3-3(a)–3-5(a). This portion corresponds to the strong motion duration defined as 'the time interval during which the central 90% of the contribution to the integral of the square of the acceleration takes place' (Trifunac and Brady, 1975). Therefore, in the context of this study, motion duration is in effect the strong motion duration.

To investigate the effect of the intensity of the input motion on the seismic response, the accelerograms are scaled to Peak Ground Accelerations (PGA) of $0.2g$–$0.6g$ with step $0.1g$, and $1.0g$.

3.3 System design, response measures, and Monte Carlo simulation

System design. The mass of the system in Figure 3-1 and the distance of each of the two elements from the center of mass, l, are set equal to one. The small-vibration lateral period in the direction of the ground motion is $T = 2\pi\sqrt{m/(2k)}$ and it will be called simply 'period', for brevity. Three periods are considered: 0.5 sec, 1.0 sec, and 1.5 sec. These periods are marked with dotted lines in the Fourier transform graphs of the input motions (Figures 3-3(b)–3-5(b)). The damping coefficient varies with the period and is calculated from the expression $c = 2\pi\zeta m/T$, assuming a value of ζ equal to 5%.

The dimensionless parameter $\gamma = l/r$ is used to characterize the radius of gyration r. Since m and l are fixed, r and the mass moment of inertia mr^2 decrease with γ. When torsion is initiated following the first yield, a reduced mass moment of inertia provides less resistance and allows larger rotations to develop. Therefore, a structure with large γ is expected to be more susceptible to torsion. The values of γ considered are 0.5, 1.0 and 1.5. Of those, $\gamma = 0.5$ results in a somewhat unrealistic plan dimension in the direction of the ground motion.

The design yield strengths of the lateral-load-resisting elements have been determined using the static force procedure in the 1994 version of the Uniform Building Code (UBC, 1994). According to the UBC, the required yield strength of the system must exceed the base shear force

$$V = \frac{Z\,I\,C}{R_w}\,W \tag{3-8}$$

in which Z, I, and R_w are zone, importance, and structural system factors, W is the seismic dead load of the system, and

$$C = \frac{1.25\,S}{T^{2/3}}\,, \quad C \le 2.75 \tag{3-9}$$

where S is the site coefficient for soil characteristics. The following values are selected: $Z = 0.40$ corresponding to Zone 4, $I = 1.0$ for standard occupancy, $S = 1.5$ corresponding to soil profile S_3 (suggested by the code for use 'in locations where the soil properties are not known in sufficient detail'), and $R_w = 8$, appropriate for building frame systems with concrete shear walls. The design yield strength of element i, $i = 1, 2$ can be calculated from

$$f_{yi,c} = V\left(\frac{k}{2k} + e_a(2l)\frac{kl}{2kl^2}\right) = V(0.5 + e_a) \tag{3-10}$$

35

where e_a is the accidental eccentricity as a percentage of the building dimension perpendicular to the direction of the static force. The value of e_a required by the UBC for nonflexible diaphragms is 5%. Therefore, the element design yield strength is $f_{yi,c} = 0.55V$. The structure has to be designed for this capacity. The uncertainty in the yield strength is represented by a perturbation about the design yield strength. The mean of F_{yi}, $i = 1, 2$, is set equal to $f_{yi,c}$ and a coefficient of variation (COV) of 15% is selected. Typical suggested coefficients of variation for the strength of reinforced concrete members range from 11% to 17% (Ellingwood et al., 1980).

For every system an associated reference system can be defined. The associated reference system has the same characteristics as the system under consideration except for the yield strengths of the resisting elements that are equal to the design yield strength $f_{yi,c}$. Therefore, the reference system constitutes the system obtained by applying the UBC provisions. It is a single-degree-of-freedom (SDOF) system that vibrates along the y-direction when subjected to an input motion in the same direction.

Response measures. The evaluation of the response of the system in Figure 3-1 is based on the following measures:

- maximum displacement $Y_{\max} = \max\{Y_{\max,i}\}$, $i = 1, 2$, where $Y_{\max,i}$ is the absolute maximum displacement of element i,

- maximum ductility $M_{\max} = \max\{M_i\}$, $i = 1, 2$, where M_i is defined as the ratio of the absolute maximum displacement to the yield displacement of element i,

- dissipated energy E_{dis}, calculated as the total area within the hysteretic loops of both elements,

- maximum rotation about center of mass $\Phi_{\max} = \max\{|\Phi(t)|\}$,

- dynamic eccentricity $\Theta(t) = \dfrac{mr^2 \ddot{\Phi}(t)}{V(2l)}$, where $\ddot{\Phi}(t)$ is the torsional acceleration, m is the mass of the system, r is the radius of gyration, V is the design base shear, and $2l$ is the system dimension perpendicular to the ground motion,

- maximum dynamic eccentricity $\Theta_{\max} = \max\{|\Theta(t)|\}$,

- $Z =$ total time of $|\Theta(t)|$ above e_a, given as percentage of the motion duration, and

- upcrossing rate N, which is equal to the number of times during the motion $|\Theta(t)|$ upcrosses level e_a, divided by the motion duration.

Of the response measures considered, the dynamic eccentricity is a random process, whereas all other measures are random variables.

Monte Carlo simulation. The one-storey system shown in Figure 3-1 is designed according to the UBC provisions as described in the first part of this section. Two restoring force models, the elastoplastic and the modified-Clough are considered (Section 3.1.1). The element yield strengths are assumed to be random variables following lognormal distributions (Section 3.1.2). The input motion is deterministic consisting of the strong motion portion of the El Centro, Taft, and Parkfield records scaled to several peak ground accelerations (Section 3.2).

In summary, the present study involves two restoring force models (elastoplastic and modified-Clough), three periods per model ($T = 0.5$, 1.0, and 1.5 sec), two correlation coefficients per period ($\rho = 1$ and 0), and, for $\rho = 0$, three values of the dimensionless radius of gyration ($\gamma = 0.5$, 1.0, and 1.5). For each of the resulting systems, 24 in all, 1000 realizations of the yield strength vector $\boldsymbol{F}_y$ are generated. A complete time-history analysis is performed for each combination of system realization and input motion. The equations of motion in (3-7) are integrated numerically by means of the central difference method, using a computer code developed for this project. Finally, the realizations of the response measures, listed earlier in this section, are analysed statistically.

3.4 Numerical results

The maximum displacement $Y_{\max}$, maximum ductility $M_{\max}$, dissipated energy E_{dis}, and maximum rotation $\Phi_{\max}$ are used to evaluate the sensitivity of the structural performance to the uncertainty in the restoring force model. The sensitivity analysis accounts for two aspects of the uncertainty:

(1) parameter uncertainty for specified restoring force model. Parameter uncertainty involves the randomness of the element yield strengths as well as uncertainty in the level of correlation between them expressed by the correlation coefficient ρ. Results for the elastoplastic model (EP) and the modified-Clough model (MC) are presented in Sections 3.4.1 and 3.4.2, respectively.

(2) model uncertainty for specified level of correlation between element yield strengths. Results for perfectly correlated yield strengths ($\rho = 1$) and independent identically distributed yield strengths ($\rho = 0$) are presented in Sections 3.4.3 and 3.4.4, respectively.

3.4.1 Parameter uncertainty. Elastoplastic model

The structure is symmetric in strength as well as in stiffness and behaves as a single-degree-of-freedom system when the element yield strengths are perfectly correlated ($\rho = 1$). When the yield strengths are independent ($\rho = 0$), the asymmetry in strength causes torsional vibrations after the yield of the weaker of the two elements.

Maximum displacement. Figures 3-6, 3-7, and 3-8 show plots of the mean and the coefficient of variation (COV) of the maximum displacement Y_{max} for all combinations of structural parameters, PGA in the range $0.2g$–$0.6g$, and input the El Centro, Taft, and Parkfield records, respectively. The mean of the maximum displacement Y_{max} increases monotonically with PGA and period T. Torsional vibrations caused by uncertainty generally increase the mean of Y_{max}. This effect is amplified as γ increases for El Centro and Parkfield, whereas for Taft the amount of the increase shows no clear dependence on the value of γ.

Under El Centro and Taft, the COV of Y_{max} as well as its variability with PGA tend to decrease with T. Although the highest values of the COV are 30.3% and 29.8% for El Centro and Taft, respectively, in most cases it does not exceed 20%. Very different trends are observed for the COV of Y_{max} under Parkfield. Specifically, it appears insensitive to period, especially for higher PGA values, consistently decreases with PGA for PGA $> 0.3g$, and decreases in the presence of torsion for $\gamma = 0.5$ and 1.0. The highest COV calculated is 15.6% which is about equal to the COV of the element yield strengths.

To facilitate comparison between motions Figure 3-9 includes plots of the mean and the COV of Y_{max} for the symmetric system ($\rho = 1$) and all three motions considered. The maximum displacement is on the average largest for the Parkfield record. This can be attributed to the fact that the structural periods considered are located in high energy areas of the Fourier transform of this record (see Figure 3-5). There is essentially no difference in the mean of Y_{max} between El Centro and Taft for $T = 0.5$ sec, but the difference increases considerably with the period.
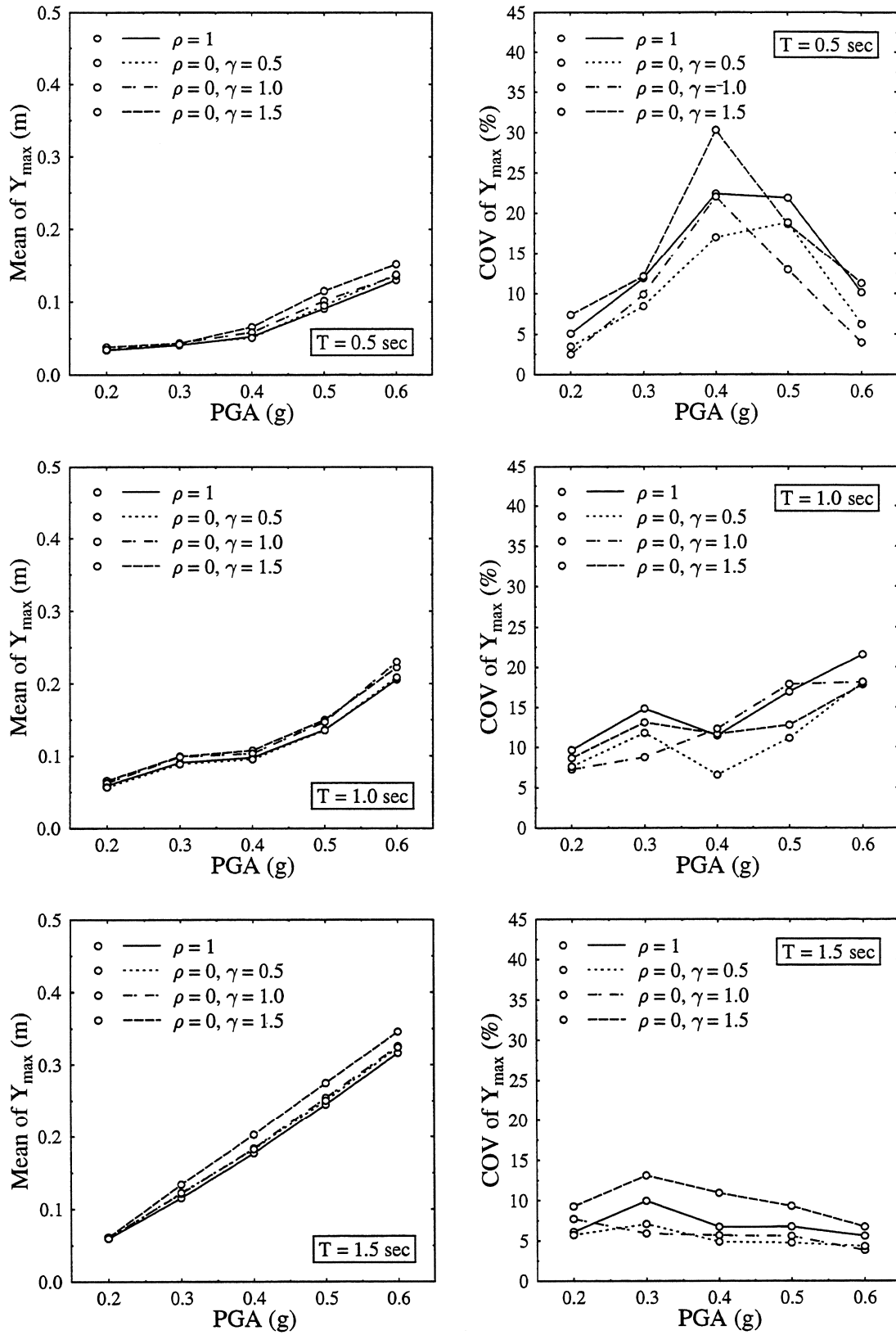
FIGURE 3-6 Mean and COV of $Y_{\max}$. EP model. Input: El Centro.
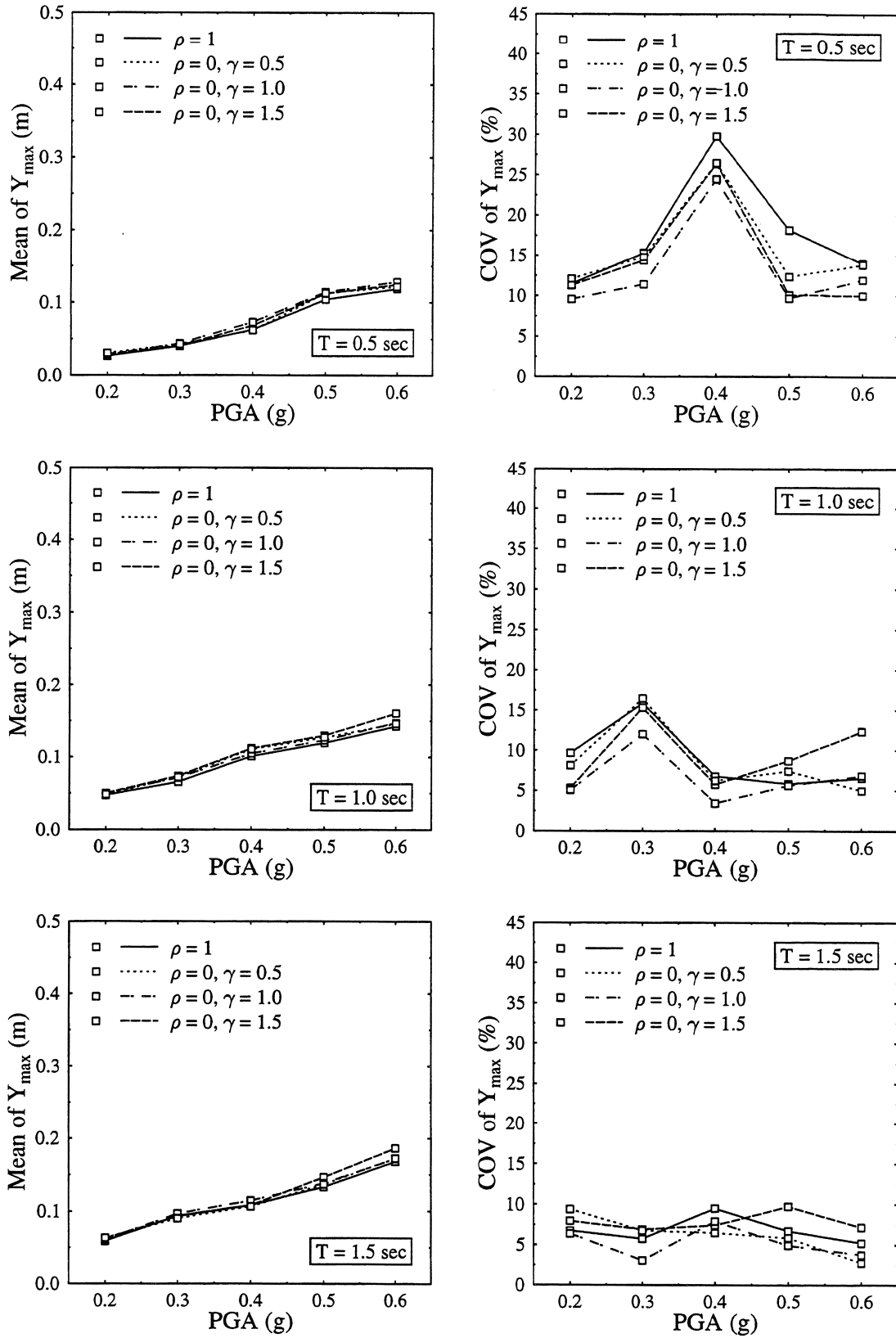
FIGURE 3-7 Mean and COV of $Y_{\max}$. EP model. Input: Taft.

40
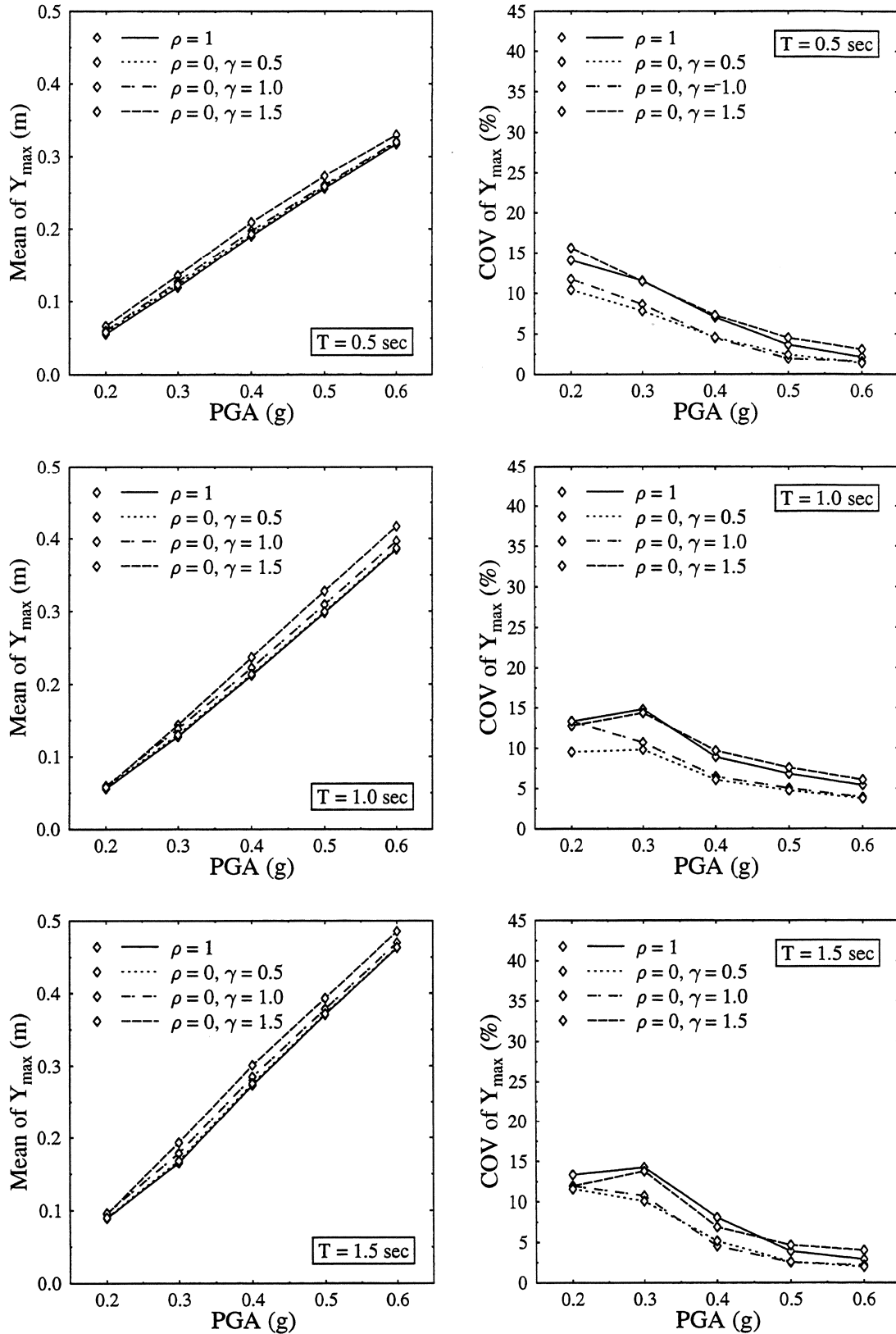
FIGURE 3-8 Mean and COV of $Y_{\max}$. EP model. Input: Parkfield.
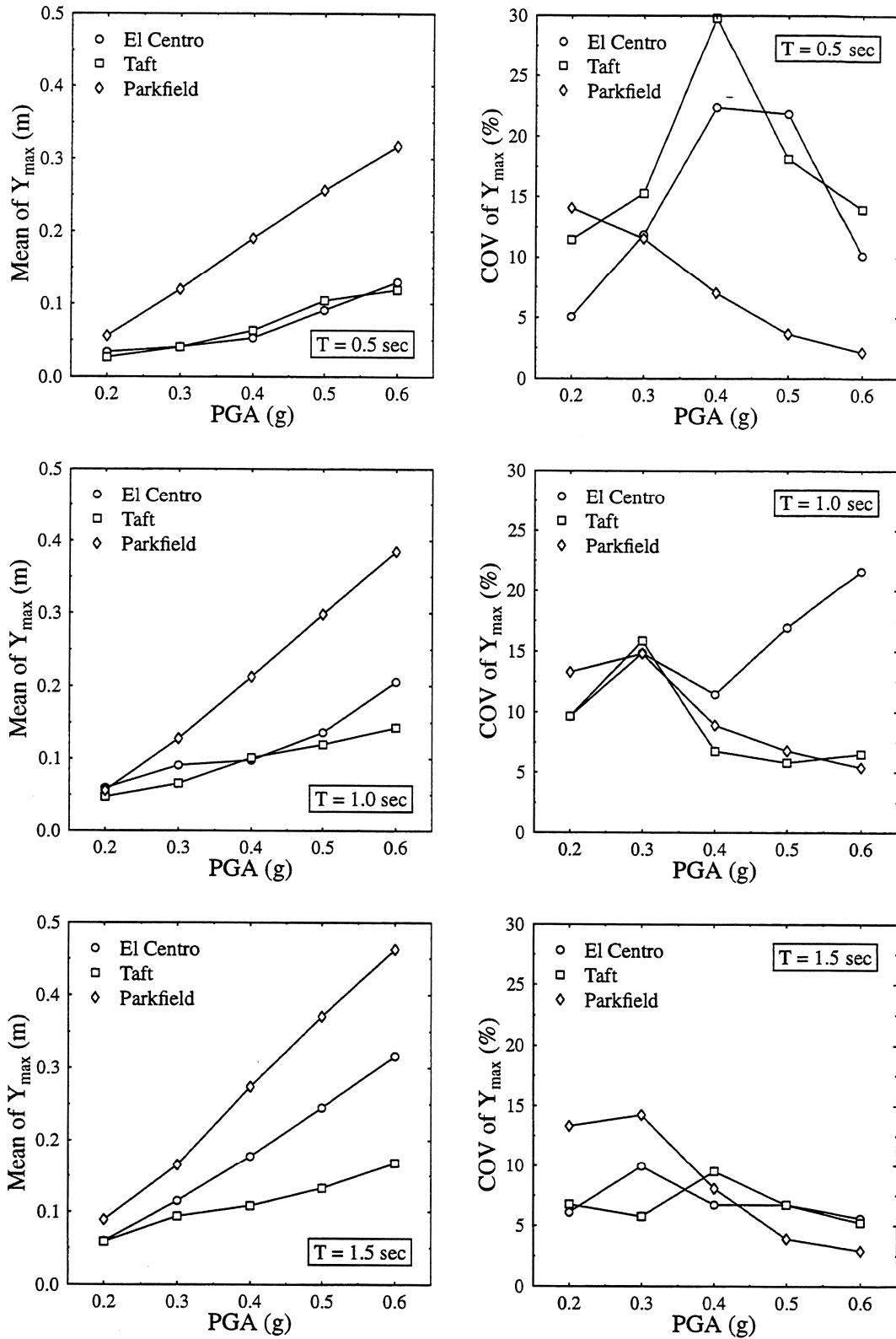
FIGURE 3-9 **Mean and COV of** Y_{max} **for perfectly correlated yield strengths. EP model.**

The plots in Figure 3-10 illustrate the effect of torsion on the mean and the COV of $Y_{\max}$ for the three input motions. The quantity $p(Y_{\max})$ is defined as the ratio of the mean of $Y_{\max}$ for $\rho = 0$ and $\gamma = 1.5$ to the mean of $Y_{\max}$ for $\rho = 1$. The quantity $q(Y_{\max})$ is the respective ratio of the coefficients of variation. In most cases an increase in the mean of the order of 10% to 20% is observed whereas the effect on the COV is rather erratic with the ratio $q(Y_{\max})$ mostly between 0.75 and 1.5.

The probability that a response measure X exceeds a level x, $P(X > x)$, is estimated as the percentage of samples with response larger than x. Figures 3-11, 3-12, and 3-13 include plots of the probability $P(Y_{\max} > y_{\max,0})$ as well as of the mean of the ratio $Y_{\max}/y_{\max,0}$ for the El Centro, Taft, and Parkfield records, respectively. The level $y_{\max,0}$ represents the maximum displacement of the associated reference system. Both the probability of exceedence and the mean ratio exhibit very different trends for the two types of ground motion. For El Centro and Taft the probability $P(Y_{\max} > y_{\max,0})$ varies widely with PGA and period. Both the probability of exceedence and the mean ratio generally increase in the presence of torsion with the exceptions mostly associated with $\gamma = 0.5$. However, the increase is not monotonic with γ. The variability of the mean ratio with the PGA decreases with the period. On the other hand, for Parkfield the probability of exceedence of $y_{\max,0}$ is rather insensitive to both PGA and period, and consistently takes values above 50%. Both the probability and the ratio increase monotonically with γ for PGA $\geq 0.3g$. The variability of the mean of $Y_{\max}/y_{\max,0}$ with PGA is not significant for all periods considered and its values tend closer to unity with increasing PGA.

Figures 3-14, 3-15, and 3-16 include plots, for El Centro, Taft, and Parkfield, respectively, of the probability that $Y_{\max}$ exceeds a level y^* equal to the statistical mean plus one standard deviation of the maximum displacement of the symmetric system ($\rho = 1$) for given period and PGA. For the symmetric system the response of less than 25% of the samples exceeds y^*. In the presence of torsion the probability of exceedence increases for $\gamma \geq 1.0$. Specifically, for $\gamma = 1.0$ it takes values mostly in the range of 20 to 40%, whereas for $\gamma = 1.5$ it exhibits much larger variability with values in most cases above 40% and as high as 60%–70% for several parameter combinations. In contrast, there is no clear trend for the effect of torsion on $P(Y_{\max} > y^*)$ when $\gamma = 0.5$. Under Parkfield the probability of exceedence for this value of γ generally decreases relative to that of the symmetric system but under El Centro and Taft both outcomes are observed for different parameter combinations.
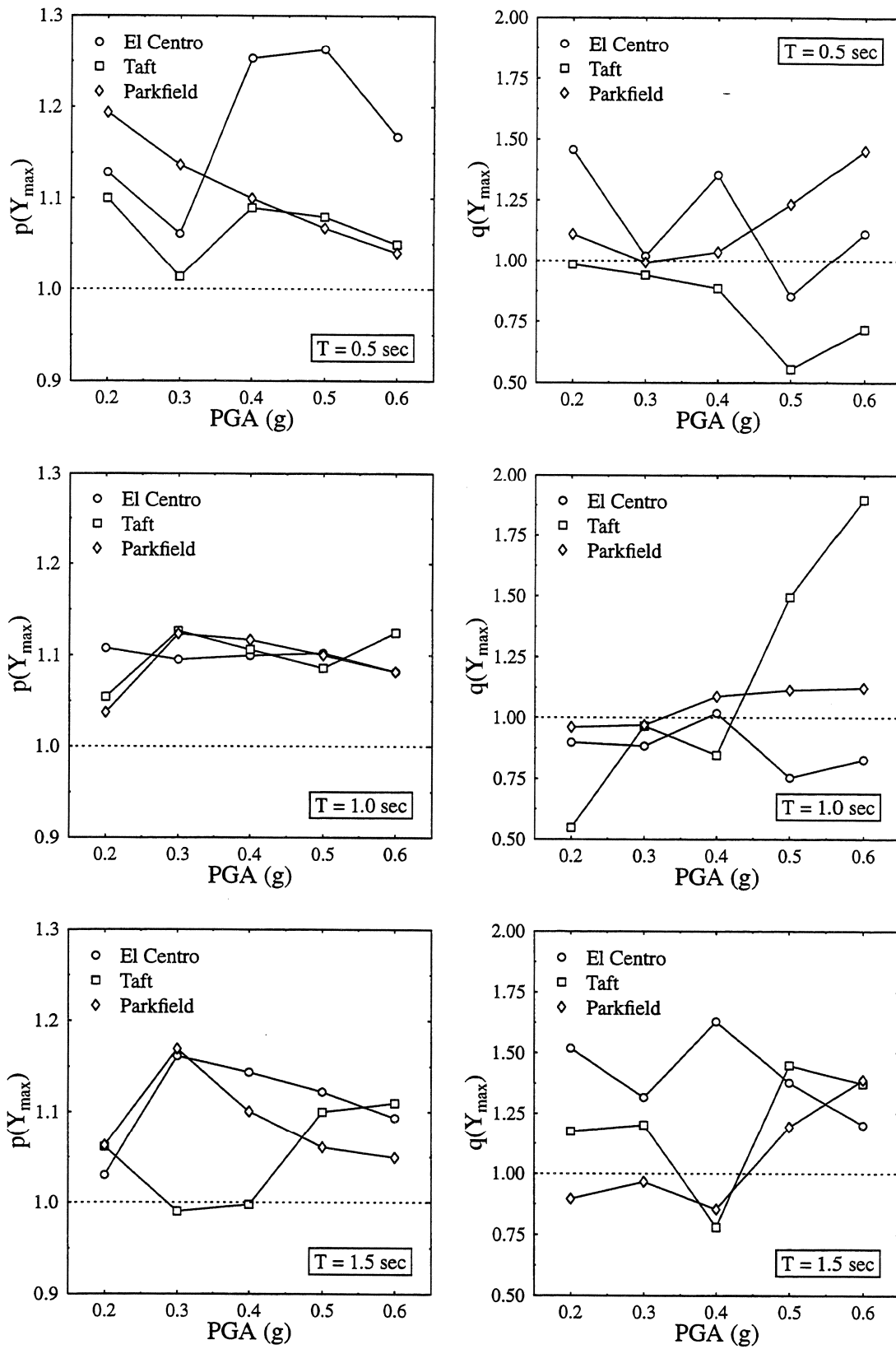
FIGURE 3-10 Ratios of mean and COV of Y_{max}. EP model.
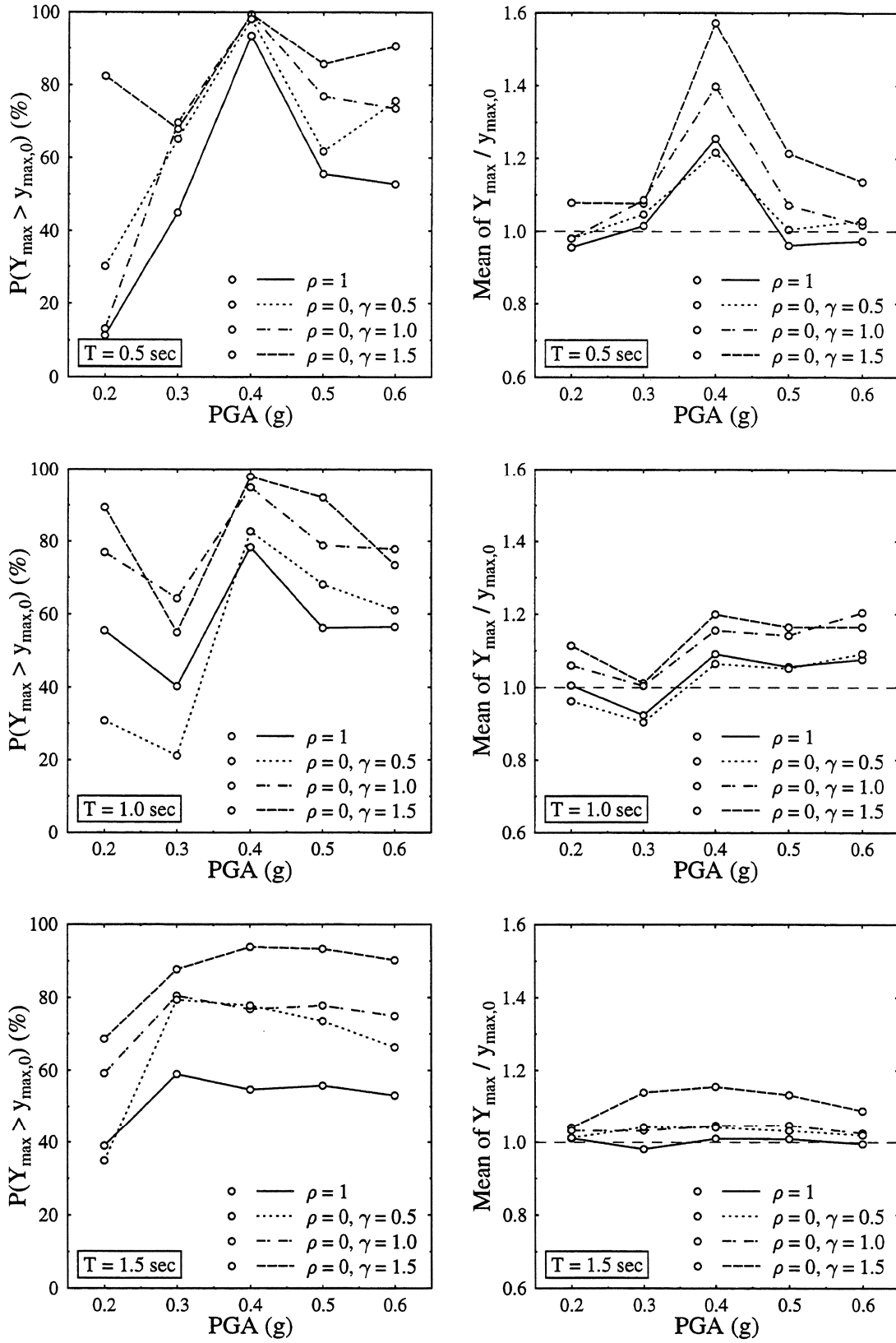
FIGURE 3-11 Comparison of Y_{max} and $y_{max,0}$. EP model. Input: El Centro.
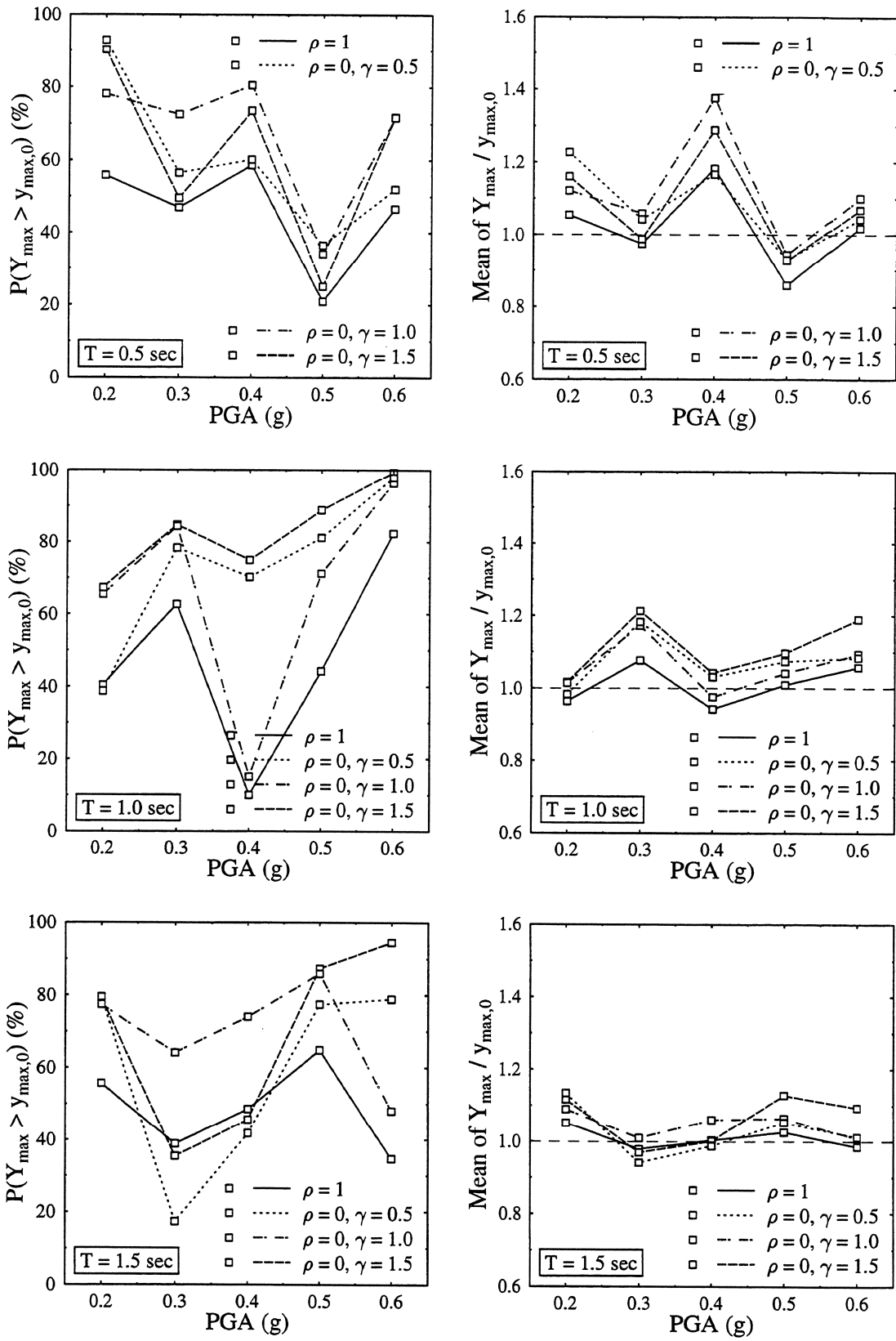
FIGURE 3-12 Comparison of Y_{max} and $y_{max,0}$. EP model. Input: Taft.
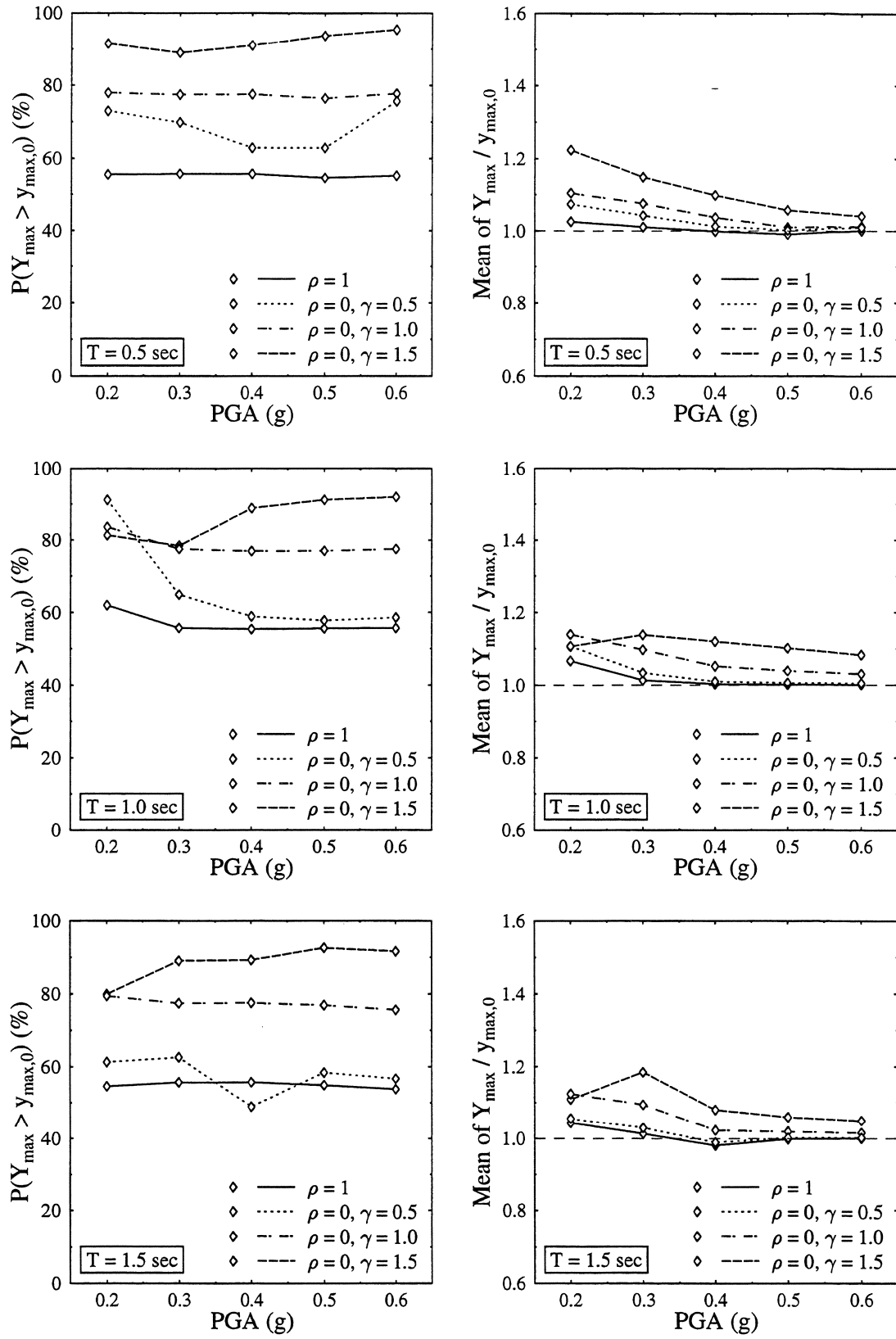
FIGURE 3-13 Comparison of Y_{max} and $y_{max,0}$. EP model. Input: Parkfield.
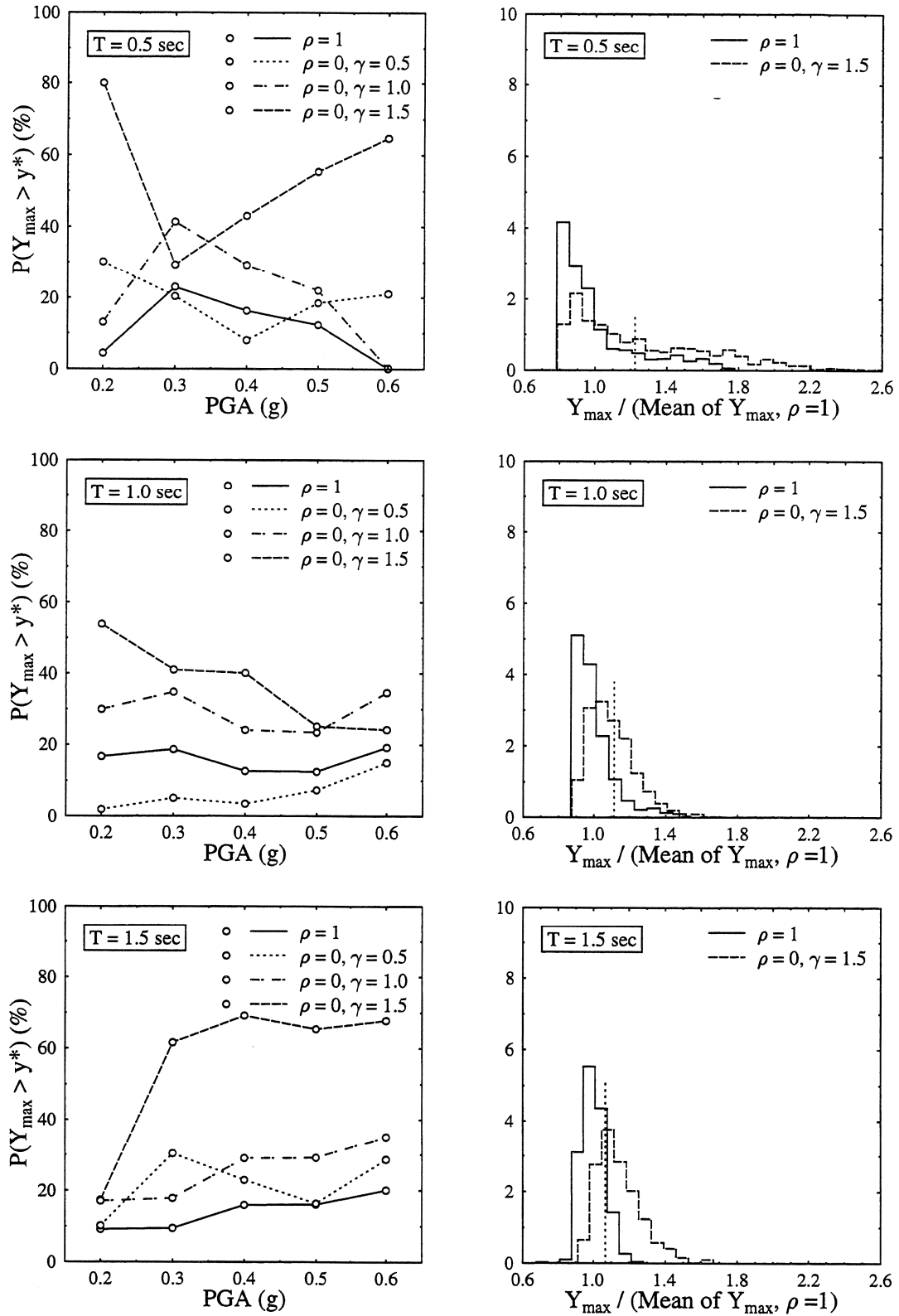
FIGURE 3-14 Probability of exceedence of level y^* and histograms of normalized maximum displacement. EP model. Input: El Centro.
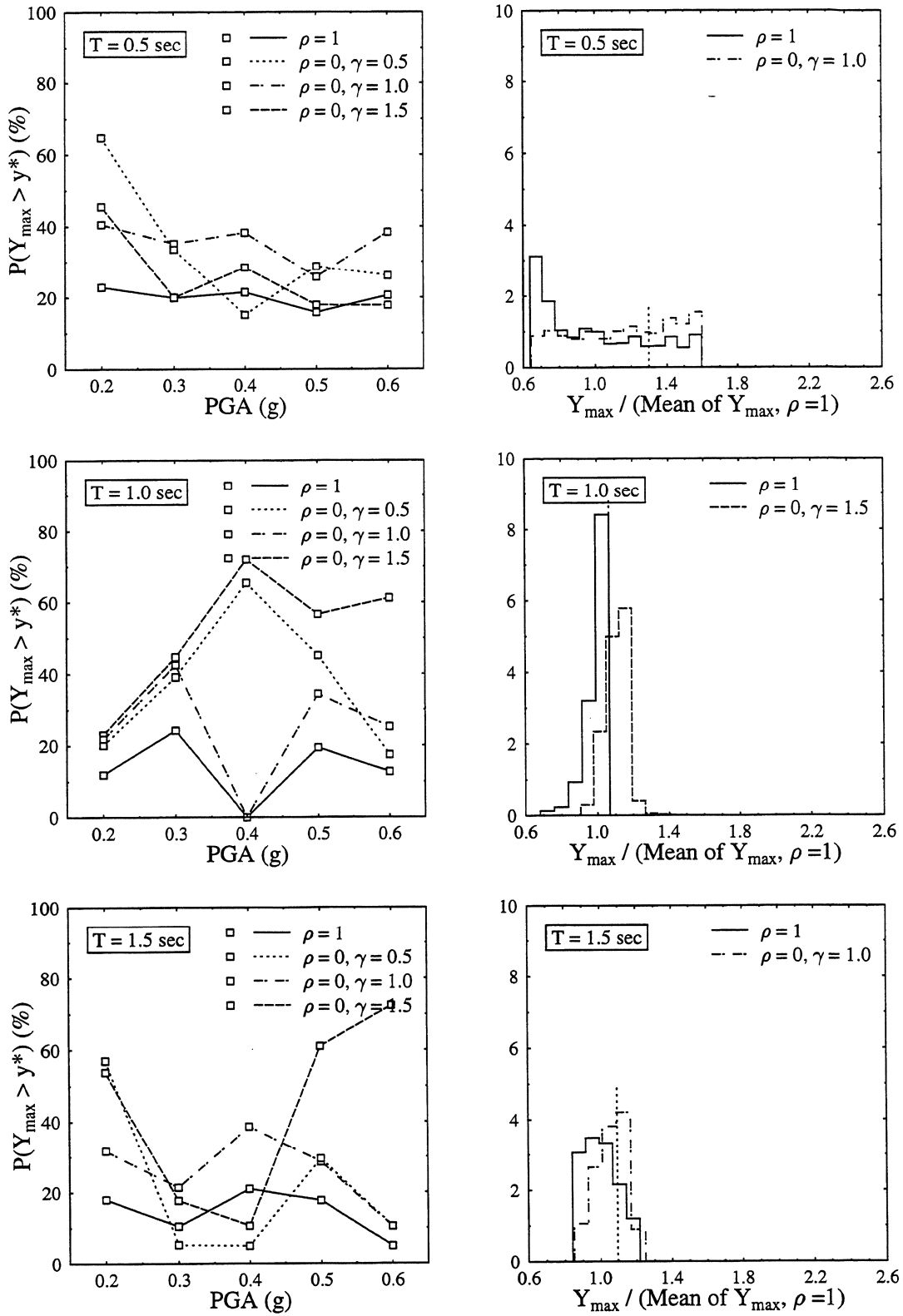
FIGURE 3-15 Probability of exceedence of level y^* and histograms of normalized maximum displacement. EP model. Input: Taft.
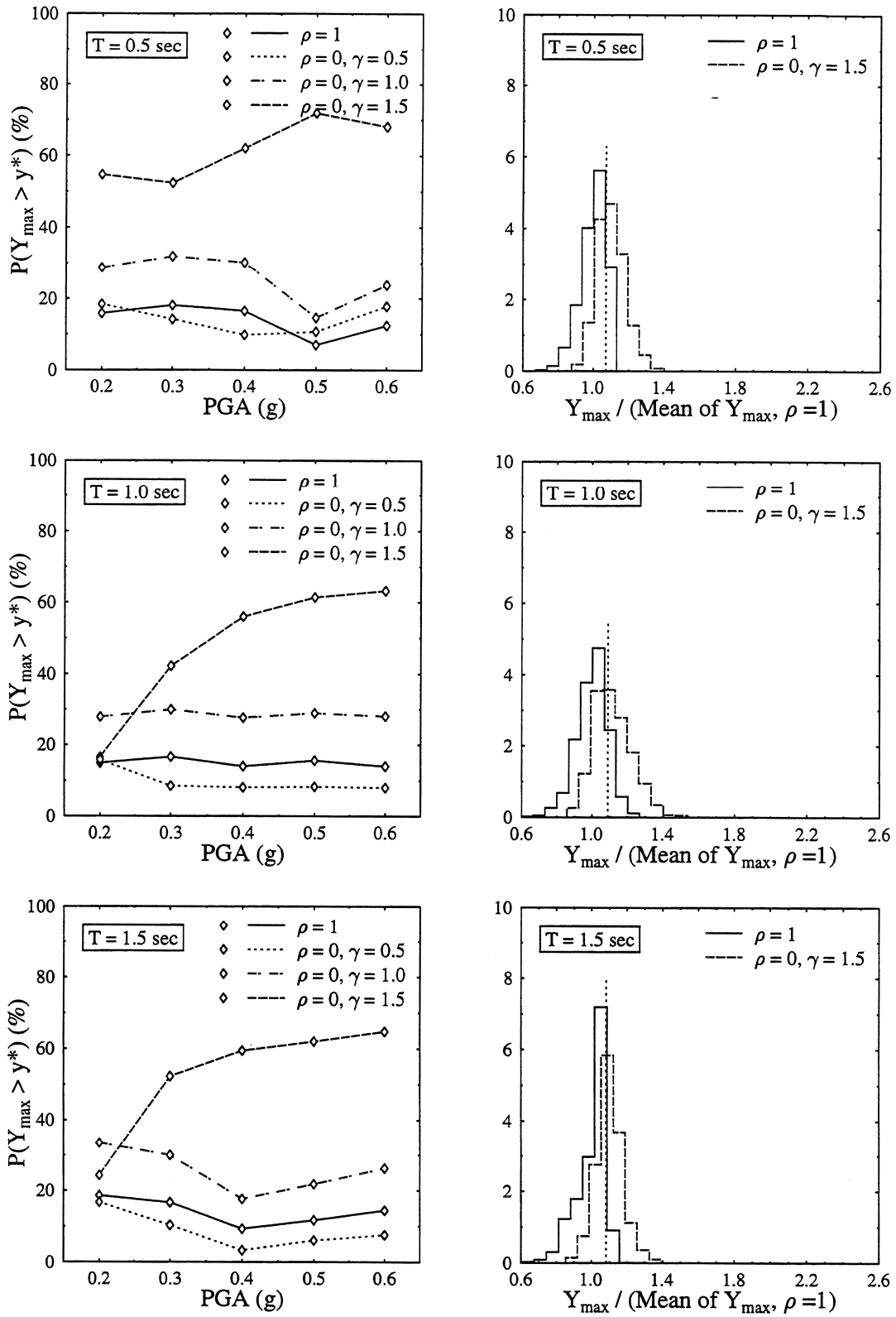
FIGURE 3-16 Probability of exceedence of level y^* and histograms of normalized maximum displacement. EP model. Input: Parkfield.

Histograms of Y_{max} normalized by the mean of the maximum displacement of the system with $\rho = 1$ are also shown in Figures 3-14–3-16. All histograms are obtained for PGA $= 0.4g$, the middle value in the range considered for the sensitivity study. The two histograms presented in each graph correspond to the symmetric system and the system with the highest probability of exceedence of level y^* for the specified PGA. The vertical dotted line marks y^*. Larger displacements are calculated with higher frequency for the system with torsion than for the symmetric system. Consequently, the shape of the histogram changes in various ways. For instance, it may spread to the right with significant increase in the extreme values (as in the top right graph of Figure 3-14 where the extreme value increases from 1.8 to 2.6), or it may extend over the same range but change from being skewed to the right to being skewed to the left (see top right graph in Figure 3-15), or again, it may shift to the right as well as change skewness (see Figure 3-16).

Maximum ductility. The trends observed for the mean and the COV of the maximum displacement apply qualitatively to the respective statistics of the maximum ductility M_{max}, with the exception that the mean of M_{max} is a decreasing function of the period (see Figures 3-17–3-19). This difference is an effect of the scaling with the yield displacement since the increase in the yield displacement with the period is much more significant than the increase in the maximum displacement. Quantitatively, all the effects of uncertainty are amplified. For example, under El Centro scaled to PGA $= 0.4g$, and for $T = 0.5$ sec and $\rho = 1$ the mean of M_{max} is 5.9. When $\rho = 0$ and $\gamma = 1.5$ the mean increases by 37%. The corresponding increase in the mean of Y_{max} is 25%.

The associated reference system is the deterministic system resulting from the application of the UBC provisions and has ductility $\mu_{max,0}$. Figures 3-20, 3-21, and 3-22 illustrate how the maximum ductility M_{max} of systems with random element yield strengths compares with $\mu_{max,0}$ for the El Centro, Taft, and Parkfield records, respectively. The plots show the probability that M_{max} exceeds values expressed as multiples of $\mu_{max,0}$. The logarithmic scale used for the ratio $\mu/\mu_{max,0}$ allows for better definition at low ductilities. Each figure includes plots for all combinations of T, ρ, and γ considered and three representative values of PGA: $0.2g$, $0.4g$, and $0.6g$.

For symmetric systems ($\rho = 1$) the probability $P(M_{max} > \mu_{max,0})$ falls mostly between 50% and 60%, which is to be expected since all realizations of the symmetric system result from a perturbation about the associated reference system. Moreover, for most parameter combinations there is negligible probability of ductilities over $2\mu_{max,0}$ with the
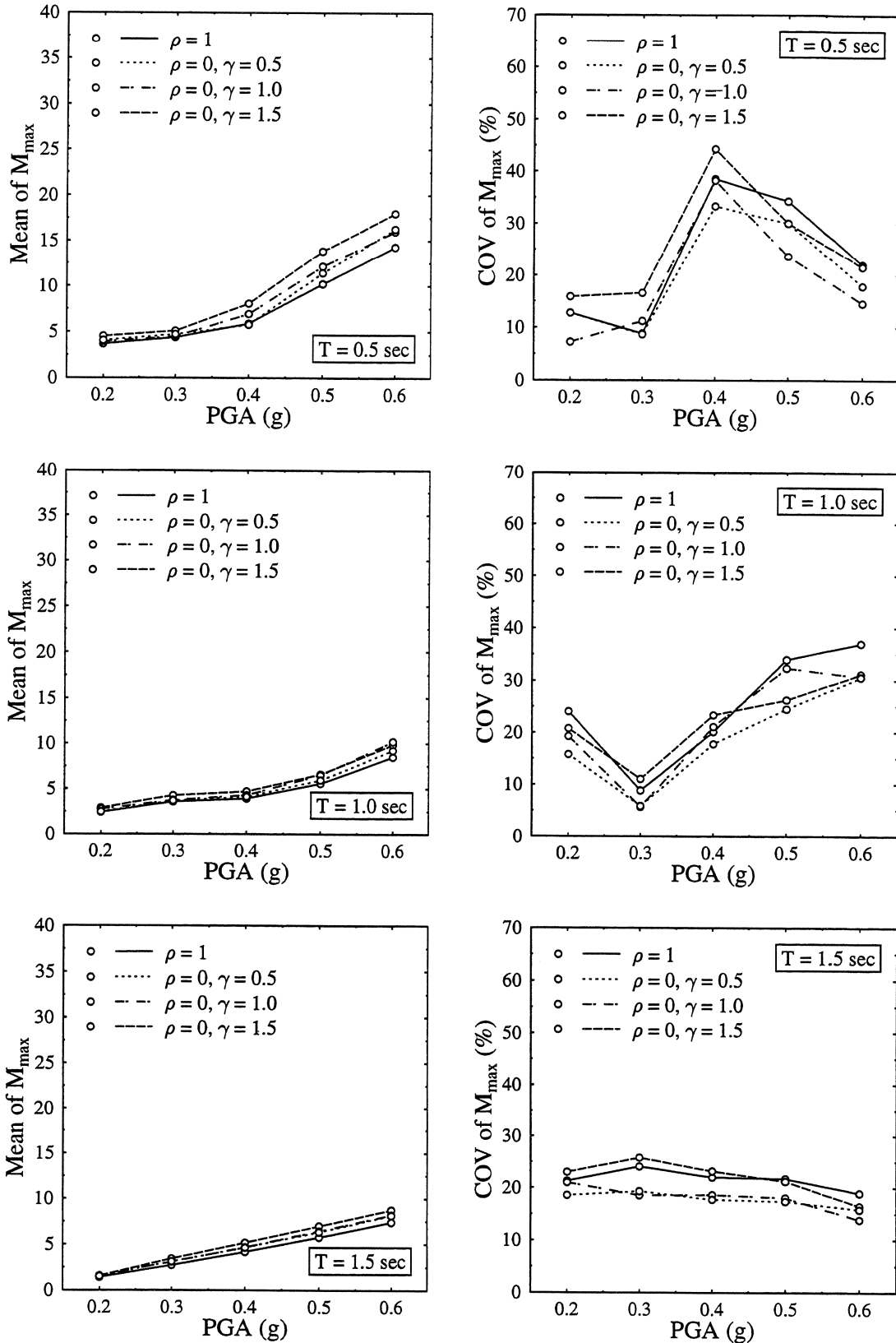
**FIGURE 3-17** Mean and COV of M_{max}. EP model. Input: El Centro.
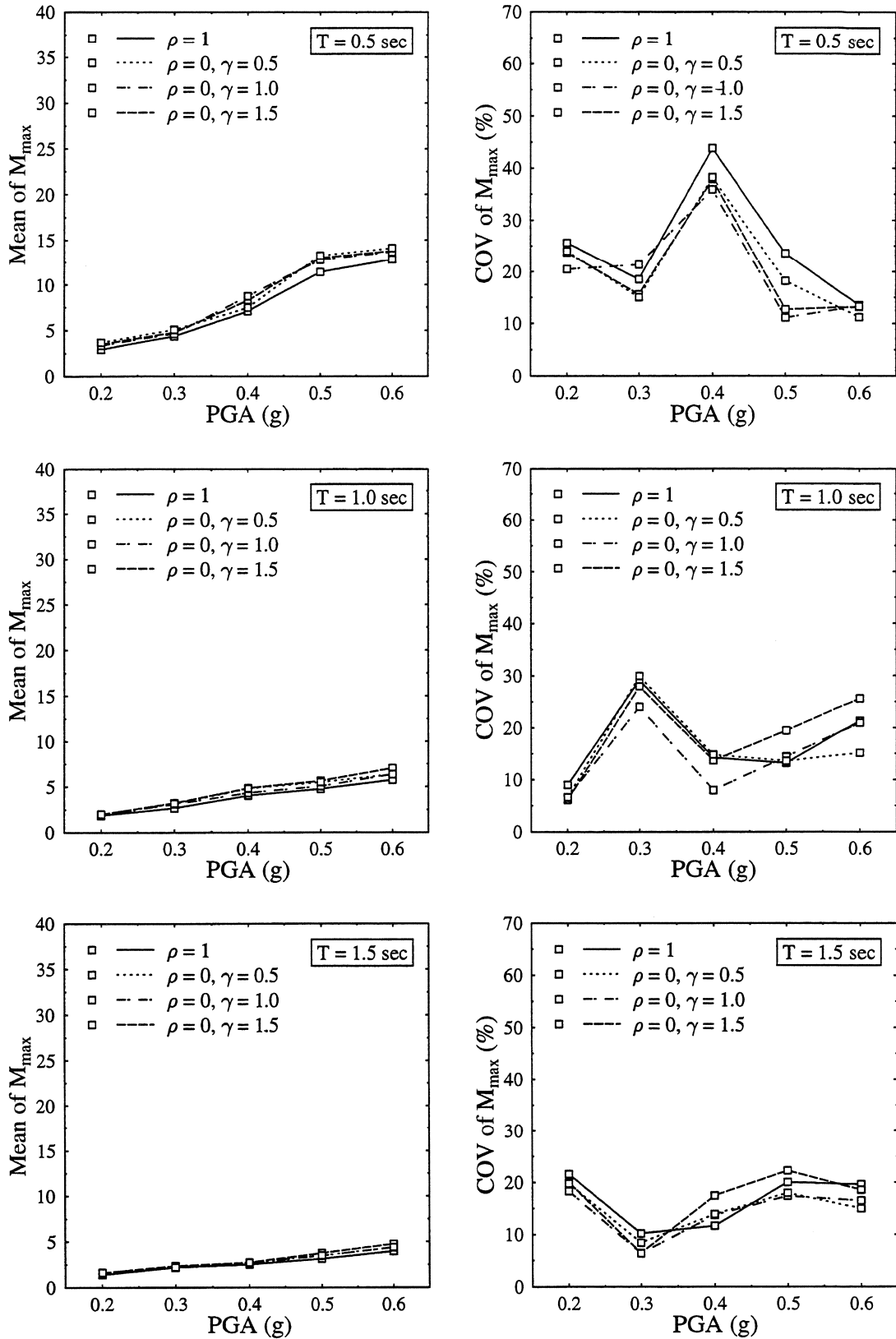
**FIGURE 3-18** Mean and COV of $M_{\max}$. EP model. Input: Taft.
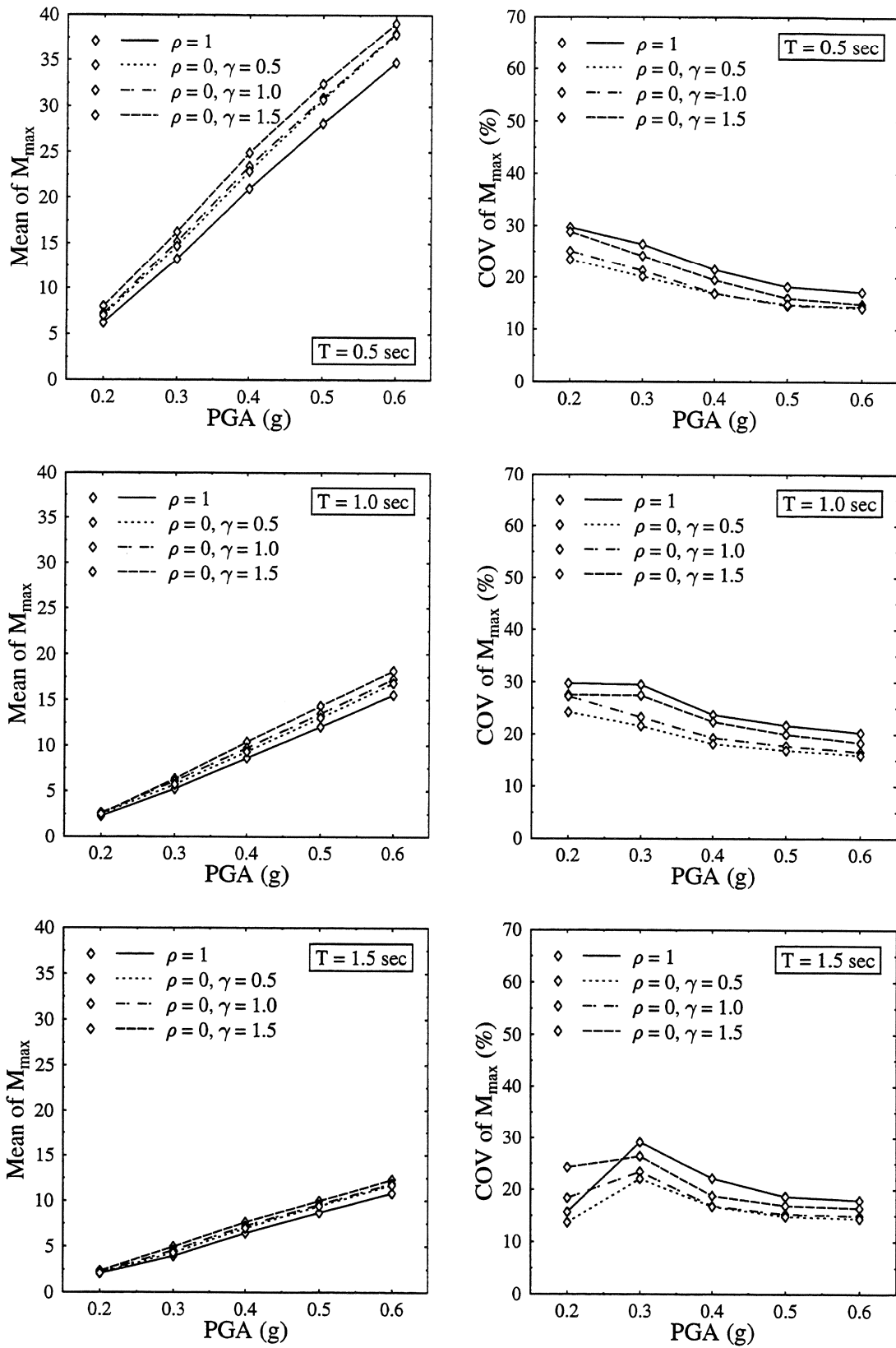
**FIGURE 3-19** Mean and COV of $M_{\max}$. EP model. Input: Parkfield.
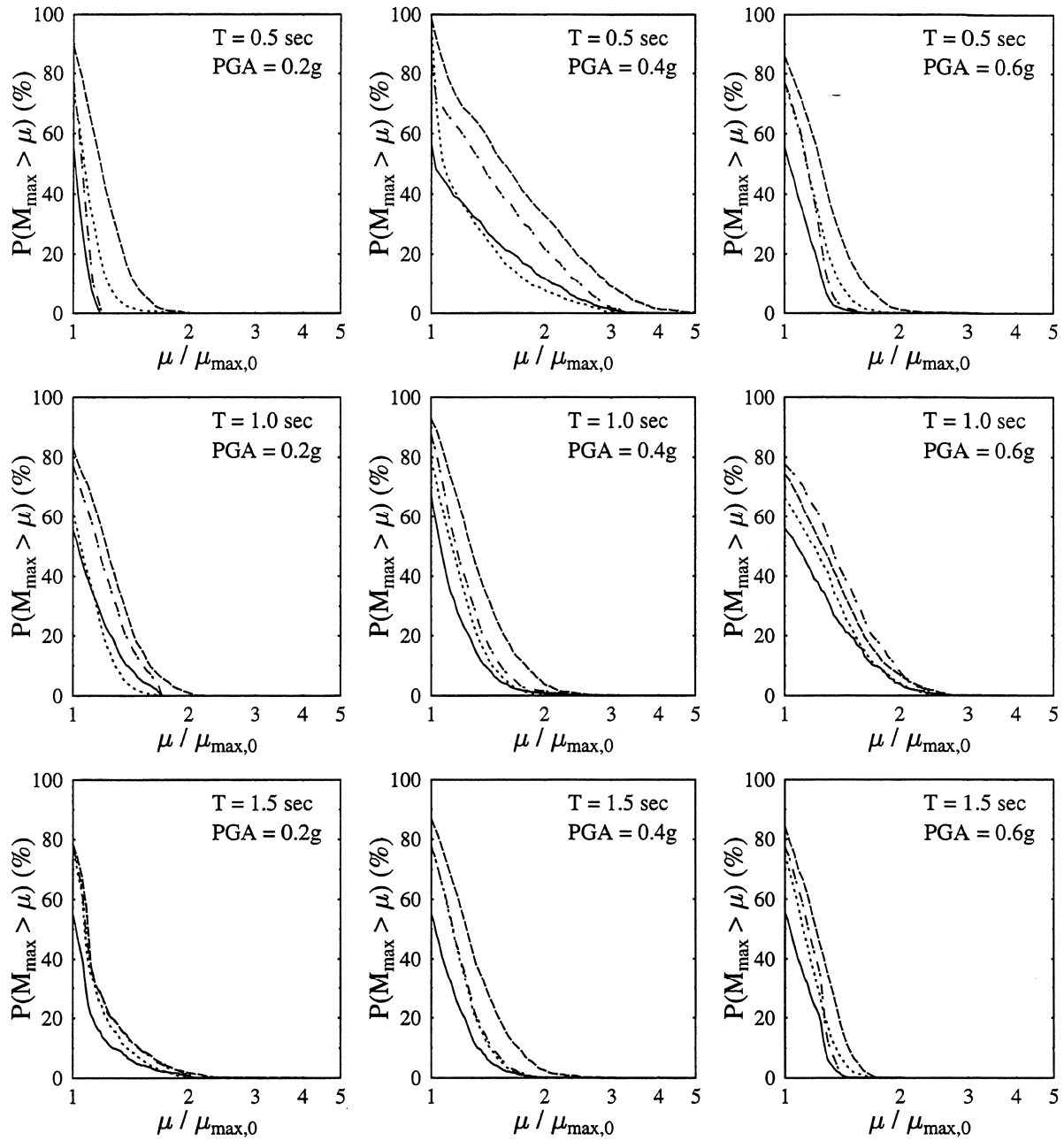
FIGURE 3-20 Probability of $M_{\max}$ exceeding $\mu_{\max,0}$. EP model. Input: El Centro. (——— $\rho = 1$; $\cdots\cdots$ $\rho = 0$, $\gamma = 0.5$; —·—· $\rho = 0$, $\gamma = 1.0$; ——— $\rho = 0$, $\gamma = 1.5$)

notable exception of the system with $T = 0.5$ sec under both El Centro and Taft scaled to PGA $= 0.4g$. Torsion tends to increase the probability of exceedence of a given level but not necessarily monotonically with γ. For asymmetric systems there is significant probability of ductility values between $2\mu_{\max,0}$ and $3\mu_{\max,0}$. Even ductilities exceeding $4\mu_{\max,0}$ are calculated for some parameter combinations.
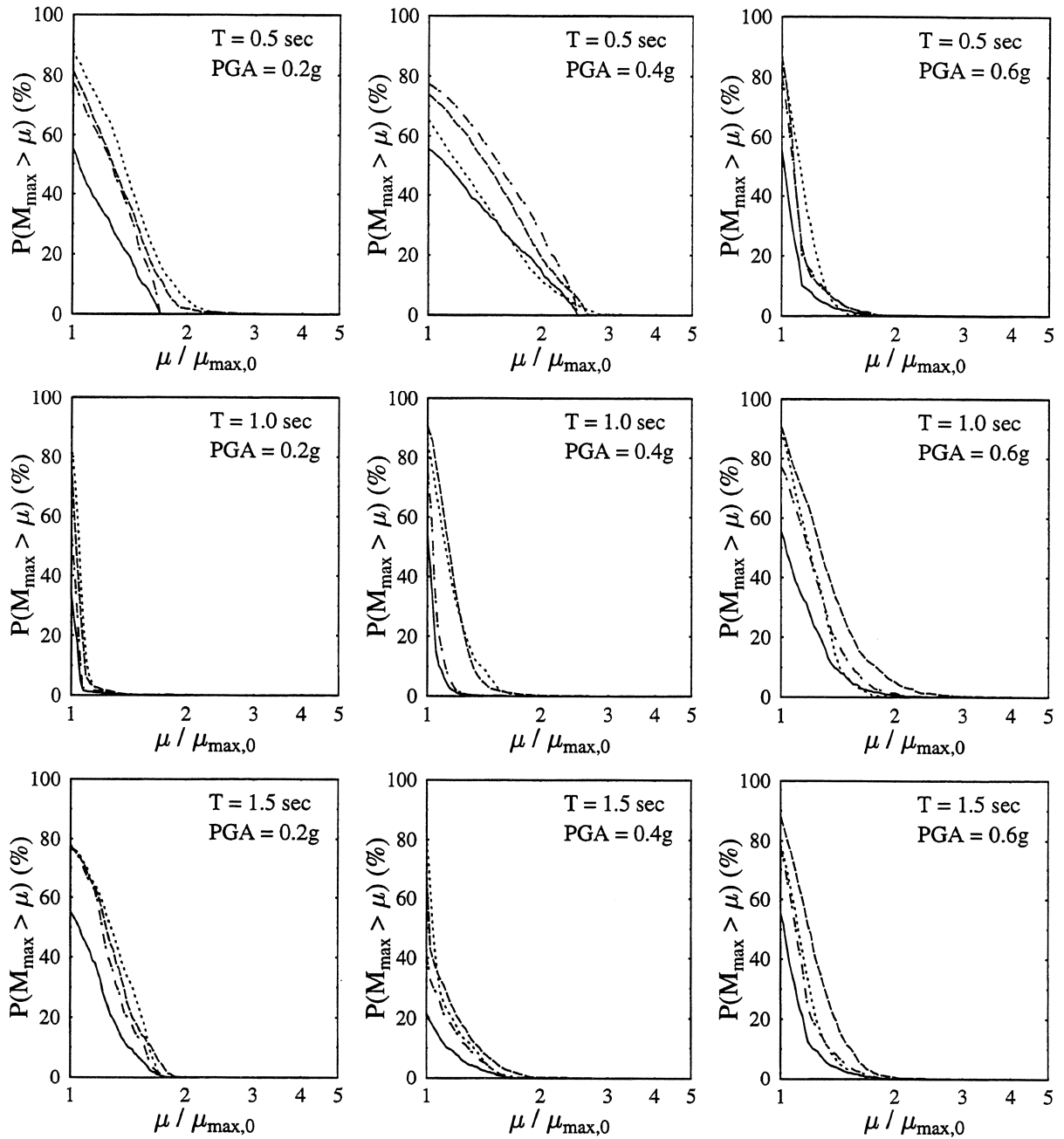
FIGURE 3-21 **Probability of** M_{max} **exceeding** $\mu_{max,0}$. **EP model. Input: Taft.**
(———— $\rho = 1$; · · · · · $\rho = 0$, $\gamma = 0.5$; —· —· $\rho = 0$, $\gamma = 1.0$; — — — $\rho = 0$, $\gamma = 1.5$)

FIGURE 3-22 Probability of M_{max} exceeding $\mu_{max,0}$. EP model. Input: Parkfield. (——— $\rho = 1$; ····· $\rho = 0$, $\gamma = 0.5$; —·—· $\rho = 0$, $\gamma = 1.0$; — — — $\rho = 0$, $\gamma = 1.5$)

Dissipated energy. The mean dissipated energy E_{dis} consistently increases with PGA, decreases with T, and is insensitive to torsional vibrations, as illustrated by Figures 3-23, 3-24, and 3-25 for El Centro, Taft, and Parkfield, respectively. The COV of E_{dis} exceeds 10% only for low PGA values and becomes very large for PGA = $0.2g$, $T = 1.5$ sec, and input either El Centro or Taft. These disproportionately large coefficients of variation are the result of the presence of almost zero mean values in the denominator of the ratio. Torsional vibrations decrease the COV of E_{dis} by approximately the same amount for all values of γ.

Figure 3-26 allows comparison of the mean and the COV of the energy dissipated by the symmetric system for different motions. The differences in the mean of E_{dis} are more pronounced for high PGA values and low periods. For $T = 1.5$ sec mean energy dissipation differs only slightly from motion to motion. For the other two periods the highest mean values are associated with Taft, followed by El Centro and then Parkfield. With input the El Centro or the Taft record the COV of E_{dis} tends to decrease with PGA whereas the opposite trend is observed for the Parkfield record.

Maximum rotation. The maximum rotation Φ_{max}, is characterized by very large coefficients of variation for all three input motions, as can be seen in Figures 3-27–3-29. Specifically, the COV exceeds 55% in all cases considered and its maximum values are 81%, 83%, and 88% for El Centro, Taft, and Parkfield, respectively. It is evident that the maximum rotation is very strongly affected by the strength uncertainty; in comparison, the COV of the element yield strengths is only 15%. The mean of Φ_{max} increases with γ for most period and PGA combinations, which supports the statement that systems with higher values of γ should be more susceptible to torsion and therefore, should develop larger rotations.

3.4.2 Parameter uncertainty. Modified-Clough model

Maximum displacement. The mean of the maximum displacement Y_{max} increases monotonically with T and PGA, as can be seen in Figures 3-30–3-32. Torsion increases the mean of Y_{max} and more so for higher values of γ. The increase in the mean is very small for systems with $T \geq 1.0$ sec subjected to the Taft record. The COV of Y_{max} in no case exceeds 15%, making the uncertainty in the maximum displacement smaller than the uncertainty in the yield strength of the lateral-load-resisting elements. Torsion affects the COV of Y_{max} in different ways depending on the value of γ. Specifically, the COV

58
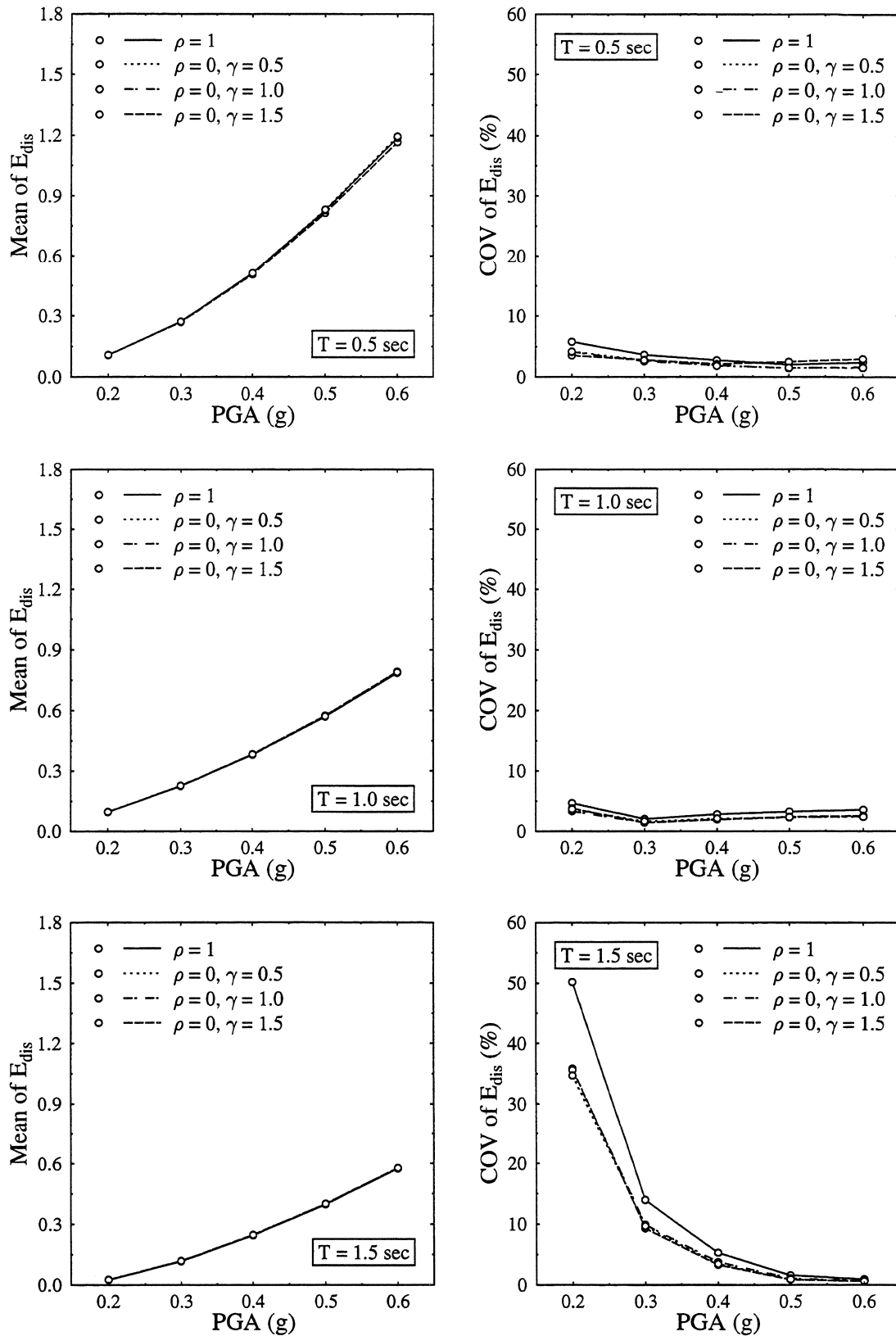
FIGURE 3-23 Mean and COV of E_{dis}. EP model. Input: El Centro.

59
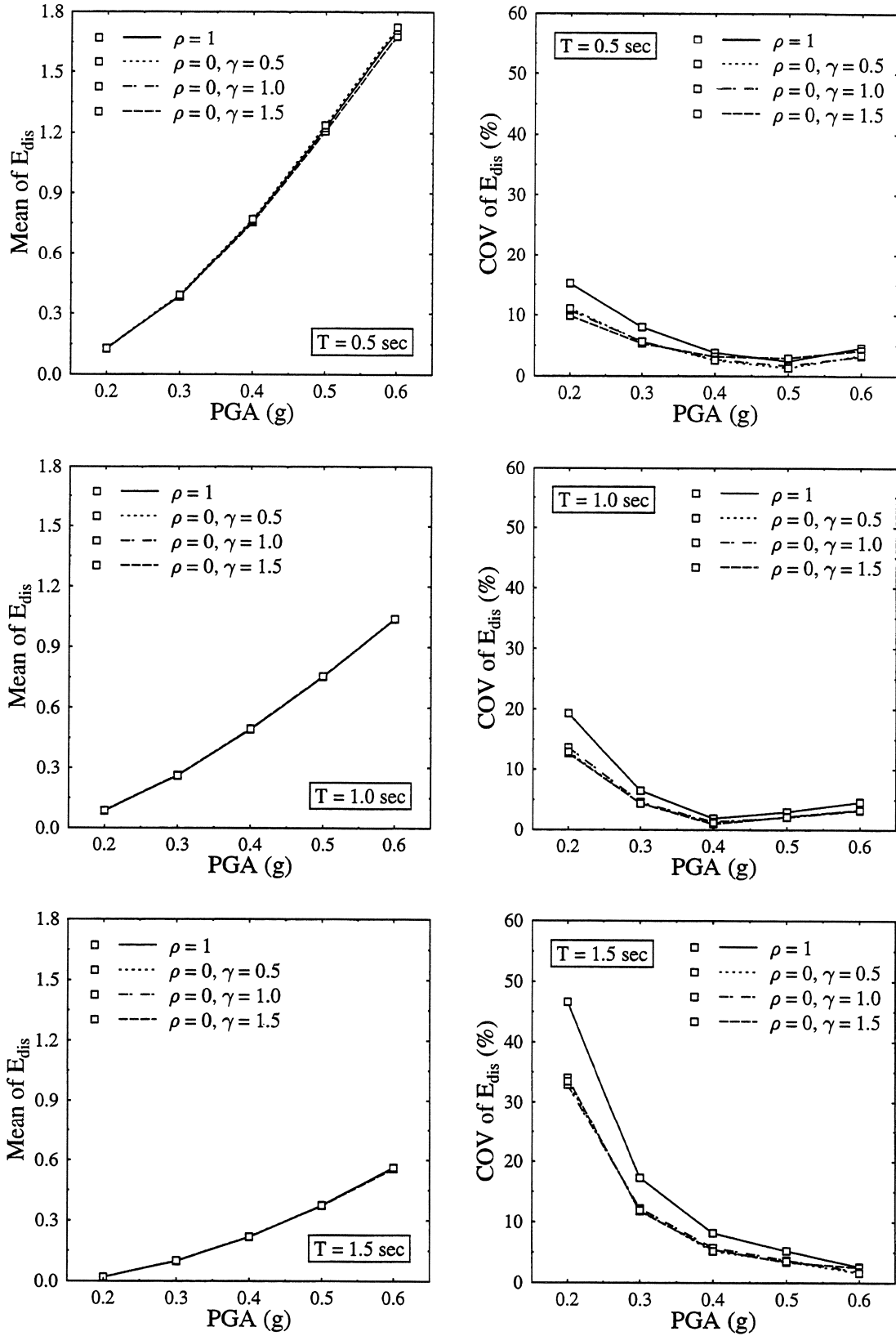
FIGURE 3-24 Mean and COV of E_{dis}. EP model. Input: Taft.
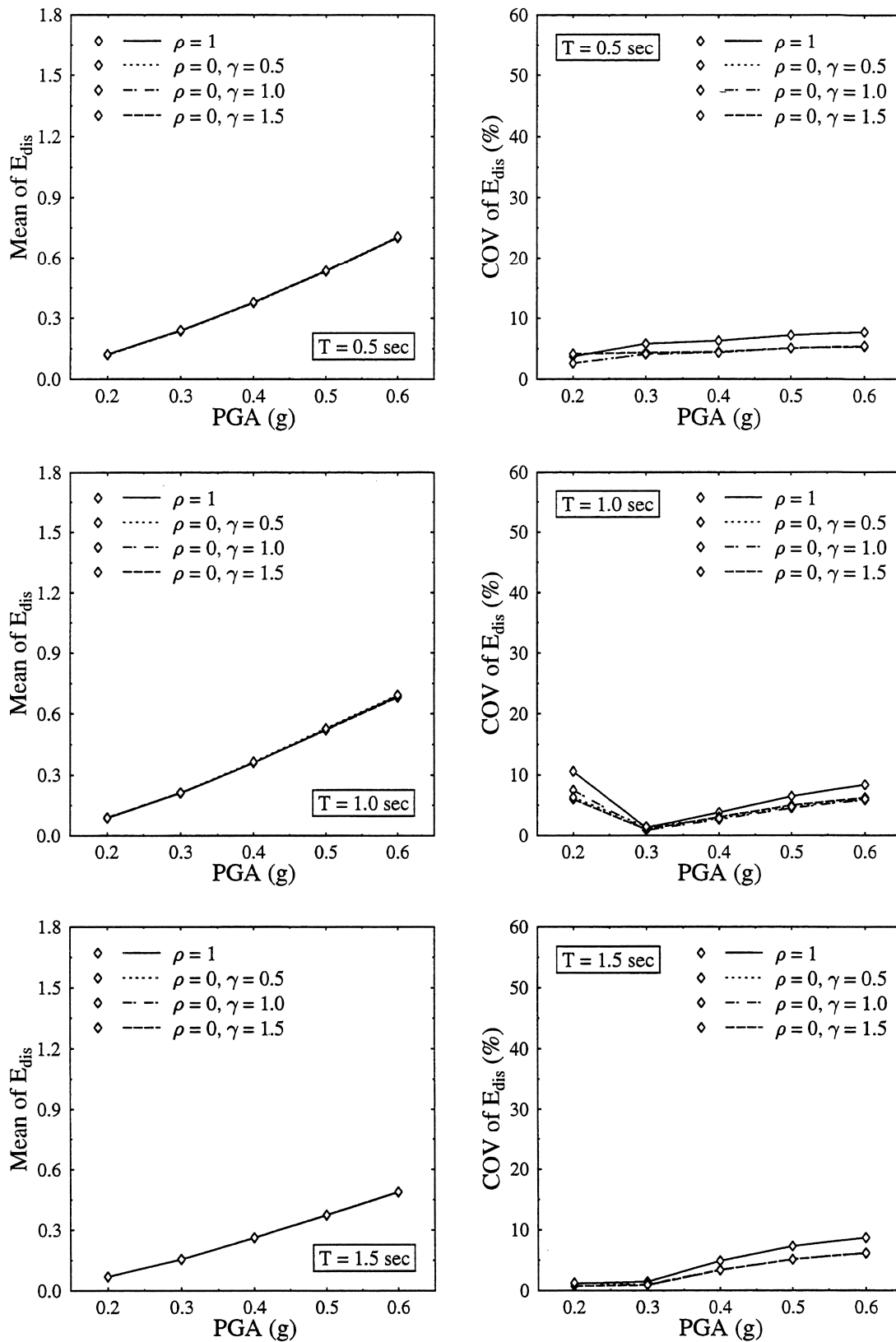
FIGURE 3-25 Mean and COV of E_{dis}. EP model. Input: Parkfield.
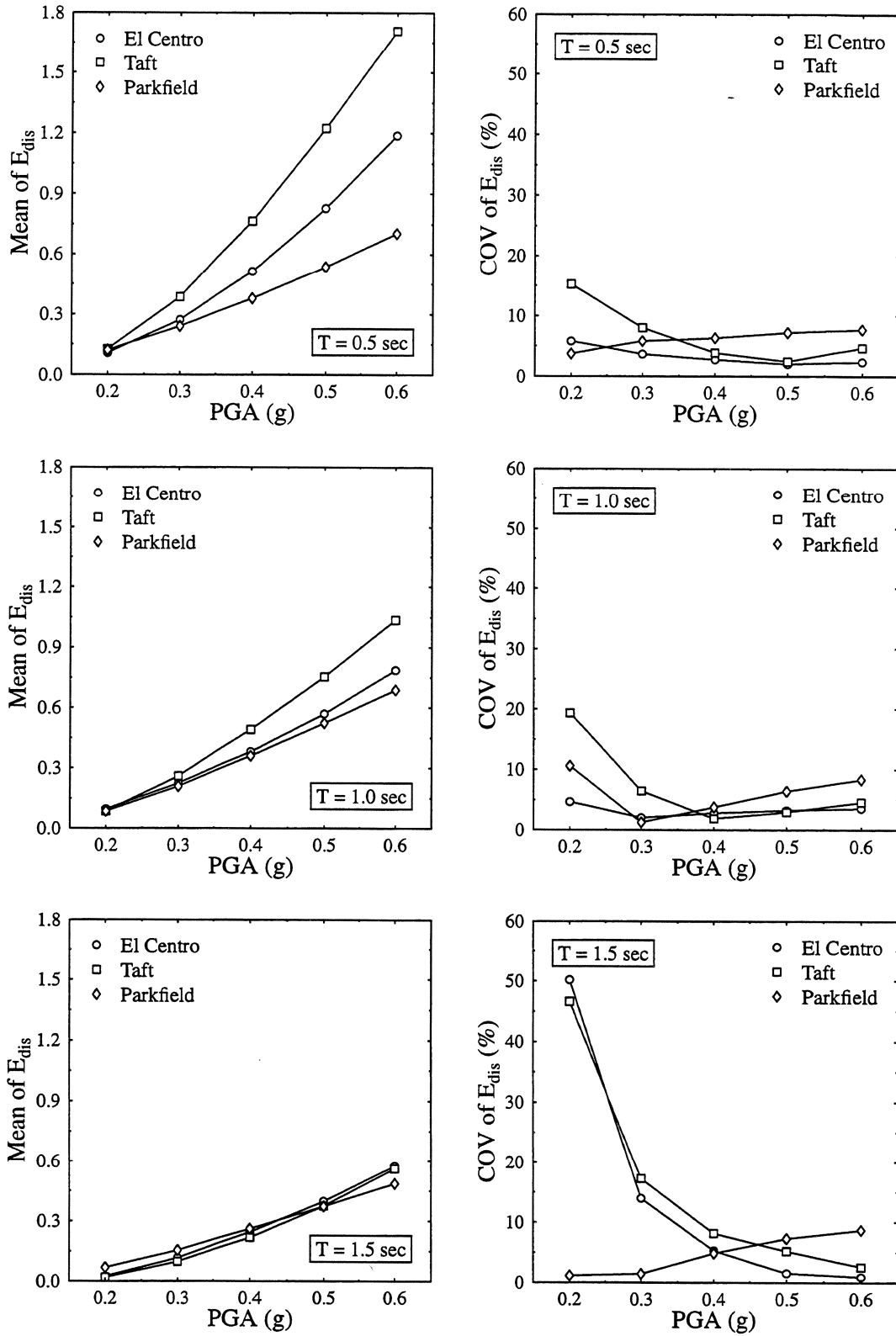
FIGURE 3-26 Mean and COV of E_{dis} for perfectly correlated yield strengths. EP model.
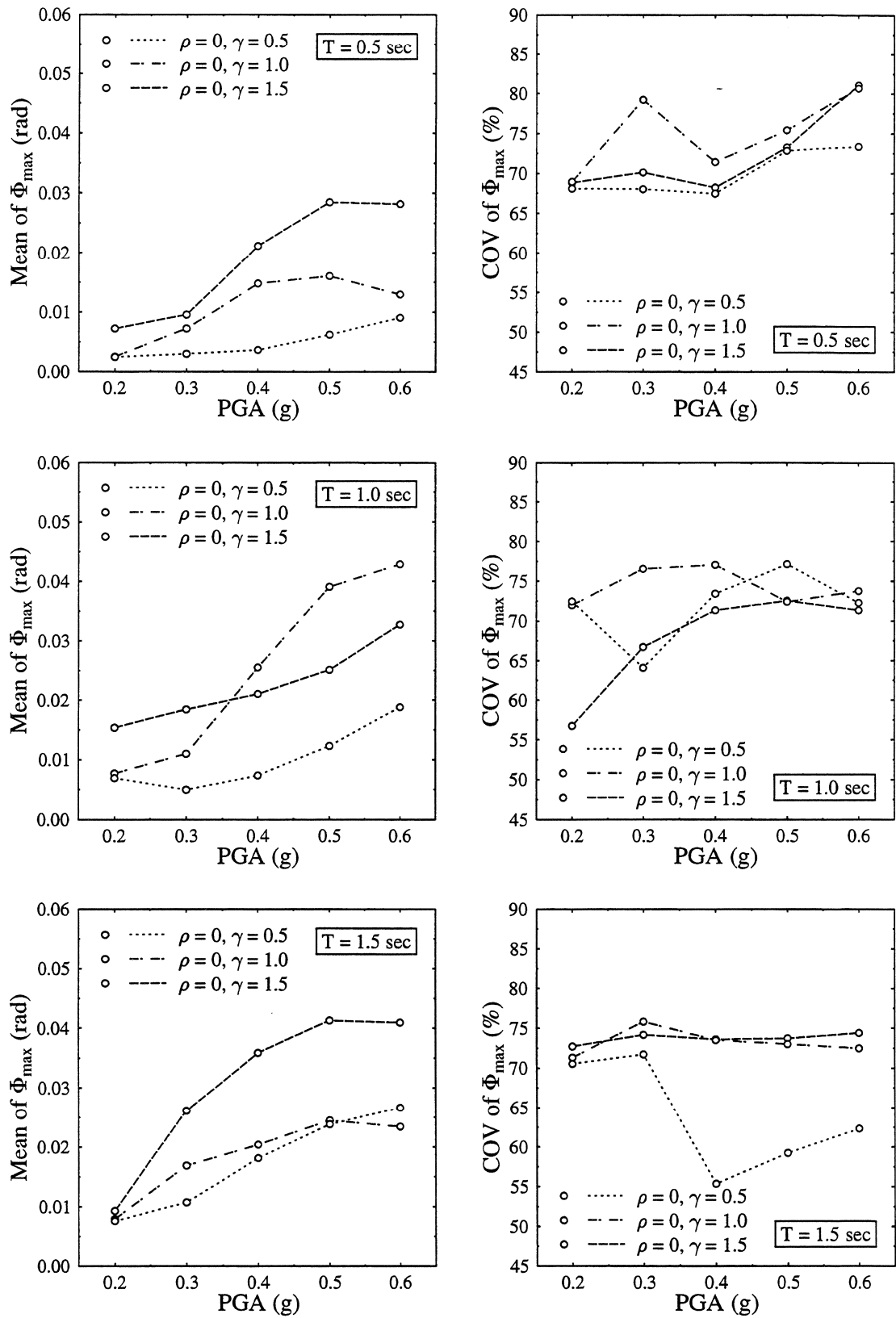
FIGURE 3-27 Mean and COV of $\Phi_{\max}$. EP model. Input: El Centro.
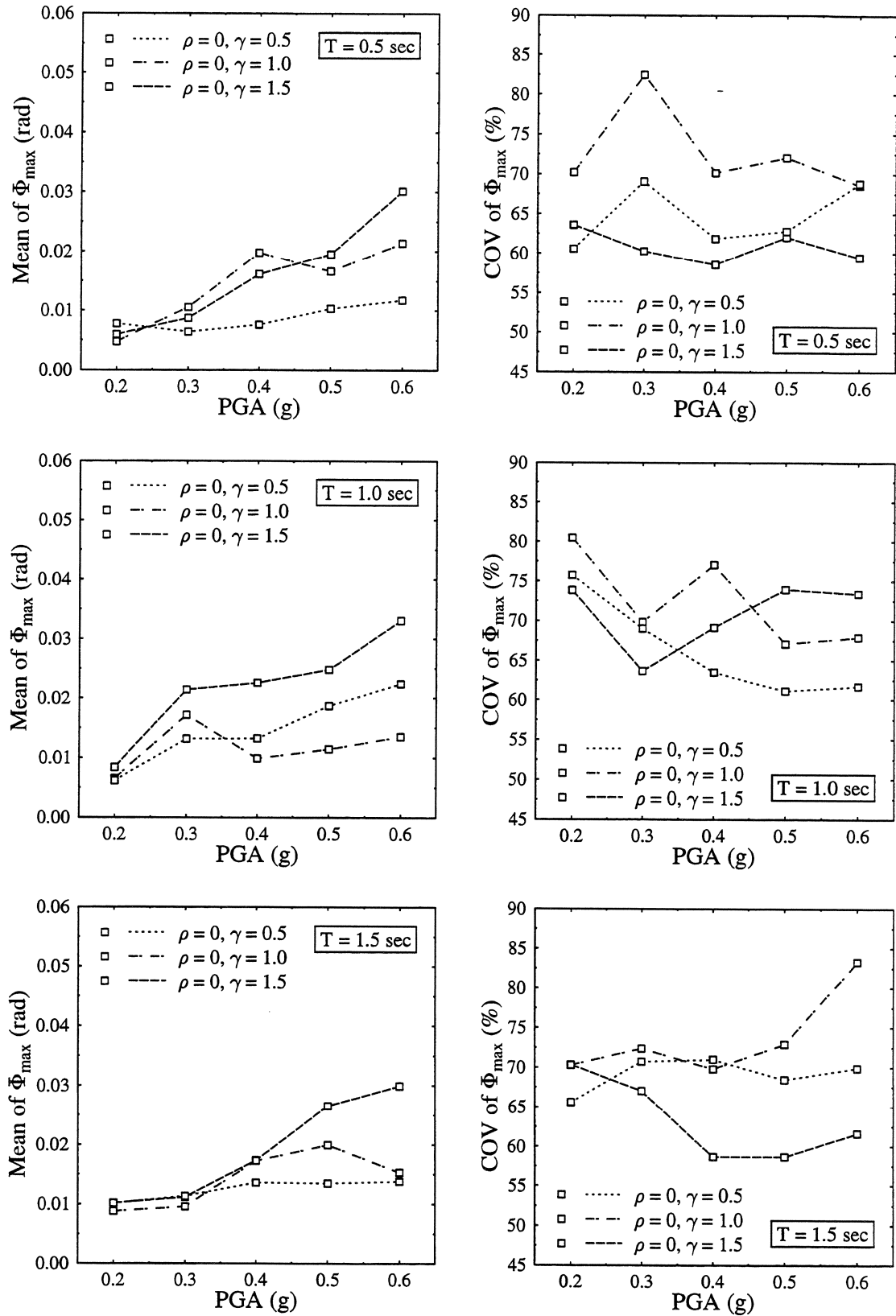
FIGURE 3-28 Mean and COV of Φ_{max}. EP model. Input: Taft.

64
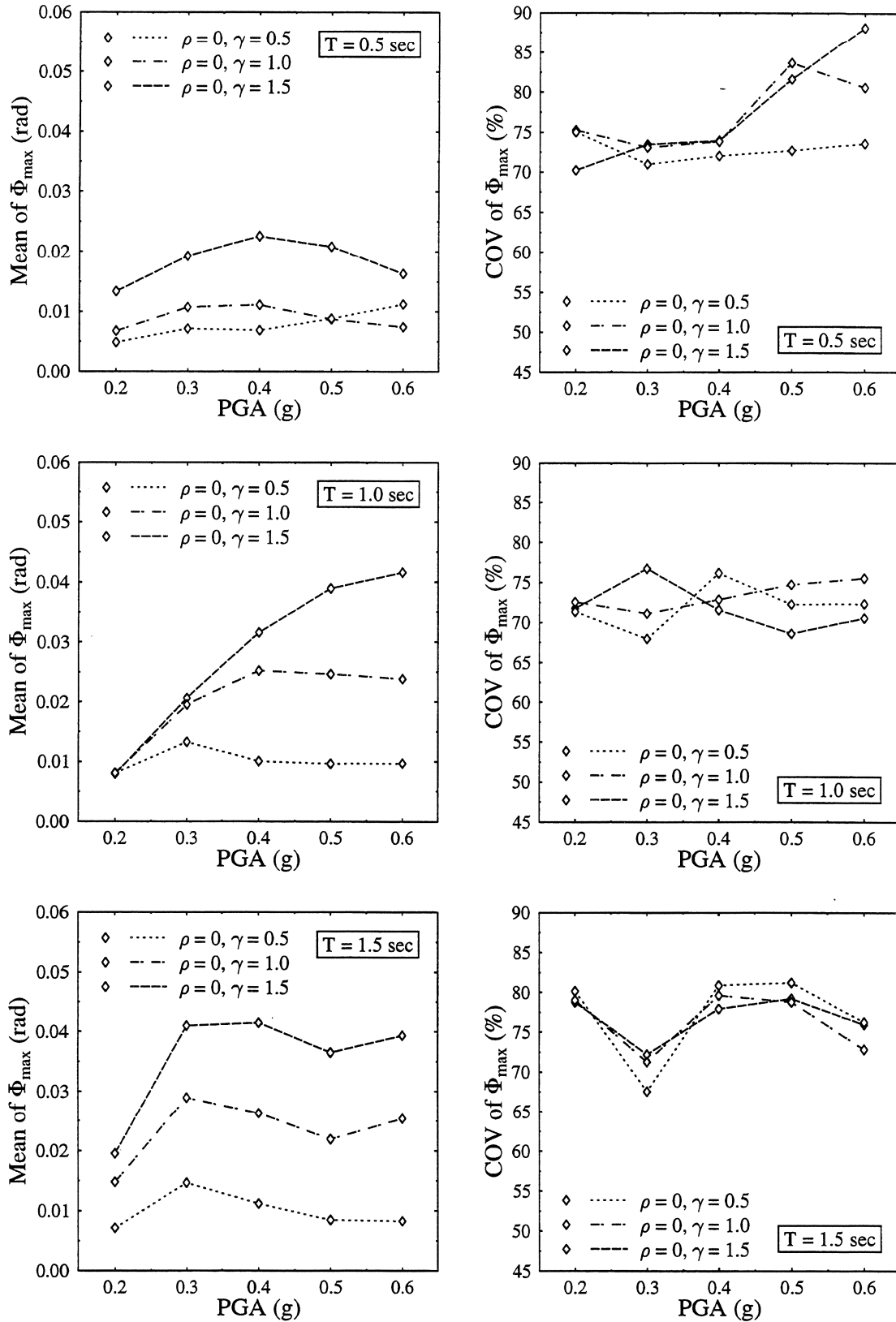
**FIGURE 3-29** Mean and COV of $\Phi_{\max}$. EP model. Input: Parkfield.
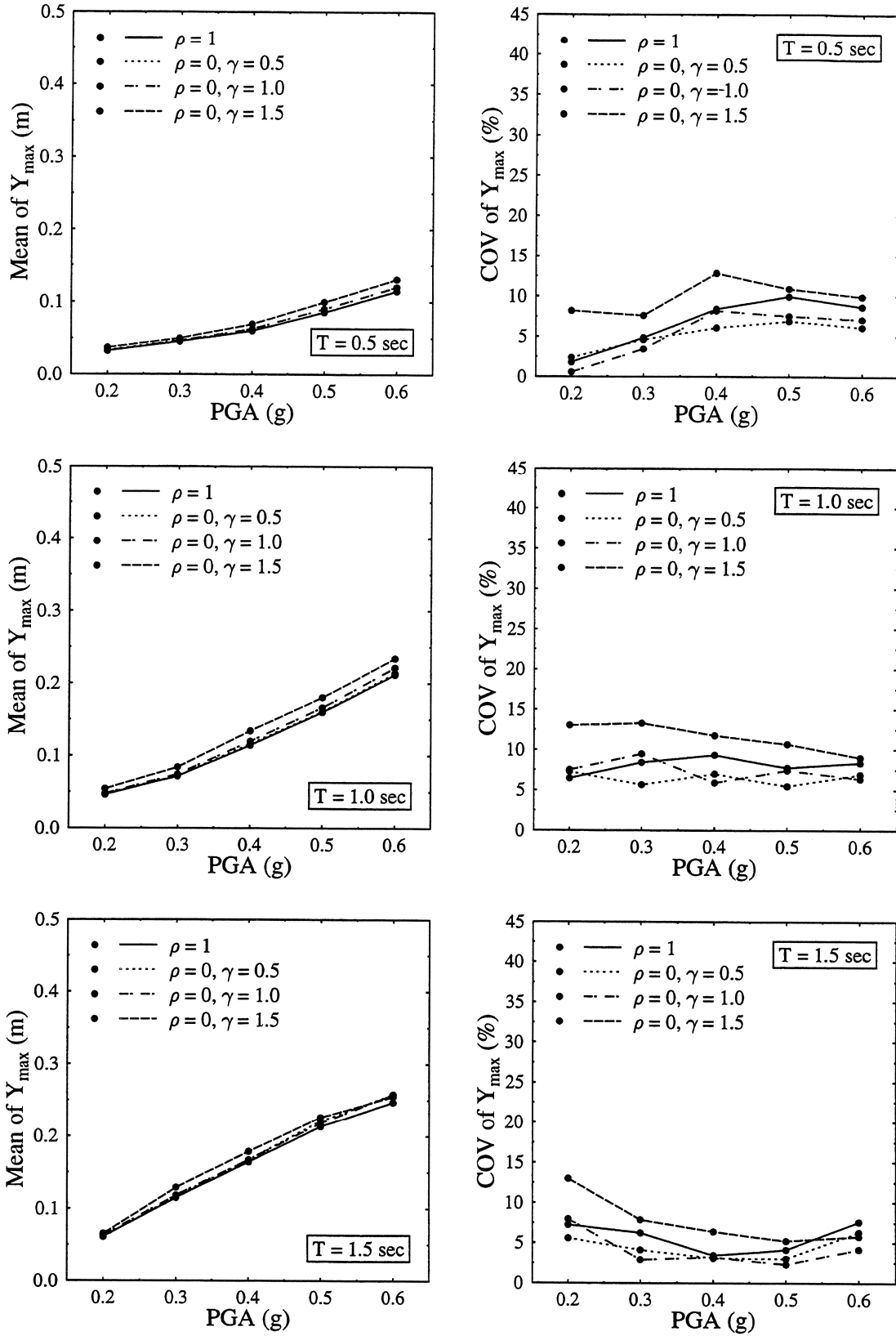
FIGURE 3-30 Mean and COV of $Y_{\max}$. MC model. Input: El Centro.
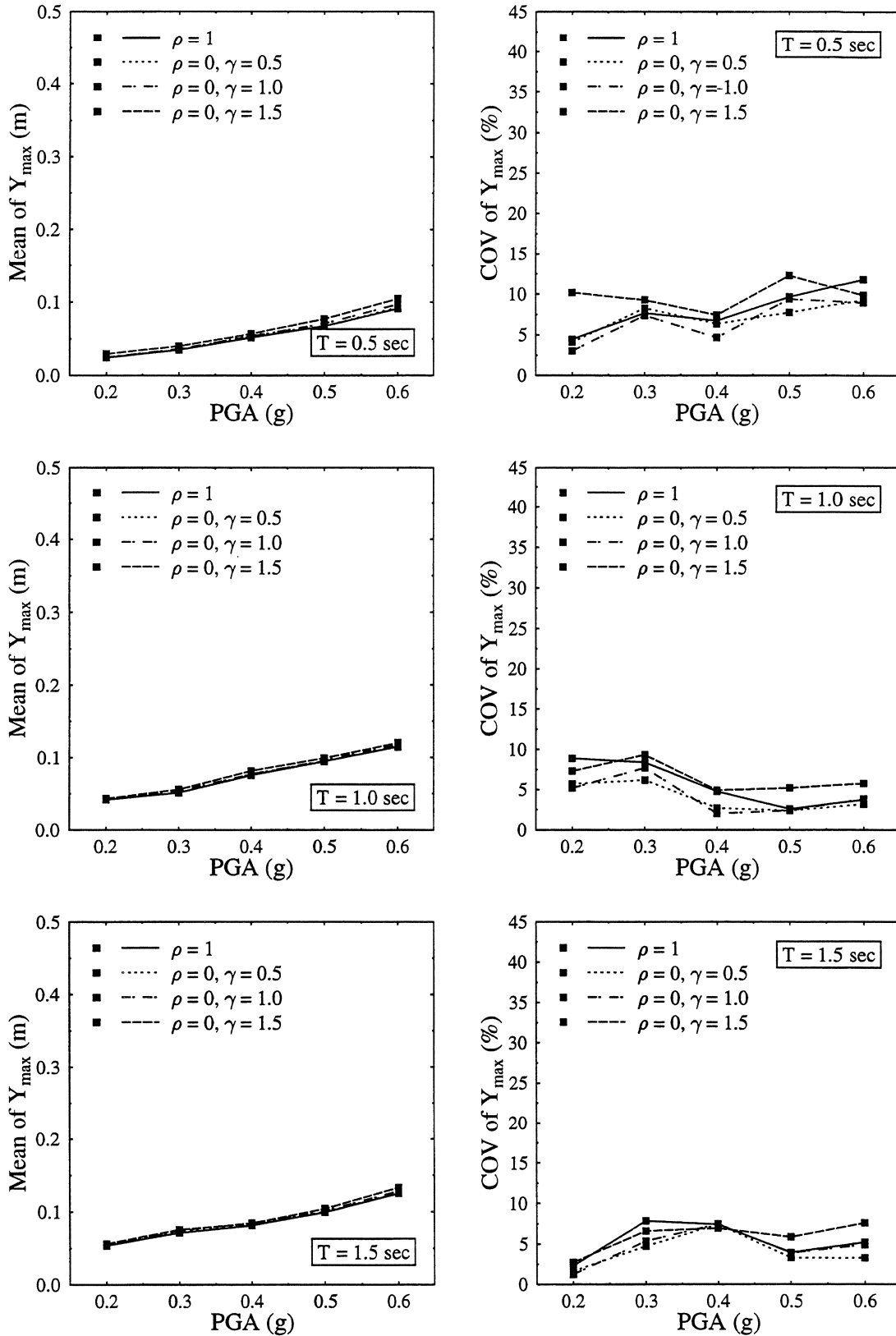
FIGURE 3-31 Mean and COV of Y_{max}. MC model. Input: Taft.
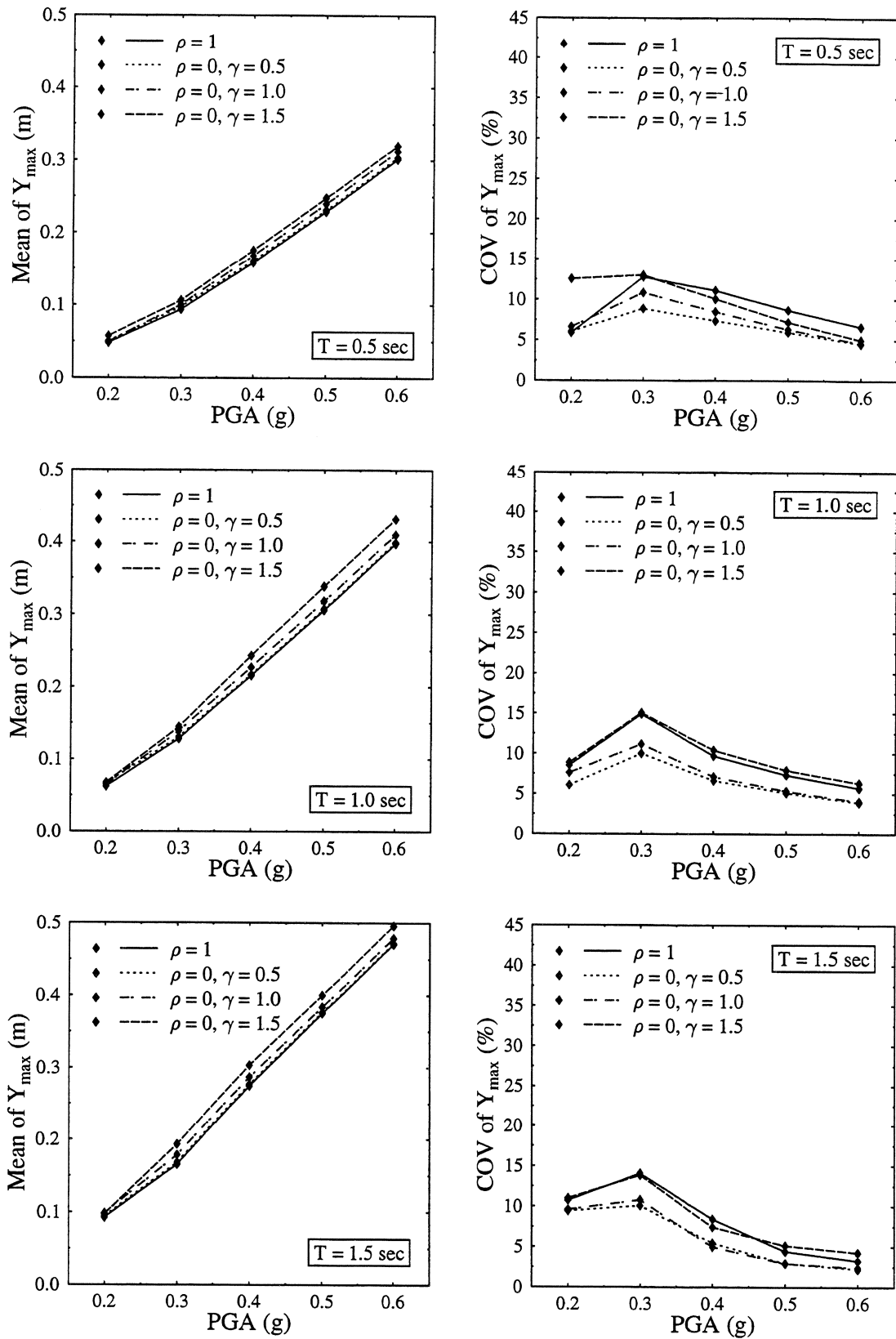
**FIGURE 3-32** Mean and COV of Y_{max}. MC model. Input: Parkfield.

generally decreases compared to the COV of the symmetric system when $\gamma \leq 1.0$ but increases when $\gamma = 1.5$. Also, under Parkfield the COV of Y_{max} decreases monotonicaly with the PGA for PGA $> 0.3g$, whereas under El Centro or Taft there is no apparent trend.

Figure 3-33 shows the mean and the COV of the maximum displacement of the system with perfectly correlated yield strengths subjected to all three input motions. The highest values of the mean for all combinations of period and PGA correspond to Parkfield, followed by El Centro, and then Taft and the differences between motions become more pronounced as the period increases. The effect of torsion on the mean and the COV of Y_{max} is further illustrated by the plots in Figure 3-34 of the ratios $p(Y_{max})$ and $q(Y_{max})$. As defined in Section 3.4.1, $p(Y_{max})$ is the ratio of the mean of Y_{max} for $\rho = 0$ and $\gamma = 1.5$ over the mean of Y_{max} for $\rho = 1$, and $q(Y_{max})$ is the respective ratio of the coefficients of variation. The increase in the mean due to torsion ranges from 3% to 21% and is particularly small for systems with $T \geq 1.0$ sec under Taft. The ratio $q(Y_{max})$ takes values from about 0.75 to about 2.0 but more often than not it exceeds unity. Therefore, torsion mostly increases the uncertainty in the maximum displacement for systems with $\gamma = 1.5$. The combination of $T = 0.5$ sec and PGA $= 0.2g$ gives exceptionally high ratios, especially under El Centro (the ratio for El Centro, not shown in the graph, is 4.5).

The probability that the maximum displacement exceeds that of the associated reference system can be very high approaching in several cases 100%, as shown in Figures 3-35–3-37. Torsion generally increases considerably the probability $P(Y_{max} > y_{max,0})$ and the increase tends to be monotonic with γ. The effect of PGA on the probability of exceedence varies from erratic for Taft to rather insignificant for Parkfield (especially for PGA $\geq 0.3g$). The mean of $Y_{max}/y_{max,0}$, also shown in Figures 3-35–3-37, generally increases with γ. It takes values mostly in the range 0.95–1.2 and it has an upper bound of 1.26.

Figures 3-38–3-40 include plots of the probability that Y_{max} exceeds the level $y*$ (defined in Section 3.4.1) and histograms of the normalized maximum displacement for PGA $= 0.4g$. The probability $P(Y_{max} > y^*)$ is lower than 25% for the symmetric system. For $\gamma = 1.0$ it remains for the most part below 40%, but for $\gamma = 1.5$ it frequently takes values in the range 50% –80%, which constitutes a very substantial increase over the symmetric system. There is no clear trend for the effect of torsion on $P(Y_{max} > y^*)$ when $\gamma = 0.5$. The two histograms presented for each period correspond to the symmetric system and the system with the highest probability of exceedence of level y^* for the specified PGA.

69
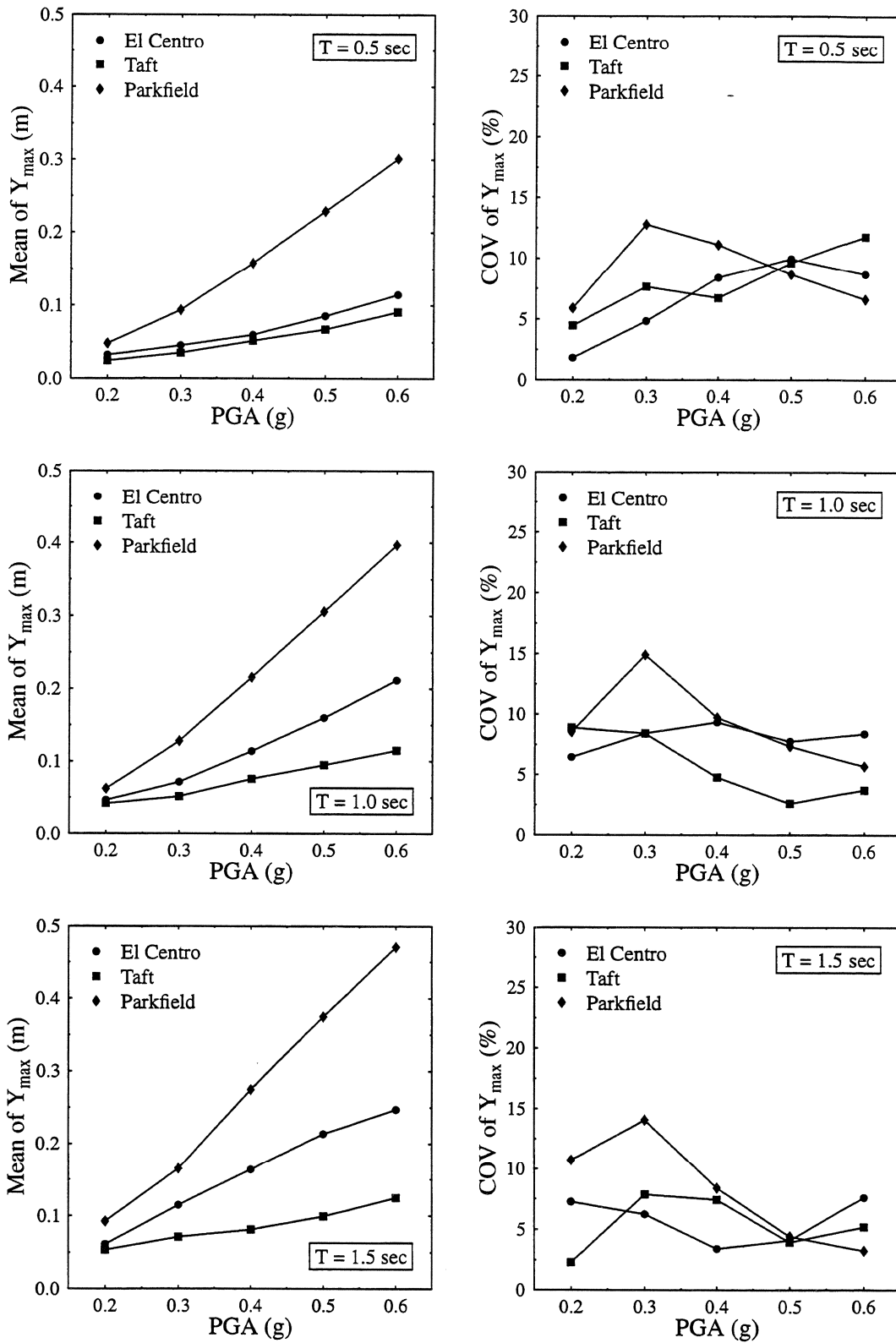
FIGURE 3-33 Mean and COV of Y_{max} for perfectly correlated yield strengths. MC model.
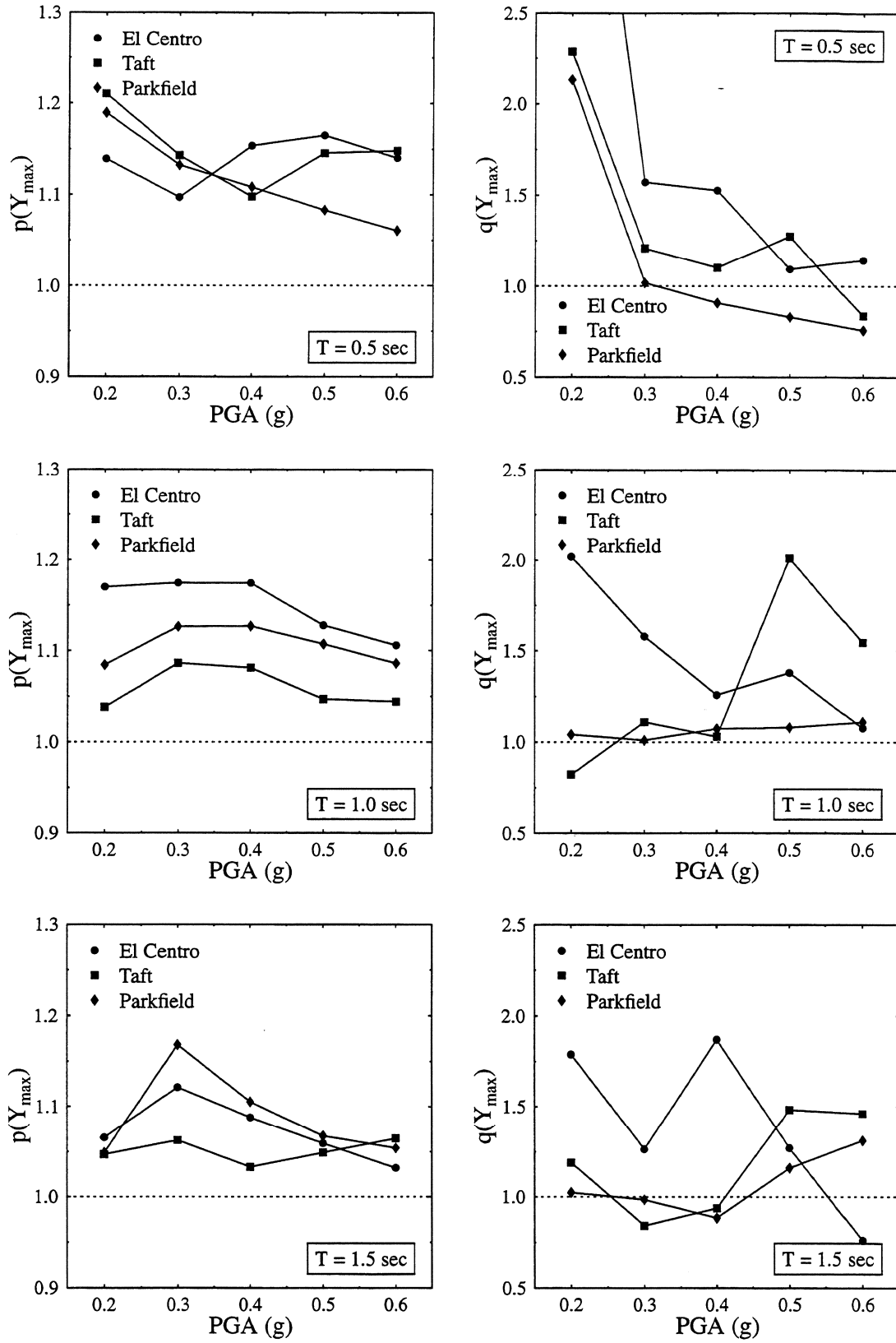
FIGURE 3-34 Ratios of mean and COV of Y_{max}. MC model.
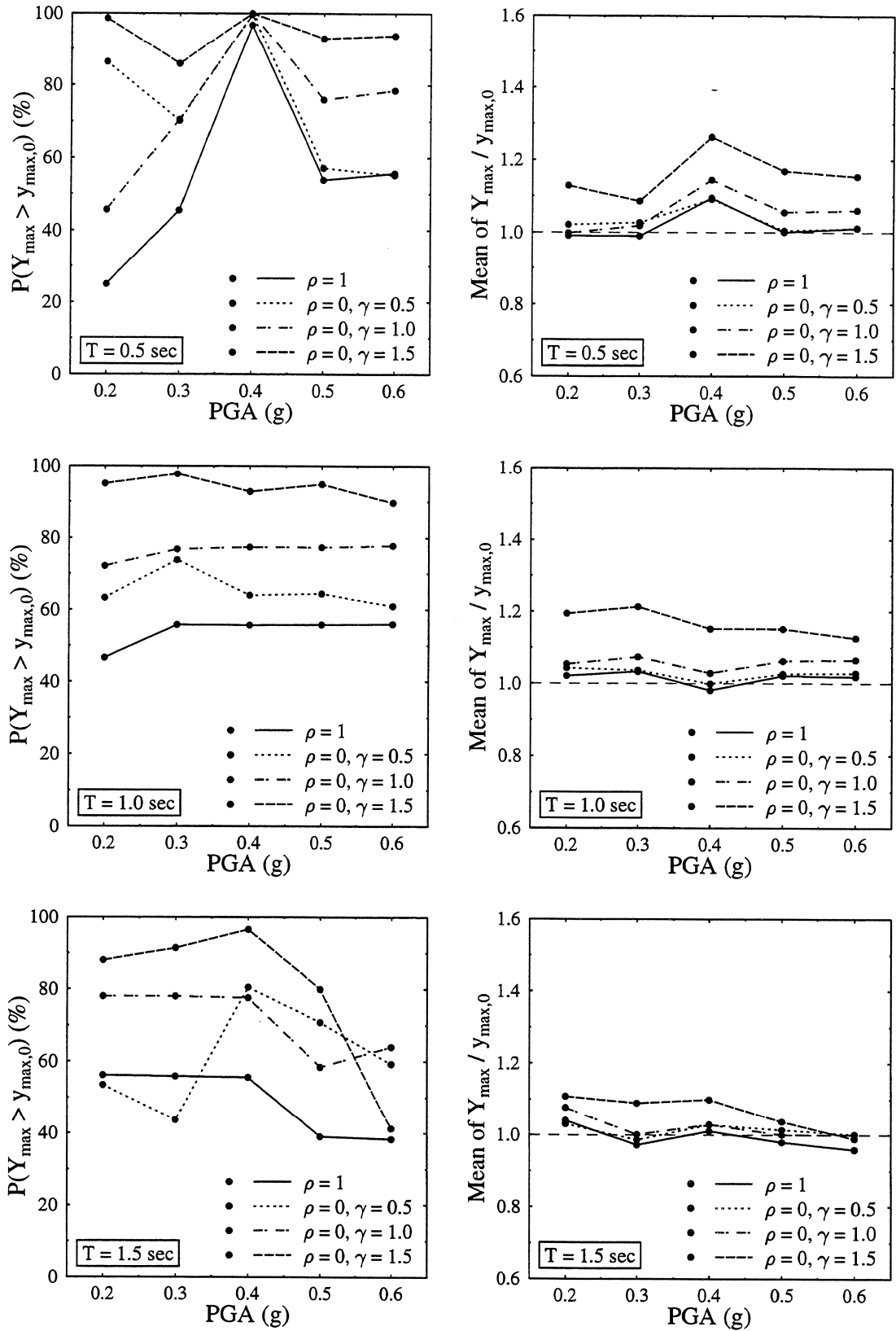
FIGURE 3-35 Comparison of Y_{max} and $y_{max,0}$. MC model. Input: El Centro.

72

FIGURE 3-36 Comparison of Y_{max} and $y_{max,0}$. MC model. Input: Taft.

FIGURE 3-37 Comparison of $Y_{\max}$ and $y_{\max,0}$. MC model. Input: Parkfield.
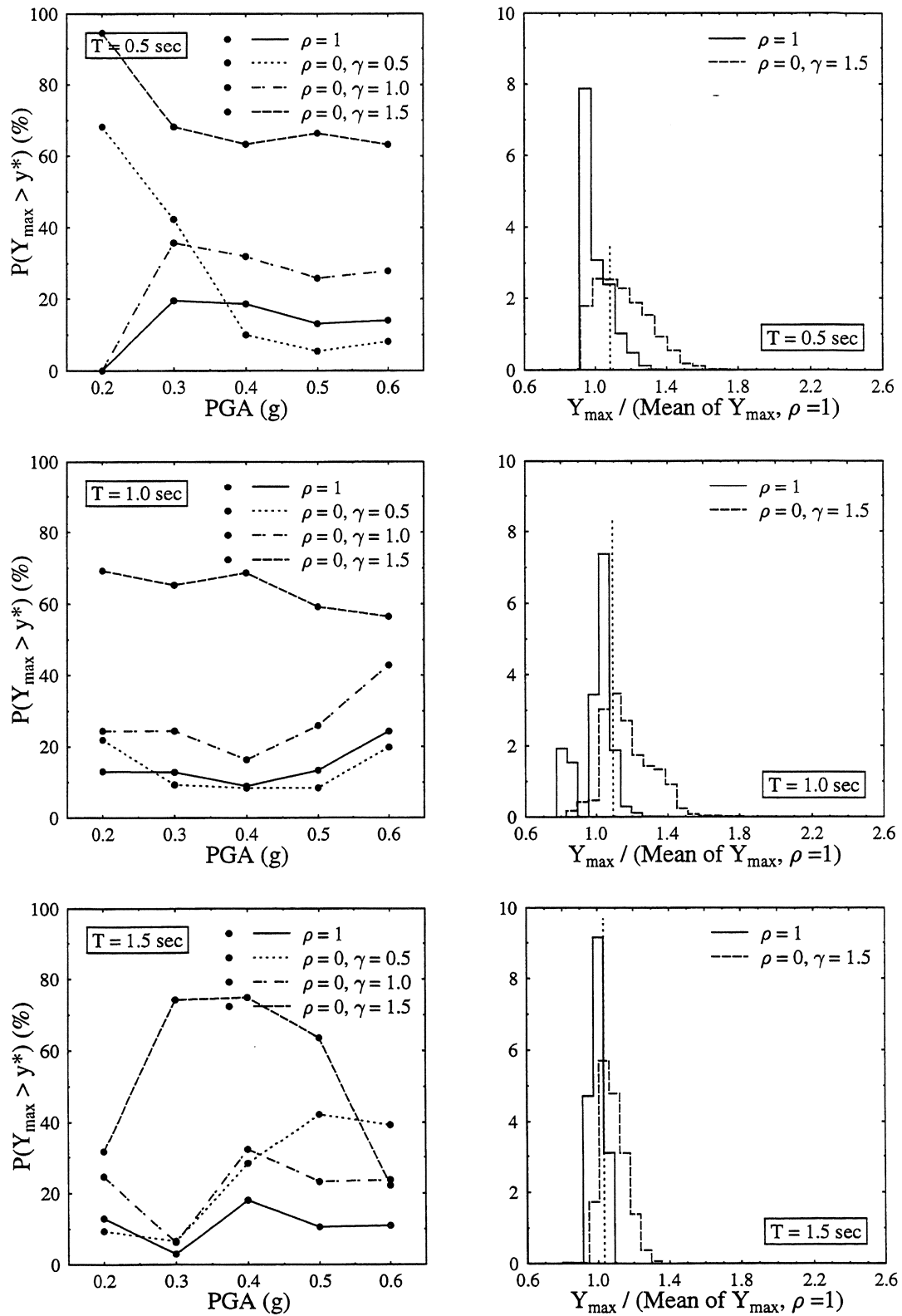
FIGURE 3-38 Probability of exceedence of level y^* and histograms of normalized maximum displacement. MC model. Input: El Centro.
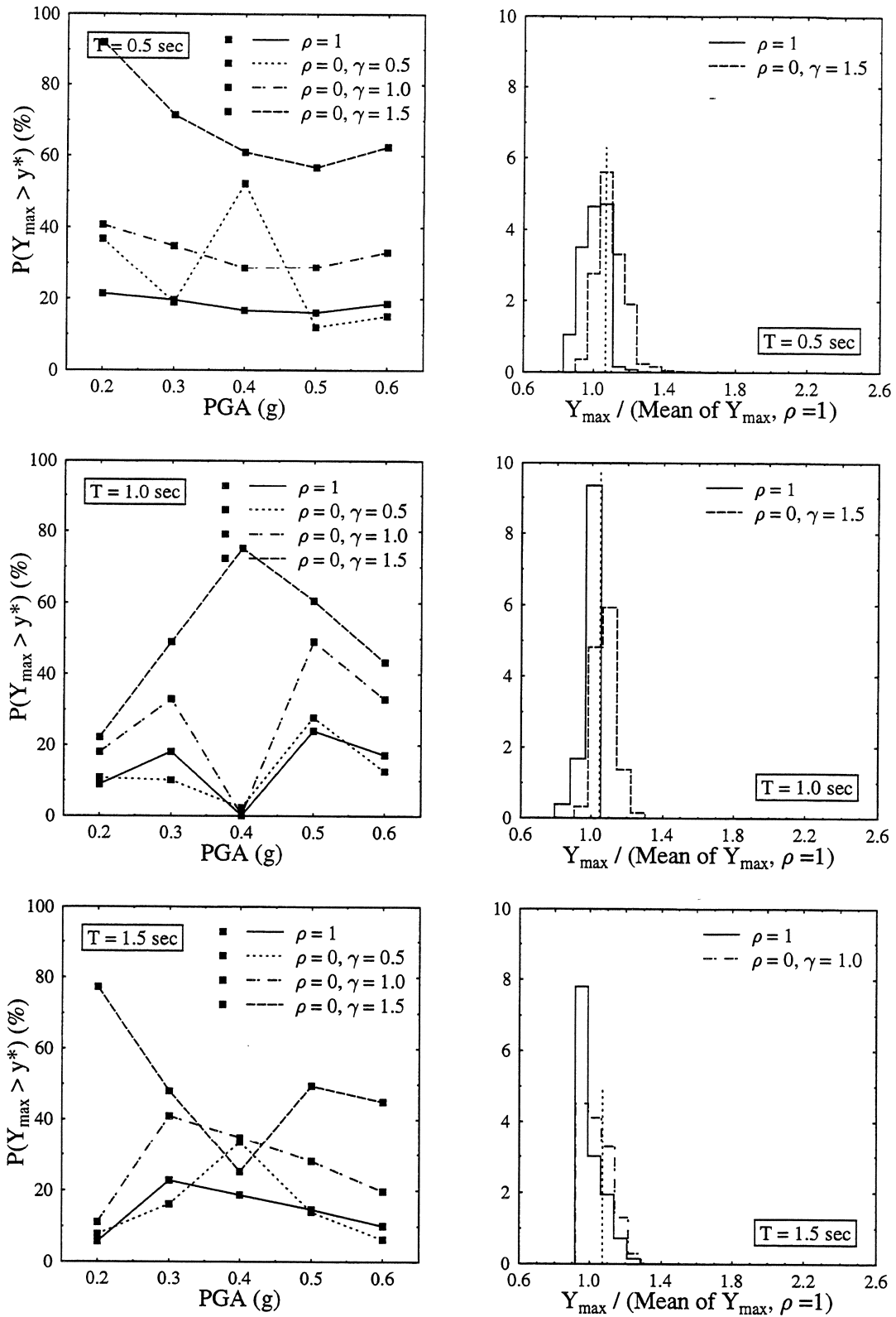
FIGURE 3-39 Probability of exceedence of level y^* and histograms of normalized maximum displacement. MC model. Input: Taft.
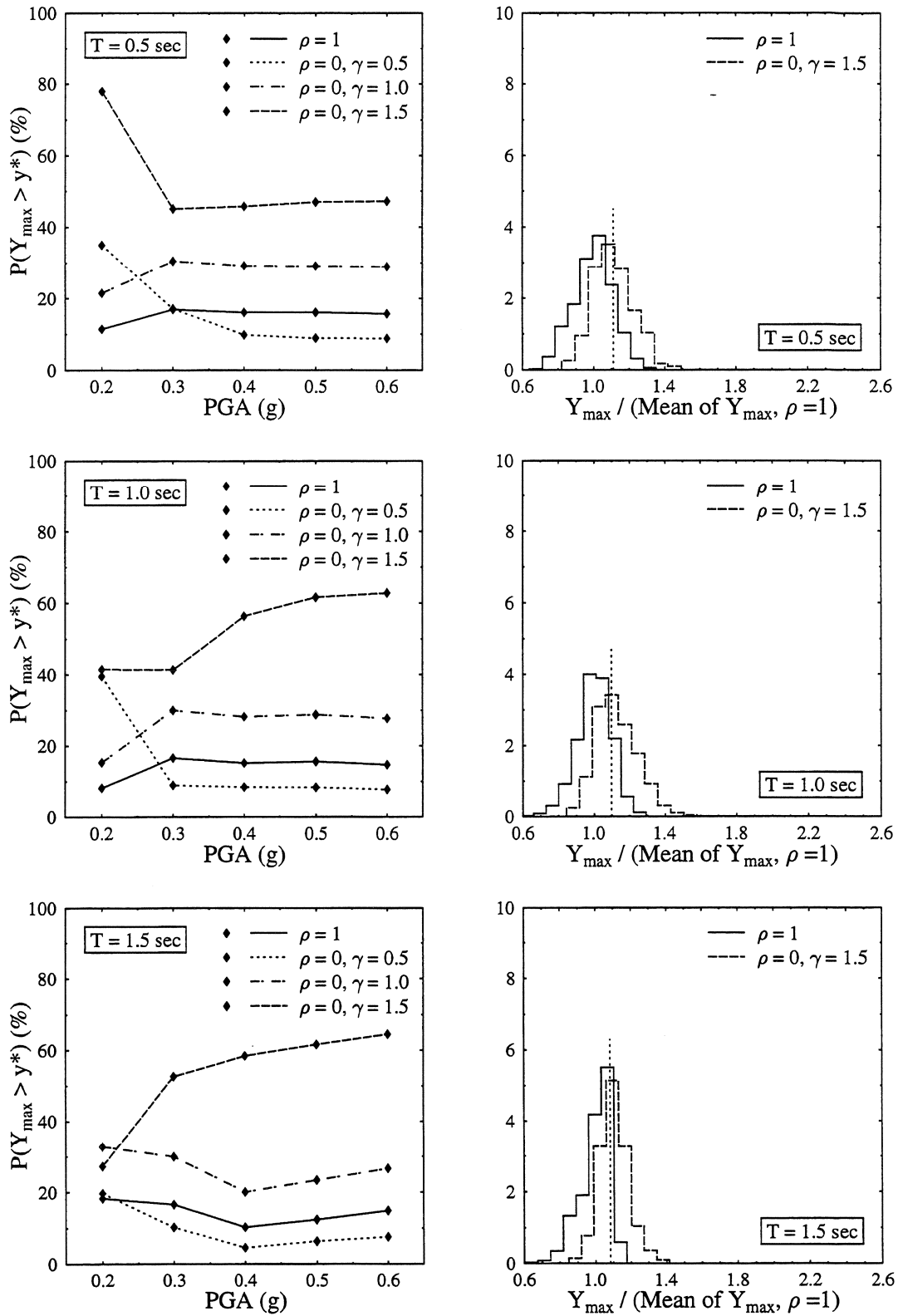
FIGURE 3-40 Probability of exceedence of level y^* and histograms of normalized maximum displacement. MC model. Input: Parkfield.

The vertical dotted line marks y^*. The histograms of systems with and without torsion differ considerably, more so for El Centro and Taft than for Parkfield.

Maximum ductility. The observations on the mean and coefficient of variation of Y_{max} transfer qualitatively to the maximum ductility M_{max}, except for the increase with the period which is reversed. Quantitatively, all the effects of uncertainty are amplified, as shown in Figures 3-41-3-43. The COV of M_{max} is about twice as high as the COV of Y_{max}.

The distribution of the maximum ductility is related to the ductility of the associated reference system $\mu_{max,0}$ by the graphs in Figures 3-44-3-46. These graphs show the probability the maximum ductility exceeds values given as multiples of $\mu_{max,0}$ and plotted on a logarithmic scale. The maximum ductility of a little more than half of the realizations of the symmetric systems exceeds $\mu_{max,0}$, but there is no significant probability of values over $2\mu_{max,0}$. The probability $P(M_{max} > \mu)$ generally increases in the presence of torsion albeit not always monotonically with γ. Ductilities over $2\mu_{max,0}$ have nonnegligible probability, especially for $\gamma = 1.5$, i.e., for the systems most susceptible to torsion. However, the probability of exceedence practically vanishes for $\mu > 3\mu_{max,0}$.

Dissipated energy. The mean of the dissipated energy E_{dis} is unaffected by torsional vibrations for all three motions considered, as can be seen in Figures 3-47-3-49. It decreases with the period whereas it increases in a practically linear relationship with PGA. The COV of E_{dis} is fairly low, exceeding 13% only for $T = 1.5$ sec and PGA $= 0.2g$, a case with mean very close to zero. Torsion decreases the COV of E_{dis} but the amount of the decrease appears insensitive to γ.

Figure 3-50 allows comparison of the mean and the COV of the energy dissipated by the symmetric system for different motions. The differences in the mean of E_{dis} are more pronounced for low periods. The COV of E_{dis} tends to increase with PGA for PGA $> 0.3g$.

Maximum rotation. Figures 3-51-3-53 show that, for all motions considered, the mean of the maximum rotation Φ_{max} increases with γ. The mean also exhibits a generally increasing trend with PGA whereas the effect of the period is unclear. The mean of Φ_{max} is considerably higher under Parkfield than under the other two input motions. The COV of Φ_{max} is very large with values mostly in the range 60%-80%.
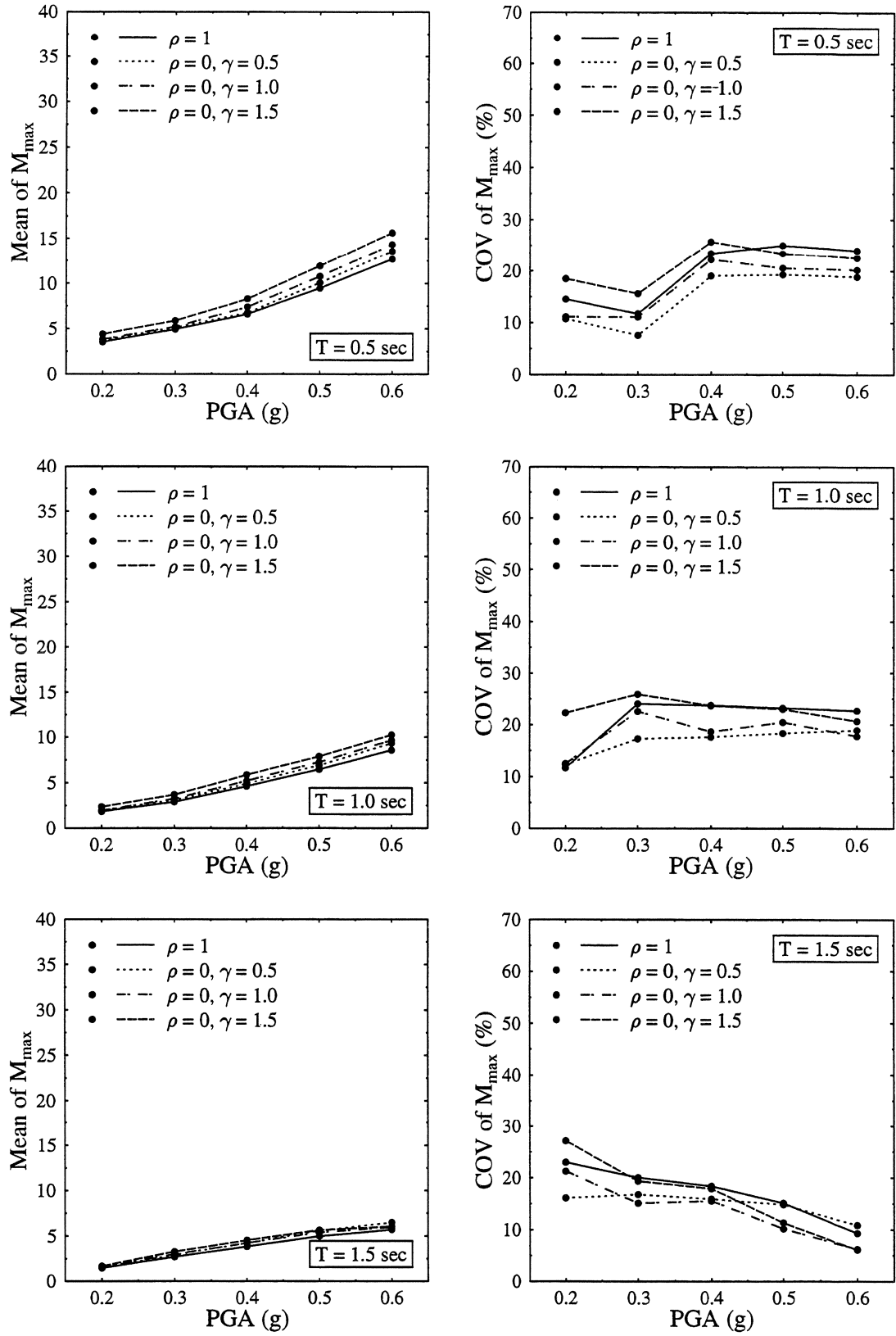
FIGURE 3-41 Mean and COV of M_{max}. MC model. Input: El Centro.
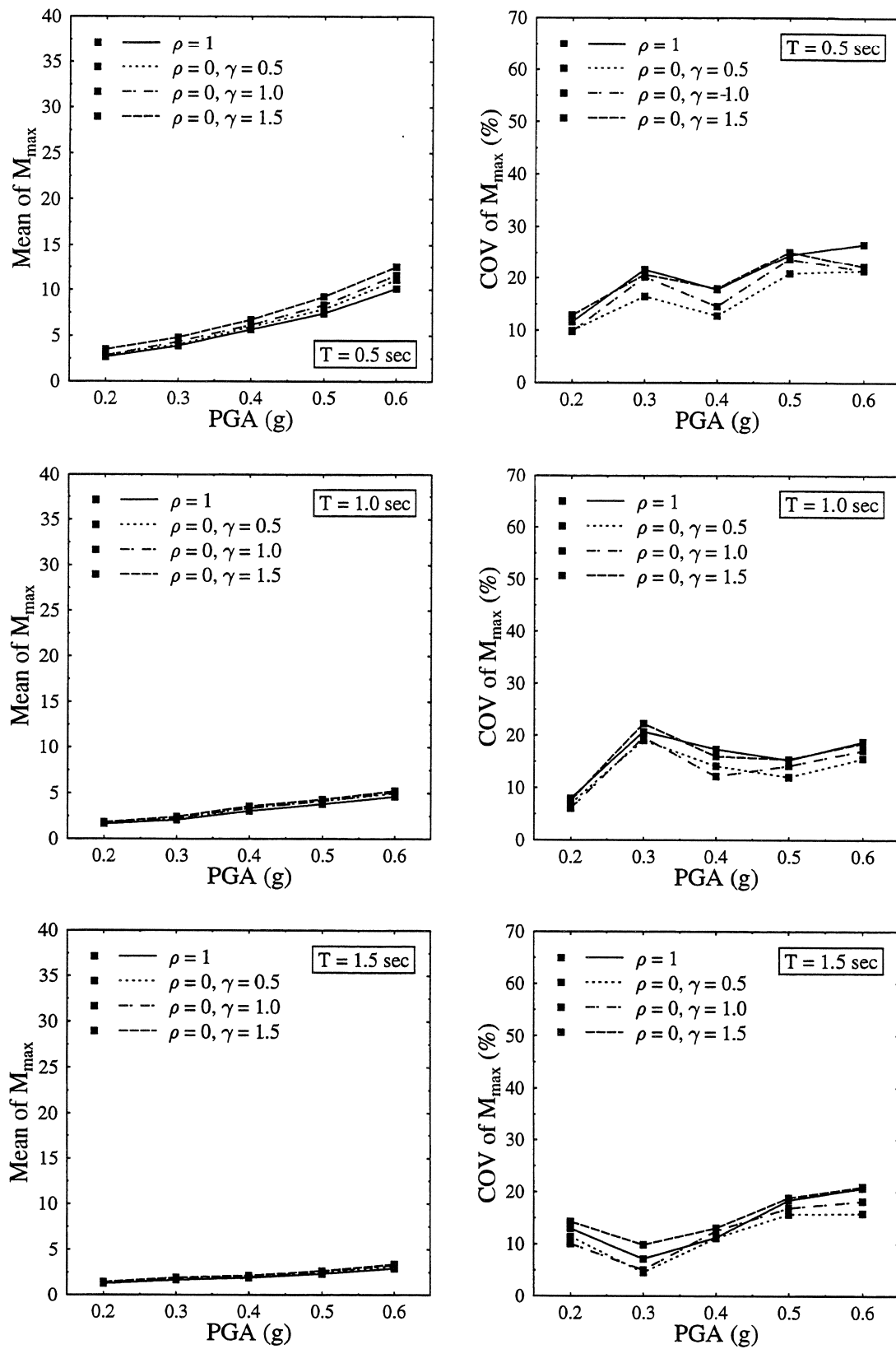
FIGURE 3-42 Mean and COV of M_{max}. MC model. Input: Taft.
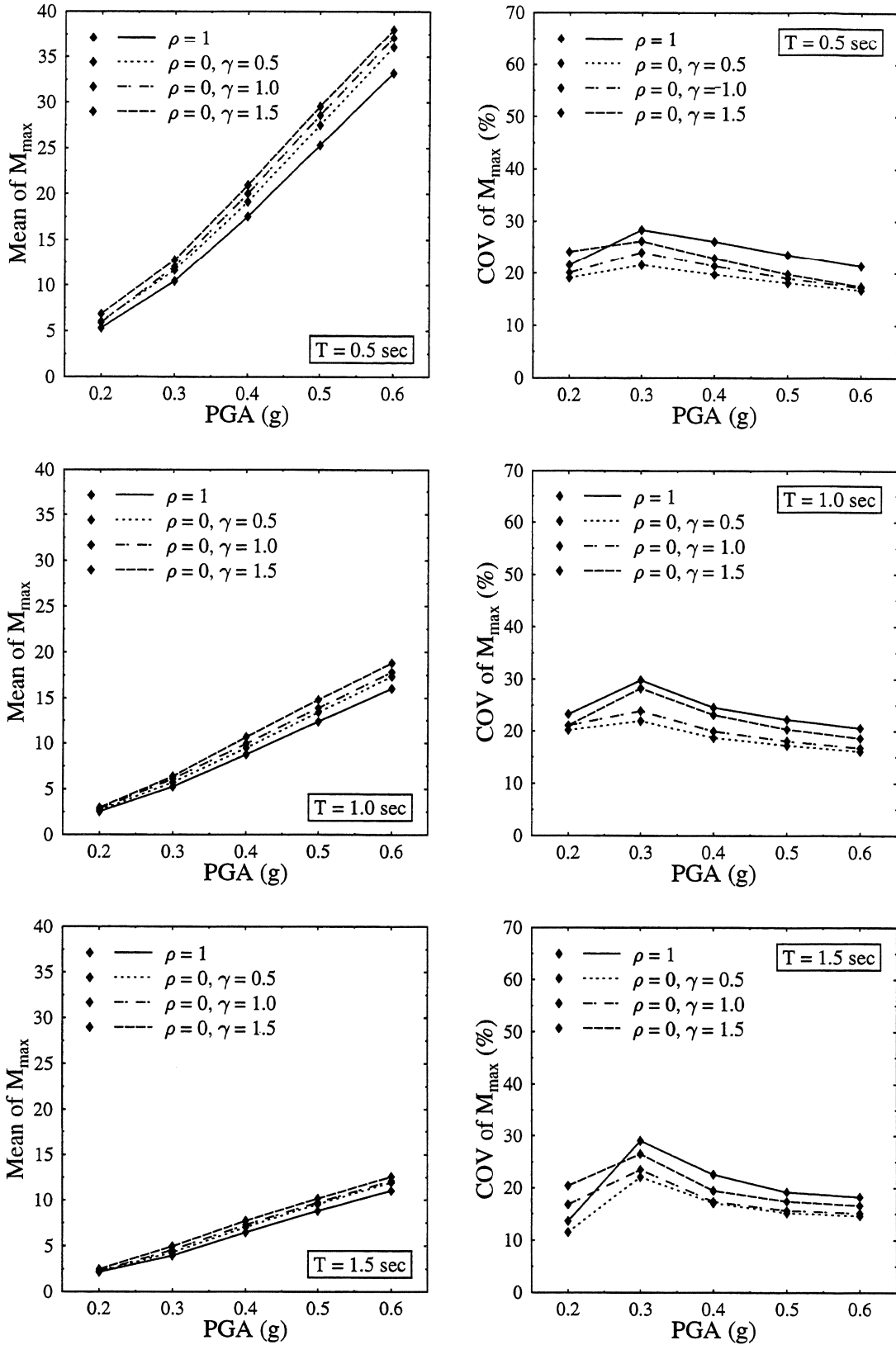
**FIGURE 3-43** Mean and COV of M_{max}. MC model. Input: Parkfield.
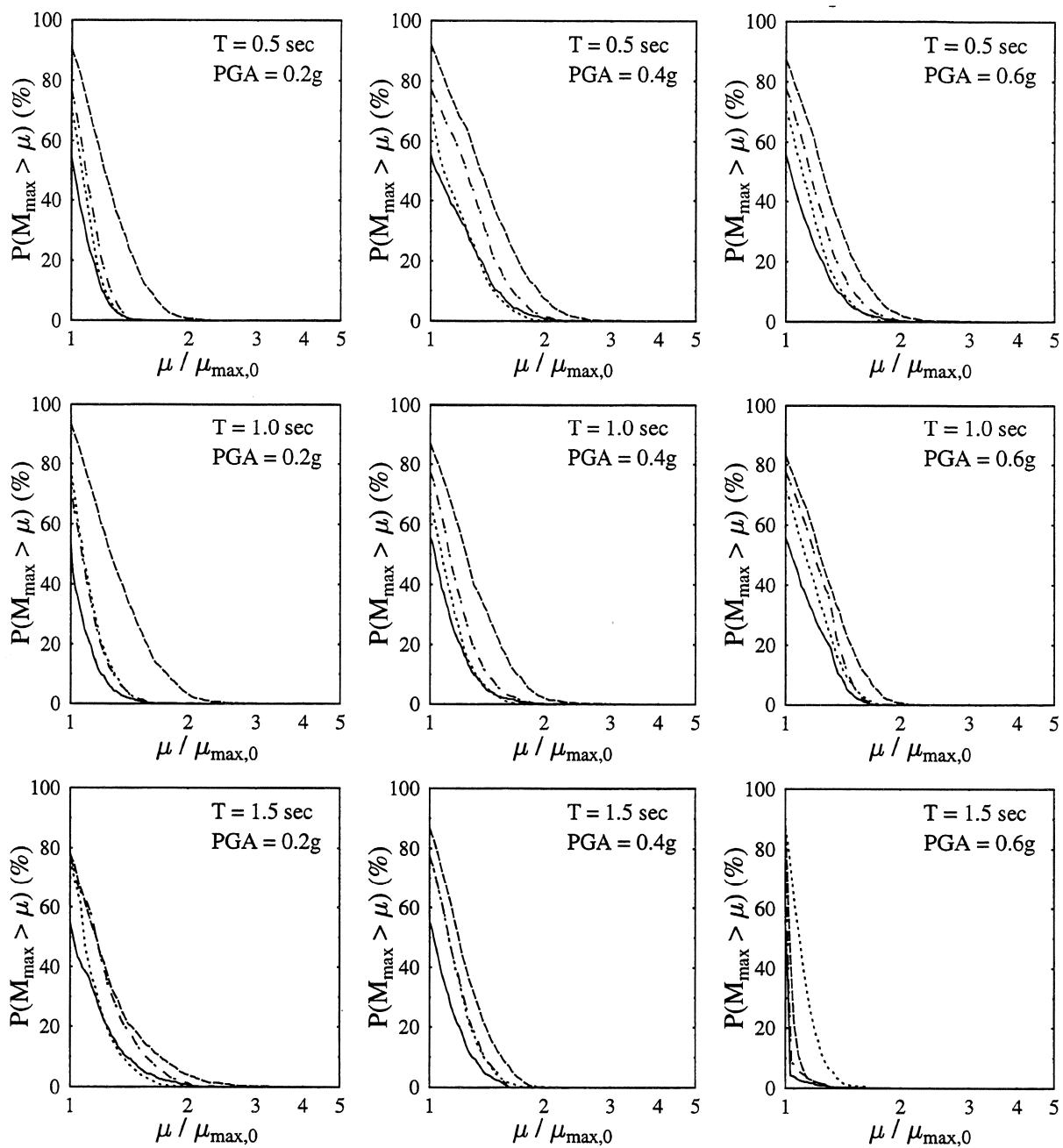
FIGURE 3-44 **Probability of** $M_{\max}$ **exceeding** $\mu_{\max,0}$. **MC model.** **Input:** **El Centro.** (——— $\rho = 1$; ····· $\rho = 0$, $\gamma = 0.5$; —·—· $\rho = 0$, $\gamma = 1.0$; — — — $\rho = 0$, $\gamma = 1.5$)
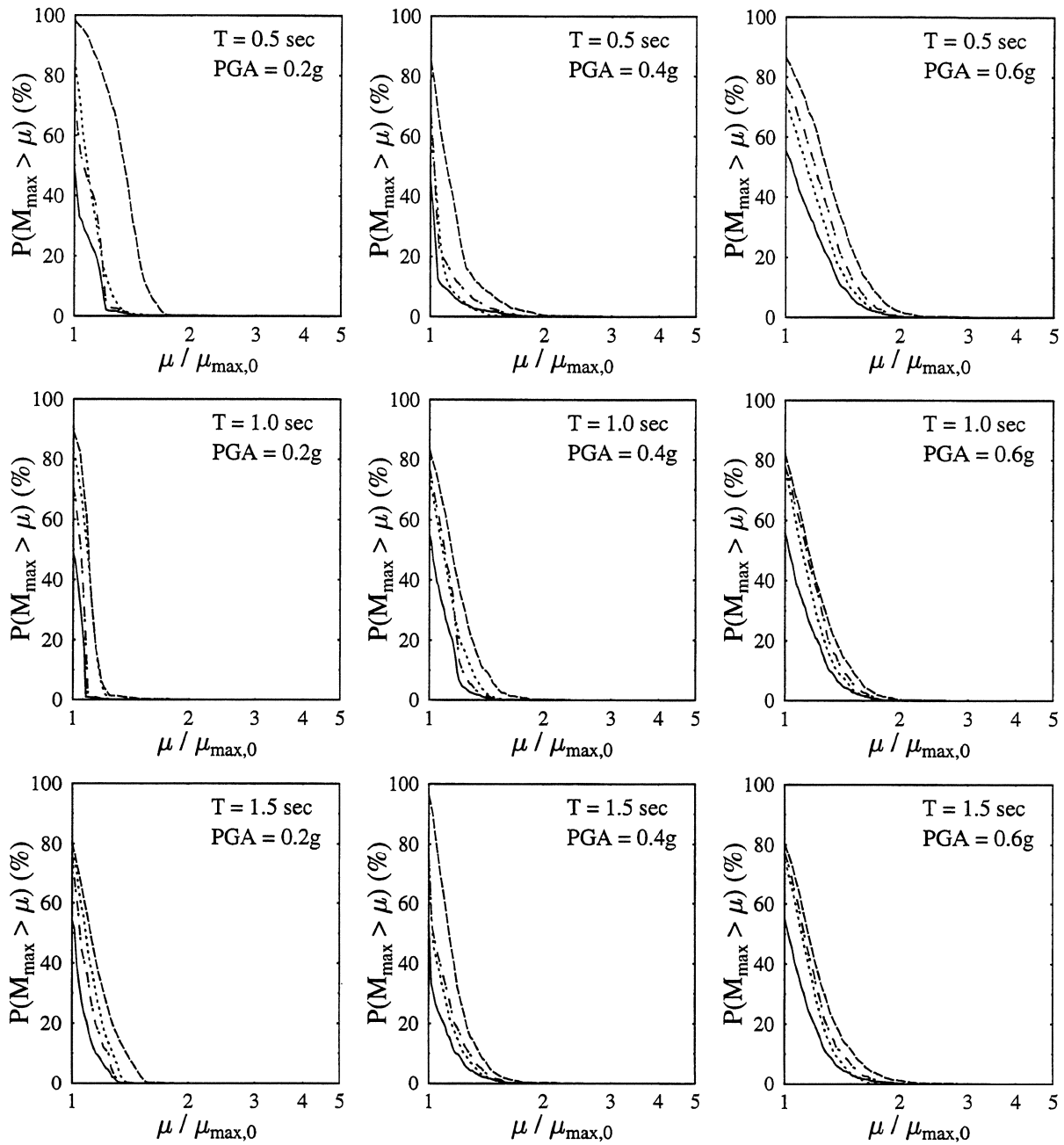
FIGURE 3-45 Probability of M_{max} exceeding $\mu_{max,0}$. MC model. Input: Taft.
(——— $\rho = 1$; $\cdots\cdots$ $\rho = 0$, $\gamma = 0.5$; —·—· $\rho = 0$, $\gamma = 1.0$; ——— $\rho = 0$, $\gamma = 1.5$)
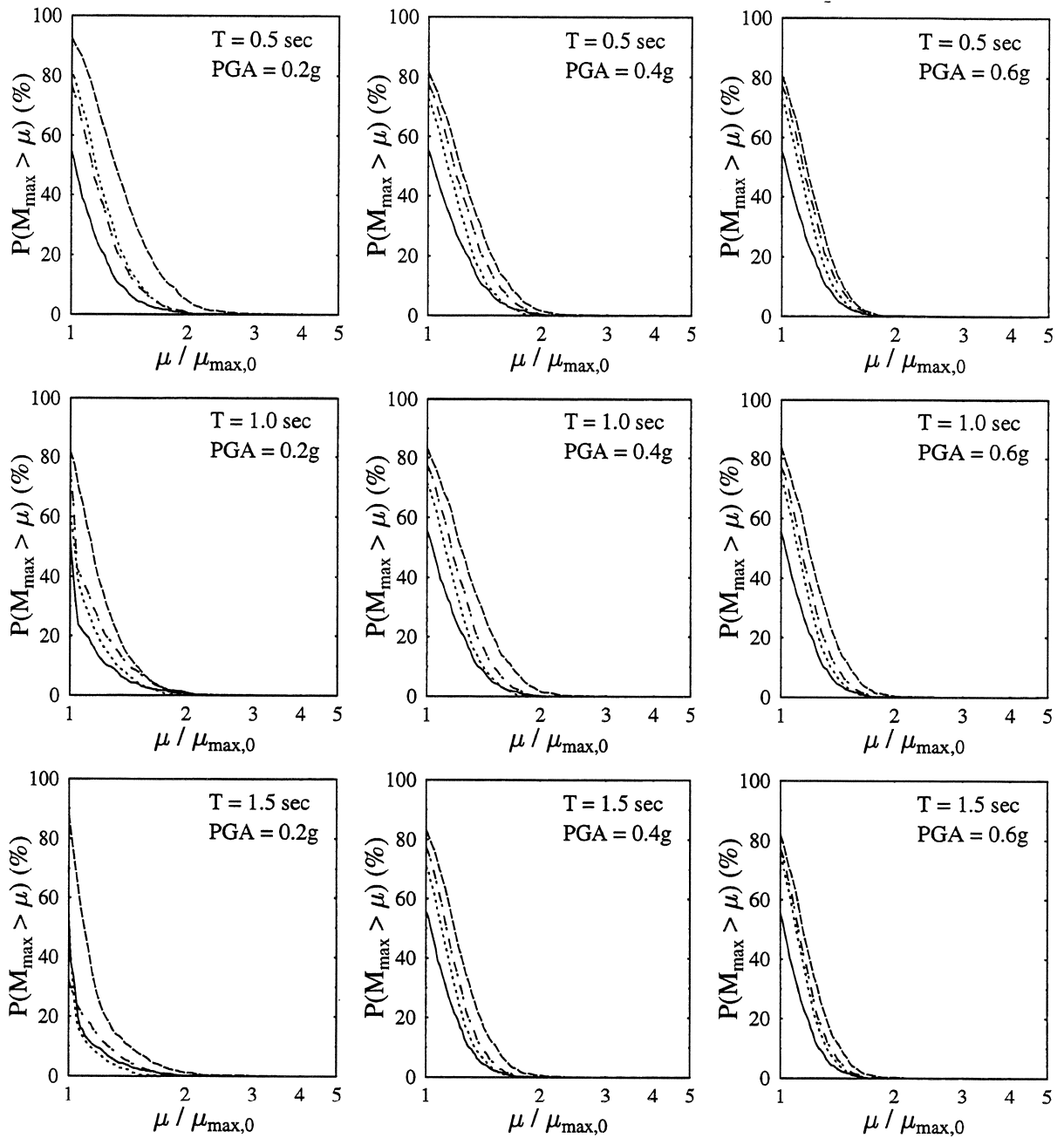
FIGURE 3-46 Probability of M_{max} exceeding $\mu_{max,0}$. MC model. Input: Parkfield. (——— $\rho = 1$; $\cdots\cdots$ $\rho = 0$, $\gamma = 0.5$; $-\cdot-\cdot$ $\rho = 0$, $\gamma = 1.0$; $---$ $\rho = 0$, $\gamma = 1.5$)
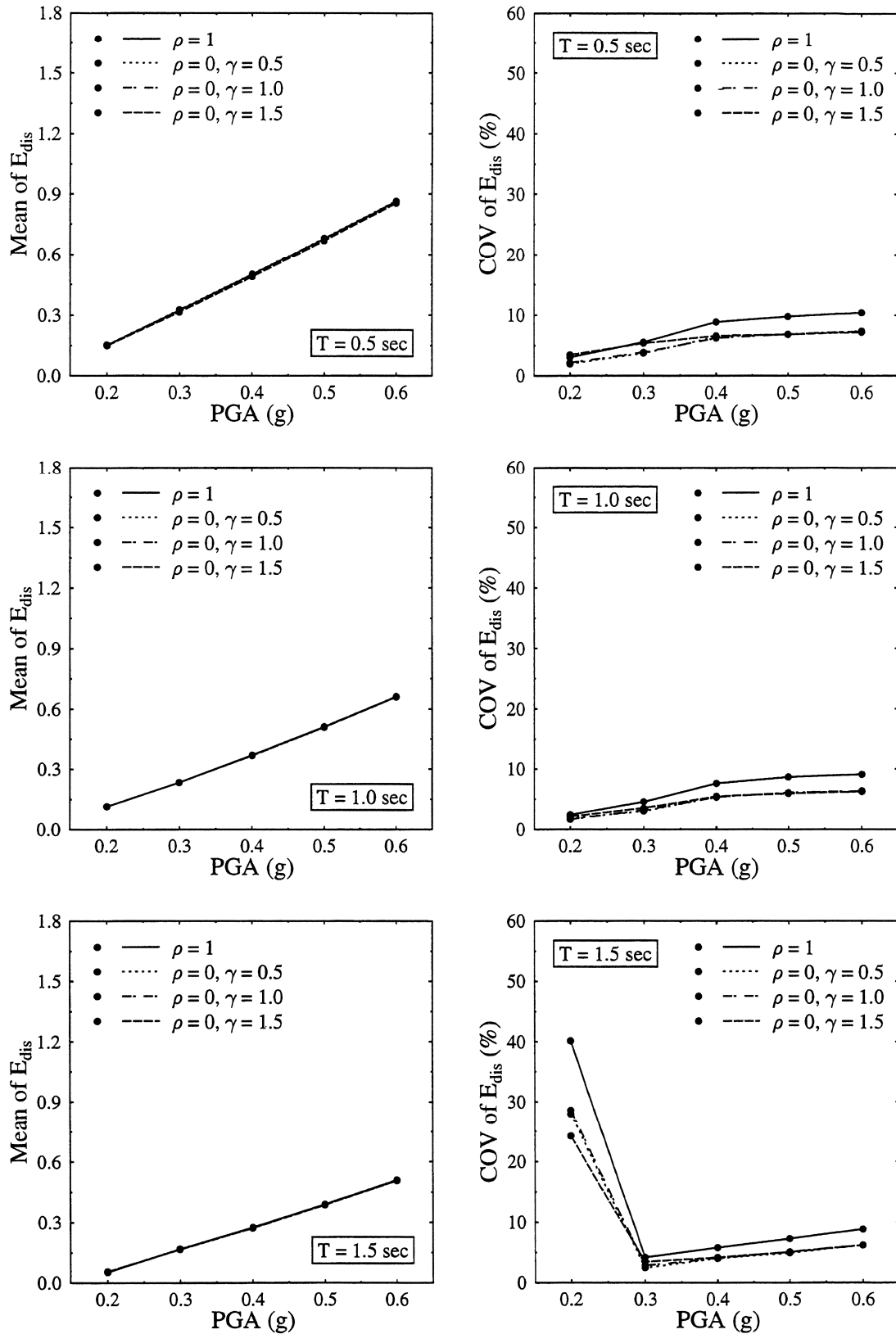
FIGURE 3-47 Mean and COV of E_{dis}. MC model. Input: El Centro.
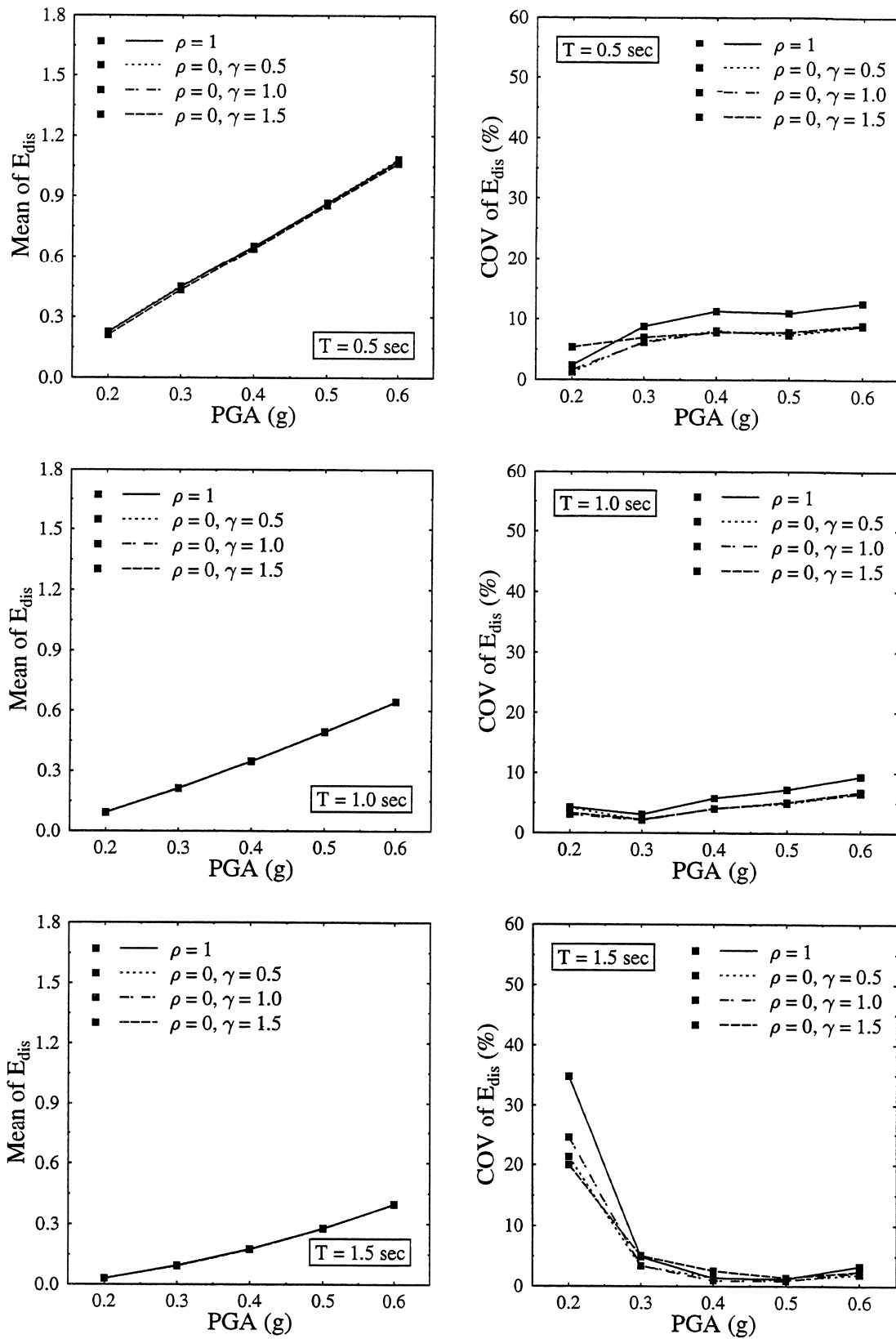
FIGURE 3-48 Mean and COV of E_{dis}. MC model. Input: Taft.

86
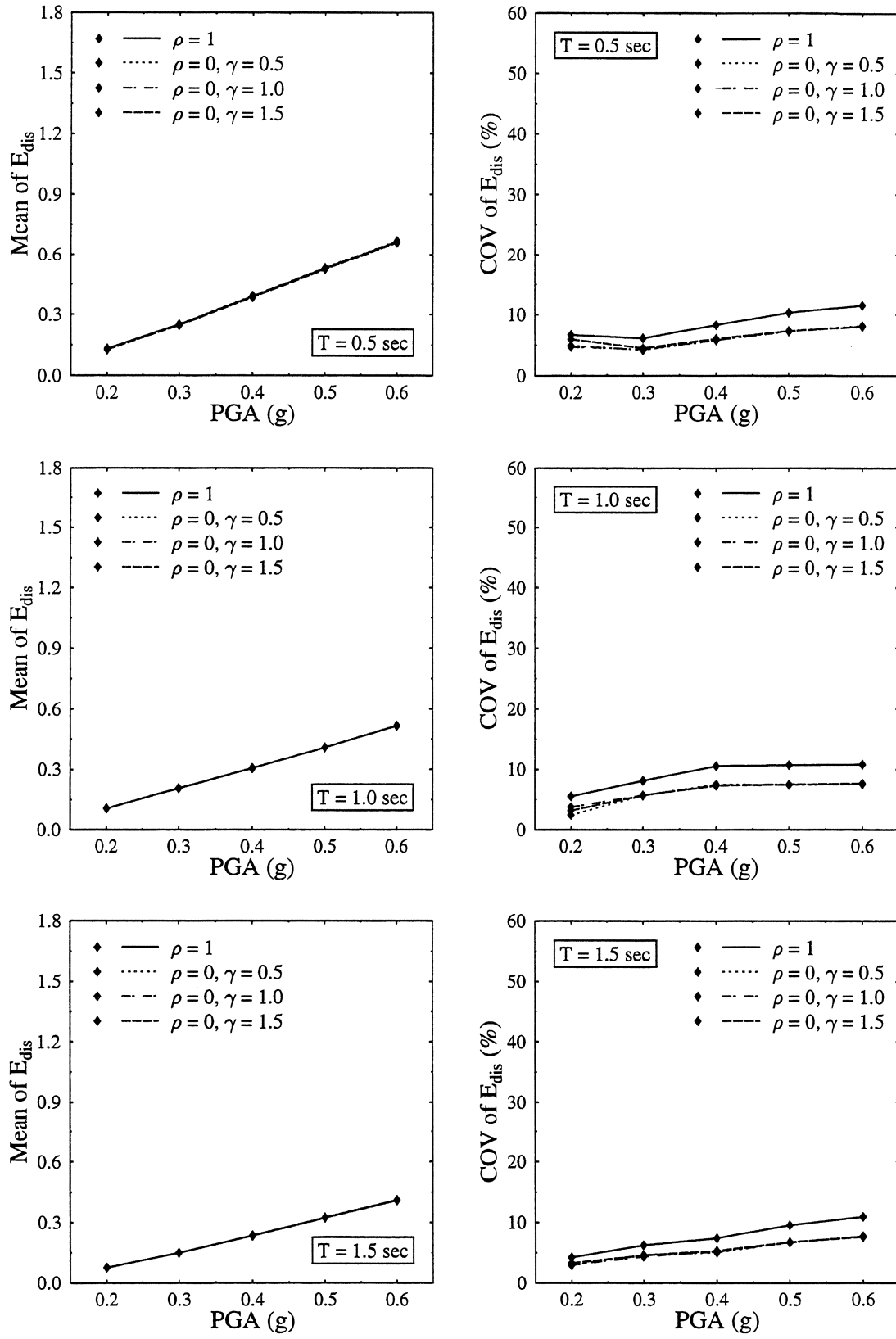
**FIGURE 3-49** Mean and COV of E_{dis}. MC model. Input: Parkfield.

87
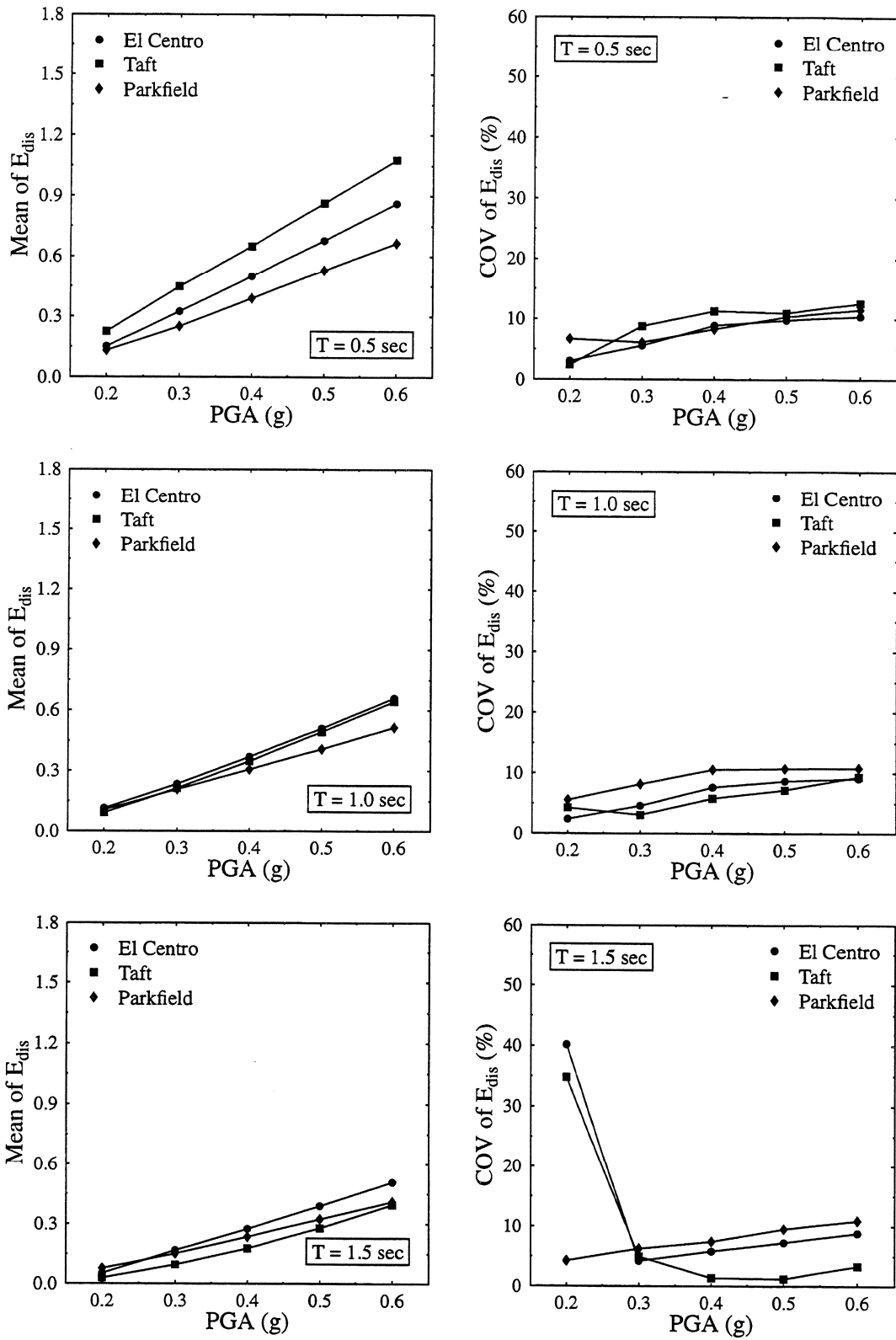
FIGURE 3-50 Mean and COV of E_{dis} for perfectly correlated yield strengths. MC model.
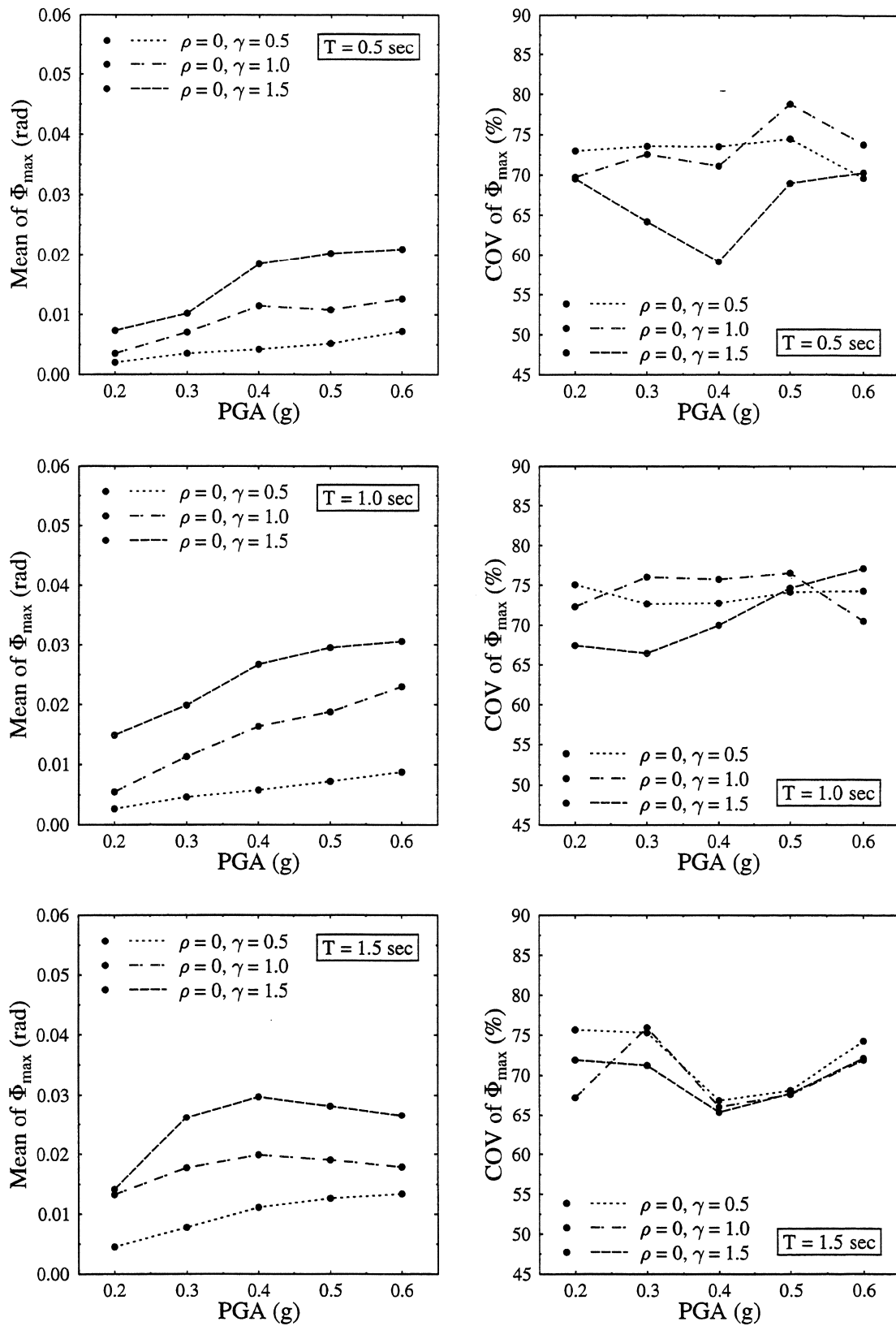
**FIGURE 3-51** Mean and COV of Φ_{max}. MC model. Input: El Centro.

89
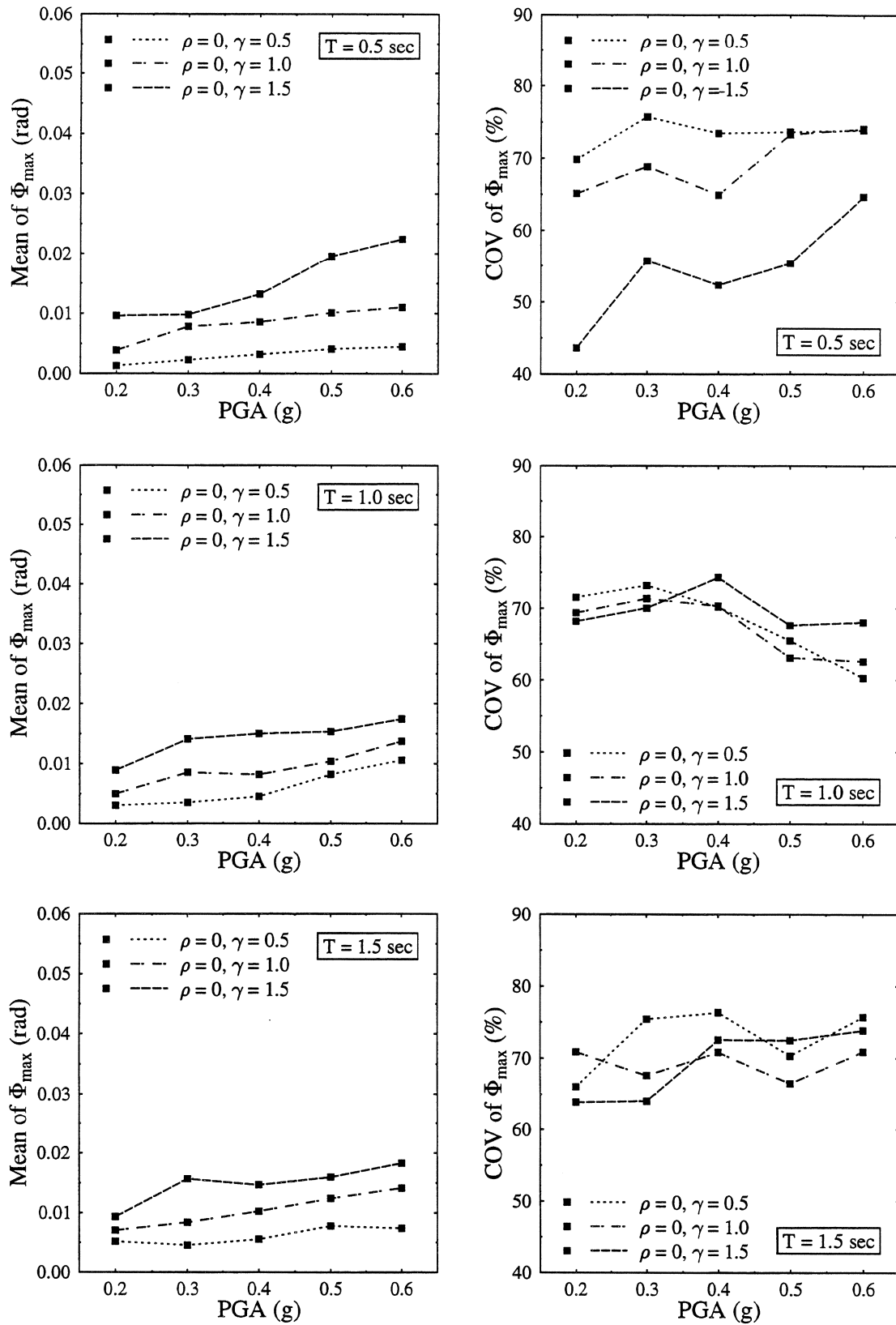
FIGURE 3-52 Mean and COV of Φ_{max}. MC model. Input: Taft.

90

FIGURE 3-53 Mean and COV of $\Phi_{\max}$. MC model. Input: Parkfield.

3.4.3 Model uncertainty. Perfectly correlated yield strengths

When the element yield strengths are perfectly correlated every realization of the structure is symmetric and experiences only translational vibrations. Therefore this section essentially deals with the sensitivity of the seismic response of a SDOF system to the uncertainty in the restoring force model. Figures 3-54, 3-55, and 3-56 include plots of the mean and the COV of the maximum displacement Y_{max}, the maximum ductility M_{max}, and the dissipated energy E_{dis}, for both the elastoplastic (EP) and the modified-Clough (MC) model, and input the El Centro, Taft, and Parkfield records, respectively. The statistics are obtained from the response of 1000 system realizations for each parameter combination.

Maximum displacement. The mean of the maximum displacement Y_{max} increases with the PGA and the period T, as expected. Under El Centro no general trend for the effect of model selection on the mean of Y_{max} is discernible. Under Taft the mean maximum displacement is consistently lower for the MC model. The same is true under Parkfield only for $T = 0.5$ sec, whereas for the other two periods considered the mean of Y_{max} appears insensitive to the model selection.

The coefficient of variation of Y_{max} exhibits the same trends under the two motions of the same type, El Centro and Taft, and markedly different trends under Parkfield. Specifically, under El Centro and Taft, and for periods of 0.5 and 1.0 sec the COV is lower for the modified-Clough than for the elastoplastic model and the difference can be quite significant. For instance, the COV of Y_{max} for $T = 0.5$ sec and input the El Centro record scaled to PGA $= 0.4g$ is 22.4% for the elastoplastic but only 8.4% for the modified-Clough model. For $T = 1.5$ sec there is no consistent trend. Under Parkfield the COV of Y_{max} is lower for the elastoplastic model for all periods and PGA $\geq 0.3g$. However, the difference between models is insignificant for the two longer periods. This last trend is also present in the histograms of the maximum displacement included in Figures 3-16 and 3-40.

The insensitivity of the maximum displacement to the selection of restoring force model for systems with $T = 1.0$ and 1.5 sec subjected to the Parkfield record scaled to PGA $\geq 0.3g$ results from the nature of this record. The strong acceleration pulses are located very close to the beginning of the strong motion portion of the record (see Figure 3-5). The time history of the response reveals that for systems with relatively long periods maximum displacement is reached at the end of the first significant inelastic excursion, until which point stiffness degradation has only minor effect, if any, on the response. As the period of
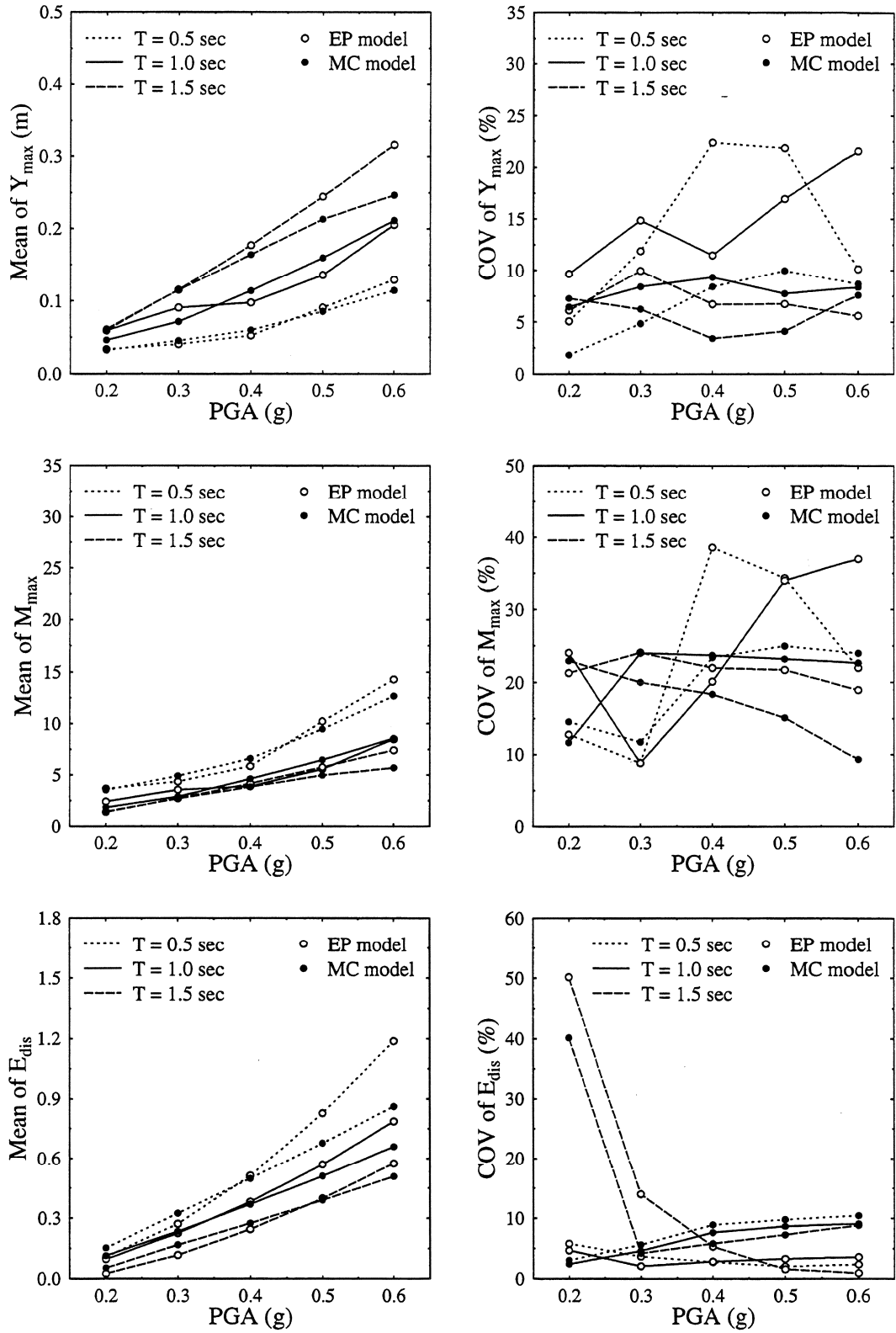
FIGURE 3-54 Mean and COV of $Y_{\max}$, $M_{\max}$, and E_{dis} for perfectly correlated yield strengths. Input: El Centro.
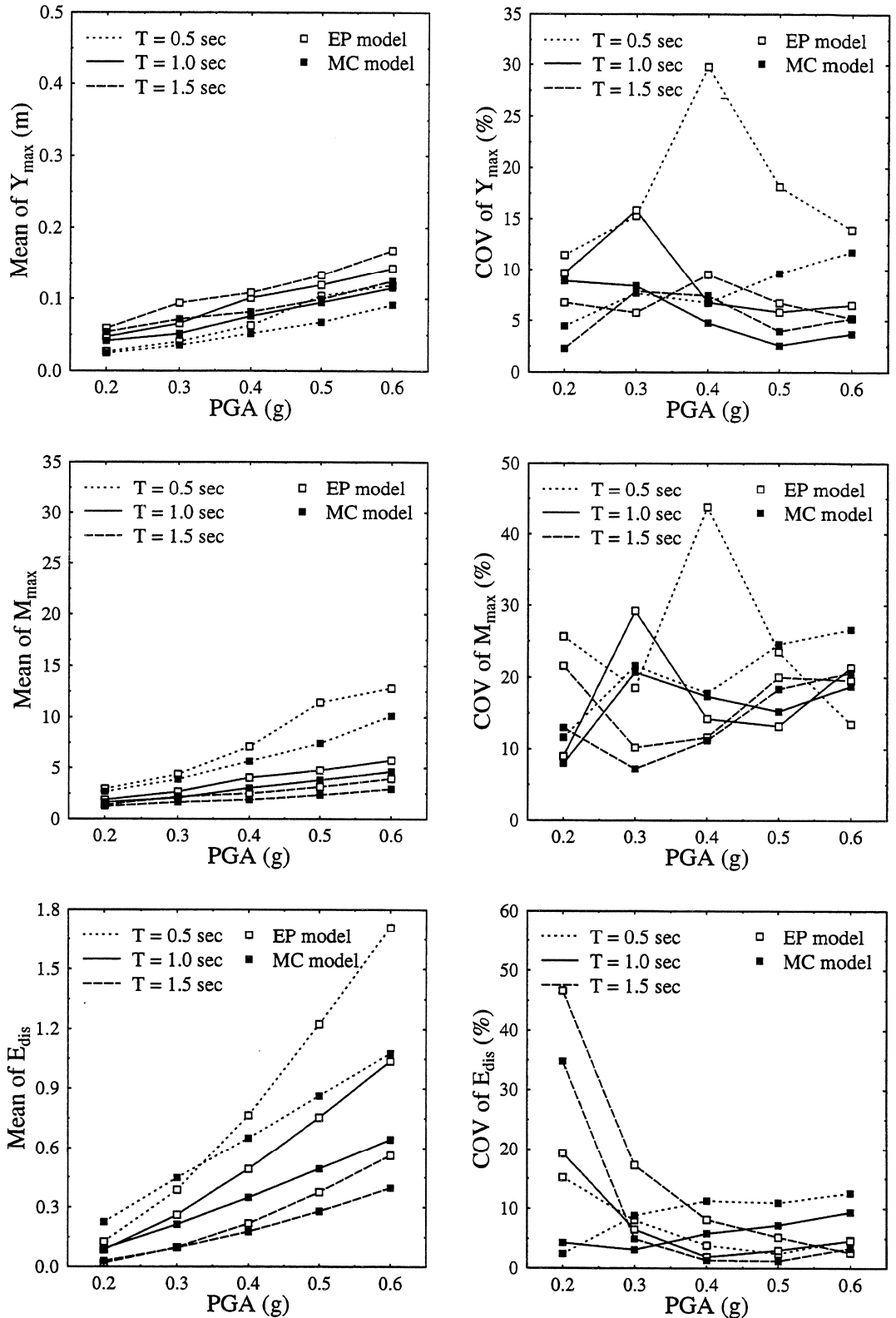
FIGURE 3-55 Mean and COV of Y_{max}, M_{max}, and E_{dis} for perfectly correlated yield strengths. Input: Taft.

94
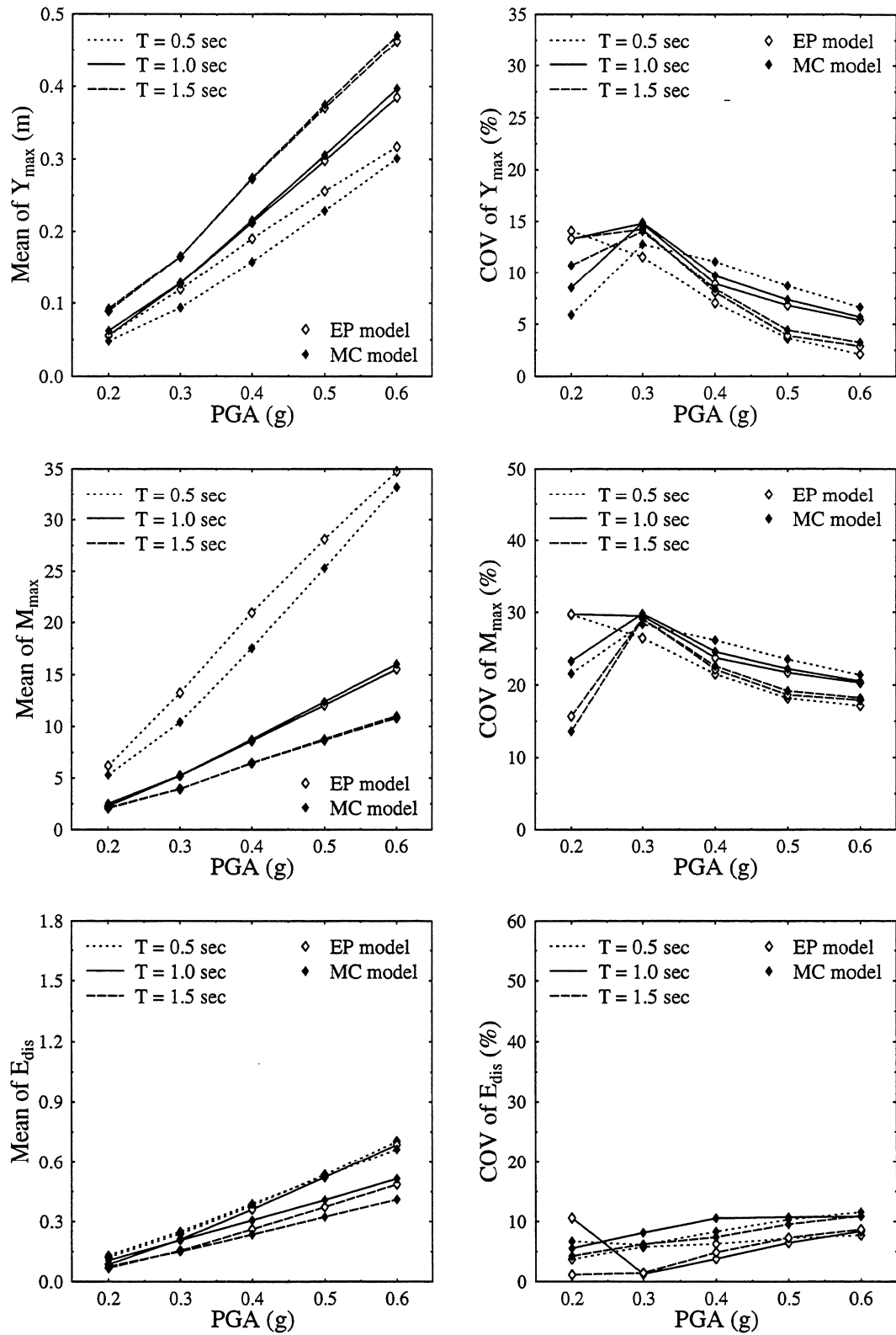
FIGURE 3-56 Mean and COV of Y_{max}, M_{max}, and E_{dis} for perfectly correlated yield strengths. Input: Parkfield.

95

the system gets shorter several inelastic excursions take place before maximum displacement is achieved and by that time the difference in the response becomes significant, as shown by the results for $T = 0.5$ sec.

Maximum ductility. The mean of the maximum ductility M_{max} increases with the peak ground acceleration but decreases with the period. Restoring force model selection affects the maximum ductility in the same way as the maximum displacement. Generally, much higher coefficients of variation are associated with the maximum ductility than with the maximum displacement, due to the scaling with the yield displacement which is also a random quantity.

Dissipated energy. The mean of the dissipated energy E_{dis} consistently increases with PGA and decreases with T. A possible explanation for the latter is that, as indicated by the mean of M_{max}, the higher period systems see relatively less inelastic action. This combined with the fact that the same systems undergo fewer hysteretic cycles explains the reduced energy dissipation. For small PGA values the MC model dissipates more energy on the average but the situation is reversed as the PGA increases (see graphs at bottom left of Figures 3-54–3-56). The differences in the mean of E_{dis} are more pronounced for larger PGA values. However, for El Centro and Taft, they diminish with increasing period. The COV of E_{dis} tends to be larger for the EP model for low PGA values but as the PGA increases the situation is reversed.

Displacement and energy ratios. Two ratios are defined to quantify the effect of model uncertainty: (1) The ratio $R_d = Y_{max,MC}/Y_{max,EP}$ for every sample, where $Y_{max,MC}$ and $Y_{max,EP}$ are the maximum displacements of two systems with identical elastic properties and yield strength but following the modified-Clough and the elasto-plastic model,respectively and (2) a similar ratio, R_e, for the dissipated energy. Both ratios are random variables. When the response of the system with MC model exceeds that of the system with EP model the ratio is larger than unity. Note that $R_d - 1 = (Y_{max,MC} - Y_{max,EP})/Y_{max,EP}$ which is the relative error in the maximum displacement if the EP model is selected over the MC. Moreover, for symmetric systems $Y_{max,MC}/Y_{max,EP}$ coincides with $M_{max,MC}/M_{max,EP}$. The last observation does not apply to systems with independent yield strengths because the maximum displacement is not necessarily associated with the same element for both restoring force models.

The graphs in each of Figures 3-57–3-59 show the mean, denoted by a thicker line, and a range of one standard deviation around it for R_d on the left and R_e on the right. The
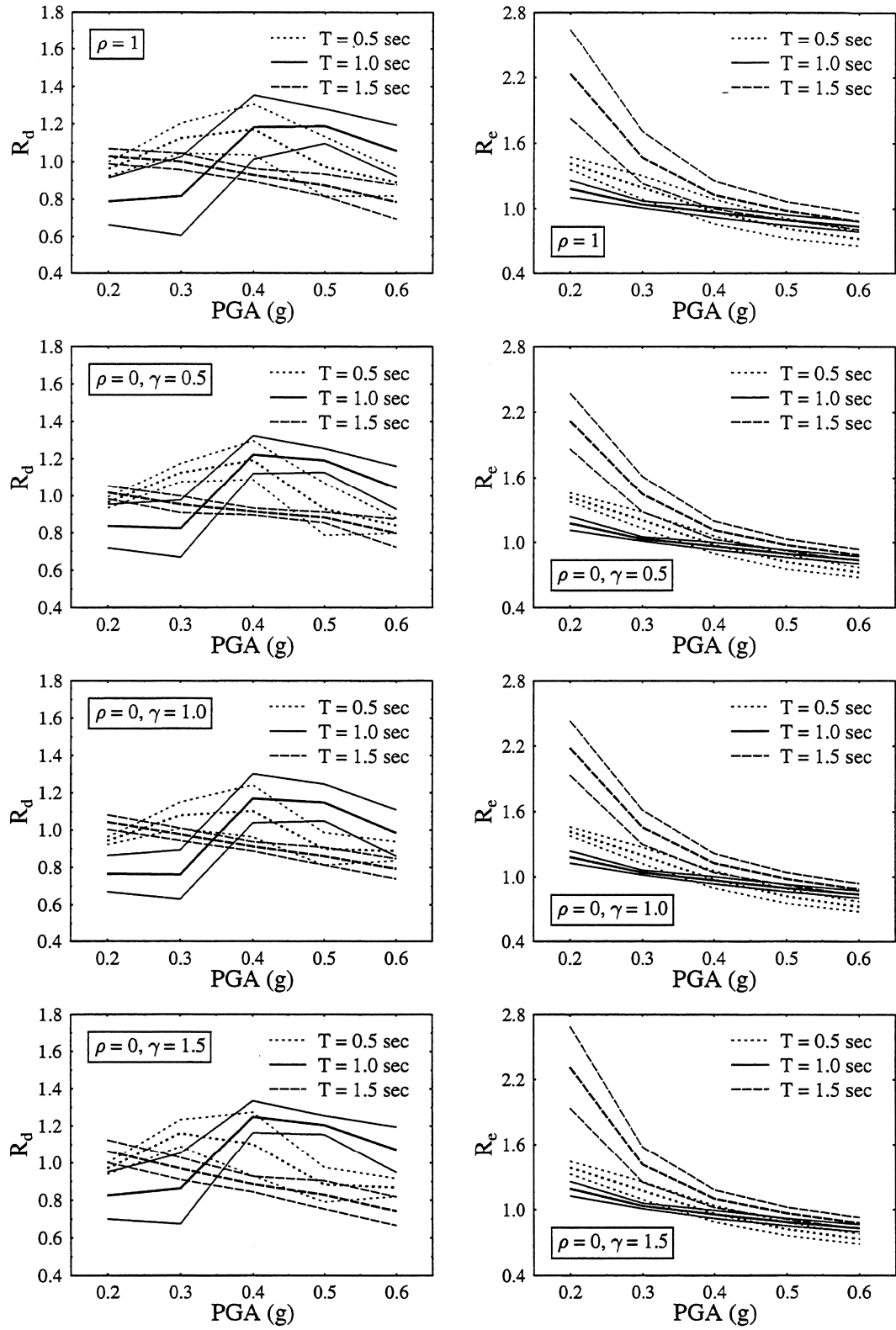
FIGURE 3-57 **Ratios of response measures of MC to EP models. Input: El Centro.**
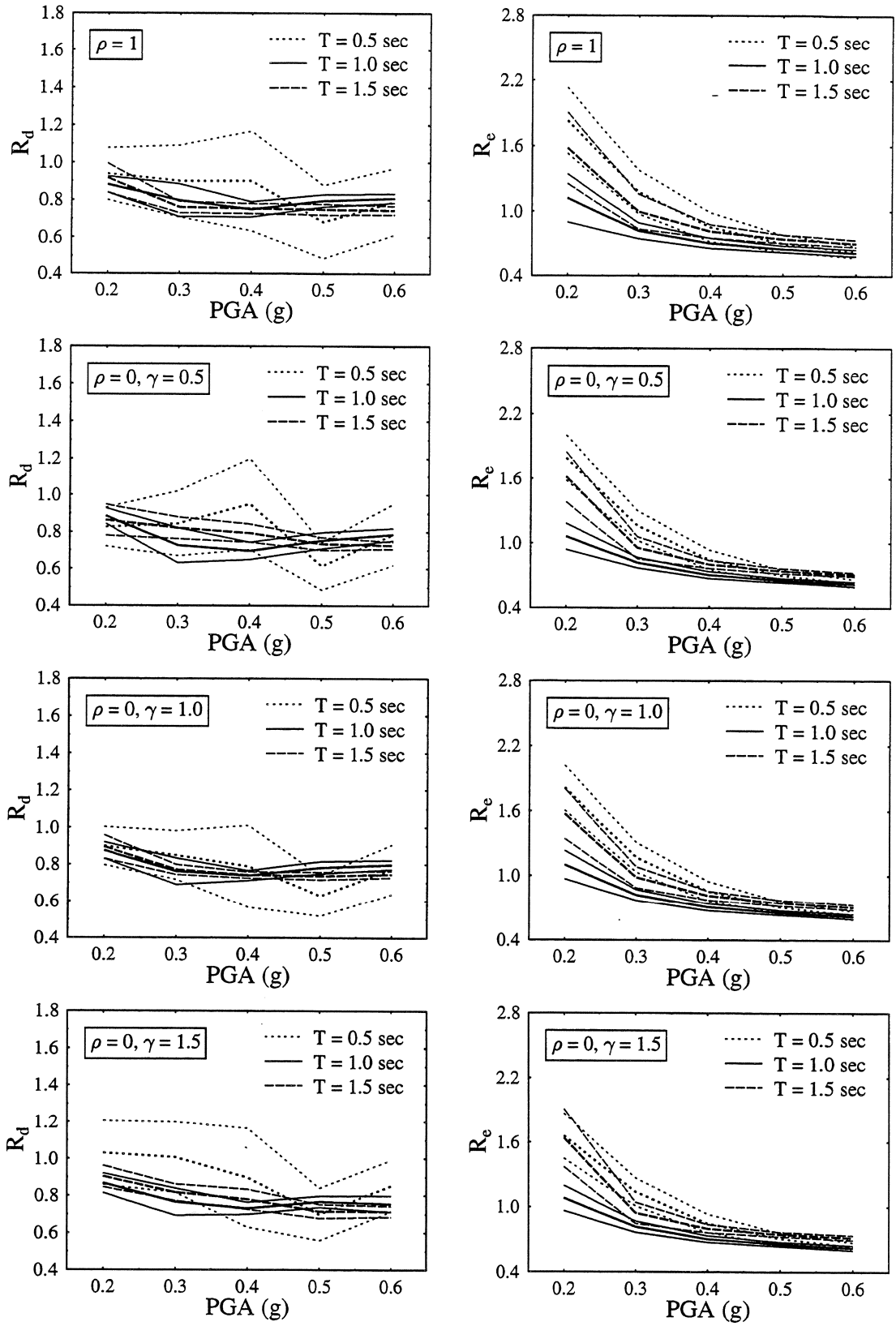
FIGURE 3-58 Ratios of response measures of MC to EP models. Input: Taft.

98
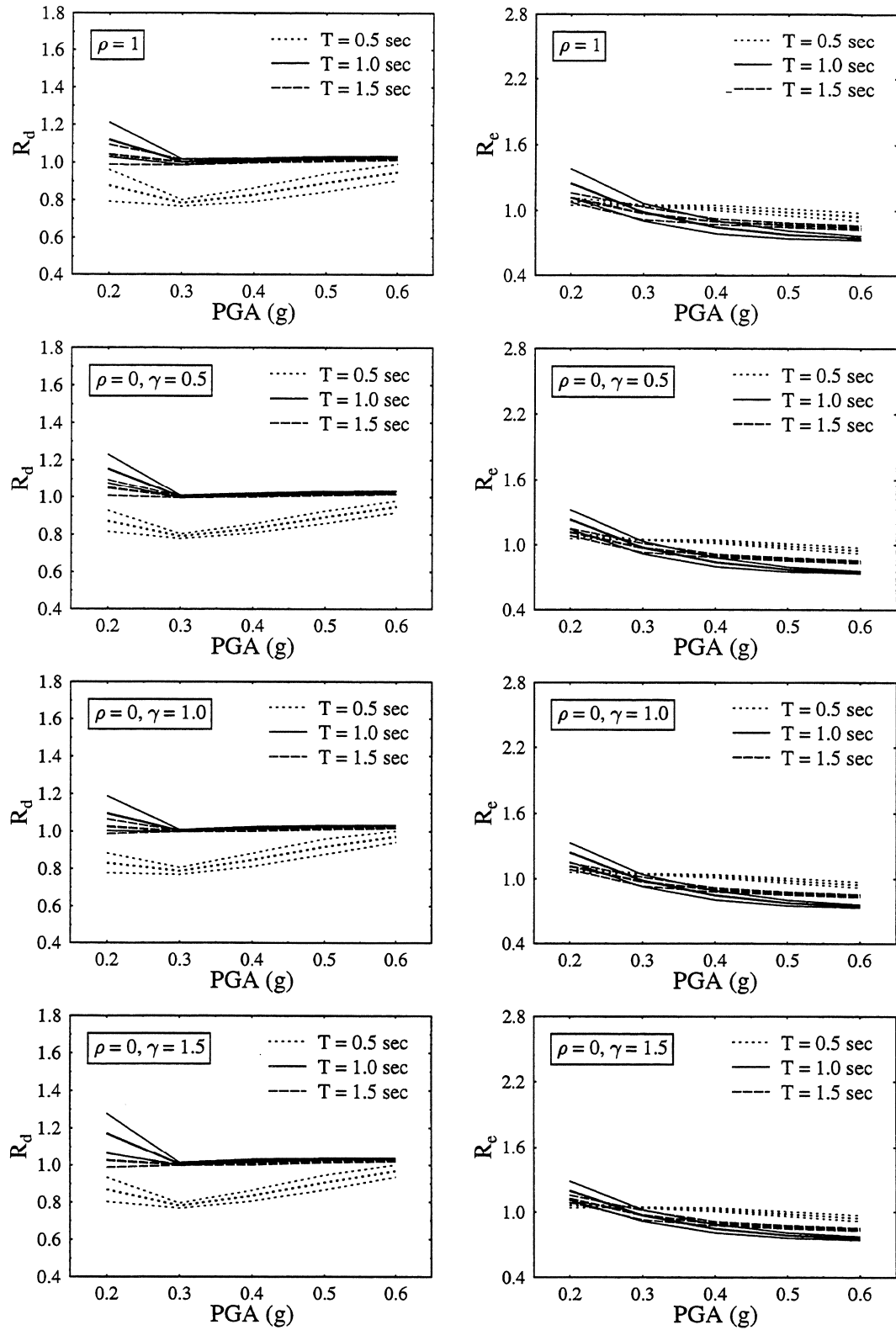
FIGURE 3-59 **Ratios of response measures of MC to EP models. Input: Parkfield.**

top two graphs refer to the case of perfectly correlated yield strengths.

Under El Centro values of the ratio R_d over one are very common especially for the two shorter periods considered. The mean and the mean-plus-one-standard-deviation of R_d can be as high as 1.19 and 1.35, respectively. Both extreme values arise for $T = 1.0$ sec. Under Taft the mean of R_d is below one, whereas the mean-plus-one-standard-deviation exceeds one only for $T = 0.5$ sec. Under Parkfield scaled to PGA $\geq 0.3g$ the maximum displacement is affected by the model selection only for $T = 0.5$ sec. For the two longer periods R_d has mean slightly larger than one and standard deviation very close to zero.

The ratio R_e consistently decreases with PGA for all motions considered. The MC model dissipates more energy than the EP model at low PGA values, but the situation is reversed as the PGA increases. This observation can be explained by the hysteretic behavior of the two models. Specifically, the EP model dissipates energy only during inelastic excursions. In contrast, the MC model starts dissipating energy after the first yield and continues at different rates throughout the motion duration. However, because of the stiffness degradation in the MC model, the area within a hysteretic loop is larger for the EP model. At low intensities the EP model shows very few loops with relatively small area since it mostly remains in the elastic range. The MC model with its continuous energy dissipation ends up with a higher total. As the intensity increases the number of hysteretic loops and the area within each loop increase for the EP model. The continuous energy dissipation by the MC model is no more sufficient to compensate for the significantly smaller area within its loops.

3.4.4 Model uncertainty. Independent yield strengths

When the element yield strengths are independent the system becomes asymmetric after the weaker of the two elements yields. From that instant on the response involves torsional, as well as lateral vibrations.

Maximum displacement. Torsion generally increases the mean of the maximum displacement Y_{max} for both the elastoplastic and the modified-Clough model. The plots of the ratio $q(Y_{max})$ for $\gamma = 1.5$ in Figures 3-10 and 3-34 show the effect of torsion on the COV of Y_{max} for the two models. When the system is subjected to the El Centro or the Taft record torsion increases the COV more often for the MC than for the EP model but the actual values of the COV tend to be lower for the MC model (see Figures 3-6, 3-30 and 3-7, 3-31). Under Parkfield and for $T = 0.5$ sec torsion increases the COV for

100

the EP whereas it mostly decreases it for the MC model but the COV values tend to be lower for the EP model (compare Figures 3-8 and 3-32). Still under Parkfield but for $T \geq 1.0$ sec the change in COV due to torsion as well as the values of the COV are generally insensitive to the model selection.

Maximum ductility. All comments on the effect of model uncertainty on Y_{max} apply to the maximum ductility as well.

Dissipated energy. The mean of the dissipated energy E_{dis} is insensitive to torsion for both models. Therefore, all observations made in Section 3.4.3 about the effect of model uncertainty on the mean of E_{dis} are valid. Reduction in the COV of E_{dis} in the presence of torsion is observed for both models. The COV tends to be higher for the EP model at low PGA values but the trend gets reversed as the PGA increases (compare Figures 3-23–3-25 with Figures 3-47–3-49).

Maximum rotation. Under El Centro or Taft the mean of the maximum rotation Φ_{max} is mostly lower for the MC model, as shown in Figures 3-27, 3-51 and 3-28, 3-48. On the contrary, under Parkfield the mean of Φ_{max} is lower for the EP model at high intensities and about the same for both models at low intensities (see Figures 3-29 and 3-53). The uncertainty in Φ_{max} is very high for both models with coefficients of variation mostly in the range of 60% to 80%.

Displacement and energy ratios. Figures 3-57–3-59 include plots of the ratios R_d and R_e, defined in Section 3.4.3, for the case of independent yield strengths ($\rho = 0$). Since these plots are similar with the ones for perfectly correlated yield strengths discussed in Section 3.4.3, the same comments apply.

3.4.5 Summary of numerical results

The tables that follow present in a concise form several of the observations from Sections 3.4.1–3.4.4. Each table corresponds to the section bearing the same title.

3.5 Conclusions

The effect on the seismic response of uncertainty in the element yield strengths is one of the issues investigated in the present study. The numerical results for one-storey systems presented in this section lead to the following conclusions:

TABLE 3-1 Parameter uncertainty. Elastoplastic model. (Section 3.4.1)

Measure	El Centro	Taft	Parkfield
Mean of Y_{max}	Increases with PGA Increases with T Increases with γ	Increases with PGA Increases with T Increased* by torsion	Increases with PGA Increases with T Increases with γ
COV of Y_{max}	Decreases* with T Max†: 30%, 22%, 13% Mostly below 20% Variability with PGA decreases with T	Decreases* with T Max†: 30%, 16%, 10% Mostly below 17% Variability with PGA decreases with T	Insensitive* to T Max†: 16%, 15%, 14% Variability with PGA insensitive to T Decreases with PGA for PGA $> 0.3g$
$P(Y_{max} > y_{max,0})$	Increased* by torsion Wide variations with PGA and T	Increased* by torsion Wide variations with PGA and T	Increases with γ for PGA $\geq 0.3g$ Rather insensitive to PGA and T
$E(Y_{max}/y_{max,0})$	Increases* with γ Variability with PGA decreases with T Max†: 1.57, 1.20, 1.16	Variability with PGA decreases with T Max†: 1.38, 1.21, 1.13	Increases with γ for PGA $\geq 0.3g$ Variability with PGA similar for all T Max†: 1.22, 1.14, 1.19
$P(Y_{max} > y^*)$	Increased by torsion for $\gamma \geq 1.0$ Below 25% for symmetric system, up to 60%–80% for $\gamma = 1.5$	Increased* by torsion for $\gamma \geq 1.0$ Below 25% for symmetric system, up to 60%–75% for $\gamma = 1.5$	Increased by torsion for $\gamma \geq 1.0$, decreased* for $\gamma = 0.5$ Below 20% for symmetric system, up to 60%–70% for $\gamma = 1.5$
Mean of E_{dis}	Increases with PGA Decreases with T Insensitive to torsion	Increases with PGA Decreases with T Insensitive to torsion	Increases with PGA Decreases with T Insensitive to torsion
COV of E_{dis}	Mostly below 10% Decreases* with PGA Decrease* by torsion is independent* of γ	Mostly below 15% Decreases* with PGA Decrease* by torsion is independent* of γ	Below 11% Increases* with PGA Decrease* by torsion is independent* of γ
Mean of Φ_{max}	Increases* with γ		Increases* with γ
COV of Φ_{max}	Range: 55%–81%	Range: 59%–83%	Range: 68%–88%

★: Denotes a trend that is present for most but not all parameter combinations
†: For periods of 0.5, 1.0, and 1.5 sec, respectively

TABLE 3-2 Parameter uncertainty. Modified-Clough model. (Section 3.4.2)

Measure	El Centro, S00E	Taft, N21E	-Parkfield, N65E
Mean of Y_{max}	Increases with PGA Increases with T Increases with γ	Increases with PGA Increases with T Increases with γ	Increases with PGA Increases with T Increases with γ
COV of Y_{max}	Below 13% Decreased* by torsion for $\gamma \leq 1.0$, increased* for $\gamma = 1.5$	Below 12% Decreased* by torsion for $\gamma \leq 1.0$, increased* for $\gamma = 1.5$	Below 15% Decreases with PGA for PGA $> 0.3g$ Decreased* by torsion for $\gamma \leq 1.0$
$P(Y_{max} > y_{max,0})$	Increases* with γ Wide variations with PGA and T	Increases* with γ Wide variations with PGA and T	Increases* with γ Insensitive* to PGA and T for PGA $\geq 0.3g$
$E(Y_{max}/y_{max,0})$	Increases* with γ Variability with PGA decreases with T Max†: 1.26, 1.21, 1.11	Increases* with γ Variability with PGA decreases with T Max†: 1.23, 1.16, 1.07	Increases with γ for PGA $\geq 0.3g$ Variability with PGA similar for all T Max†: 1.22, 1.15, 1.19
$P(Y_{max} > y^*)$	Increased by torsion for $\gamma \geq 1.0$ Below 25% for symmetric system, up to 60%–80% for $\gamma = 1.5$	Increased by torsion for $\gamma \geq 1.0$ Below 25% for symmetric system, up to 60%–80% for $\gamma = 1.5$	Increased by torsion for $\gamma \geq 1.0$, decreased* for $\gamma = 0.5$ Below 20% for symmetric system, up to 50%–70% for $\gamma = 1.5$
Mean of E_{dis}	Increases almost linearly with PGA Decreases with T Insensitive to torsion	Increases almost linearly with PGA Decreases with T Insensitive to torsion	Increases almost linearly with PGA Decreases with T Insensitive to torsion
COV of E_{dis}	Mostly below 10% Increases* with PGA Decrease* by torsion is independent* of γ	Mostly below 15% Increases* with PGA Decrease* by torsion is independent* of γ	Below 12% Increases* with PGA Decrease* by torsion is independent* of γ
Mean of Φ_{max}	Increases with γ Increases* with PGA	Increases with γ Increases* with PGA	Increases with γ Increases* with PGA
COV of Φ_{max}	Range: 59%–79%	Range: 44%–76%	Range: 66%–83%

*: Denotes a trend that is present for most but not all parameter combinations
$\dagger$: For periods of 0.5, 1.0, and 1.5 sec, respectively

TABLE 3-3 Model uncertainty. Perfectly correlated yield strengths. (Section 3.4.3)

Measure	El Centro, S00E	Taft, N21E	Parkfield, N65E
Mean of Y_{max}	Increases with PGA Increases with T	Increases with PGA Increases with T MC < EP	Increases with PGA Increases with T MC < EP for $T = 0.5$, MC $\simeq$ EP for $T \geq 1.0$
COV of Y_{max}	MC < EP for $T \leq 1.0$	MC < EP for $T \leq 1.0$	MC > EP for PGA $\geq$ $0.3g$, but difference slight for $T \geq 1.0$
Mean of M_{max}	Increases with PGA Decreases* with T	Increases with PGA Decreases with T MC < EP	Increases with PGA Decreases with T MC < EP for $T = 0.5$, MC $\simeq$ EP for $T \geq 1.0$
COV of M_{max}			MC > EP for PGA $\geq$ $0.3g$, but difference slight for $T \geq 1.0$
Mean of E_{dis}	Increases with PGA Decreases with T MC > EP for small PGA's, it reverses as PGA increases Models converge as T increases	Increases with PGA Decreases with T MC > EP for small PGA's, it reverses as PGA increases Models converge as T increases	Increases with PGA Decreases with T MC > EP for small PGA's, it reverses as PGA increases
COV of E_{dis}	MC < EP for small PGA's, it reverses as PGA increases	MC < EP for small PGA's, it reverses as PGA increases	Mostly MC > EP
R_d	(Mean + Std) of R_d often above 1.0, with max 1.35	(Mean + Std) of R_d above 1.0 only for $T = 0.5$, with max 1.17	(Mean + Std) of R_d significantly above 1.0 only for $T \geq 1.0$ and PGA = $0.2g$, with max 1.21 Std is negligible for $T \geq 1.0$ and PGA $\geq$ $0.3g$.
R_e	Decreases with PGA Significantly over 1.0 for small PGA's	Decreases with PGA Significantly over 1.0 for small PGA's	Decreases with PGA Exceeds 1.0 for small PGA's

$\star$: Denotes a trend that is present for most but not all parameter combinations

TABLE 3-4 Model uncertainty. Independent yield strengths. (Section 3.4.4)

Measure	El Centro, S00E	Taft, N21E	Parkfield, N65E
Mean of Y_{max}		MC < EP	MC < EP for $T = 0.5$, MC $\simeq$ EP for $T \geq 1.0$
	Increases with γ for both models	Increases with γ for MC only	Increases with γ for both models
COV of Y_{max}	Mostly MC < EP	Mostly MC < EP but difference decreases with T	MC > EP for PGA $\geq$ 0.3g, but difference slight for $T \geq 1.0$
	Increased by torsion more often for the MC than for the EP model	Increased by torsion more often for the MC than for the EP model	Increased by torsion for the MC but decreased* for the EP model
Mean of E_{dis}	Insensitive to torsion for both models	Insensitive to torsion for both models	Insensitive to torsion for both models
	MC > EP for small PGA's, it reverses as PGA increases	MC > EP for small PGA's, it reverses as PGA increases	MC > EP for small PGA's, it reverses as PGA increases
	Models converge as T increases	Models converge as T increases	
COV of E_{dis}	Decreased* by torsion for both models	Decreased* by torsion for both models	Decreased* by torsion for both models
	MC < EP for small PGA's, it reverses as PGA increases	MC < EP for small PGA's, it reverses as PGA increases	Mostly MC > EP
Mean of Φ_{max}	Mostly MC < EP	Mostly MC < EP	MC $\simeq$ EP for small PGA's, MC > EP as PGA increases
R_d	(Mean + Std) of R_d often above 1.0, with max 1.34	(Mean + Std) of R_d above 1.0 only for $T = 0.5$, with max 1.20	(Mean + Std) of R_d significantly above 1.0 only for $T \geq 1.0$ and PGA = 0.2g, with max 1.28. Std is negligible for $T \geq 1.0$ and PGA $\geq$ 0.3g.
R_e	Decreases with PGA	Decreases with PGA	Decreases with PGA
	Significantly over 1.0 for small PGA's	Significantly over 1.0 for small PGA's	Exceeds 1.0 for small PGA's

*: Denotes a trend that is present for most but not all parameter combinations

105

- As expected, the mean of the maximum displacement $Y_{\max}$, the maximum ductility $M_{\max}$, and the dissipated energy E_{dis}, increases monotonically with the peak ground acceleration (PGA).

- The mean of $Y_{\max}$ increases with the small-vibration lateral period T whereas the mean of $M_{\max}$ and E_{dis} decreases.

- Torsion caused by uncertainty in the element yield strengths results in increase in the mean of $Y_{\max}$ and $M_{\max}$. However, the mean value of E_{dis} is insensitive to variations in the mass moment of inertia of the structure as well as to the uncertainty in the element yield strengths.

- The coefficients of variation of E_{dis} and $Y_{\max}$ are relatively small, whereas $M_{\max}$ and especially the maximum rotation $\Phi_{\max}$ have large coefficients of variation. For example, the coefficient of variation of $\Phi_{\max}$ can be as high as 88% when the coefficient of variation of the element yield strengths is 15%.

- The uncertainty in the element yield strengths results in ductilities up to about twice the ductility of the code-designed deterministic system when the yield strengths are perfectly correlated. When they are independent there is significant probability of ductilities three and even four —for some parameter combinations— times that of the code-designed system.

This study also addresses the question whether the choice of the elastoplastic restoring force model over the modified-Clough is conservative. The numerical results for one-storey systems indicate that:

- Maximum displacement can be larger for the modified-Clough than for the elastoplastic model. This observation is most prevalent under El Centro, less so under Taft where it holds only for systems with $T = 0.5$ sec, whereas under Parkfield it applies only to PGA $= 0.2g$ and $T \geq 1.0$ sec.

- Dissipated energy can be lower for the modified-Clough than for the elastoplastic model, more so for higher peak ground accelerations.

These observations suggest that if the modified-Clough were the correct restoring force model, the use of the elastoplastic model instead would not necessarily be conservative, since it might underestimate displacements and overestimate energy dissipation.

SECTION 4

MULTI-STOREY SYSTEMS

The focus of the present study is the effects of system uncertainty on the response and design of building structures. Sources of system uncertainty considered are the functional form of the restoring force model of the lateral-load-resisting elements and the parameters of this model.

The first part of the study, presented in Sections 3 and 5.1, involves a simple structural model consisting of a rigid slab supported by two lateral-load-resisting elements (see Figure 3-1). The simplicity of this model offers three advantages: (1) it allows for large numbers of samples to be considered in Monte Carlo simulation, (2) it makes possible to investigate multiple values of deterministic system parameters as well as scalings of the input motion and (3) it facilitates interpretation of the observed response. However, it is evident that this one-storey model is just an idealization for research purposes, not a realistic structure. This raises the issue whether observations on the response of the simple model translate, even qualitatively, to the behavior of actual buildings. In an attempt to address this issue as well as to investigate the effects of system uncertainty on multi-storey systems the second part of this study employs a seven-storey building designed according to code specifications. This building, although still somewhat idealized, could conceivably be built with small modifications, for instance, a stairwell.

The assumptions made for the study of multi-storey systems reflect as closely as possible those made earlier for one-storey systems. The input is still deterministic consisting of two acceleration records. The population of available restoring force models is represented by the same two: the elastoplastic and the modified-Clough. Of the model parameters, the yield strength is once more treated as a lognormally distributed random variable. This uncertainty in the structural element yield strengths can give rise to torsional response in nominally symmetric systems, i.e., systems symmetric in the elastic range which become asymmetric following yield. The reasons for these choices and their repercussions are discussed in more detail in the introduction to Section 3.

To the writers' best knowledge this is the first study of the effects of system uncertainty on the seismic response of a realistic multi-storey building that extends beyond parametric investigations to treat yield strengths as random variables and to account for them by means of Monte Carlo simulation.

4.1 Structural model

The structure considered is a seven-storey reinforced concrete frame-shear wall building with plan view and elevation as shown in Figure 4-1. The rigid rectangular floor slabs are supported by four and eight moment-resisting frames in the x- and y-directions, respectively. The shear walls occupy the middle span of the end frames along the y-direction and are aligned with the input motion. The mass is uniformly distributed on the slabs, which places the centers of mass of the floors at their respective geometric centroids. Moreover, all centers of mass lie on the same vertical line. A similar structure is found in the study by Sedarat and Bertero (Sedarat and Bertero, 1990) from which the basic outline and most member dimensions were drawn.

Typical member cross sections are shown in Figure 4-2. Member dimensions are constant for all storeys but their reinforcement varies. All beams have the same cross section (Figure 4-2(a)). The interior columns are square (Figure 4-2(b)), whereas those on the long sides of the building are rectangular (Figure 4-2(c)) with their long side along the x-axis, to compensate for the absence of shear walls in that direction. Each shear wall consists of a panel and two edge columns (Figure 4-2(d)).

4.1.1 Restoring force models

For analysis purposes, all members are represented by their centroidal axis and remain elastic throughout whereas all inelastic deformations are taken by flexural springs at member ends, as well as, in some cases, shear and axial springs. Beams have only flexural springs; shear deformations are ignored and axial ones are not allowed because of the rigid slab assumption. Columns have noninteracting flexural and axial springs; shear deformations are ignored as being negligible in comparison with those of the shear walls in the direction of interest, i.e., that of the input motion.

The panels in the shear walls are modeled as line elements with flexural, shear, and axial springs. No interaction between the various springs in a member is considered. The edge columns are modeled as axial members with pins at their ends in the plane of the wall but they are allowed out-of-plane bending. Compatibility between panel and edge columns is enforced by plane section assumption at floor levels.

All flexural and shear springs in the structure follow the same restoring force model. A detailed description of the two models selected for this study, the elastoplastic and the

(a) plan view
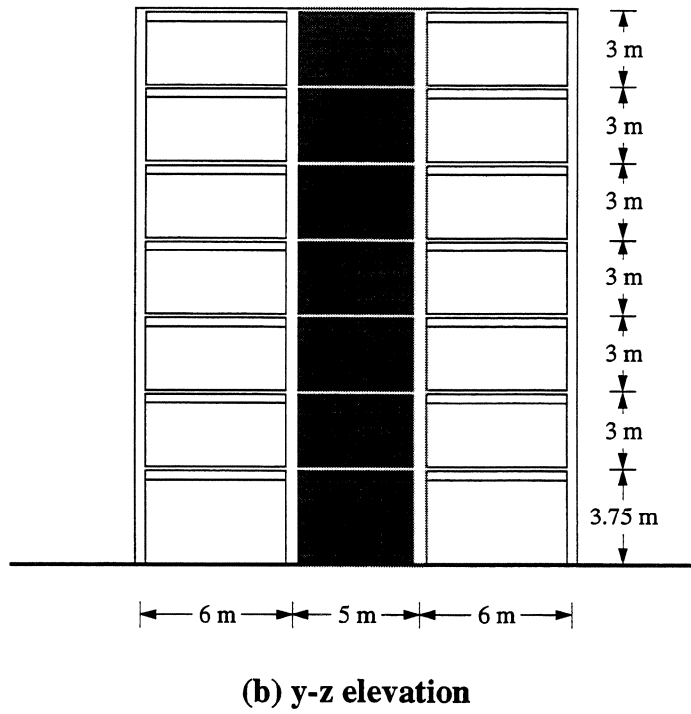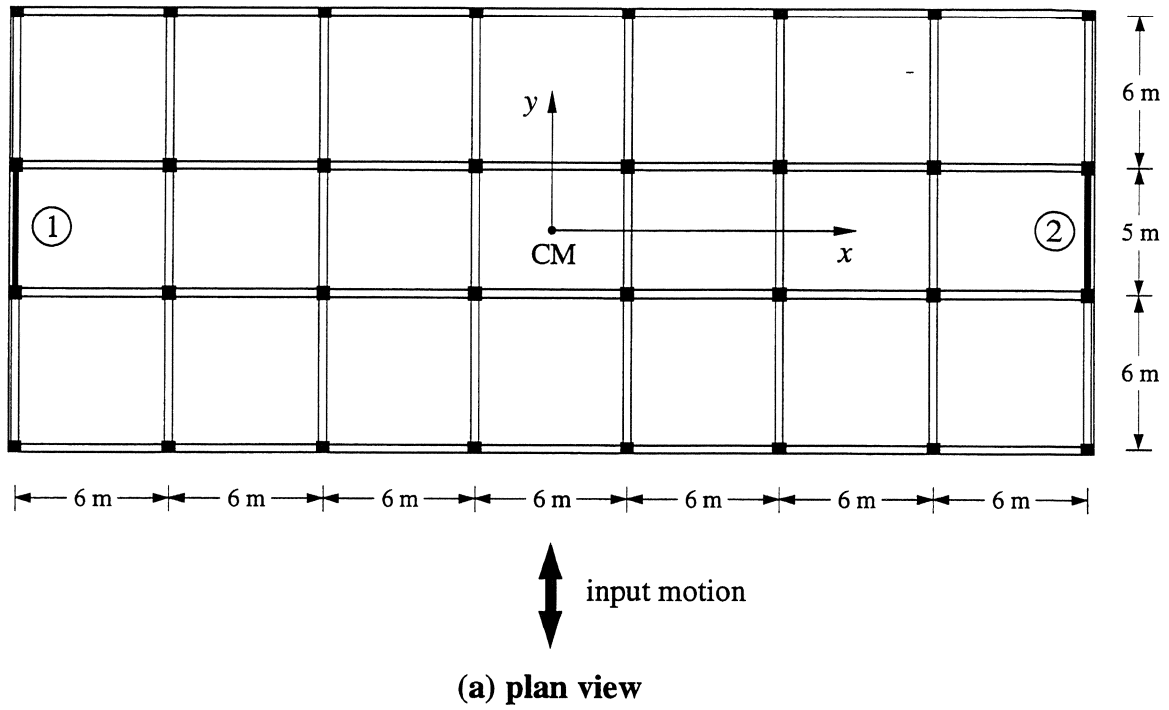
(b) y-z elevation

FIGURE 4-1 Plan view and elevation of 7-storey building.

(a) beam

(b) interior column

(c) perimeter column

(d) shear wall
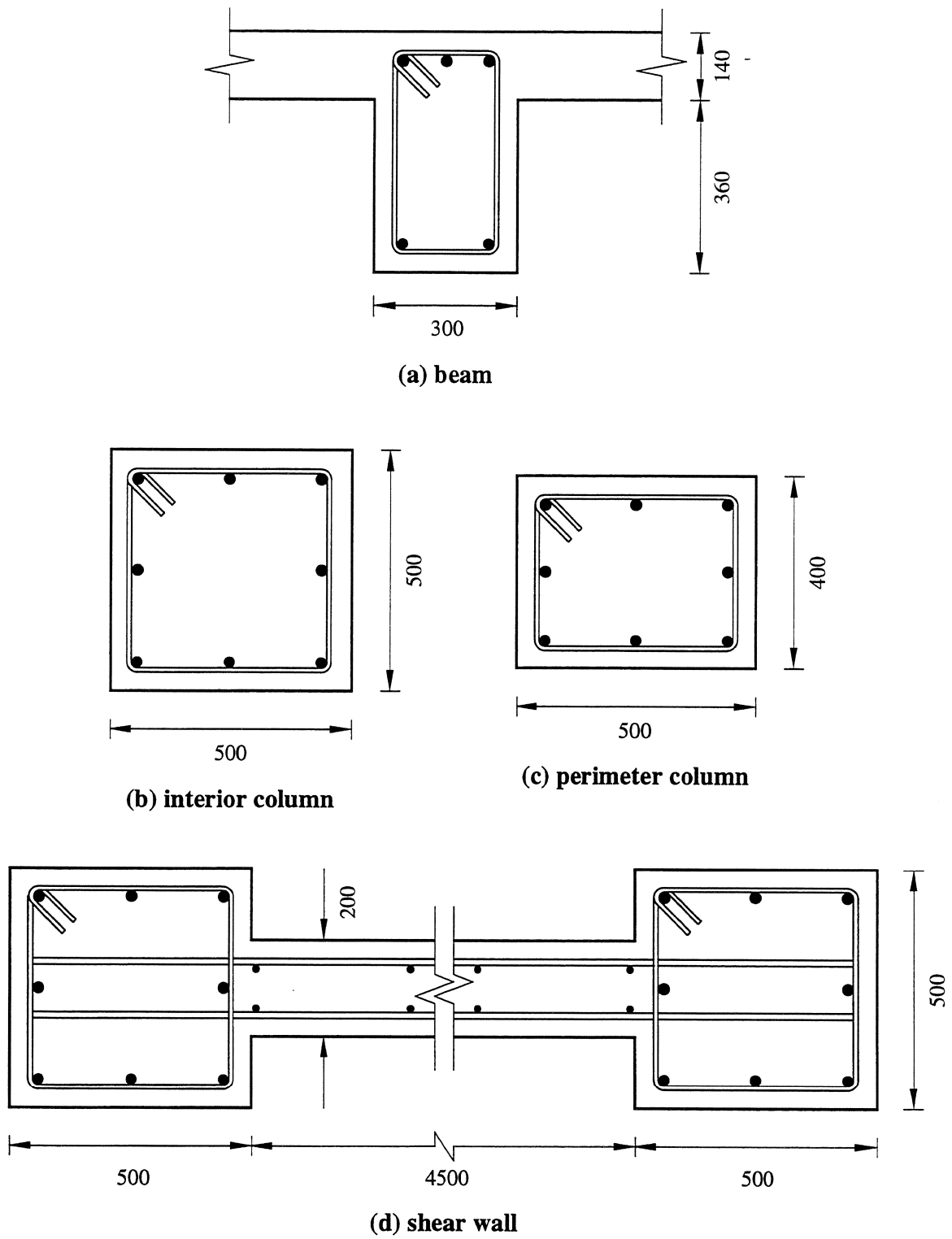
FIGURE 4-2 Typical member cross sections (all dimensions in mm).
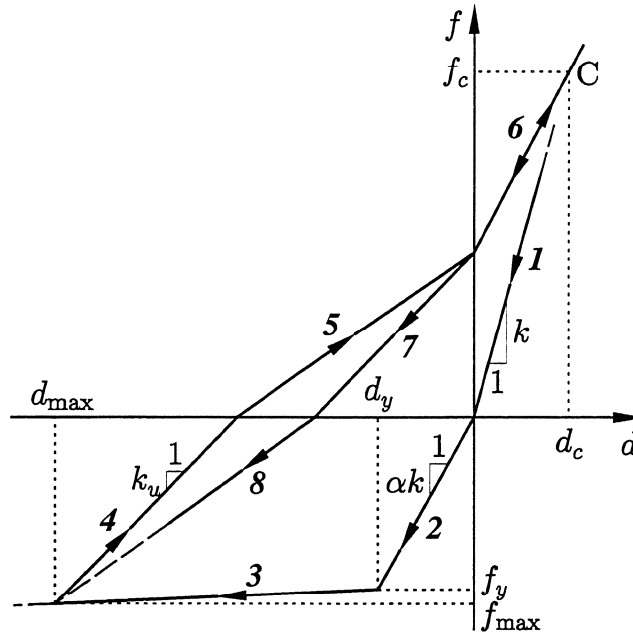
FIGURE 4-3 Axial restoring force model.

modified-Clough, is given in Section 3.1.1. Their essential difference is that the modified-Clough model accounts for stiffness degradation at the expense of somewhat increased complexity.

In effect, for the part of the study devoted to multi-storey systems the elastoplastic model is approximated by a bilinear model with post-yield stiffness to elastic stiffness ratio $\beta = 1\%$. The small post-yield stiffness is necessary to avoid numerical instability. However, for reasons of simplicity this quasi-elastoplastic model will be referred to as elastoplastic. The same ratio of 1% is assigned to the bilinear backbone curve of the modified-Clough model.

Axial springs follow a hysteretic model devised by the author of the computer code employed in the analysis of the multi-storey systems. This model, shown in Figure 4-3, has a backbone curve defined by the elastic stiffness in compression k, the tensile strength f_y, the ratio of elastic stiffness in tension and compression α, and the ratio of post-yield stiffness in tension to elastic stiffness in compression β. The sign convention for this model is that compressive forces and displacements are positive. Unloading in tension (branch 4) follows stiffness $k_u = (f_c - f_{max})/(d_c - d_{max})$ where f_{max} and d_{max} are the maximum tensile force and displacement, respectively, and $f_c = \eta |f_y|$ and $d_c = f_c/k$ are the coordinates of point C, with η a parameter of the model. After the restoring force

reverses sign the stiffness for loading in compression (branch 5) is αk if $|d_{\max}| \leq |d_y|$, or $\alpha k (f_c - f_{\max})(d_c - dy) / [(f_c - f_y)(d_c - d_{\max})]$ otherwise. Once displacement becomes compressive and as long as it remains so the model follows the path defined by the zero-displacement point and point C (branch 6). Further tensile deformation occurs with slope k_u (branch 7) up to the intersection with the displacement axis, and along the path defined by the intersection point and point $(f_{\max}, d_{\max})$ (branch 8) afterwards. The parameters α, β, and η are set to the values recommended by the author of the model, i.e., 0.5, 0.001, and 2.0, respectively.

4.1.2 Random parameters of restoring force model

The seven-storey building in Figure 4-1 is assumed to be perfectly symmetric about the x-axis of its plan. Moreover, all beams and individual columns symmetrically located about the y-axis are assumed to be deterministic and identical.

Each segment of a wall delimited by two consecutive floors is considered a separate *wall element*. The behavior of the wall element in its own plane is modeled by five noninteracting springs: two flexural, one shear, and one axial for the panel portion and two axial, one for each of the edge columns. Geometrically, the shear walls are symmetrically located about the y-axis. The elastic stiffnesses of the pairs of wall elements in each storey are assumed to be deterministic and identical.

The yield strengths of the springs modeling each wall element are the random variables F_{yi}, $i = 1, \ldots, 5$, with means μ_i and variances σ_i^2. These random variables are assumed to be perfectly correlated and lognormally distributed. The choice of the lognormal distribution is arbitrary but physically admissible since it does not allow for negative strength values. The assumption of perfect correlation is dictated by the fact that the five springs represent the same physical entity. The variables F_{yi} are related to the random variable X through the system of independent equations

$$F_{yi} = \exp(\tilde{\mu}_i + \tilde{\sigma}_i X), \quad i = 1, \ldots, 5 \tag{4-1}$$

where $X \sim N(0, 1)$ and

$$\tilde{\mu}_i = \ln \frac{\mu_i}{\sqrt{1 + \alpha_i^2}} \tag{4-2}$$

$$\tilde{\sigma}_i^2 = \ln(1 + \alpha_i^2) \tag{4-3}$$

are the parameters of the associated normal distribution with $\alpha_i = \sigma_i / \mu_i$ being the coefficient of variation of variable i.

112

The sets of springs in any two wall elements are assumed to be independent. This is considered a reasonable assumption for wall elements that are part of the same shear wall, as well as for elements belonging to different walls, since it is usual construction practice to erect the walls segmentally, storey by storey.

4.1.3 Equations of motion

CANNY-E (CANNY-E, 1995), a computer code capable of performing three-dimensional inelastic dynamic analysis of building structures, has been used to calculate the seismic response of the building in Figure 4-1. In this program, the structure is idealized as a set of rigid nodes connected by deformable members. Because of the rigid floor slab assumption the displacement of each floor level is described by the translations of its center of mass in the x- and y-directions and the rotation about the center of mass. Consequently, any node at floor level is limited to at most three independent degrees-of-freedom: vertical translation and rotations about x- and y-axes.

The equations of motion for the nodal degrees-of-freedom are

$$m\ddot{X} + c\dot{X} + F = -m\ddot{x}_g \tag{4-4}$$

where X = vector of nodal displacements, m = mass matrix, c = damping matrix, F = vector of restoring forces, and $\ddot{x}_g$ = ground acceleration.

The nodal displacements are random variables due to the strength uncertainty in the restoring force model.

4.2 Input motions

The deterministic input for this part of the study consists of the strong motion portion of two earthquake records, also used in the one-storey part of the study: (1) the S00E component of the El Centro record from the 1940 Imperial valley earthquake and (2) the N65E component of the Cholame Shandon record from the 1966 Parkfield earthquake, or as they are referred to, the 'El Centro' and 'Parkfield' records, respectively. Plots of both accelerograms and of their Fourier transforms can be seen in Figures 3-3 and 3-5. It is pointed out once more that any further reference to 'motion' actually implies 'strong motion', since this is the part of the record used.

The third record in the one-storey part of the study, 'Taft', is not considered because

analysis of the seven-storey building is far more time consuming and computer resources are limited. The selection of motions is based on the following rationale: (1) El Centro is included as the most widely used record in seismic response studies providing increased potential for future comparisons; (2) Taft is the longest of the three records and belongs in the same category of input motions as El Centro, namely of motions characterized by irregular accelerograms and fairly uniform energy content over a wide band of frequencies; (3) Parkfield, as representative of a different category of motions with few pronounced acceleration pulses, should allow for observations that are less specific to the input motion considered.

El Centro has a Peak Ground Acceleration (PGA) of $0.35g$. In an effort to establish some equivalency between the two motions Parkfield is scaled so that the total energy dissipated by the symmetric elastoplastic system (see Section 4.3 for description) is the same for both motions. The PGA of the scaled record is $0.43g$ versus the recorded peak value of $0.49g$.

4.3 System design and modeling, response measures, and Monte Carlo simulation

System design. The building in Figure 4-1 is designed according to the provisions in the 1994 version of the Uniform Building Code (UBC) for reinforced concrete structures resisting forces induced by earthquake motions. Lateral loads have been determined by the static force procedure.

The building design has been aided by the computer code ETABS (ETABS, 1995). This program can perform three-dimensional linear static and dynamic analysis of buildings. Its nonlinear capabilities are limited to the modeling of base isolation devices. When used in its design capacity, ETABS takes as input overall building and member dimensions, material properties, vertical dead and live loads, the Code to be used for seismic design, and the parameters required for the static force procedure. Based on those, the program performs linear static analysis of the building under all code-required load combinations and, with the assistance of design post processors, provides the designer with reinforcement area requirements. It is the responsibility of the designer to select and position the reinforcement bars as well as to verify satisfaction of provisions on minimum reinforcement ratio, maximum allowable bar spacing, etc.

The compressive strength of the concrete is taken as 25 MPa and the yield strength of the reinforcing steel as 414 MPa (60 ksi). The dead load on the building consists of the self weight of the structure and uniform floor loads of 0.86 kN/m^2 and 1.63 kN/m^2 for the roof and all other floors, respectively, accounting for nonstructural elements such as roofing, floor finishes and partitions. The corresponding uniform live loads are taken as 0.96 kN/m^2 and 1.92 kN/m^2.

In the UBC the total design base shear in a given direction is determined from the expression

$$V = \frac{Z I C}{R_w} W \qquad (4\text{-}5)$$

in which Z, I, and R_w are zone, importance, and structural system factors, W is the seismic dead load of the system, and

$$C = \frac{1.25 S}{T^{2/3}}, \quad C \leq 2.75 \qquad (4\text{-}6)$$

where S is the site coefficient for soil characteristics. The following values are selected: $Z = 0.40$ corresponding to Zone 4, $I = 1.0$ for standard occupancy, $S = 1.5$ corresponding to soil profile S_3 (suggested by the code for use 'in locations where the soil properties are not known in sufficient detail'), and $R_w = 12$, appropriate for concrete special moment-resisting frames, i.e., frames detailed to provide ductile behavior. The accidental eccentricity required by the UBC for nonflexible diaphragms is $e_a = 5\%$ of the building dimension perpendicular to the direction of the shear force.

System modeling for inelastic dynamic analysis. At the time of the earthquake the structure will be carrying its dead load plus some unknown fraction of the live load used in its design. This fraction is arbitrarily taken as 60%. Therefore, the floors of the building in Figure 4-1 are assigned masses corresponding to the dead load plus 60% of the live load. The same combination of gravity loads is used to calculate initial actions on the members, i.e., generalized forces present at the onset of the ground motion. The damping is mass and elastic stiffness proportional with coefficients calculated by assigning modal damping $\zeta = 5\%$ to the first and third small-vibration lateral modes in the direction of the ground motion. The natural frequencies of these modes are 8.02 rad/sec and 72.1 rad/sec, respectively.

The members of the building resulting from the design procedure outlined earlier in this section are modeled in CANNY by sets of inelastic springs, as described in Section 4.1.1. The yield strengths of these springs, calculated from the structure as designed, are consid-

115

ered the 'design' yield strengths. The resulting system has two axes of symmetry. Consequently, it vibrates along the y-direction when subjected to an input motion in the same direction. The first small-vibration period of this system in the y-direction is 0.78 sec.

Yield strength uncertainty is limited to the springs modeling shear walls (Section 4.1.2) and is represented by a perturbation about the design yield strength. The mean of F_y for each of these springs is set equal to the corresponding design value. The common coefficient of variation (COV) for all wall springs is set to 15%, in keeping with the assumption made for one-storey systems.

Response measures. The evaluation of the response of the system in Figure 4-1 is based on the following measures:

- interstorey wall displacement $Y_w(t)$, i.e., the displacement of a shear wall between consecutive floor levels,

- maximum interstorey displacement $Y_{\max} = \max\{\max\{|Y_{wi}(t)|\}\}$, $i = 1, 2$, where $Y_{wi}(t)$ is the interstorey displacement of wall i,

- maximum interstorey rotation $\Phi_{\max}$, defined as the maximum in absolute value of the difference in rotation between consecutive floors,

- dissipated energy E_{dis}, calculated as the total area within the hysteretic loops of the springs modeling individual members or groups of members,

- dynamic eccentricity $\Theta(t)$, which for storey k, $k = 1, \ldots, 7$, is defined as $\Theta_k(t) = \sum_{i=k}^{7} m_i r_i^2 \ddot{\Phi}_i(t) \Big/ (V_k b)$, where $\ddot{\Phi}_i(t)$, m_i, and r_i are the torsional acceleration, mass, and radius of gyration of floor i, $i = 1, \ldots, 7$, V_k is the design storey shear, and b is the building dimension perpendicular to the ground motion,

- maximum dynamic eccentricity $\Theta_{\max} = \max\{|\Theta(t)|\}$,

- Z = total time of $|\Theta(t)|$ above e_a, given as percentage of the motion duration, and

- upcrossing rate N, which is equal to the number of times during the motion $|\Theta(t)|$ upcrosses level e_a, divided by the motion duration.

Of the response measures considered, the interstorey wall displacement and the dynamic eccentricity are random processes, whereas all other measures are random variables.

116

Monte Carlo simulation. The seven-storey building shown in Figure 4-1 is designed according to the UBC provisions for seismic design of reinforced concrete structures as described in the first part of this section. In its modeling for inelastic dynamic analysis the flexural and shear behavior of its members are represented by springs with quasi-elastoplastic (bilinear with 1% post-yield stiffness ratio) or modified-Clough restoring force models (Section 4.1.1). Throughout axial springs follow a third model, described in Section 4.1.1. The yield strengths of the springs modeling wall elements (segments of wall between consecutive floors) are assumed to be lognormally distributed random variables, perfectly correlated within a wall element but independent from one wall element to any other (Section 4.1.2). The input motion is deterministic consisting of the El Centro record and a scaled version of the Parkfield record with PGA = 0.43g.

The study of multi-storey systems, as the earlier of one-storey systems, is based on Monte Carlo simulation. Each set of yield strength values generated is assigned to what constitutes a realization of the seven-storey system. Assuming a restoring force model (either elastoplastic or modified-Clough) and an input motion (either El Centro or Parkfield) a complete time-history analysis of this system realization is performed. The equations of motion (Section 4-4) are integrated numerically by means of the Newmark-β method with $\beta = 1/4$. The four combinations of restoring force model and input motion result in four sets of realizations of the response measures listed earlier in this section, which are analyzed statistically.

The number of realizations considered is necessarily limited by the required computer time per time-history analysis and the available computer resources. The long analysis time is due partly to the increased complexity of the system and partly to the solution algorithm in CANNY-E. Specifically, this algorithm solves a linearized problem in each time step but does not iterate for equilibrium. The resulting unbalanced forces are carried over to the next step. When the restoring force model is characterized by large slope discontinuities, as are both models considered in this study, the time step, Δt, must be severely reduced to prevent the unbalanced forces from leading to numerical instability. Preliminary analyses indicated that although $\Delta t \leq 10^{-3}$ sec is sufficient to avoid divergence, $\Delta t \leq 2 \times 10^{-4}$ sec is necessary to restrict the numerical errors caused by the unbalanced forces within acceptable limits. With this time step, analysis of a system realization with elastoplastic model subjected to the 24.4 sec strong motion portion of the El Centro record using a 200 MHz Pentium processor takes about two hours. Moreover, each analysis with the modified-Clough model takes about 1.5 times as long as with the

elastoplastic due to the more frequent stiffness changes and associated LU-factorizations.

Weighing all the above factors, the number of realizations considered is 150 and 100 for the elastoplastic and modified-Clough models, respectively. The first one hundred realizations for each model have identical envelope curves and differ only in the presence or not of stiffness degradation during cycling.

4.4 Numerical results

The interstorey wall displacement Y_w, maximum interstorey displacement Y_{max}, maximum interstorey rotation Φ_{max}, and dissipated energy E_{dis} are used to evaluate the effects of strength uncertainty on the seismic response of the seven-storey system under consideration. Whenever possible, the statistics of these response measures are related to the respective response measures of the symmetric system with the same restoring force model subjected to the same input motion.

While all wall elements remain elastic the symmetry of the building is preserved. Therefore, for input motion in the y-direction the floor slabs experience only translation in that same direction. However, once any of the springs in the walls yields symmetry is lost and the floor slabs develop rotations about their respective centers of mass.

The deterministic system with spring yield strengths equal to the means of the assumed distributions is perfectly symmetric and it remains so throughout the motion. The response measures of this system are compared, whenever applicable, to the average values of the respective measures produced by Monte Carlo simulation.

4.4.1 Interstorey wall displacement

The amount of stress in a shear wall depends on its interstorey displacement $Y_w(t)$. From a given sample time history of $Y_w(t)$ it is possible to calculate for what fraction of the motion the process $|Y_w(t)|$ takes values above displacement level w. Figures 4-4–4-7 show the median and 90% confidence interval of the time above w, for the range of w values encountered in the realizations of $|Y_w(t)|$. The 90%-confidence interval implies that 90% of the sample values for the specific displacement level lie between the upper and lower envelope curves leaving out 5% of the values on either side.

Each figure shows seven storey plots for one of the four motion and restoring force model
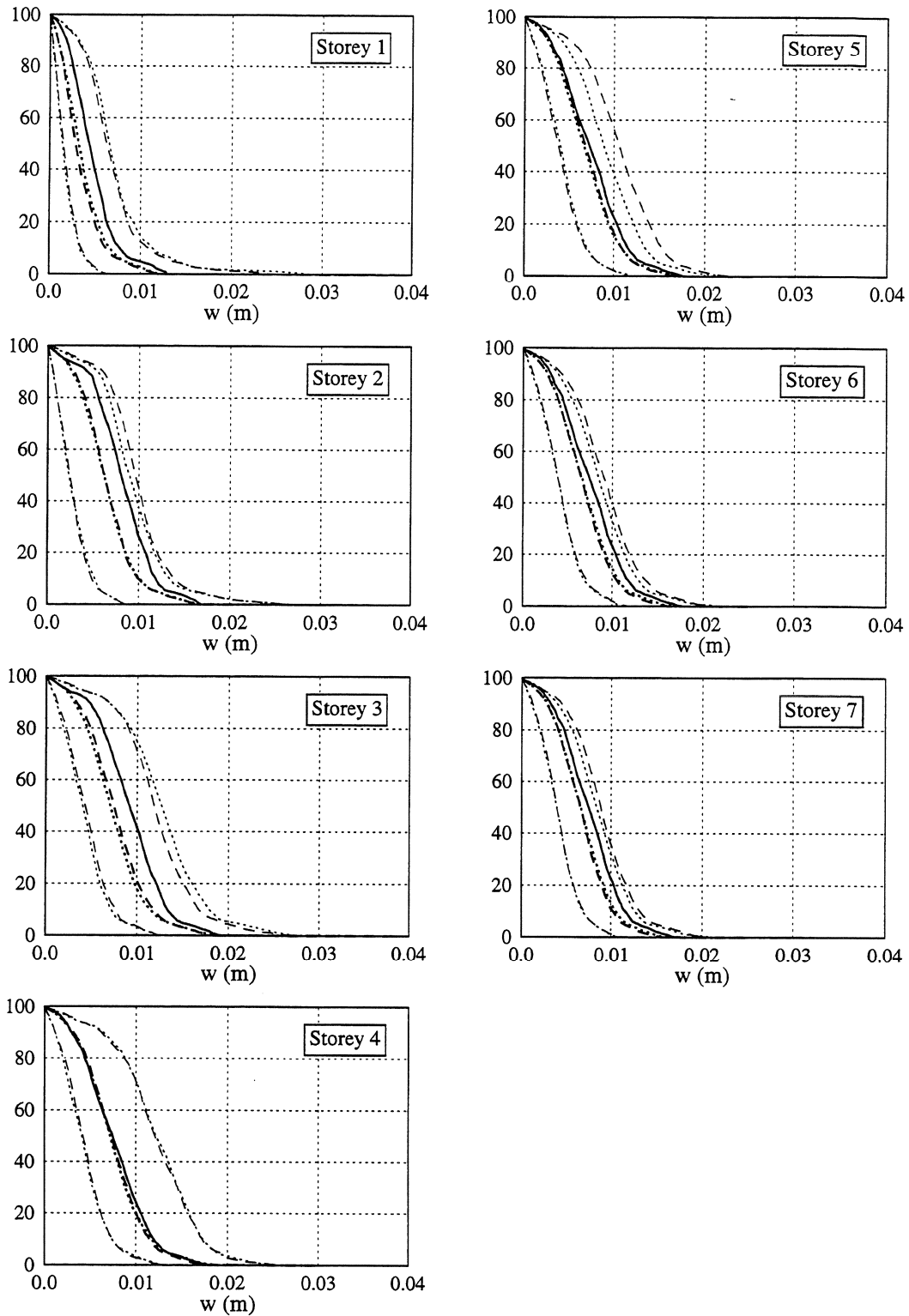
FIGURE 4-4 Percentage of motion duration over which $|Y_w(t)|$ exceeds level w. EP model. Input: El Centro. (—— symmetric system; ····· wall 1; – – – wall 2)

119
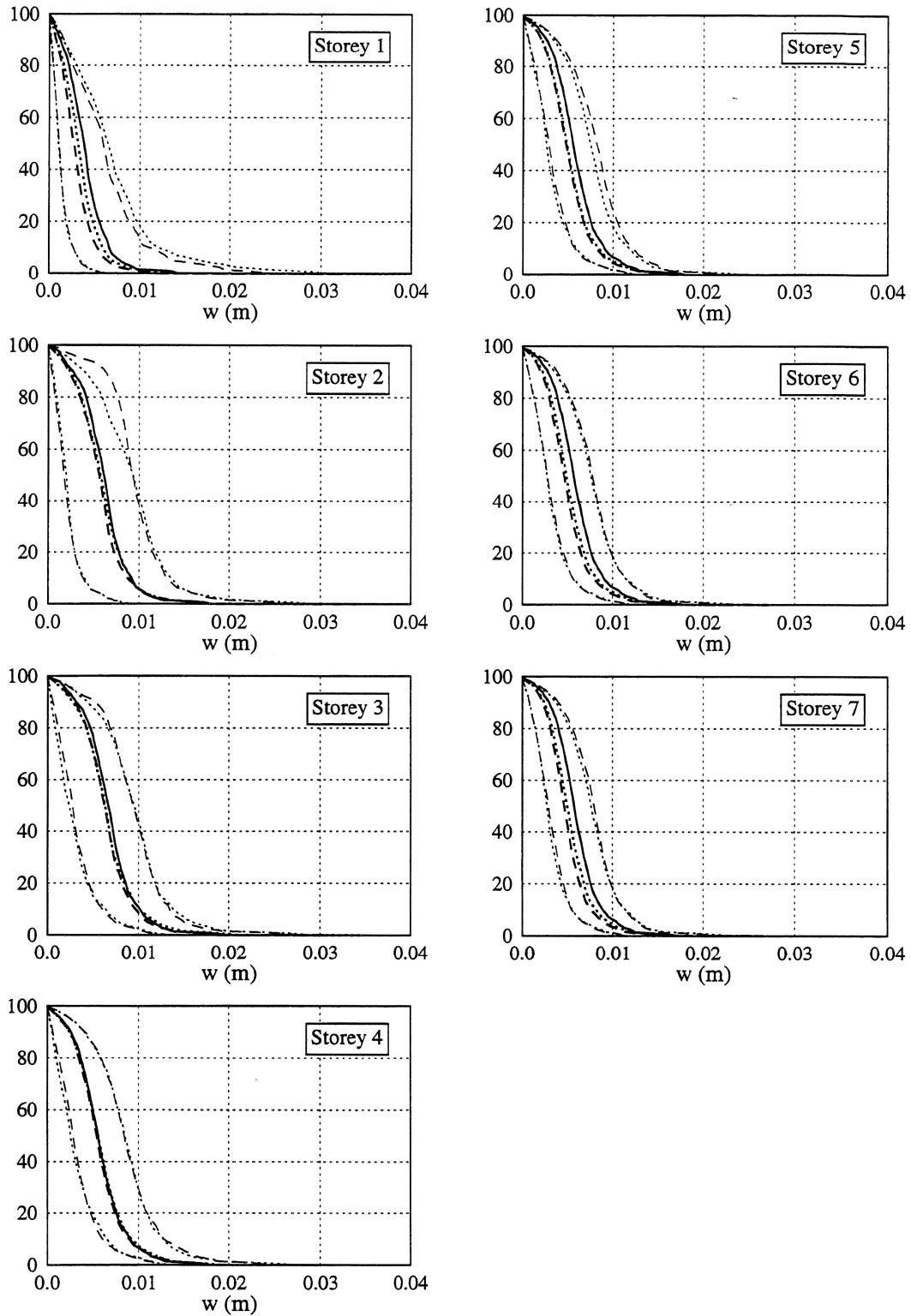
FIGURE 4-5 Percentage of motion duration over which $|Y_w(t)|$ exceeds level w. MC model. Input: El Centro. (—— symmetric system; ····· wall 1; — — — wall 2)

120
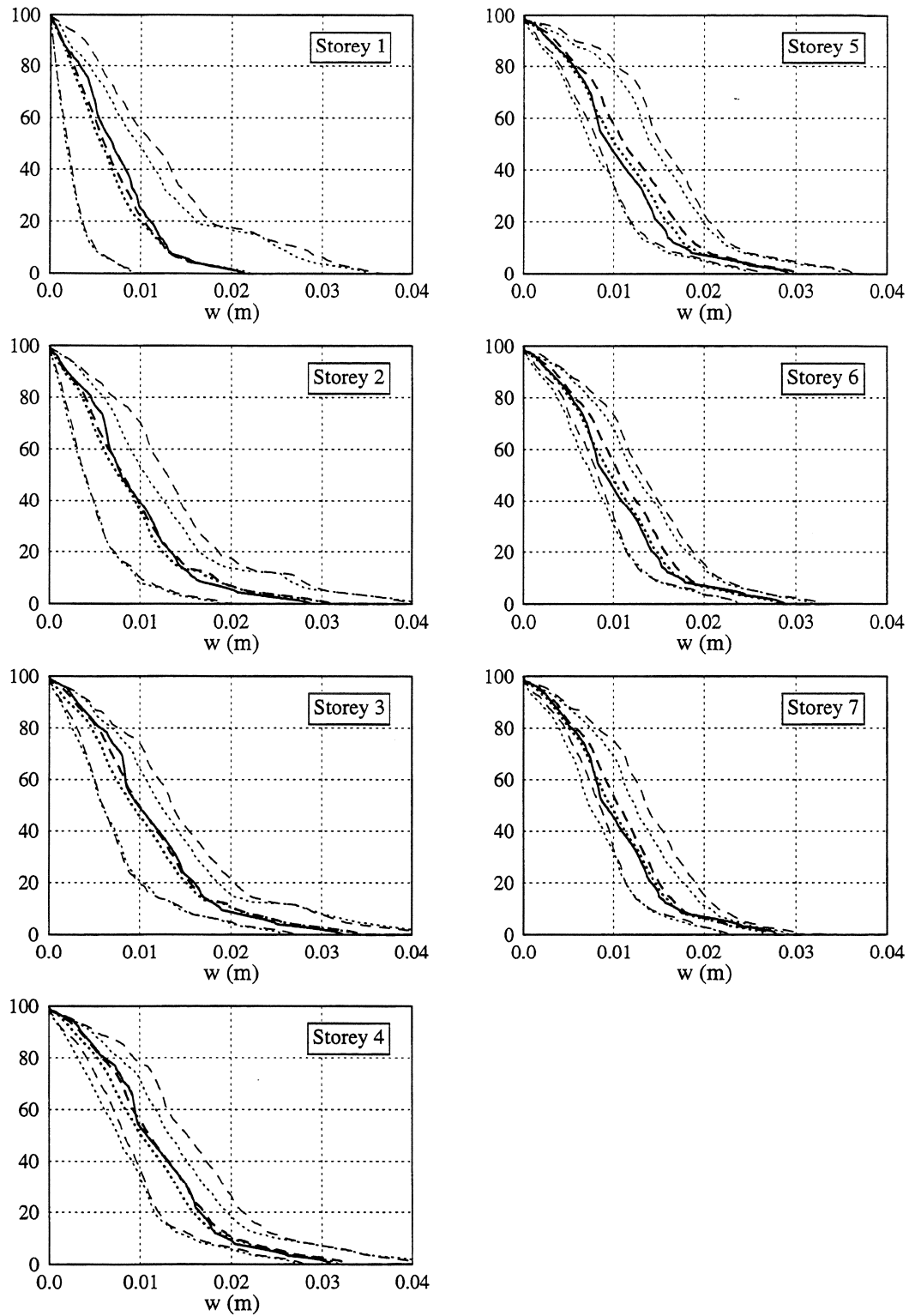
FIGURE 4-6 Percentage of motion duration over which $|Y_w(t)|$ exceeds level w. EP model. Input: Parkfield. (——— symmetric system; · · · · · wall 1; — — — wall 2)

121
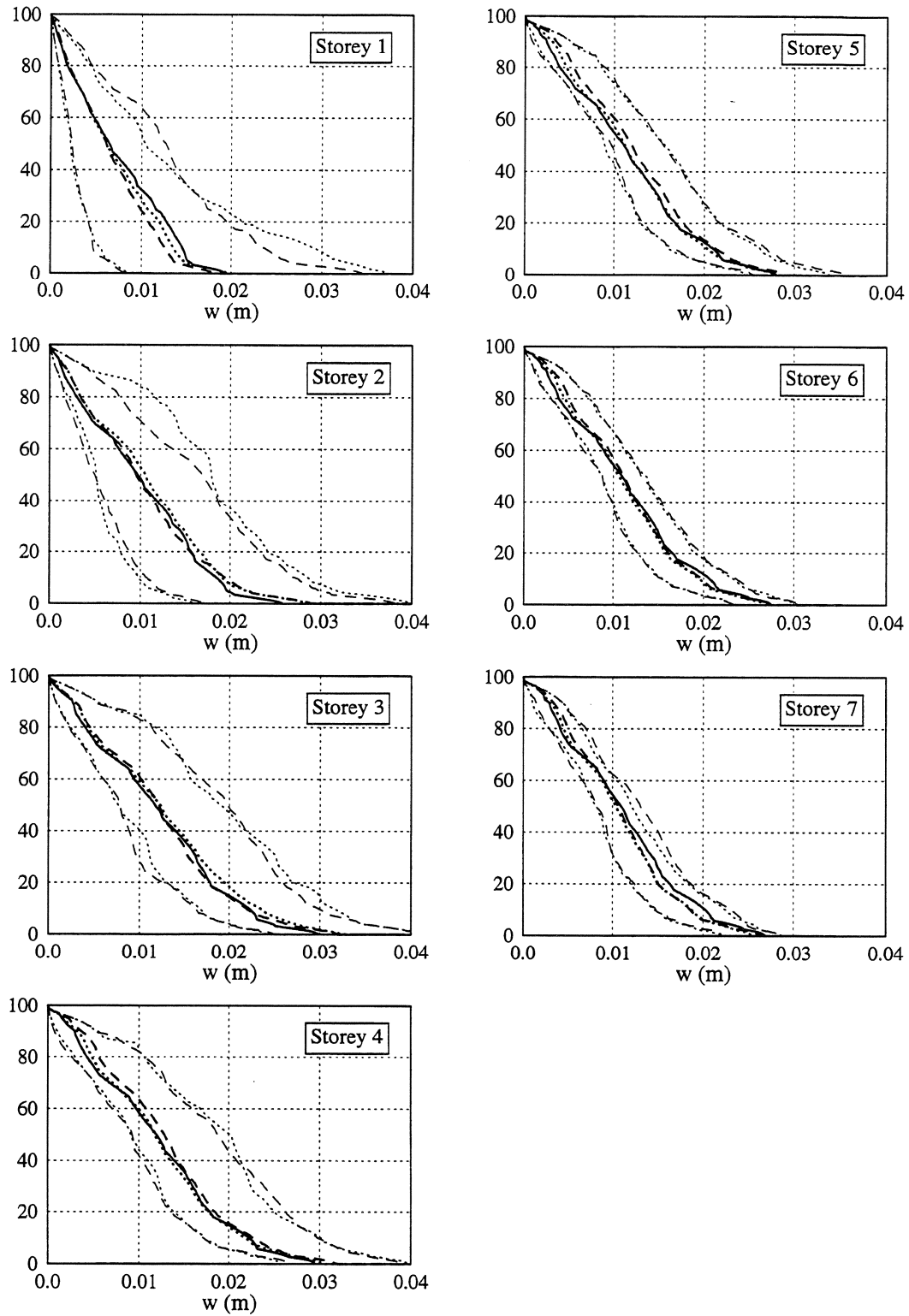
FIGURE 4-7 Percentage of motion duration over which $|Y_w(t)|$ exceeds level w. MC model. Input: Parkfield. (——— symmetric system; · · · · · wall 1; — — — wall 2)

combinations. The dotted and dashed lines correspond to walls 1 and 2, respectively, as marked in Figure 4-1. Thicker lines denote the median. The continuous line in each plot corresponds to the deterministic symmetric system in which both walls undergo identical displacements for input motion acting in their direction. Asymptotically, i.e., for sufficiently large number of realizations the curves corresponding to the two walls would be indistinguishable. It is evident from the plots that especially for the upper envelope curves 100 or 150 realizations are not sufficient. Nevertheless, the agreement between walls is quite satisfactory for the lower envelope curve and the median.

In most graphs the wall median curves are statistically indistinguishable from the response of the symmetric system. The only notable differences are observed under El Centro, especially in the three lowest storeys in Figure 4-4 where the median curves lie significantly lower.

Any given level of interstorey wall displacement is exceeded for longer fraction of the motion duration under Parkfield, particularly so for higher displacement levels. It is also evident that $Y_w(t)$ reaches higher values under Parkfield.

4.4.2 Maximum interstorey displacement

The maximum interstorey displacement $Y_{\max}$ defined as the maximum maximorum of the magnitude of the interstorey wall displacements gives an indication of the maximum stress on the wall system for a given system realization. The mean of $Y_{\max}$ is compared in Figure 4-8 with the maximum interstorey displacement of the symmetric system $y_{\max,0}$. The probability of $Y_{\max}$ exceeding $y_{\max,0}$ is calculated as the percentage of sample values of $Y_{\max}$ above $y_{\max,0}$. It starts from about 50% in the top storey and gets as high as 94%, although its specific values are not very reliable because of the limited number of samples. The ratio of the mean of $Y_{\max}$ to $y_{\max,0}$ shown in the right plot is consistently larger than one. This indicates that the yield uncertainty and the resulting torsional response increase on the average the maximum interstorey displacement. The ratio exhibits an increasing trend from the top storey down. There is no clear trend for the effect of either input motion or restoring force model on the probability of exceedence or the ratio.

The actual values of the mean of $Y_{\max}$ are shown in Figure 4-9 along with its coefficient of variation (COV). The mean of $Y_{\max}$ increases with height up to the third storey and then decreases resulting in similar top- and first-storey values. The effect of the input motion on the mean of $Y_{\max}$ is very pronounced with values under Parkfield as much as
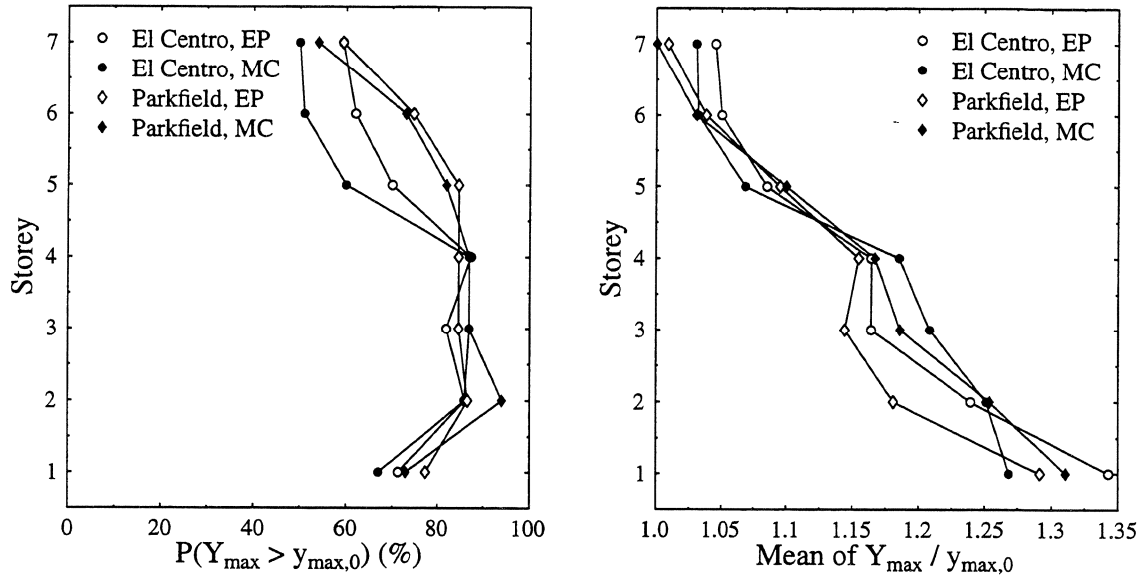
FIGURE 4-8 Comparison of Y_{max} and $y_{max,0}$.

70% higher than under El Centro. On the other hand the effect of restoring force model is from minor to practically none, as for the top three storeys under El Centro.

When considering the coefficients of variation of all response measures of the seven-storey system one should be aware that part of the calculated values is statistical variation caused by the relatively small number of realizations. The COV of Y_{max} in all storeys above the
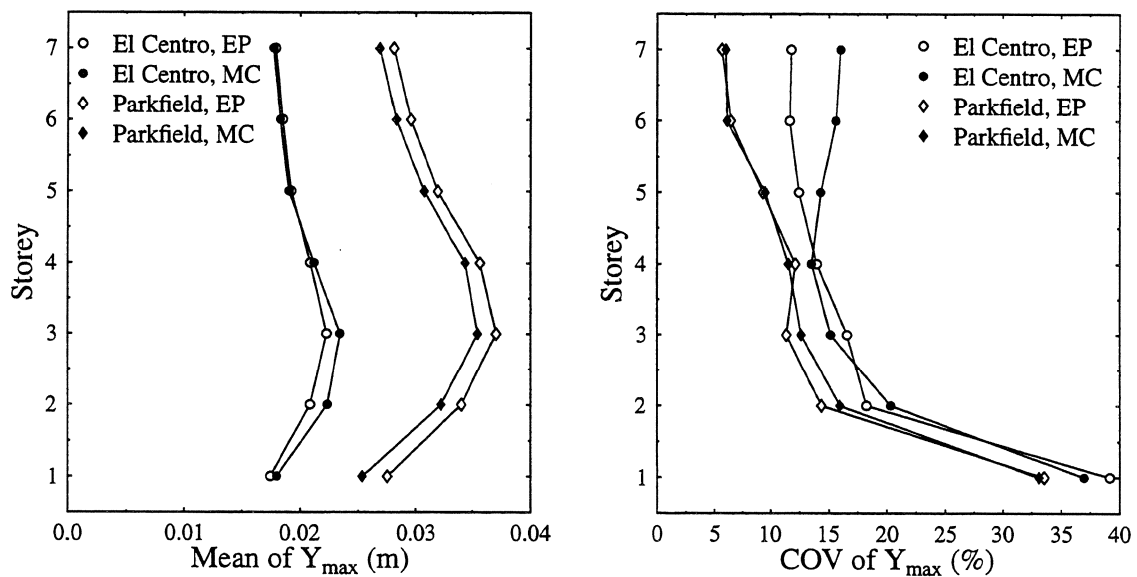
FIGURE 4-9 Mean and COV of maximum interstorey displacement Y_{max}.

124

first does not exceed 20% whereas in the first storey it ranges from 33% to 39%. It is also consistently lower under Parkfield, mostly due to the higher mean values, although the standard deviation (not shown) is actually larger for storeys up to the fifth.

Displacement ratio. In order to quantify the effect of model uncertainty the following ratio is defined in each storey: $R_d = Y_{max,MC}/Y_{max,EP}$ for each of the first 100 samples common to both models, where $Y_{max,MC}$ and $Y_{max,EP}$ are the maximum interstorey displacements of two systems with identical elastic properties and yield strengths but following the modified-Clough and the elastoplastic model, respectively. The ratio R_d is a random variable. When the response of the system with MC model exceeds that of the system with EP model the ratio is larger than unity. Note that $R_d - 1 = (Y_{max,MC} - Y_{max,EP})/Y_{max,EP}$ which coincides with the relative error in the maximum displacement if the EP model is selected over the MC.

The graphs in Figure 4-10 show the mean of R_d, denoted by the thicker line, and a range of one standard deviation around it. Under El Centro it is more likely than not that the maximum interstorey displacement for the MC model will exceed that for the EP in the lower four storeys. The highest ratio values are calculated in the first storey. The opposite holds true under Parkfield. There is small probability of the response for the MC model exceeding that for the EP, as evidenced by the mean-plus-one-standard-deviation values of about one in most storeys and the consistently below one mean values.
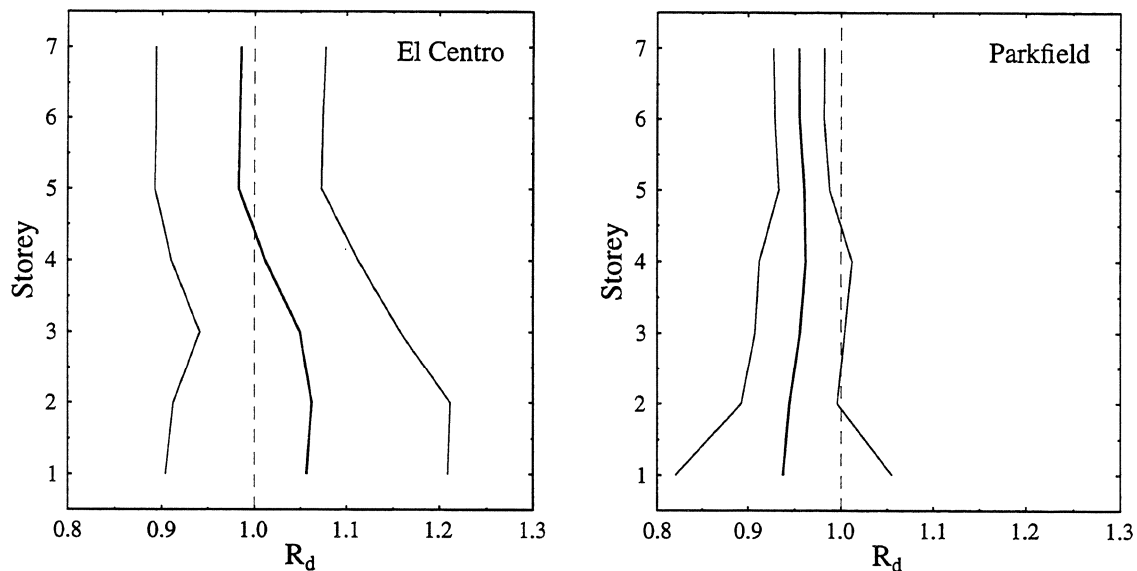
FIGURE 4-10 Ratio of maximum interstorey displacement of MC to EP model.

4.4.3 Maximum interstorey rotation

The mean of the maximum interstorey rotation Φ_{max} shown in the first graph of Figure 4-11 is fairly constant for the first two or three storeys and then decreases with height. It is mostly lower under El Centro but it not clear how it is affected by the model selection. The COV of Φ_{max}, seen in the second graph of the same figure, exceeds 45% in all cases. Its values in the first floor are particularly high, between 69% and 78%, a trend observed previously in conjunction with the COV of Y_{max} (Figure 4-9).
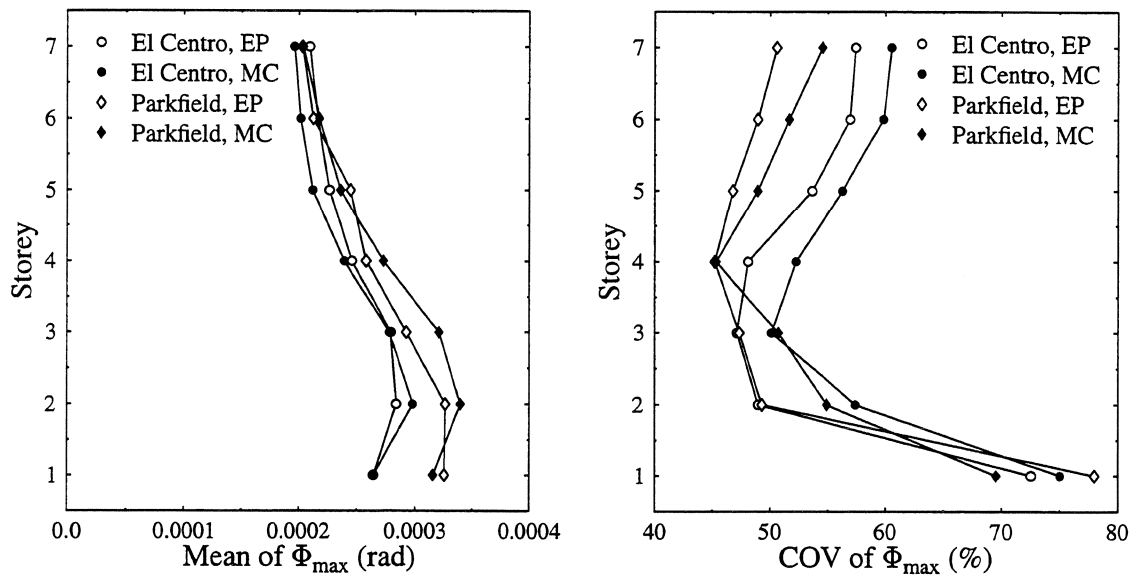
FIGURE 4-11 Mean and COV of maximum interstorey rotation Φ_{max}.

4.4.4 Dissipated energy

The seven-storey building under consideration has been designed as special moment-resisting frame-wall system. According to this design philosophy, frames and walls collaborate in energy dissipation during seismic response. In order to identify their contributions each storey is divided into a frame and a wall subsystem. All inelastic springs in a frame subsystem have completely deterministic parameters whereas all springs in a wall subsystem have random yield strengths.

Figure 4-12 shows the sample mean of the dissipated energy E_{dis} as well as the energy dissipated by the symmetric system. The difference between total and frame energy lines, identified on the graphs, is the wall energy. The mean of the frame energy is fairly constant over the height of the building and differs little from the frame energy in the symmetric system. The walls dissipate energy mostly below the fourth floor and
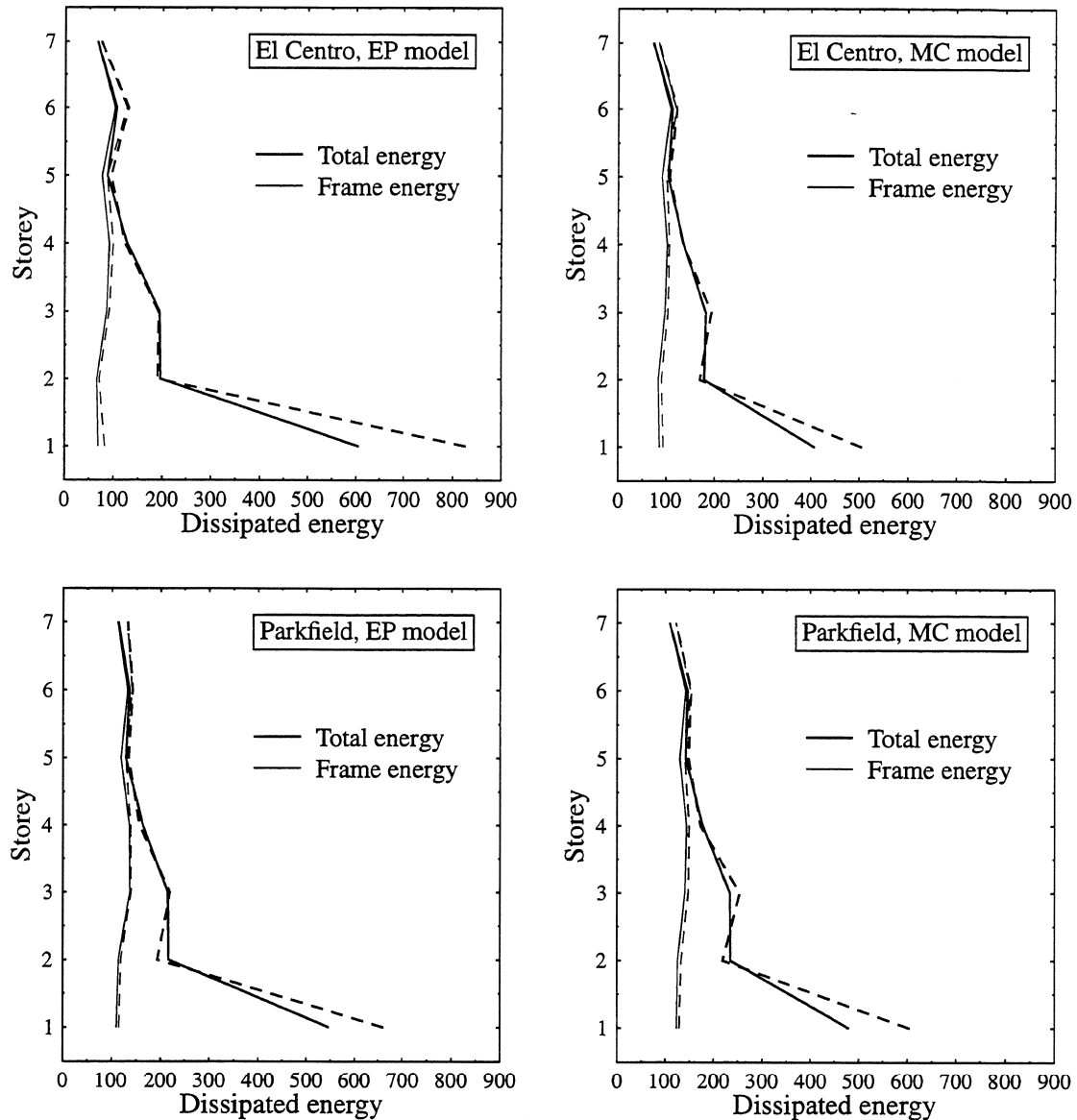
FIGURE 4-12 Dissipated energy (——— sample mean; ——— symmetric system).

especially, as expected, in the first storey. The walls in the first floor of the asymmetric systems dissipate on the average less energy than the same storey walls of the symmetric system. Under Parkfield, the mean of E_{dis} changes only slightly between models. Under El Centro the wall energy is considerably lower for the MC model, especially in the first storey.

The uncertainty in the wall energy, expressed by the COV in Figure 4-13, is very high, particularly compared with the uncertainty in the frame energy. This is to be expected since the uncertainty in the frame energy is a second level effect caused by the uncertain

127
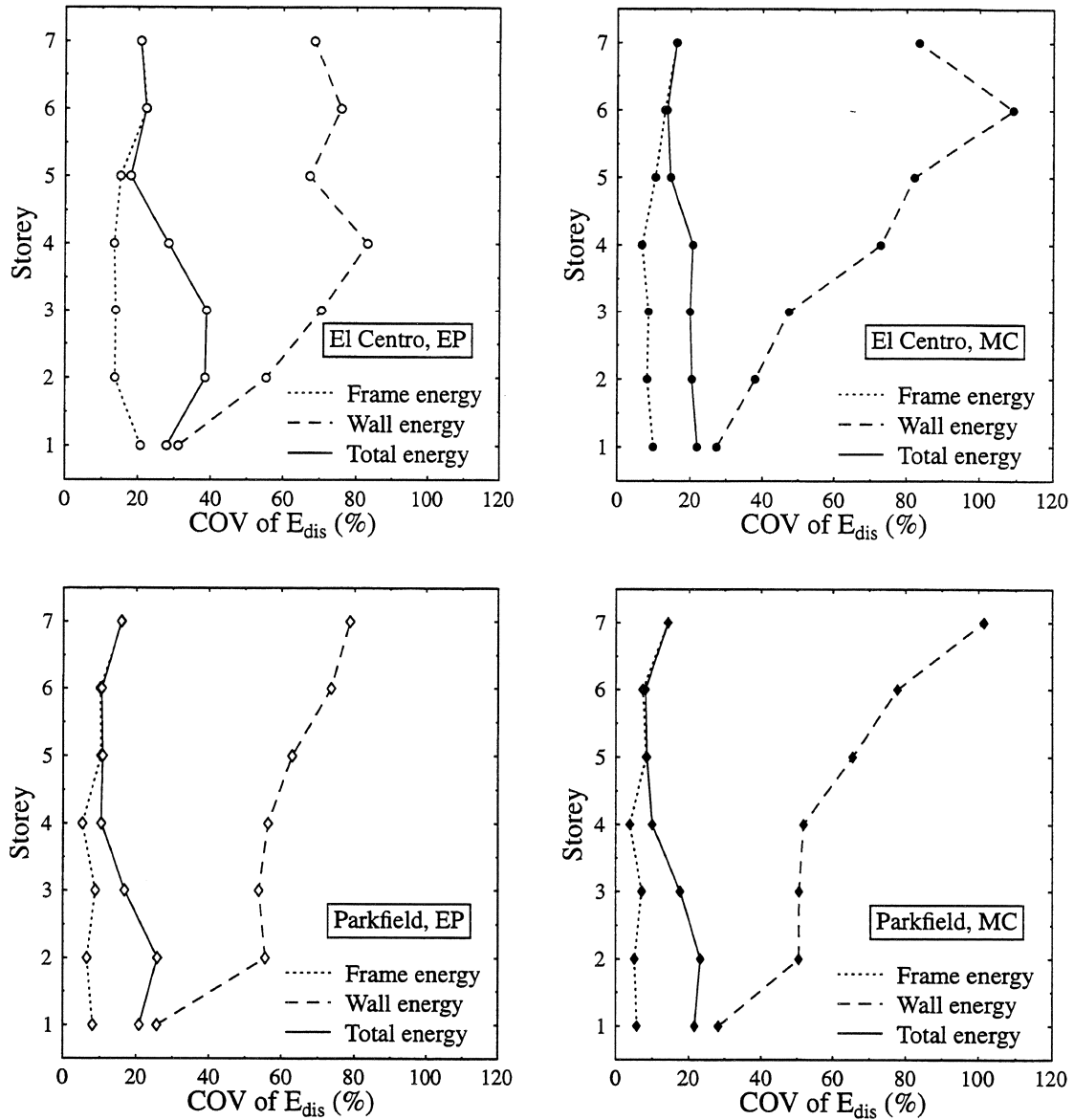
FIGURE 4-13 Coefficient of variation of dissipated energy.

strengths of the wall springs. The disproportionately large coefficients of variation of the wall energy in the higher storeys are caused by the practically zero mean values in the same storeys. The COV of the total energy lies mostly below 25% with the exception of the combination of EP model and El Centro which gives COV as high as 39%. Moreover, the COV of the total energy tends to be lower for the MC model.

Statistics of the energy dissipated over all storeys are listed in Table 4-1. It is notable that the frames (inspection of detailed results, not shown here, reveals that it is mostly the beams) dissipate on the average 40% to 60% of the total energy. The mean of the total

TABLE 4-1 Statistics on system energy dissipation.

Input	Model	Subsystem	Mean(E_{dis})	COV(E_{dis})	Mean($E_{\text{dis}}/e_{\text{dis},0}$)
El Centro	EP	Frame	556.3	12.22	0.881
		Walls	829.7	15.75	0.827
		Total	1386.0	13.12	0.848
	MC	Frame	640.8	7.23	0.917
		Walls	553.2	11.40	0.894
		Total	1194.0	7.57	0.906
Parkfield	EP	Frame	861.9	7.22	0.942
		Walls	659.6	11.02	0.910
		Total	1521.5	6.21	0.928
	MC	Frame	915.5	5.39	0.940
		Walls	609.7	12.38	0.872
		Total	1525.2	6.72	0.911

energy dissipated by the system is insensitive the model selection under Parkfield but it is 16% higher for the EP than for the MC model under El Centro. The coefficients of variation are generally low, lower than the COV assumed for the uncertain yield strengths. The asymmetric systems dissipate on the average less energy than their respective deterministic symmetric systems, as indicated by the mean of the ratio $E_{\text{dis}}/e_{\text{dis},0}$.

Energy ratio. A ratio between dissipated energies for the two restoring force models on a per sample basis is defined in a similar way as the displacement ratio in Section 4.4.2. The mean of the ratio $R_e = E_{\text{dis,MC}}/E_{\text{dis,EP}}$ as well as a range of one standard deviation around it are plotted in Figure 4-14.

Under El Centro the mean of the ratio R_e for the total energy is above one in all storeys above the second with a highest value of 1.25. However, the first storey in which a large portion of the energy dissipation takes place, is expected to have less energy dissipated for the MC model. As a matter of fact, with all storey energies summed up the mean of R_e for the whole system is 0.92 which shows that the first storey dominates the energy dissipation of the system. The spread of ratio values is fairly constant with height.

Under Parkfield, R_e for the total energy has small variability, between about 0.8 and 1.2.
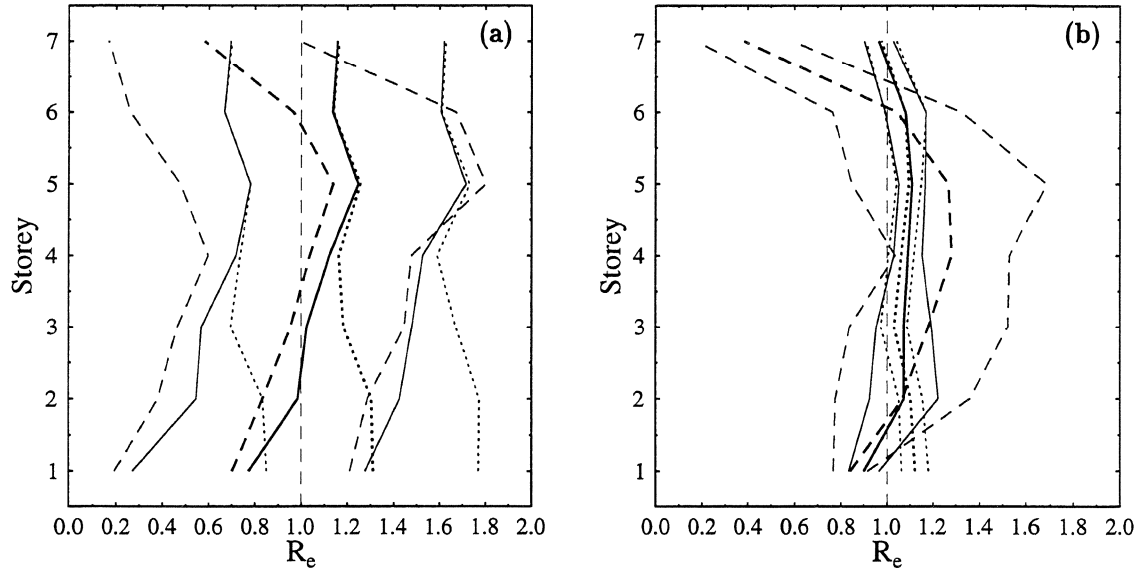
FIGURE 4-14 **Ratio of dissipated energy of MC to EP model.** **(a) Input:** **El Centro. (b) Input: Parkfield.** ($\cdots\cdots$ frames; $---$ walls; —— total.)

Its mean is above one in most storeys but below one in the first storey which eventually compensates for the rest and as it turns out the mean of R_e for the whole system is unity.

4.5 Conclusions

One of the objectives of this study is to investigate the sensitivity of the seismic response to yield strength uncertainty. Numerical results from the seven-storey frame-shear wall building with random yield strengths in the wall springs indicate that:

- Torsion caused by strength uncertainty leads to maximum interstorey displacements with mean values consistently higher than the respective displacements of the deterministic symmetric system. The increase is the more significant the lower the storey and it can be as much as 35%.

- The coefficients of variation of the maximum interstorey displacement Y_{max} and the total energy dissipated by the system are relatively small with the exception of Y_{max} in the first storey for which it is roughly 35%. On the other hand, the coefficient of variation of the maximum interstorey rotation can be as high as 78% when the coefficient of variation of the random yield strengths is 15%.

- The mean of Y_{max} increases with height up to the third storey and subsequently decreases resulting in similar top- and first-storey values.

- Torsion results in decrease in the mean of the total energy dissipated in the first storey, the largest by far among all storeys, compared to the energy dissipated in the same storey by the symmetric system.

Another issue addressed by the present study is whether the choice of the simple elasto-plastic restoring force model over the more sophisticated modified-Clough is conservative. Numerical results from the seven-storey system suggest that:

- Maximum interstorey displacement can be larger for the modified-Clough than for the elastoplastic model. This is more likely than not under El Centro and especially in the lower four storeys whereas it is rather improbable under Parkfield with the possible exception of the first storey.

- Dissipated energy tends to be lower for the modified-Clough than for the elastoplastic model, particularly in the first storey where a significant portion of the energy dissipation takes place.

These observations suggest that if the modified-Clough were the correct restoring force model, the use of the elastoplastic model instead, would not necessarily be conservative.

SECTION 5

CODE EVALUATION

The static force procedure of the Uniform Building Code (UBC, 1994) requires that accidental torsion be considered in seismic design. This accidental torsion at a given storey can be determined for nonflexible diaphragms by assuming the mass of that story is displaced from the calculated center of mass a distance equal to 5% of the building dimension perpendicular to the direction of the static force. As stated in the 1991 version of the UBC, the accidental torsion is introduced "to account for the uncertainties in locations of loads". The same accidental torsion provision is included in the 1994 version of the code, except that no reason for its necessity is offered any more.

The supplement to the National Building Code of Canada (NBCC, 1985) lists several sources of accidental torsion: "variations in the estimates of the relative rigidities, uncertain estimates of dead and live loads at the floor levels, addition of wall panels and partitions after completion of the building, variation of the stiffness with time, and inelastic or plastic action". A similar list can be found in the commentary of the New Zealand Standard (NZS, 1992): "limitations of stiffness calculation, degree of accuracy of assumptions, mass variation, construction variations, and, in severe earthquakes, asymmetric failure of torsion resisting elements". Both the Canadian and the New Zealand code specify accidental torsion due to an eccentricity of 10% of the building dimension perpendicular to the direction of loading. The fact that this value is double the one required by the UBC raises the issue of which of the two values, if any, is the appropriate one.

Only one source of accidental torsion is considered in this study: the uncertainty in material properties and, more specifically, in yield strength. A nominally symmetric system with yield strength uncertainty can experience torsional vibrations following yield. The objective is to determine whether the UBC provisions for accidental torsion are satisfactory for this case. The code evaluation is based on comparison between the UBC-specified accidental eccentricity and the dynamic eccentricity, defined as the ratio of the dynamic torsional moment to the storey shear force given by the same code. Sections 5.1 and 5.2 cover, respectively, the one-storey and multi-storey systems considered. Section 5.3 deals with similarities and differences in the trends observed for the two types of system. All conclusions drawn in the context of code evaluation are limited to the systems and input

133

motions considered and therefore should not be construed as a general assessment of the validity of the code provisions on accidental eccentricity.

5.1 One-storey systems

The two lateral-load-resisting elements of the structural model shown in Figure 5-1 are assumed to have independent yield strengths ($\rho = 0$) following identical lognormal distributions (equations (3-2)–(3-6)). The lognormal distribution is arbitrary but physically admissible since it does not allow for negative strength values. Because of the independence of yield strengths, the inelastic response of the system involves torsion. Both the elastoplastic and the modified-Clough restoring force models are considered. The small-vibration lateral period in the direction of the ground motion T, called 'period' for brevity, is taken equal to 0.5, 1.0, and 1.5 sec. The dimensionless parameter $\gamma = l/r$ is used to characterize the radius of gyration r. Since mass m and l are fixed, r and the mass moment of inertia mr^2 decrease with γ. When torsion is initiated following yield of the weakest element, a reduced mass moment of inertia provides less resistance and allows larger rotations to develop. Therefore, a system with large γ is expected to be more susceptible to torsion. The values of γ considered are 0.5, 1.0 and 1.5. The system is designed according to the UBC provisions as described in Section 3.3.
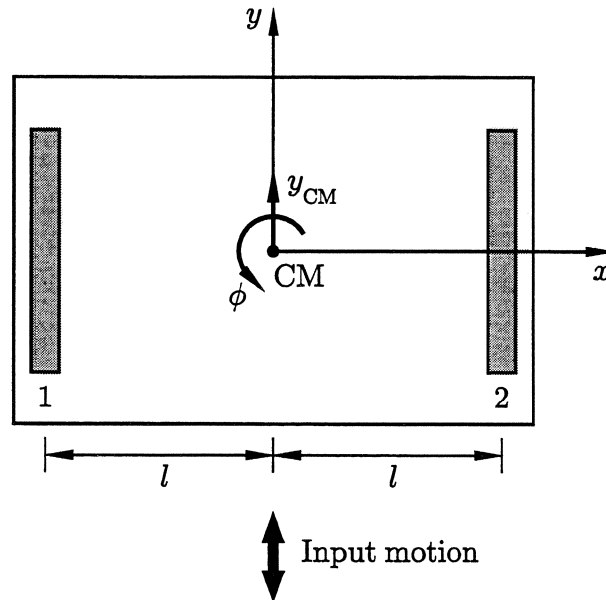
FIGURE 5-1   Structural model (same as Figure 3-1).

Input consists of the strong motion portions of the El Centro, Taft, and Parkfield acceleration records (see Section 3.2). Each record is scaled to peak ground accelerations of $0.2g$–$0.6g$ with step $0.1g$, and $1.0g$. In the context of this study the term 'motion' is used as an abbreviation for 'strong motion'.

Code evaluation is based on the following response measures:

- dynamic eccentricity $\Theta(t) = \dfrac{mr^2\,\ddot{\Phi}(t)}{V\,(2l)}$, where $\ddot{\Phi}(t)$ is the torsional acceleration, m is the mass of the system, r is the radius of gyration, V is the design base shear, and $2l$ is the system dimension perpendicular to the ground motion,

- maximum dynamic eccentricity $\Theta_{\max} = \max\{|\Theta(t)|\}$,

- Z = total time of $|\Theta(t)|$ above the code-specified accidental eccentricity e_a, given as percentage of the motion duration, and

- upcrossing rate N, which is equal to the number of times during the motion $|\Theta(t)|$ upcrosses level e_a, divided by the motion duration.

Numerical results are obtained for systems with two restoring force models, three periods per model, and three values of the parameter γ per period. For each of the above systems Monte Carlo simulation with 1000 realizations of the element yield strengths is performed.

5.1.1 Dynamic eccentricity

Figure 5-2 shows time history samples of the dynamic eccentricity $\Theta(t)$ for system realizations corresponding to various combinations of restoring force model and parameters T and γ. All time histories in the figure result from the same input motion, namely the El Centro record scaled to peak ground acceleration of $0.4g$. Sample systems with the same period are assigned the same pair of element yield strengths. Consequently, the differences between time histories are due to the model and/or the value of γ but not to the yield strength values.

Comparison of the plots in Figure 5-2 provides some insight on the way the evolution in time of $\Theta(t)$ is affected by variations in the system parameters. The parameter γ affects the time history most drastically, as shown by the pair of graphs in each row. This is to be expected since γ controls the torsional response of the system and the dynamic eccentricity is just a scaled form of the torsional acceleration.
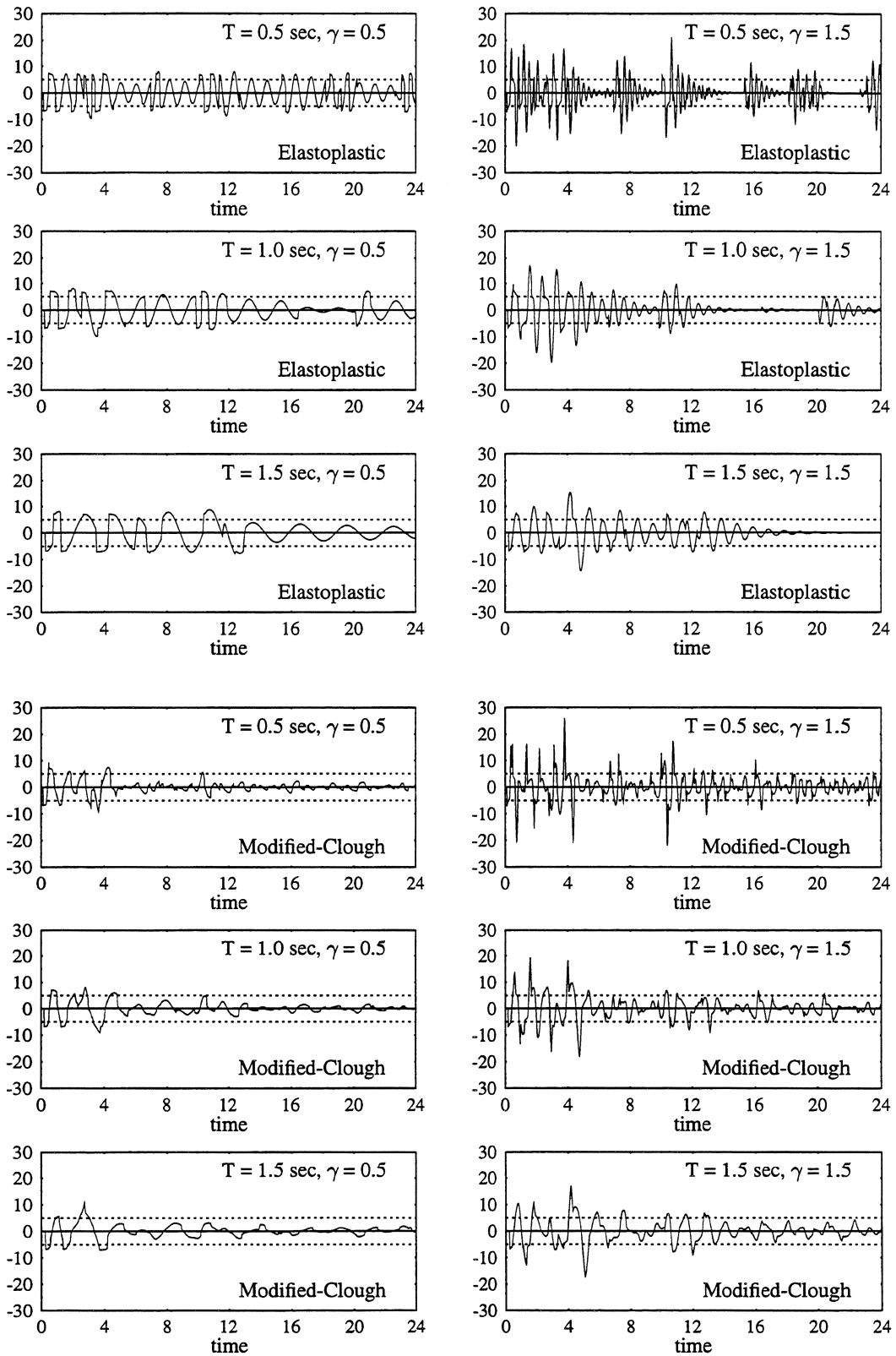
FIGURE 5-2 Dynamic eccentricity time history for sample systems. Input: El Centro scaled to PGA = 0.4g.

The restoring force model appears to be very influential, as well. Comparison of the graphs in the top and bottom half of Figure 5-2 reveals essential differences associated with the model selection. The time histories for the elastoplastic model are characterized by three major phases. The first phase occurs when only one of the elements is in yield and is associated with a build up in torsional accelerations. During the second phase both elements are in yield and the only change in torsional acceleration is due to the viscous damping. The third phase is present while both elements are elastic. During this time translation and rotation are decoupled. In the absence of torsional component in the input motion, the torsional response during this phase is damped free vibration. The periods of damped free vibration are easiest to identify in the time history sample at top right of Figure 5-2 (for instance, between 4.5 and 6.5 sec or 7.5 and 10 sec, approximately). If the elements remain in the elastic range long enough the torsional acceleration and, therefore, the dynamic eccentricity may return to zero. At some point during the free vibration in torsion one of the two elements may yield again and the response goes back to first phase.

In contrast, for the modified-Clough model the two elements never behave elastically after their initial yield. Consequently, translation and rotation remain coupled throughout the rest of the motion and the free vibration is absent from the graphs in the bottom half of the figure. Moreover, some level of dynamic eccentricity is observed at all times after initial yield.

The time history samples in Figure 5-2 show that the dynamic eccentricity varies considerably in time. It would therefore be useful to devise some measure of the magnitude of $|\Theta(t)|$. Only the absolute value of $\Theta(t)$ needs to be considered since the sign of the dynamic eccentricity is of no consequence in the context of code evaluation. The process $|\Theta(t)|$ is neither ergodic nor stationary. Because it is nonergodic, sampling in time is not equivalent to sampling at a fixed time across the ensemble. Moreover, due to the lack of stationarity, sampling across the ensemble at various fixed times would yield very different histograms. Taking the above two comments into account, the desired measure can be obtained through the following procedure: Realizations of $|\Theta(t)|$ for given system parameters and input motion are sampled at fixed times t_i, $i = 1, \ldots, n$, yielding a histogram f_i at each time t_i. Next, a mixture of histograms f is defined as $f = (1/n) \sum_{i=1}^{n} f_i$. The n fixed-time histograms are assigned equal weights assuming that observation of the process at any of these times is equally likely. The histogram f provides an overall measure of the magnitude of $|\Theta(t)|$.

TABLE 5-1 **Estimates of the mean of $|\Theta(t)|$ and one, two, and three standard deviations above it (all values in %).**

Sys	El Centro				Taft				Parkfield			
	Mean + k std deviations				Mean + k std deviations				Mean + k std deviations			
	$k=0$	$k=1$	$k=2$	$k=3$	$k=0$	$k=1$	$k=2$	$k=3$	$k=0$	$k=1$	$k=2$	$k=3$
S1	2.38	5.22	8.06	10.90	3.20	6.08	8.96	11.84	3.10	6.30	9.50	12.70
S2	2.30	5.56	8.82	12.08	3.05	7.62	12.19	16.76	2.25	5.72	9.19	12.66
S3	2.17	4.59	7.01	9.43	2.49	5.29	8.09	10.89	3.35	6.63	9.91	13.19
S4	1.90	4.92	7.94	10.96	2.73	6.25	9.77	13.29	4.11	8.86	13.61	18.36
S5	2.09	4.59	7.09	9.59	2.86	5.84	8.82	11.80	3.48	6.88	10.28	13.68
S6	1.86	4.51	7.16	9.81	1.96	4.50	7.04	9.58	3.44	7.11	10.78	14.45
S7	0.76	2.04	3.32	4.60	1.00	2.51	4.02	5.53	1.73	4.14	6.55	8.96
S8	2.05	4.85	7.65	10.45	2.13	5.00	7.87	10.74	2.01	5.35	8.69	12.03
S9	0.86	2.18	3.50	4.82	1.30	3.03	4.76	6.49	1.66	4.29	6.92	9.55
S10	1.74	4.24	6.74	9.24	2.65	5.98	9.31	12.64	2.52	5.99	9.46	12.93
S11	1.24	3.08	4.92	6.78	1.29	2.99	4.69	6.39	1.90	4.63	7.36	10.09
S12	1.87	4.35	6.83	9.31	1.89	4.56	7.23	9.90	2.64	6.31	9.98	13.65
	1.77	4.18	6.59	9.00	2.21	4.97	7.73	10.49	2.68	6.02	9.36	12.69

Table 5-1 lists the mean ($k=0$) and the mean plus one, two, and three standard deviations obtained from the histogram f of $|\Theta(t)|$ for several system configurations, labeled S1–S12. Systems S1–S6 follow the elastoplastic model whereas systems S7–S12 follow the modified-Clough. Systems S1, S2, S7, and S8 have $T = 0.5$ sec, S3, S4, S9, and S10 have $T = 1.0$ sec, and the rest have $T = 1.5$ sec. Finally, odd numbered systems have $\gamma = 0.5$ and even numbered ones have $\gamma = 1.5$, representing the two extreme values of this parameter considered in the study. All three input motions are scaled to the same PGA of $0.4g$. For each system configuration 100 realizations of $|\Theta(t)|$ were sampled at 1 sec intervals for El Centro and Taft, and at 0.25 sec intervals for Parkfield. The strong motion portion of the Parkfield record is much shorter than those of the other two records and it was sampled more frequently in order to end up with comparable numbers of sampling points per realization for all three input motions.

The last row of Table 5-1 shows the statistical mean of the quantities in the columns averaged over the set of systems S1–S12. Compared with the values in this last row, the UBC-specified accidental eccentricity of 5% places above, at, and below the mean plus

one standard deviation mark for the El Centro, Taft, and Parkfield records, respectively. The 10% accidental eccentricity value suggested by other codes falls either above or at about the mean plus three standard deviations point for El Centro and Taft, respectively. However, for Parkfield it places slightly above the mean plus two standard deviations mark.

From the mixture of histograms $f = (1/n) \sum_{i=1}^{n} f_i$, where f_i are histograms of $|\Theta(t)|$ at fixed times t_i, one can obtain the percentage of values of $|\Theta(t)|$ exceeding specified eccentricity levels. This percentage is plotted versus eccentricities in the range 5% to 25% in Figures 5-3(a)–5-5(a) for all even numbered systems in the set S1–S12, i.e., the systems with $\gamma = 1.5$. Each figure shows results for one of the input motions considered and the PGA is $0.4g$ in all cases. The six curves in Figure 5-3(a) in the order in which they intersect the y-axis starting from the top correspond to systems S2, S4, S6, S8, S12, and S10. Similarly, the order in Figure 5-4(a) is S2, S4, S10, S12, S6, and S8 and in Figure 5-5(a) is S4, S6, S12, S10, S2, and S8.

The range of percentages for each eccentricity level is better illustrated by the envelope curves shown in Figures 5-3(b)–5-5(b). Although the majority of $|\Theta(t)|$ values lie below
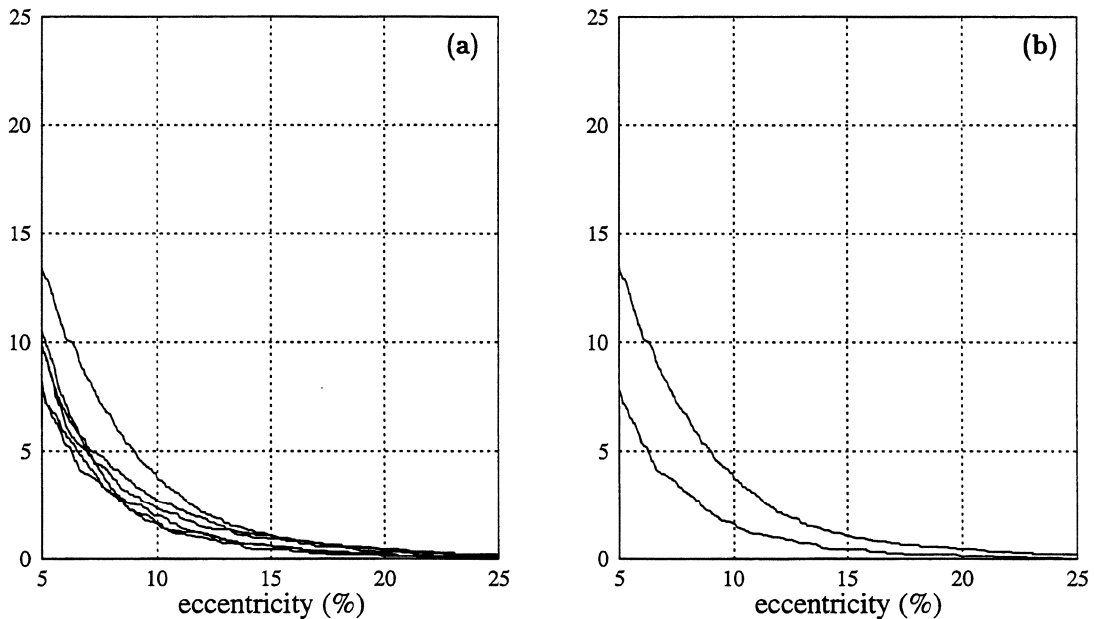
FIGURE 5-3 Percentage of absolute dynamic eccentricity values above specified eccentricity levels. Input: El Centro scaled to PGA $= 0.4g$. (a) Results for EP and MC models, $T = 0.5$, 1.0, and 1.5 sec, and $\gamma = 1.5$. (b) Envelopes of results in (a).
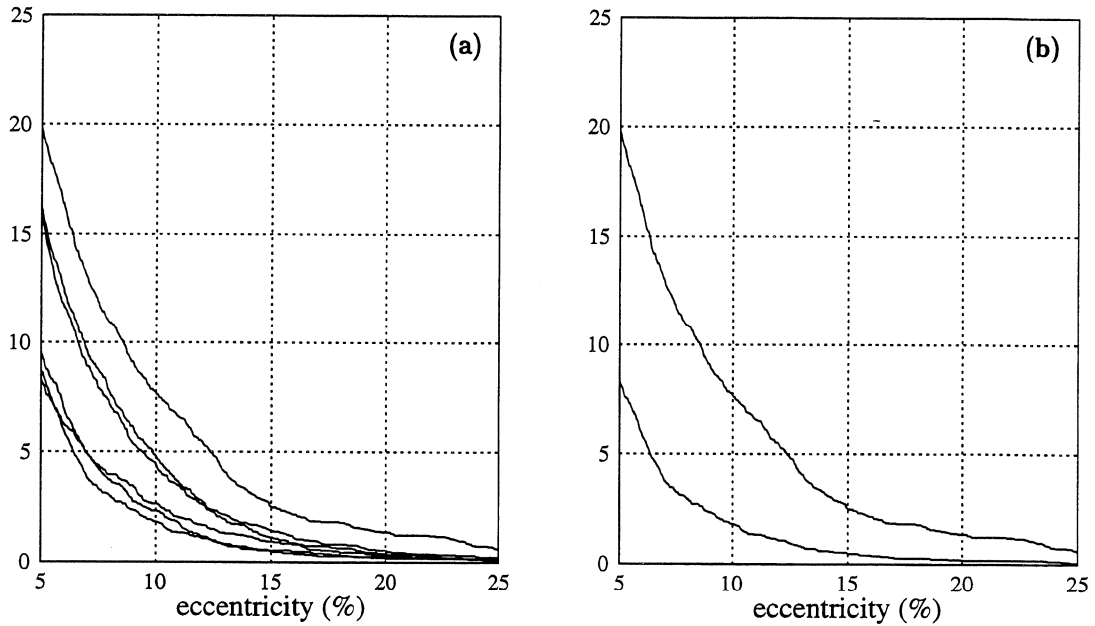
FIGURE 5-4 Percentage of absolute dynamic eccentricity values above specified eccentricity levels. Input: Taft scaled to PGA = $0.4g$. (a) Results for EP and MC models, $T = 0.5$, 1.0, and 1.5 sec, and $\gamma = 1.5$. (b) Envelopes of results in (a).
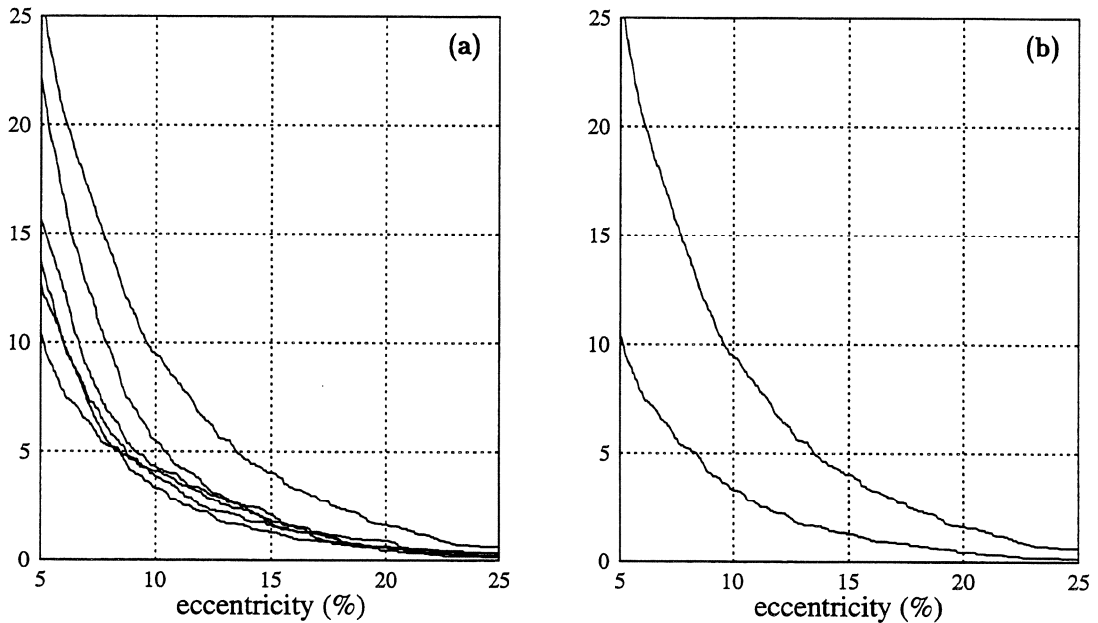
FIGURE 5-5 Percentage of absolute dynamic eccentricity values above specified eccentricity levels. Input: Parkfield scaled to PGA = $0.4g$. (a) Results for EP and MC models, $T = 0.5$, 1.0, and 1.5 sec, and $\gamma = 1.5$. (b) Envelopes of results in (a).

140

the 5% accidental eccentricity specified by the UBC, a considerable percentage exceeds the code eccentricity. This percentage is roughly 8%–13% for El Centro, 8%–20% for Taft, and 10%–26% for Parkfield. Moreover, the percentage of values above the 10% eccentricity level (approximately 1.5%–4%, 2%–8%, and 3.5%–9.5% for El Centro, Taft, and Parkfield, respectively) is still quite significant. Therefore, no clear justification can be offered for choosing 5% or 10% as the appropriate accidental eccentricity.

5.1.2 Maximum dynamic eccentricity

The maximum dynamic eccentricity $\Theta_{\max}$ is compared with the accidental eccentricity $e_a = 5\%$ specified by the UBC. The left-column graphs in Figures 5-6–5-11 show the mean of $\Theta_{\max}$. The graphs on the right of the same figures include two sets of curves, represented by lines of different thickness. The thicker lines represent the probability $P(\Theta_{\max} > e_a)$, estimated as the percentage of samples of $\Theta_{\max}$ that exceed e_a. This is essentially the probability of the absolute dynamic eccentricity $|\Theta(t)|$ exceeding e_a at any time during the strong motion. It is based on instantaneous values of the dynamic eccentricity and therefore, it contains no information on how brief or prolonged the stay above e_a may be. This information is provided by the sets of thinner lines on the graphs, which indicate the mean of Z, i.e., the percentage of the motion duration that $|\Theta(t)|$ is expected to spend above e_a.

Elastoplastic model. The mean of $\Theta_{\max}$ exceeds 5% for almost all system parameter and PGA combinations, as shown in Figures 5-6, 5-7, and 5-8 corresponding to the El Centro, Taft, and Parkfield records, respectively. For the systems least susceptible to torsion ($\gamma = 0.5$) the mean of $\Theta_{\max}$ remains below 10% but, as γ increases, values between 10% and 20% are frequently encountered. The mean of $\Theta_{\max}$ tends to increase with PGA, as well as, with the parameter γ. Under El Centro and Parkfield the increase with γ is monotonic. Under Taft the trend is not as consistent but the highest values are still associated with $\gamma = 1.5$. The uncertainty in $\Theta_{\max}$ is large; its coefficient of variation (not shown) ranges between 60% and 80%.

The probability $P(\Theta_{\max} > e_a)$, shown with thick lines in the right-column graphs of Figures 5-6–5-8 is generally high with most values in the range 40%–85%. It tends to increase with γ whereas it remains relatively unaffected by the increase in PGA for accelerations over $0.4g$.

The mean of Z, the total time above e_a, is represented by the set of thin lines. It
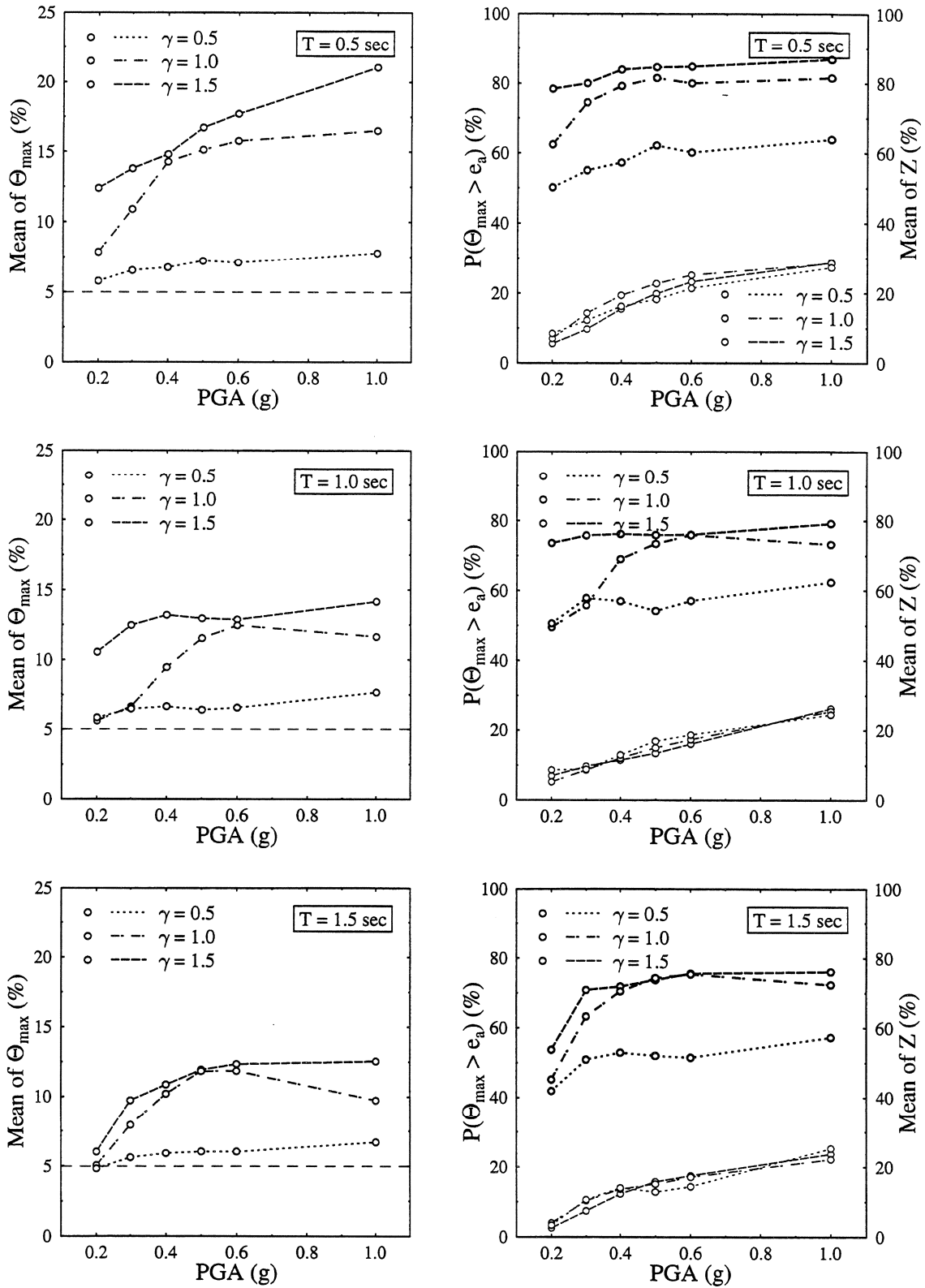
FIGURE 5-6 Mean of Θ_{max}, probability of exceedence of e_a by Θ_{max}, and mean of Z. EP model. Input: El Centro.
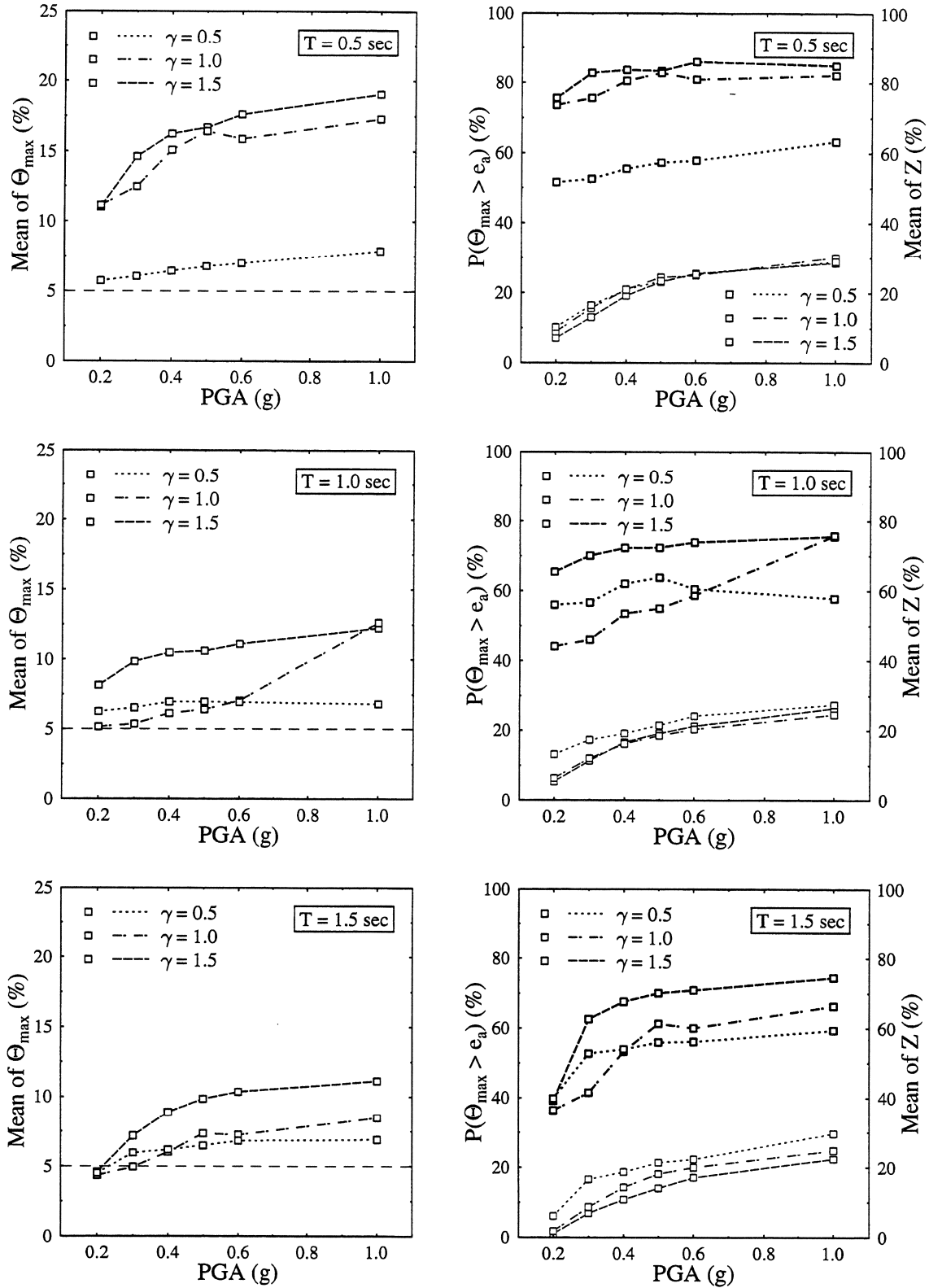
FIGURE 5-7 Mean of $\Theta_{\max}$, probability of exceedence of e_a by $\Theta_{\max}$, and mean of Z. EP model. Input: Taft.

143
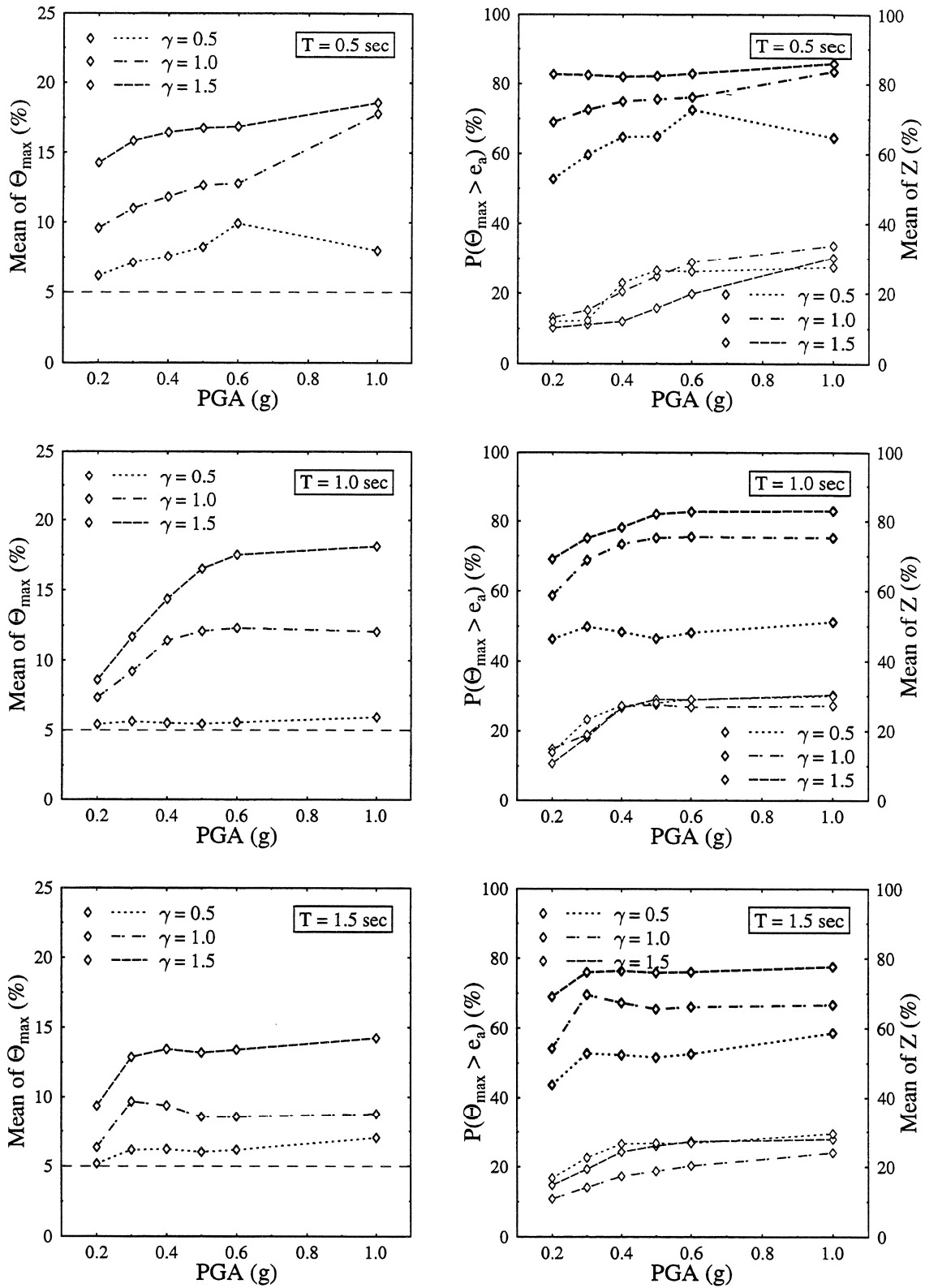
FIGURE 5-8 Mean of Θ_{max}, probability of exceedence of e_a by Θ_{max}, and mean of Z. EP model. Input: Parkfield.
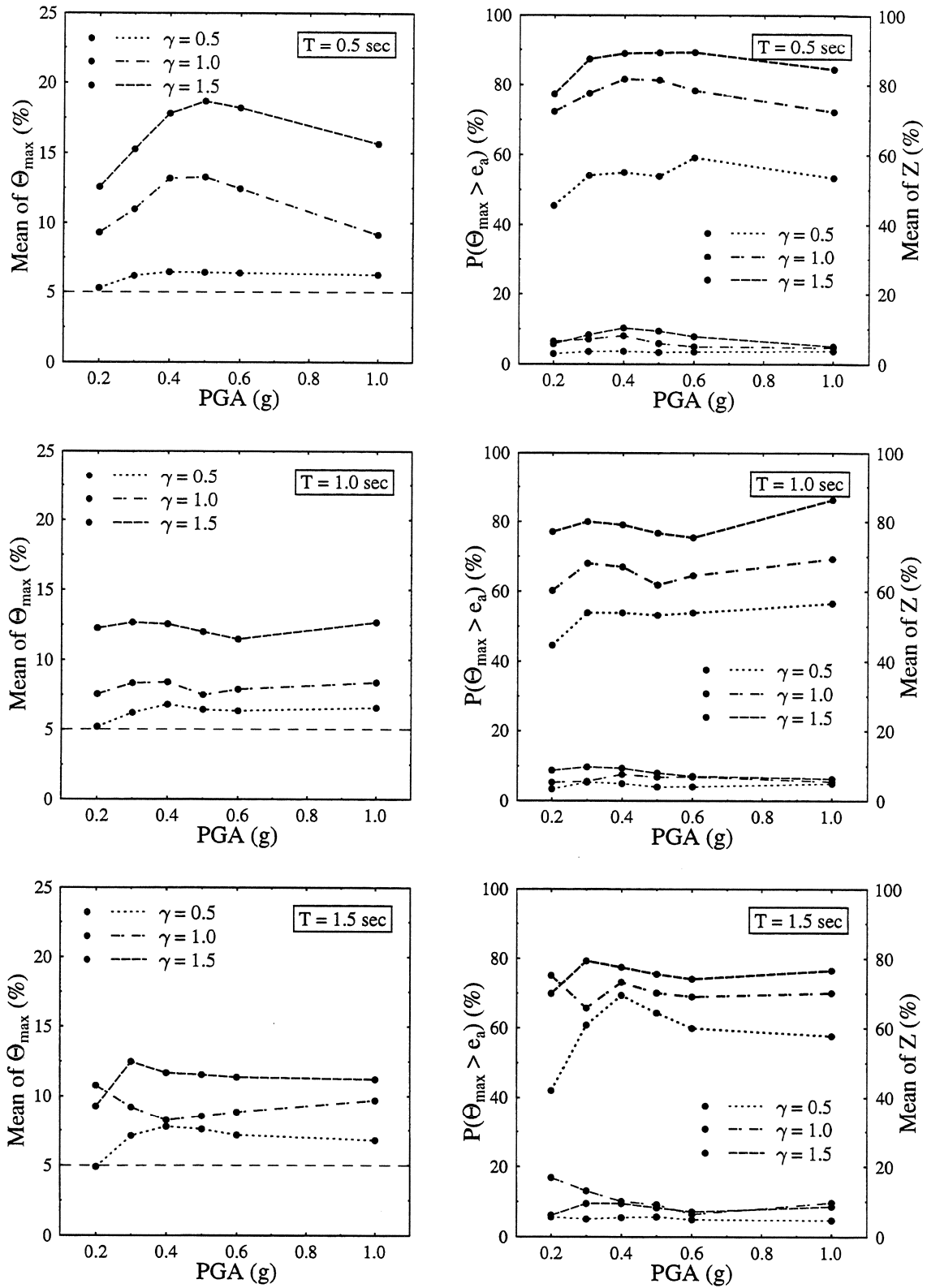
FIGURE 5-9 Mean of $\Theta_{\max}$, probability of exceedence of e_a by $\Theta_{\max}$, and mean of Z. MC model. Input: El Centro.
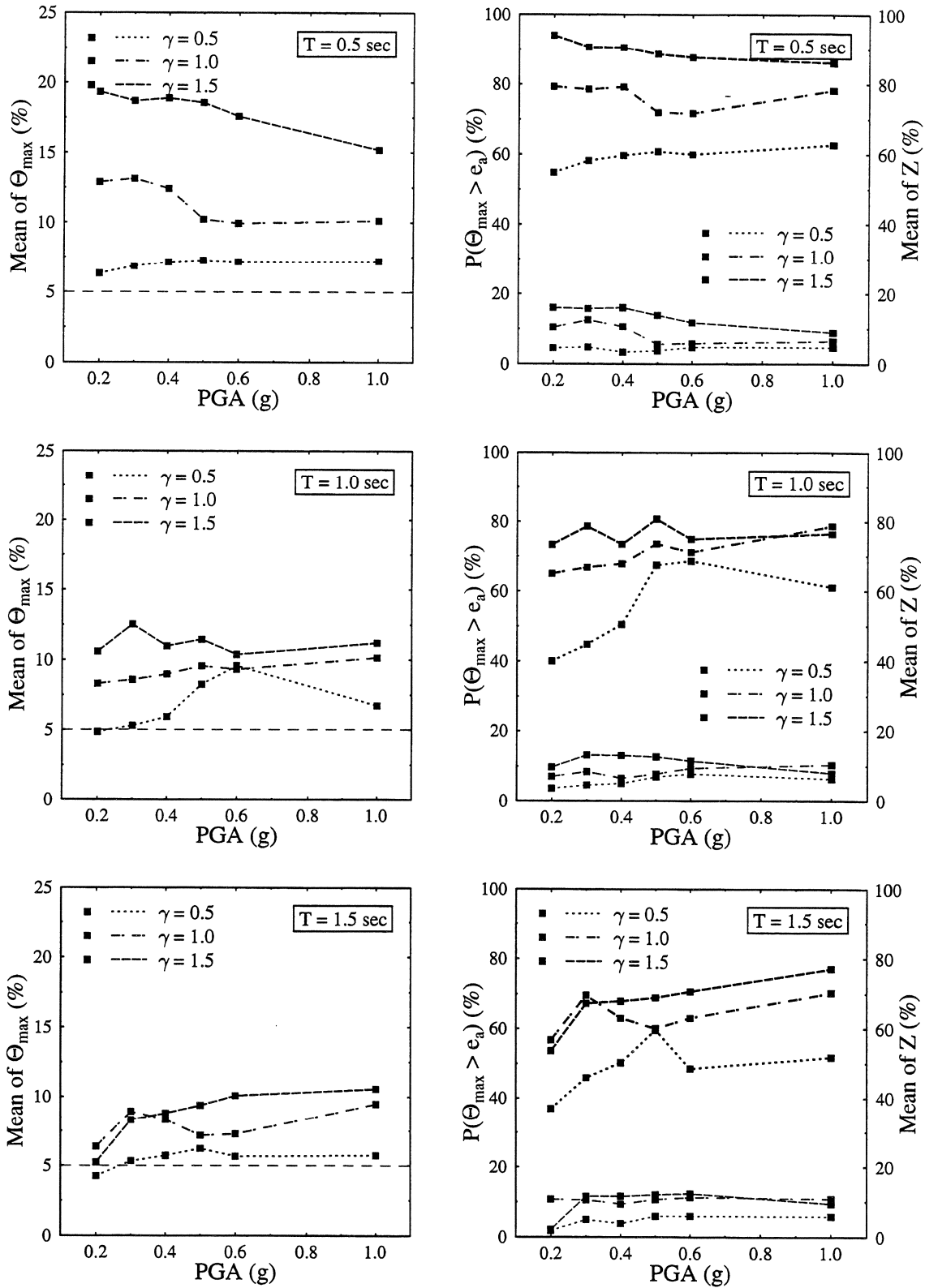
FIGURE 5-10 Mean of Θ_{max}, probability of exceedence of e_a by Θ_{max}, and mean of Z. MC model. Input: Taft.

146
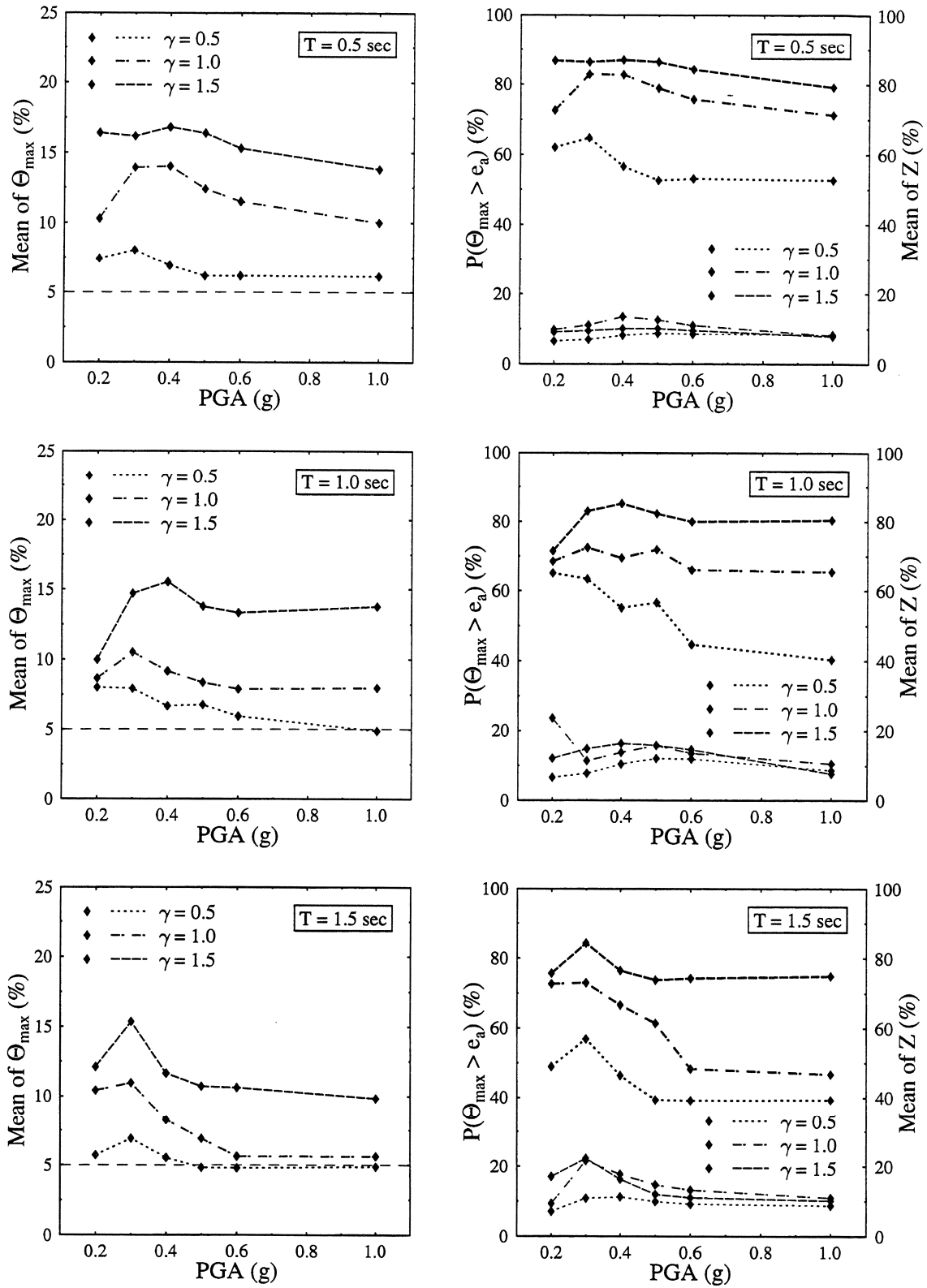
FIGURE 5-11 Mean of $\Theta_{\max}$, probability of exceedence of e_a by $\Theta_{\max}$, and mean of Z. MC model. Input: Parkfield.

consistently increases with PGA with highest values in the range of 25% to 35% of the motion duration. Even for PGA = 0.2g, the process $|\Theta(t)|$ is expected to spend 5% to 15% of the motion above e_a. The effect of the torsional parameter γ on the mean of Z is not clear. Although systems with $\gamma = 1.5$ are most likely to exceed e_a at any time during the motion, as indicated by the probability $P(\Theta_{\max} > e_a)$, they do not necessarily spend on the average more time above e_a than systems with $\gamma = 0.5$.

Modified-Clough model. The mean of the maximum dynamic eccentricity, shown in Figures 5-9–5-11 exceeds the code accidental eccentricity of 5% for most system parameter and PGA combinations, reaching values as high as 20%. It tends to increase with γ with very few exceptions observed at low peak ground accelerations. The effect of the input motion intensity is unclear since both increase and decrease with the PGA are observed on occasion. The coefficient of variation of $\Theta_{\max}$ is high with most values in the range 50% to 80%.

The maximum dynamic eccentricity exceeds the code accidental eccentricity with probability $P(\Theta_{\max} > e_a)$, shown with thick lines in the right-column graphs of Figures 5-9–5-11. This probability generally increases with γ but it is not clear how it is affected by increasing peak ground accelerations. Most of its values fall between 40% and 90%.

The mean of the total time above e_a, shown with thin lines, remains below 17%, 16%, and 24% of the motion duration for the El Centro, Taft, and Parkfield records, respectively. Moreover, it is fairly insensitive to variations in PGA and its highest values tend to be associated with PGA $\leq 0.4g$. The relationship between γ and the mean of Z is not always monotonic, but more often than not the mean increases with γ.

Comparison. The results presented in this section are characterized mostly by similarities between the two restoring force models, such as:

— The mean of the maximum dynamic eccentricity $\Theta_{\max}$ takes values roughly between 5% and 20%. Therefore, it generally exceeds the code-specified accidental eccentricity $e_a = 5\%$.

— The uncertainty in $\Theta_{\max}$ is high, with most coefficients of variation between 60% and 80%.

— The probability of the absolute dynamic eccentricity $|\Theta(t)|$ exceeding e_a at any time during the motion is represented by $P(\Theta_{\max} > e_a)$. It is high, exceeding 40% for

$\gamma = 0.5$ and increasing even further with γ, up to 85% or 90% for $\gamma = 1.5$.

— The absolute dynamic eccentricity is expected to spend a significant fraction of the motion duration above e_a. The mean of Z in most cases ranges from 3% to 15% and from 5% to 30% for the modified-Clough and the elastoplastic models, respectively.

One clear difference between models relates to the effect of PGA on the mean of Z, the total time above e_a. For the elastoplastic model this time clearly increases with the PGA, whereas for the modified-Clough model it appears rather insensitive to variations in PGA. Consequently, on the average, $|\Theta(t)|$ spends a smaller fraction of the motion duration above e_a for the modified-Clough than for the elastoplastic model, especially at higher earthquake intensities.

5.1.3 Total time above code eccentricity

The probability that the absolute dynamic eccentricity will exceed the code-specified accidental eccentricity e_a is covered in Section 5.1.2. In the same section, plots of the mean of Z, the total time above e_a, are presented (see Figures 5-9–5-11) and discussed. In order to form a more complete picture, it would be useful to know with what probability the total time spent above e_a will be longer than a specified percentage a of the motion duration. Values of the absolute dynamic eccentricity above e_a should cause less concern if they occur over just a small fraction of the motion duration.

Figures 5-12–5-17 show graphs of the probability $P(Z > a)$ versus the duration percentage a. Each figure includes plots for all combinations of T and γ, and, in order to avoid clatter, three representative values of PGA, $0.2g$, $0.4g$, and $0.6g$, represented by lines of increasing width. The value at $a = 0$ represents the percentage of samples for which the absolute dynamic eccentricity exceeds e_a at any time during the motion. For example, a probability of 70% at $a = 0$ indicates that the dynamic eccentricity of 30% of the samples remains below e_a throughout the motion.

Elastoplastic model. Figures 5-12, 5-13, and 5-14 show graphs of the probability $P(Z > a)$ for the El Centro, Taft, and Parkfield records, respectively. Under El Centro and Taft and for a given a there is a clear tendency for the probability $P(Z > a)$ to increase with the PGA. This trend is not as prevalent under Parkfield. In any case, this probability can be quite sensitive to variations in PGA.

149
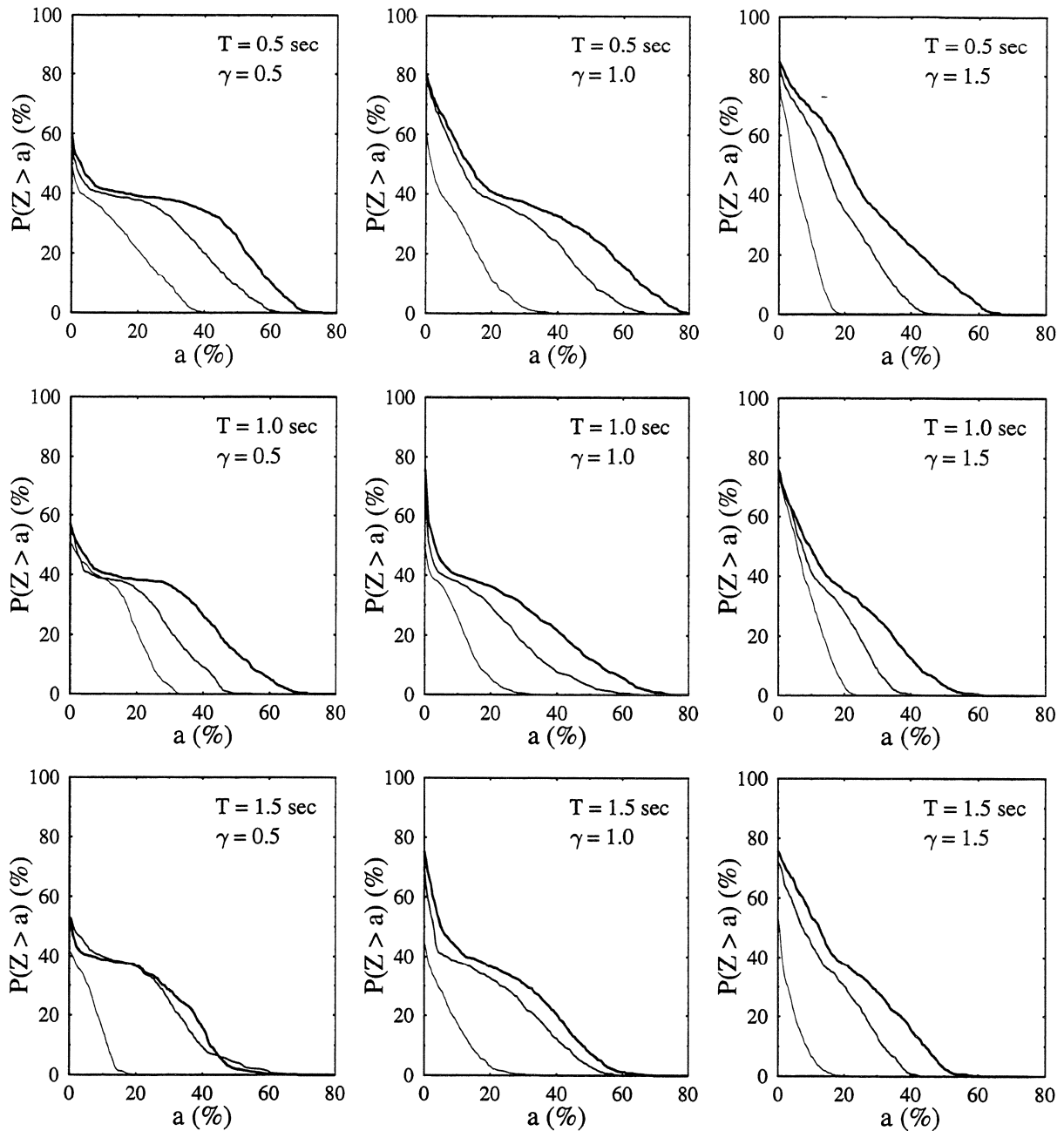
FIGURE 5-12 **Probability of exceedence of level** a **by** Z. **EP model. Input: El Centro. (Lines in increasing width correspond to** PGA $= 0.2g$, $0.4g$, **and** $0.6g$.**)**

The probability values at $a = 0$ indicate that, as γ increases, it becomes more likely that the absolute dynamic eccentricity will spend some amount of time above e_a. The same increasing tendency with γ is still evident at low values of a, but as a increases the trend reverses. For instance, under El Centro scaled to PGA $= 0.4g$ and for $T = 0.5$ sec, the probabilities that the total time above e_a exceeds 10% of the strong motion duration are
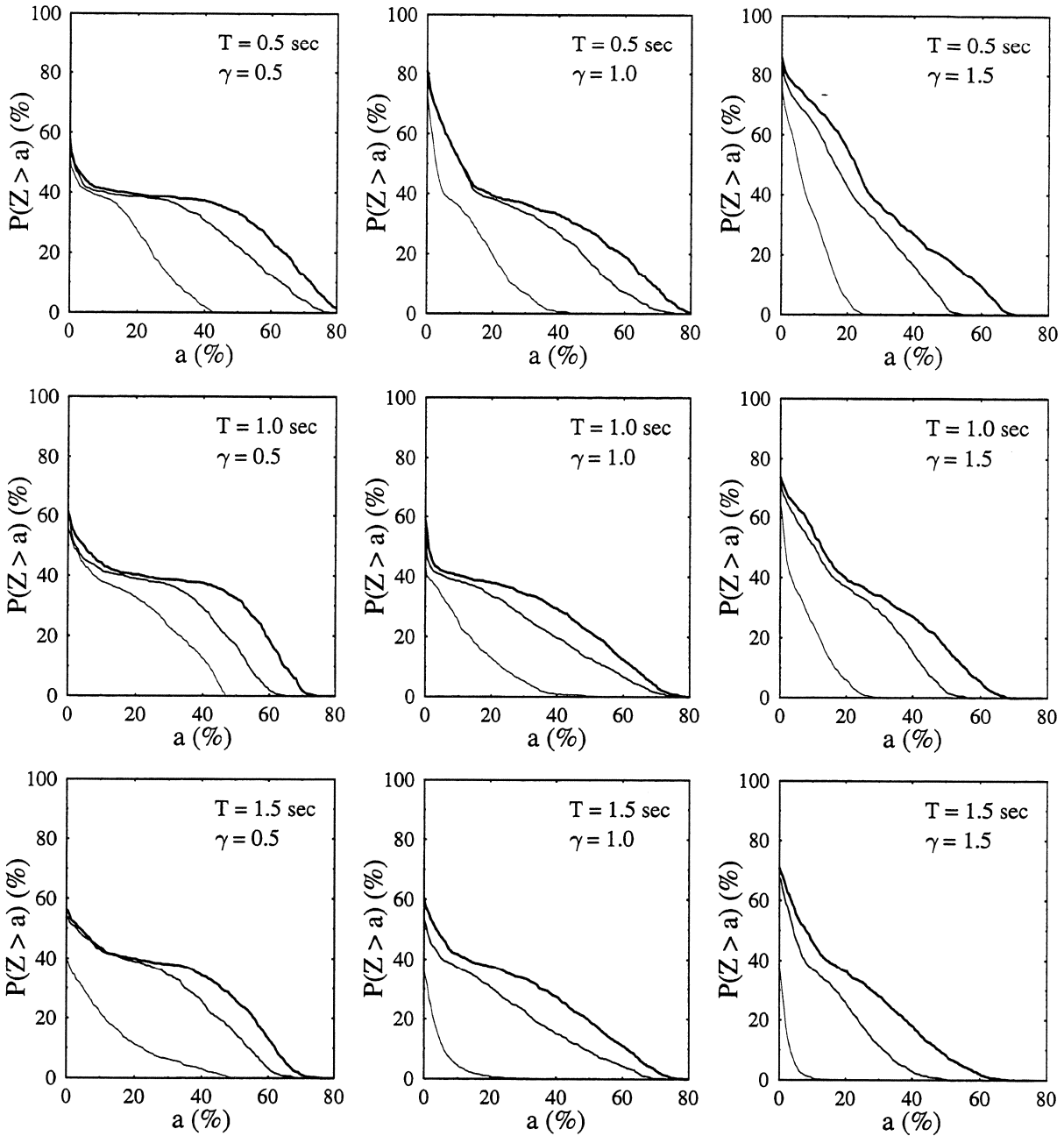
FIGURE 5-13 Probability of exceedence of level a by Z. EP model. Input: Taft. (Lines in increasing width correspond to PGA $= 0.2g$, $0.4g$, and $0.6g$.)

40%, 51%, and 61% for $\gamma = 0.5$, 1.0, and 1.5, respectively. When a increases to 30% the corresponding probabilities become 32%, 33%, and 18%.

It is apparent from the plots in Figures 5-12–5-14 that, even for the rather low earthquake intensity represented by a PGA of $0.2g$, there is nonnegligible probability of Z values as

151
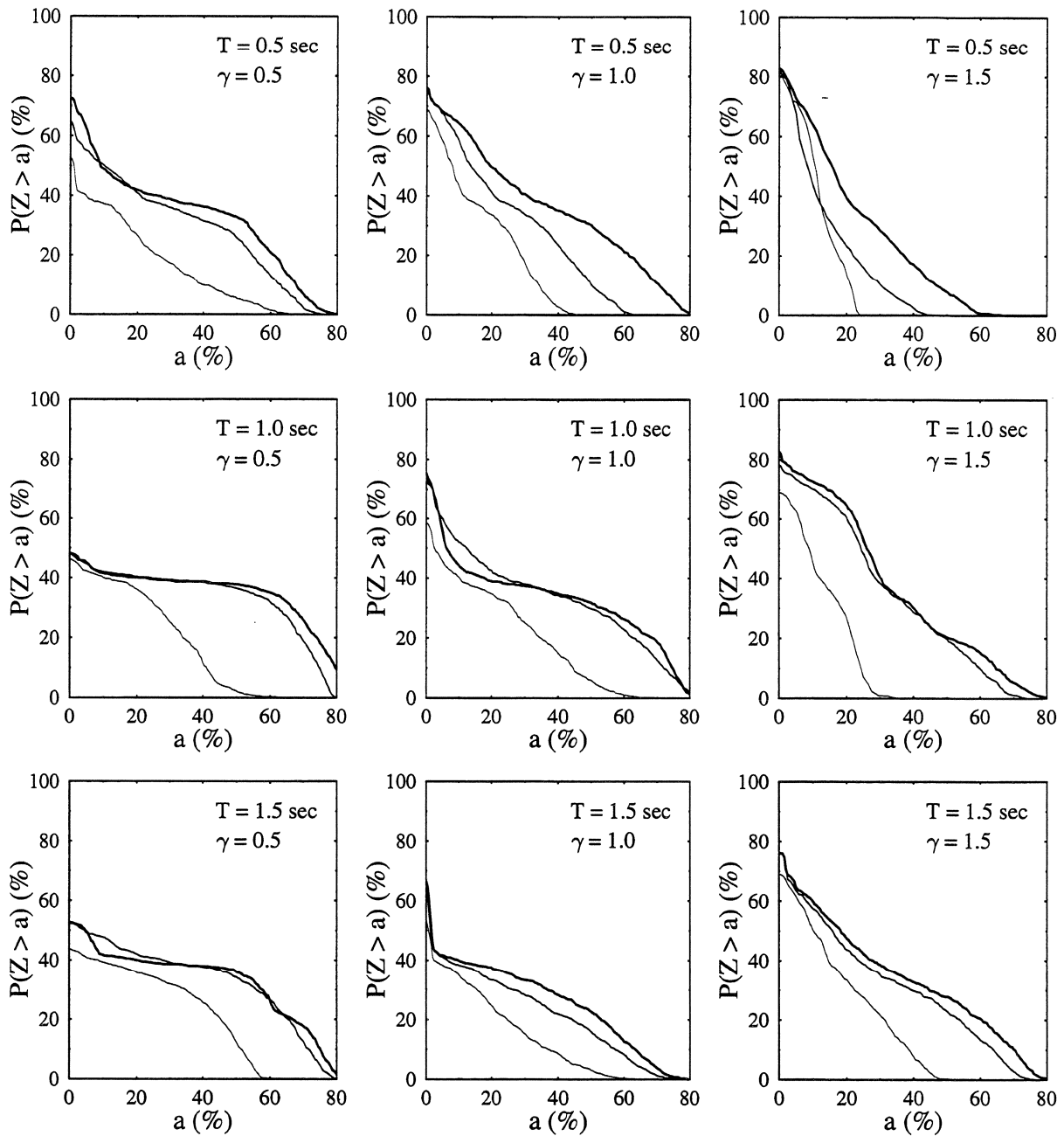
FIGURE 5-14 **Probability of exceedence of level** a **by** Z. **EP model. Input: Parkfield. (Lines in increasing width correspond to PGA** $= 0.2g$, $0.4g$, **and** $0.6g$.)

high as 20%–40% under El Centro and Taft and even higher (40%–60%) under Parkfield. In general, the highest values of Z are observed for Parkfield, followed by Taft, and then El Centro.

Modified-Clough model. Figures 5-15–5-17 show the probability $P(Z > a)$ for the

152
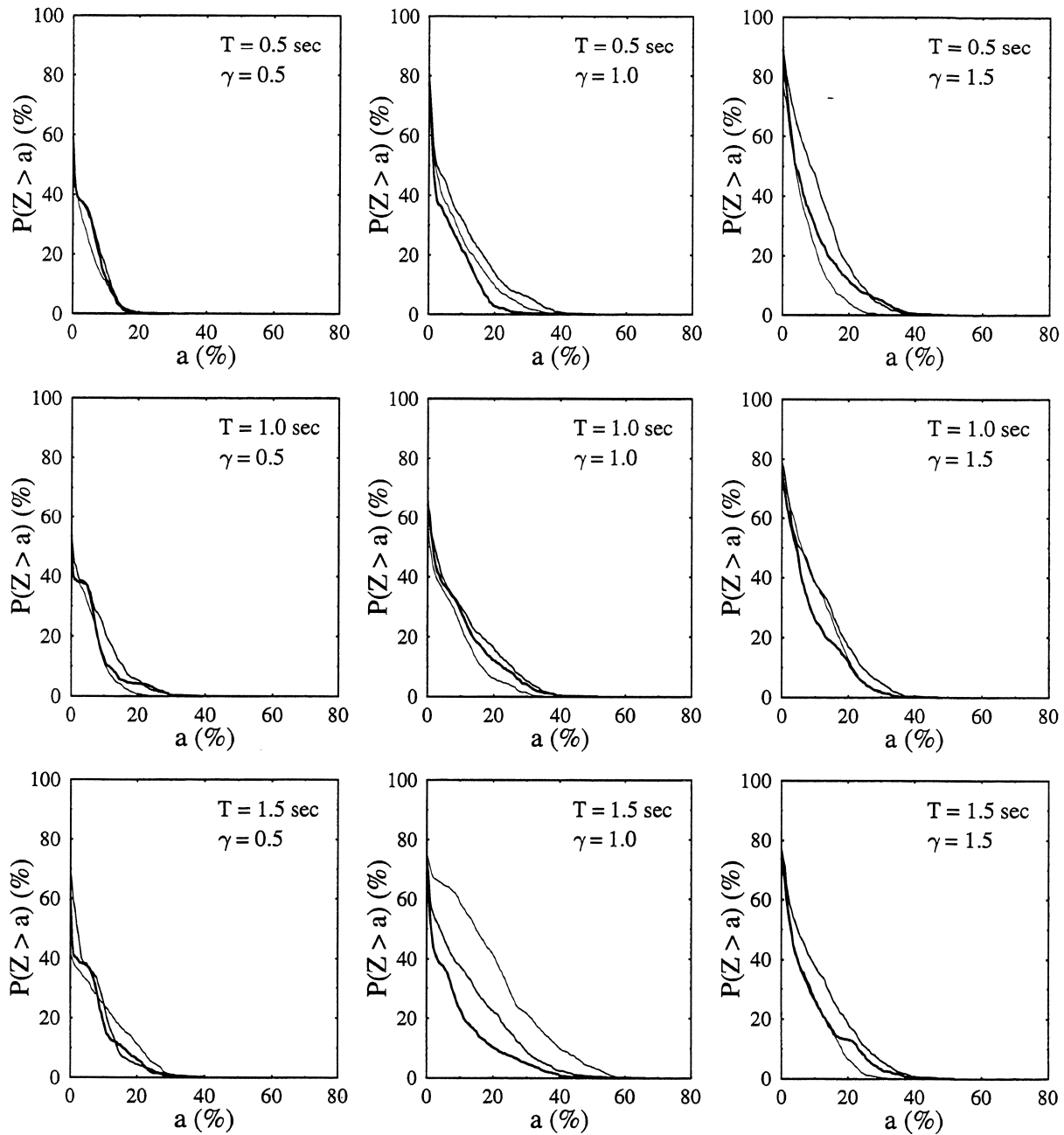
FIGURE 5-15 Probability of exceedence of level a by Z. MC model. Input: El Centro. (Lines in increasing width correspond to PGA $= 0.2g$, $0.4g$, and $0.6g$.)

modified-Clough model. There is no indication of a monotonic increase or decrease of this probability with the PGA. In fact, for the two motions of the first type, i.e., El Centro and Taft, it appears rather insensitive to variations in PGA. The probability of exceedence tends to increase with γ, a trend more evident at low values of a. Under El Centro, the probability curves do not extend beyond $a = 40\%$ in most cases. Under Taft, durations
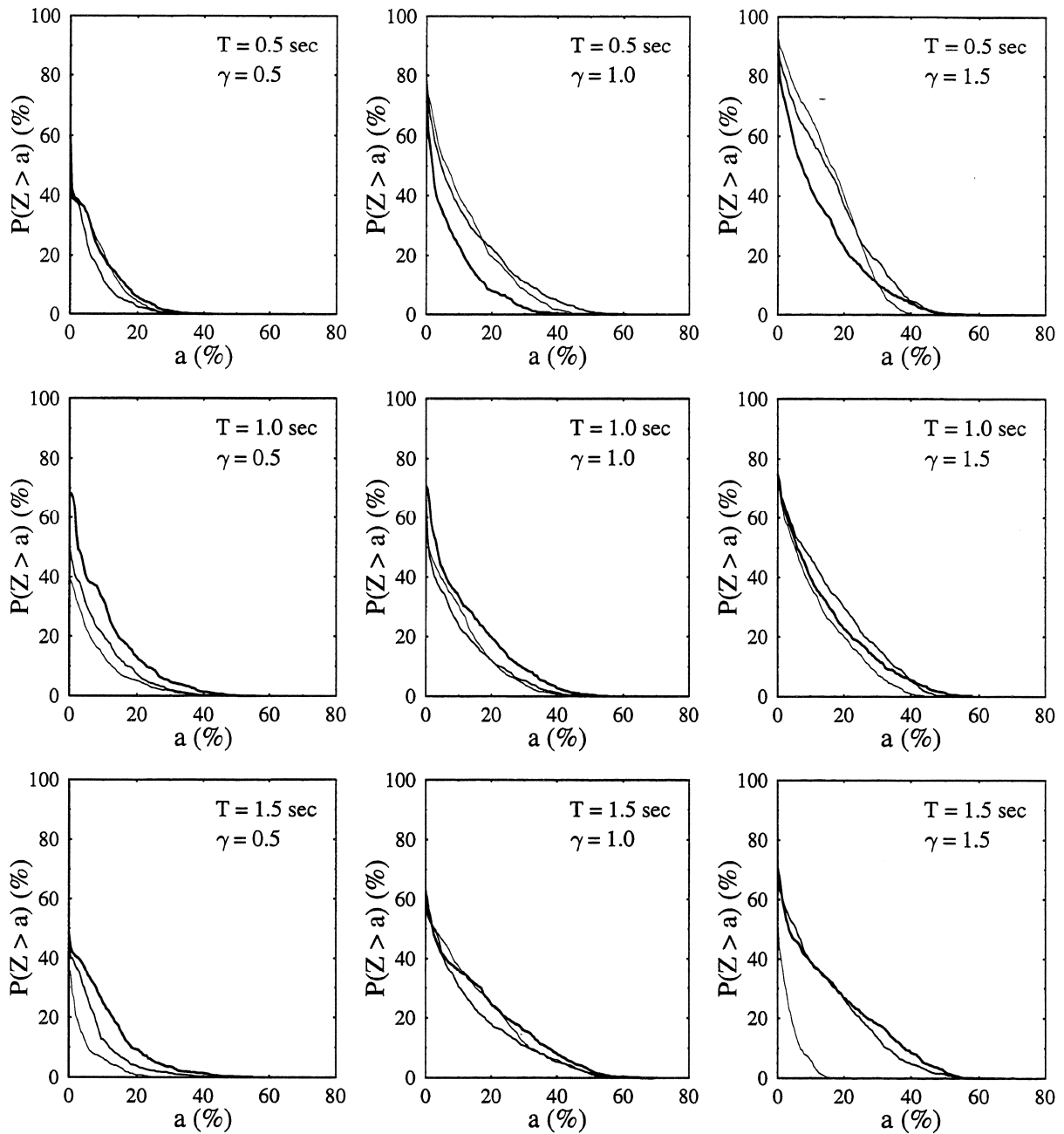
FIGURE 5-16 Probability of exceedence of level a by Z. MC model. Input: Taft. (Lines in increasing width correspond to PGA = $0.2g$, $0.4g$, and $0.6g$.)

up to about 50% have significant probability of occurrence, whereas under Parkfield even higher values of Z (between 60% and 70%) are possible.

Comparison. The total time $|\Theta(t)|$ spends above e_a, Z, is significantly affected by the selection of restoring force model. The numerical results show that:
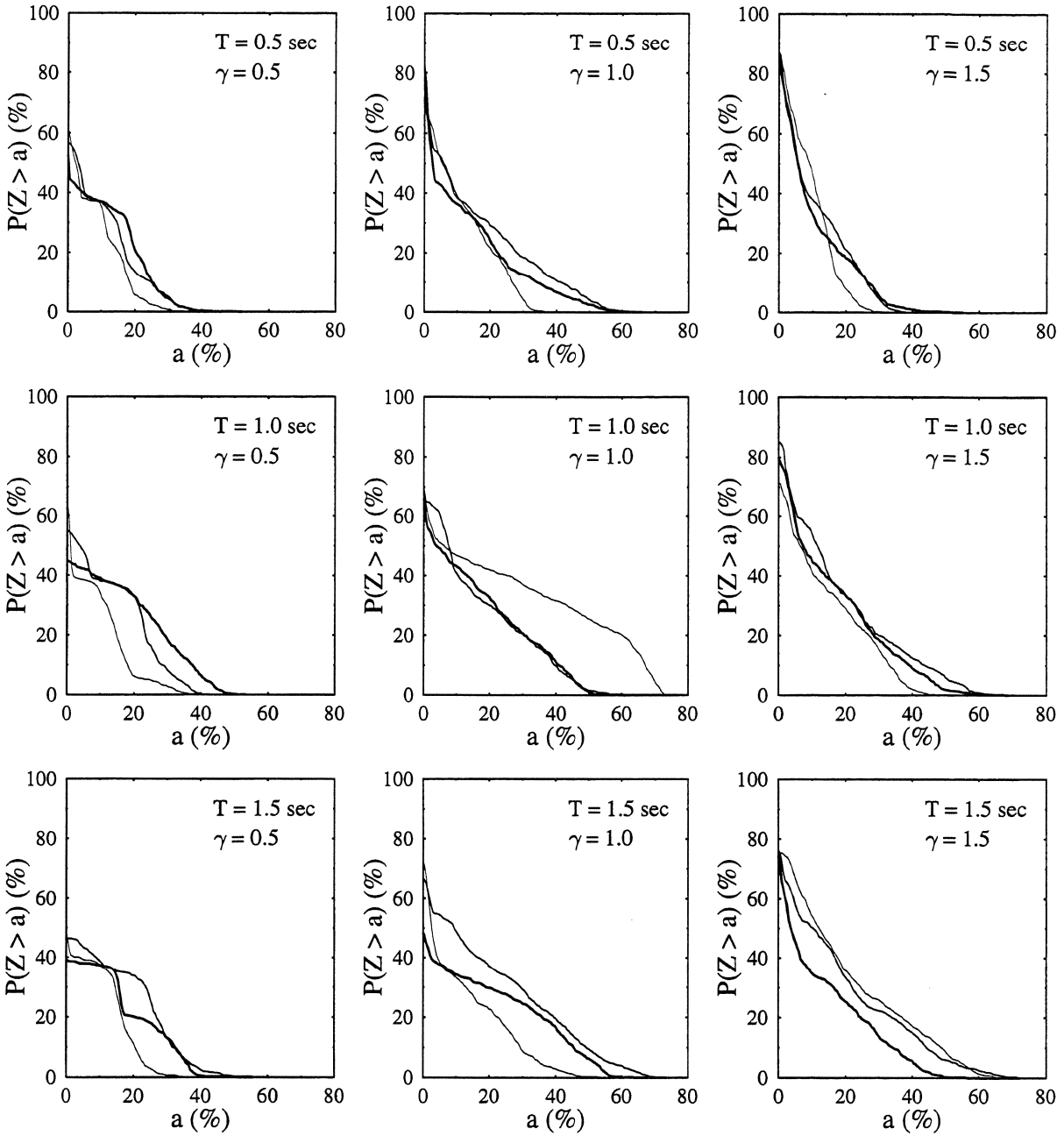
FIGURE 5-17 Probability of exceedence of level a by Z. MC model. Input: Parkfield. (Lines in increasing width correspond to PGA $= 0.2g$, $0.4g$, and $0.6g$.)

— The mean of Z is lower for the modified-Clough than for the elastoplastic model, especially at higher peak ground accelerations (see also Section 5.1.2).

— Much higher values of Z are associated with the elastoplastic model, especially for systems with low γ where the extreme Z values for the elastoplastic model are two

or three times as high as for the modified-Clough.

— The probability $P(Z > a)$ is far more sensitive to variations in PGA for the elasto-plastic than for the modified-Clough model.

— For the elastoplastic model the probability curves exhibit a distinct plateau when $\gamma = 0.5$. This plateau, present for all three input motions, becomes less evident as γ increases. For the modified-Clough model such a plateau can be identified only under Parkfield.

5.1.4 Mean upcrossing rate

The mean upcrossing rate provides information on how frequently the absolute dynamic eccentricity upcrosses a specified eccentricity level. The rates listed in Tables 5-2 and 5-3, for the elastoplastic and the modified-Clough models, respectively, refer to the accidental eccentricity $e_a = 5\%$, specified by the UBC. Each table contains results for the three input motions and all system parameter combinations.

Elastoplastic model. The mean upcrossing rate generally increases with the PGA, as well as with γ. The absolute dynamic eccentricity upcrosses e_a about twice as often when $\gamma = 1.5$ than when $\gamma = 0.5$. In contrast, the mean upcrossing rate decreases with the period T. The rates for $T = 1.5$ sec are about one third of those for $T = 0.5$ sec. As to the effect of the type of ground motion, the highest mean upcrossing rates are associated with Taft and Parkfield for $T = 0.5$ sec and $T \geq 1.0$ sec, respectively.

Modified-Clough model. The mean upcrossing rate generally increases with γ; for $\gamma = 1.5$ it is three to four times as high as for $\gamma = 0.5$ when $T \geq 1.0$ sec, whereas for $T = 0.5$ sec the ratio climbs into the five to seven range. The rate is rather insensitive to variations in PGA for $T = 1.0$ and 1.5 sec. A decreasing tendency with the period is evident for all values of γ but only for $\gamma = 1.5$ the rate consistently decreases with T.

Comparison. The mean upcrossing rate of level e_a by $|\Theta(t)|$ is quite sensitive to the restoring force model selection. Comparison of the results in Tables 5-2 and 5-3 indicates that:

— The mean upcrossing rate tends to be higher for the elastoplastic model. The difference between models is more pronounced at shorter periods and higher peak ground accelerations.

TABLE 5-2 Mean upcrossing rate of level e_a by the absolute dynamic eccentricity. EP model.

Input	T (sec)	γ	PGA (g)					
			0.2	0.3	0.4	0.5	0.6	1.0
El Centro	0.5	0.5	0.4424	0.6553	0.8003	0.8826	1.0010	1.1893
		1.0	0.5823	1.0643	1.3605	1.5659	1.7094	1.8264
		1.5	0.6174	1.0952	1.6413	2.0253	2.3103	2.6308
	1.0	0.5	0.2218	0.2212	0.3546	0.4464	0.4926	0.6521
		1.0	0.2356	0.3657	0.5117	0.6342	0.7210	0.9475
		1.5	0.3788	0.4802	0.5889	0.7198	0.8997	1.3622
	1.5	0.5	0.0717	0.2054	0.2463	0.2367	0.2954	0.4458
		1.0	0.1322	0.3020	0.3678	0.3908	0.4367	0.6087
		1.5	0.1174	0.2896	0.4842	0.5873	0.6345	0.8974
Taft	0.5	0.5	0.5247	0.7942	0.9882	1.0889	1.1402	1.2397
		1.0	0.7029	1.2143	1.5199	1.6570	1.6602	1.8977
		1.5	0.8442	1.4200	2.0346	2.3739	2.5000	2.5904
	1.0	0.5	0.3198	0.4560	0.5182	0.5955	0.6557	0.7385
		1.0	0.3117	0.5522	0.7081	0.7787	0.8313	0.9501
		1.5	0.3556	0.6857	0.9327	1.0344	1.1536	1.3690
	1.5	0.5	0.1123	0.2780	0.3205	0.3793	0.4013	0.5210
		1.0	0.0677	0.2776	0.4313	0.5261	0.5704	0.6799
		1.5	0.0553	0.3165	0.4717	0.6048	0.7170	0.8843
Parkfield	0.5	0.5	0.5259	0.5165	0.9928	1.0863	1.0560	1.0101
		1.0	0.8808	0.9651	1.3418	1.5568	1.8371	1.9678
		1.5	0.9247	0.9835	1.1853	1.5638	1.9144	2.6037
	1.0	0.5	0.3823	0.5845	0.6054	0.5967	0.6132	0.6163
		1.0	0.6207	0.7738	0.9679	0.9016	0.8554	0.8234
		1.5	0.5934	1.0175	1.4062	1.3892	1.3075	1.3486
	1.5	0.5	0.2738	0.3427	0.3825	0.4026	0.4006	0.4996
		1.0	0.3148	0.3802	0.4628	0.4980	0.5414	0.6188
		1.5	0.5250	0.6989	0.8510	0.9039	0.9304	0.9152

TABLE 5-3 Mean upcrossing rate of level e_a by the absolute dynamic eccentricity. MC model.

Input	T (sec)	γ	PGA (g) 0.2	0.3	0.4	0.5	0.6	1.0
El Centro	0.5	0.5	0.1638	0.1816	0.1601	0.1475	0.1542	0.1593
		1.0	0.5432	0.6060	0.6454	0.4753	0.4004	0.3825
		1.5	0.6358	0.8731	1.0414	0.9377	0.8323	0.5756
	1.0	0.5	0.1053	0.1607	0.1386	0.1274	0.1338	0.1627
		1.0	0.2342	0.2564	0.3453	0.3126	0.3138	0.2692
		1.5	0.4361	0.5117	0.5120	0.4568	0.4219	0.4310
	1.5	0.5	0.1291	0.1176	0.1382	0.1317	0.1231	0.1160
		1.0	0.3926	0.3214	0.3059	0.2847	0.2187	0.2880
		1.5	0.2572	0.3513	0.3713	0.3447	0.3059	0.3675
Taft	0.5	0.5	0.2635	0.2622	0.1783	0.1913	0.2391	0.2434
		1.0	0.7830	0.9408	0.7932	0.4744	0.5249	0.5244
		1.5	1.6013	1.4779	1.4411	1.2616	1.1330	0.9779
	1.0	0.5	0.1407	0.1739	0.1925	0.2403	0.2601	0.2201
		1.0	0.3097	0.3797	0.3163	0.3953	0.4601	0.5032
		1.5	0.5300	0.7058	0.7120	0.7199	0.6789	0.5370
	1.5	0.5	0.0528	0.1270	0.1020	0.1447	0.1371	0.1410
		1.0	0.3103	0.3141	0.2920	0.3554	0.3715	0.3395
		1.5	0.1198	0.4806	0.4777	0.4996	0.5150	0.4701
Parkfield	0.5	0.5	0.3236	0.3148	0.3220	0.3186	0.3062	0.2773
		1.0	0.7255	0.8857	1.1032	1.0116	0.9109	0.6011
		1.5	0.7266	0.8733	1.0147	1.0809	1.0468	0.8437
	1.0	0.5	0.2207	0.2050	0.2358	0.2806	0.2260	0.1493
		1.0	0.8282	0.4927	0.5475	0.5966	0.4968	0.3584
		1.5	0.6902	0.8657	0.8544	0.7827	0.6860	0.4733
	1.5	0.5	0.1983	0.1679	0.1662	0.1562	0.1427	0.1451
		1.0	0.3577	0.5412	0.4463	0.3768	0.3199	0.2724
		1.5	0.7001	0.6794	0.5059	0.4657	0.4616	0.3672

— Although the rate increases with γ for both models, the increase is much sharper for the modified-Clough model.

— The mean upcrossing rate appears more sensitive to variations in PGA for the elastoplastic than for the modified-Clough model.

5.1.5 Conclusions

The adequacy of the UBC provisions to account for accidental torsion caused by strength uncertainty is evaluated based on a simulation study of one-storey systems. The response measures employed are the dynamic eccentricity $\Theta(t)$, defined as the ratio of the dynamic torsional moment to the base shear force given by the code, the maximum dynamic eccentricity in absolute value, the upcrossing rate of the code accidental eccentricity level $e_a = 5\%$ by $|\Theta(t)|$, and the total time of $|\Theta(t)|$ above e_a. Numerical results show that:

- The mean of the maximum dynamic eccentricity exceeds the code accidental eccentricity e_a for all system parameter combinations and all peak ground accelerations over $0.2g$.

- The probability that $|\Theta(t)|$ will exceed e_a at any time during the motion is high. It ranges mostly from 40% to 85% for the elastoplastic model and from 40% to 90% for the modified-Clough.

- The process $|\Theta(t)|$ spends on the average about 5%–30% and 3%–15% of the motion duration above e_a for the elastoplastic and the modified-Clough models, respectively.

- There is significant probability that the total time above e_a may exceed 40% of the motion duration even for peak ground accelerations not exceeding $0.4g$.

- Of the three motions considered, El Centro, Taft, and Parkfield, the latter appears to place the highest demands on the one-storey systems investigated, especially for $T \geq 1.0$ sec. A higher percentage of values of $|\Theta(t)|$ exceed e_a under this motion. Also, $|\Theta(t)|$ tends to both upcross level e_a more frequently and spend a larger fraction of the motion above it.

- Use of the modified-Clough versus the elastoplastic model generally results in $|\Theta(t)|$ spending a smaller fraction of the motion duration above e_a, as well as, in less frequent upcrossings of level e_a.

If inelastic time-history analysis is to be used as part of the design process a restoring force model has to be selected. The issue of appropriate restoring force model does not arise in the seismic design codes since inelastic response is considered only implicitly through the reduction in the base shear. Based on the present study of one-storey systems, the elasto-plastic model appears to be more conservative than the modified-Clough. Specifically, Figures 5-3(a)–5-5(a) show that, for systems differing only in the restoring force model, the percentage of $|\Theta(t)|$ values exceeding $e_a = 5\%$ is generally higher for the elastoplastic model. Moreover, as observed earlier, the absolute dynamic eccentricity of systems following the elastoplastic model tends to upcross level e_a more frequently, as well as, spend a larger fraction of the motion duration above e_a.

In summary, for the one-storey systems and the input motions considered, the 5% accidental eccentricity in the UBC provisions appears inadequate for the source of accidental torsion considered in this study, namely the uncertainty in the element yield strengths. Moreover, results presented in Table 5-1 and Figures 5-3–5-5 suggest that the 10% accidental eccentricity, required, among others, by the Canadian and the New Zealand codes, albeit superior to the 5% in the UBC, may still be inadequate. Therefore, no clear justification can be offered for choosing between the two accidental eccentricity values.

5.2 Multi-storey systems

The shear walls of the seven-storey building in Figure 5-18 are modeled by inelastic springs with uncertain yield strengths. The lognormally distributed yield strengths are assumed to be perfectly correlated for the segment of a wall within a given storey but independent from one segment to another in the same or different storeys (Section 4.1.2). Because of the independence of yield strengths, the inelastic response of the system may involve torsion. Springs used to model flexural and shear behavior of structural members follow either the elastoplastic (EP) or the modified-Clough (MC) model (Sections 3.1.1 and 4.1.1). The building is designed in accordance with the UBC provisions as described in Section 4.3.

Input is deterministic and consists of the strong motion portions of the El Centro and Parkfield earthquake records (Sections 3.2 and 4.2). El Centro is used as recorded whereas Parkfield is scaled to peak ground acceleration of $0.43g$.

Code evaluation for multi-storey systems is based on the following response measures:

(a) plan view
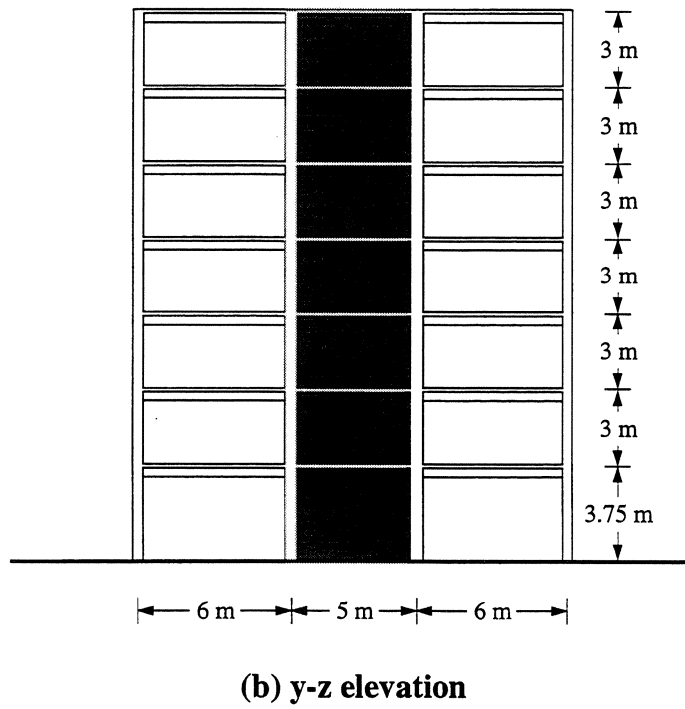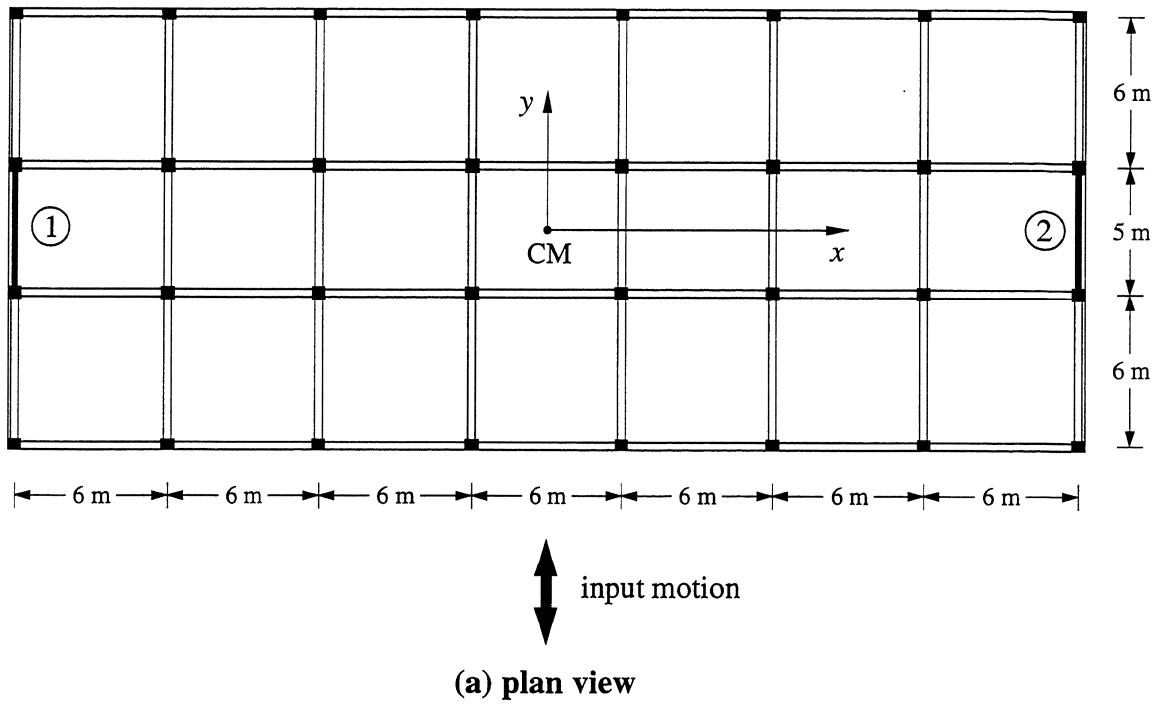
(b) y-z elevation

FIGURE 5-18 Plan view and elevation of 7-storey building (same as Figure 4-1).

161

- dynamic eccentricity $\Theta(t)$, which for storey k, $k = 1, \ldots, 7$, is defined as $\Theta_k(t) = \sum_{i=k}^{7} m_i r_i^2 \ddot{\Phi}_i(t) \Big/ (V_k\, b)$, where $\ddot{\Phi}_i(t)$, m_i, and r_i are the torsional acceleration, mass, and radius of gyration of floor i, $i = 1, \ldots, 7$, V_k is the design storey shear, and b is the building dimension perpendicular to the ground motion,

- maximum dynamic eccentricity $\Theta_{\max} = \max\{|\Theta(t)|\}$,

- Z = total time of $|\Theta(t)|$ above e_a, given as percentage of the motion duration, and

- upcrossing rate N, which is equal to the number of times during the motion $|\Theta(t)|$ upcrosses level e_a, divided by the motion duration.

Motion duration in this case is in effect the strong motion duration. The response measures for code evaluation mirror one to one those used in the study of one-storey systems.

Numerical results are obtained from 150 and 100 system realizations for the elastoplastic and modified-Clough models, respectively, subjected in turn to the El Centro and Parkfield records.

5.2.1   Dynamic eccentricity

For a given time history realization of the absolute value of the dynamic eccentricity $\Theta(t)$ it is possible to calculate for what percentage of the motion duration $|\theta(t)|$ exceeds a specified eccentricity level. From the set of 100 or 150 similar sample values one may calculate statistics such as the median and 90%-confidence interval shown in Figures 5-19 and 5-20, for the El Centro and Parkfield records, respectively. The plots cover eccentricities in the range 0 to 50%. The 90%-confidence interval implies that 90% of the sample values for the specific eccentricity level lie between the upper and lower envelope curves leaving out 5% of the values on either side. Full and dashed lines represent the elastoplastic and modified-Clough models, respectively and the medians are denoted by thicker lines.

Both median and envelope curves in Figures 5-19 and 5-20 are essentially identical from storey to storey with the exception of slightly lower values at the top storey. The results for the two restoring force models are practically indistinguishable under Parkfield whereas under El Centro significantly lower percentages of the motion duration are associated with the modified-Clough model. For instance, for a 5% eccentricity the median is about 45% for the elastoplastic and 32% for the modified-Clough. Moreover, for the elastoplastic

162
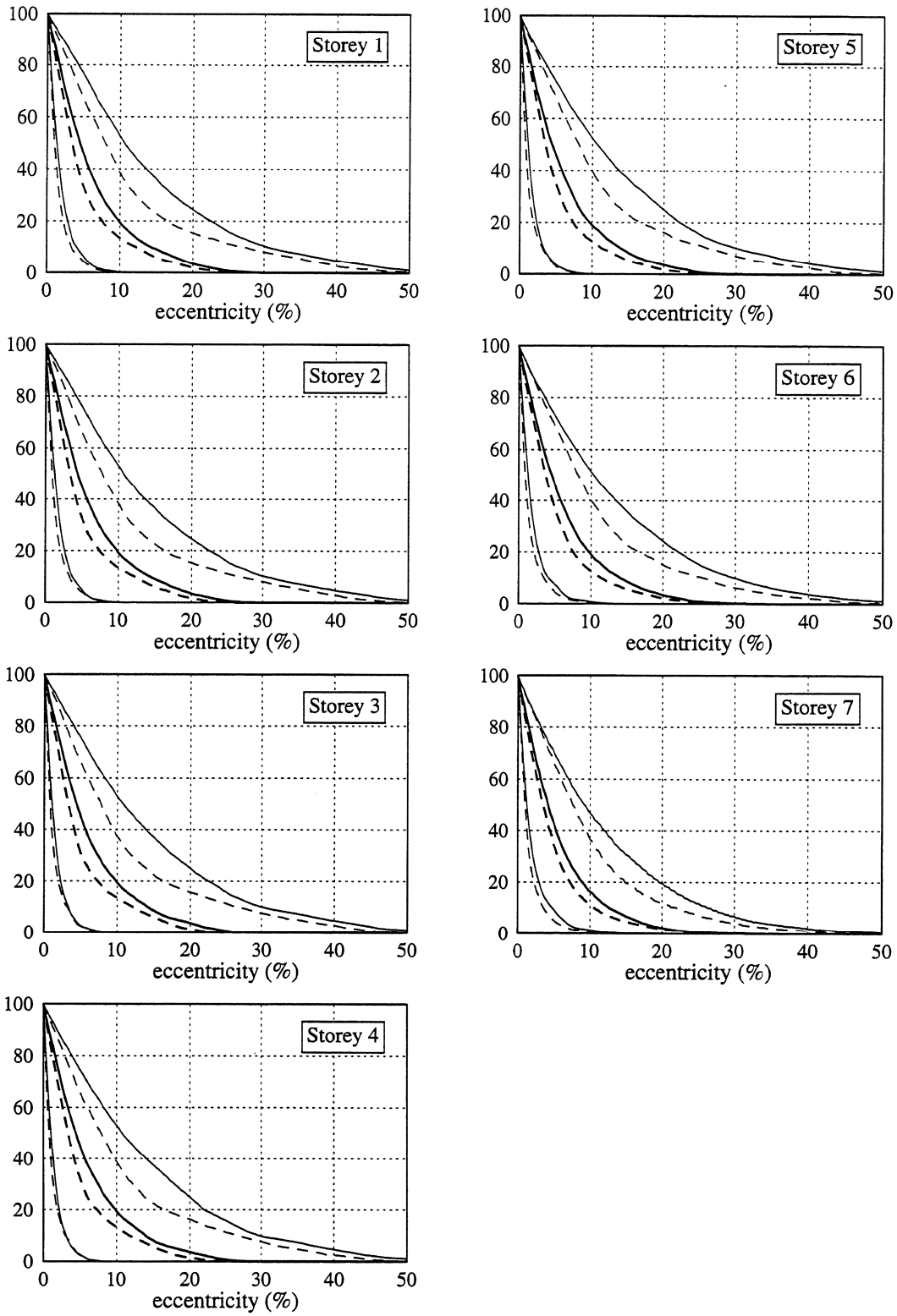
FIGURE 5-19 Percentage of motion duration for which $|\Theta(t)|$ exceeds specified eccentricity levels. Input: El Centro. (——— EP model; – – – MC model)

163
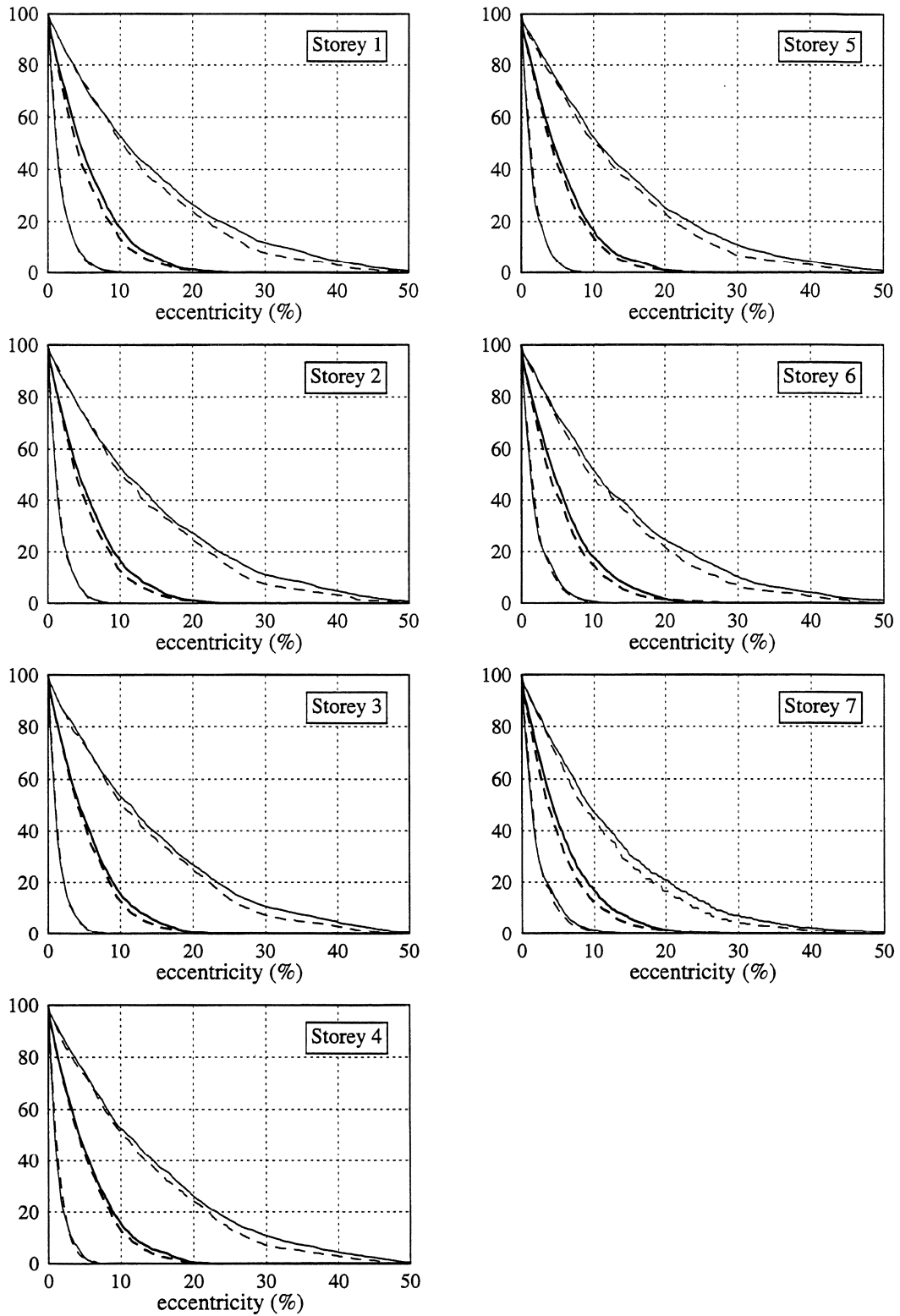
FIGURE 5-20 Percentage of motion duration for which $|\Theta(t)|$ exceeds specified eccentricity levels. Input: Parkfield. (——— EP model; − − − MC model)

TABLE 5-4 Estimates of the mean and standard deviation of $|\Theta(t)|$ for seven-storey building (all values in %).

	El Centro				Parkfield			
	Elastoplastic		Mod.-Clough		Elastoplastic		Mod.-Clough	
Storey	Mean	Std.	Mean	Std.	Mean	Std.	Mean	Std.
1	6.71	7.72	5.28	6.47	6.52	7.38	5.94	6.62
2	6.65	7.70	5.19	6.42	6.43	7.32	5.88	6.57
3	6.58	7.68	5.10	6.36	6.35	7.27	5.80	6.51
4	6.55	7.67	5.10	6.33	6.35	7.25	5.78	6.48
5	6.60	7.67	5.23	6.33	6.45	7.28	5.82	6.49
6	6.62	7.59	5.35	6.29	6.54	7.27	5.84	6.47
7	6.07	6.84	5.00	5.73	6.09	6.65	5.37	5.93

model there is very little difference in the results from the two input motions, with a tendency for somewhat higher values under El Centro.

The measure of the magnitude of $|\theta(t)|$ devised in Section 5.1.1 is equally applicable to the storey dynamic eccentricities. This measure consists of a mixture of histograms $f = (1/n) \sum_{i=1}^{n} f_i$, where f_i are histograms of $|\Theta(t)|$ at fixed times t_i, $i = 1, \ldots, n$. Since complete time histories are available for all realizations of the seven-storey building $|\theta(t)|$ is sampled at 0.005 sec intervals, which is the recording step for the system response.

From the storey histograms f one can obtain estimates of: (1) the mean and standard deviation of $|\theta(t)|$, listed in Table 5-4 and (2) the percentage of values of $|\Theta(t)|$ exceeding specified eccentricity levels, plotted in Figure 5-21 for eccentricities in the range 5% to 25%. The UBC-specified accidental eccentricity of 5% falls below of just at the mean values in the table. The 10% accidental eccentricity suggested by other codes places below the mean plus standard deviation level.

Each curve in the plots in Figure 5-21 corresponds to a storey dynamic eccentricity for either the elastoplastic or the modified-Clough model. In both plots two sets of curves can be identified corresponding exactly to the two restoring force models, with the upper set belonging to the elastoplastic. The single line in each set corresponds to the top storey. The percentage of dynamic eccentricity values above 5% is quite high, between 32% and 42%, under El Centro and even higher, between 37% and 44% under Parkfield. The

165
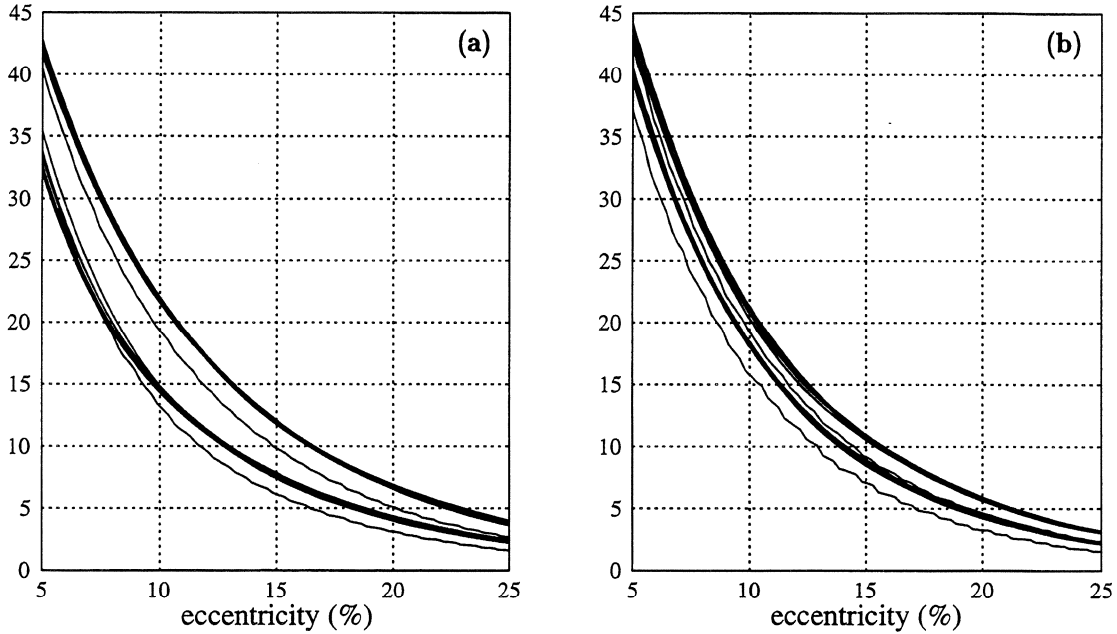
FIGURE 5-21 Percentage of absolute dynamic eccentricity values above specified eccentricity levels. (a) Input: El Centro. (b) Input: Parkfield.

respective percentages for the 10% eccentricity level are still high at 13%–22% and 16%–22%. Nothing in the above results suggests that a 10% accidental eccentricity requirement is more appropriate than the 5% in the UBC.

5.2.2 Maximum dynamic eccentricity

The mean of the maximum dynamic eccentricity $\Theta_{\max}$ is compared with the UBC accidental eccentricity $e_a = 5\%$ in Figure 5-22. It is obvious that the mean of $\Theta_{\max}$ is much larger than 5% for all restoring force models and input motion combinations. There is not much variation from storey to storey but there is a clear tendency for somewhat lower values from the 2nd to the 5th storey. Lower values are also consistently associated with the modified-Clough model under the same input motion, and the Parkfield record for the same restoring force model.

The uncertainty in $\Theta_{\max}$ is quite high; its coefficient of variation takes values between 38% and 58%. The probability that the maximum dynamic eccentricity exceeds e_a is between 99% and 100%. Therefore, it is virtually certain that at some point during the motion $|\Theta(t)|$ will exceed e_a.

166
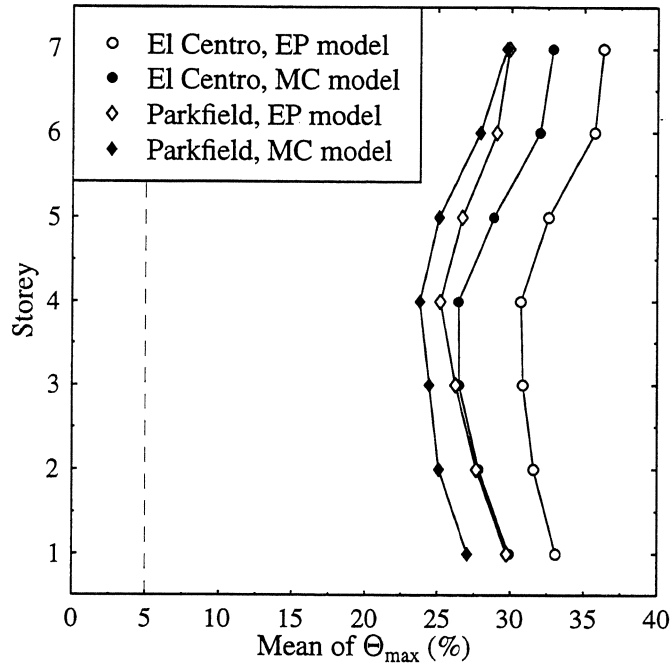
FIGURE 5-22 Mean of maximum dynamic eccentricity

5.2.3 Total time above code eccentricity

As discussed in the previous section there is extremely high probability that the magnitude of the dynamic eccentricity will exceed the code accidental eccentricity sometime during the motion. The results in Figure 5-23 indicate what percentage of the motion duration is $|\Theta(t)|$ expected to spend above e_a.

The mean of Z, the total time above e_a, is quite significant ranging from 32% to 44% of the motion duration. It is practically constant with height with the exception of somewhat lower values at the top storey. For the elastoplastic model it is practically the same under either of the two motions whereas the effect of the input is more pronounced for the modified-Clough model. Finally, for both motions considered the mean of Z is consistently higher for the modified-Clough model.

Additional information on the distribution of Z is provided in Figure 5-24, illustrating the probability that the total time above e_a will be longer than a specified percentage a of the motion duration. There are seven curves in each plot, one for each of the seven storeys in the building. Identifying the curves is pointless since for all practical purposes they are indistinguishable, save for the isolated one visible at higher values of a which corresponds to the 7th storey.

167
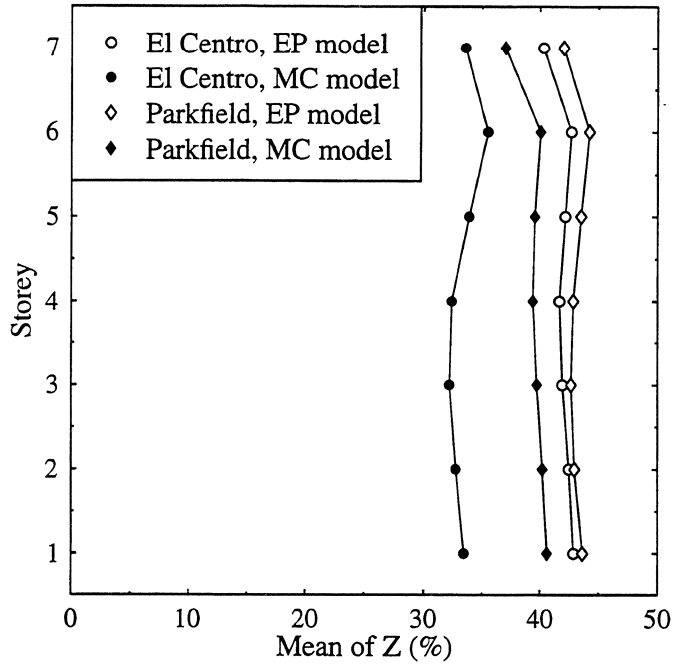
FIGURE 5-23 Mean of total time above code eccentricity
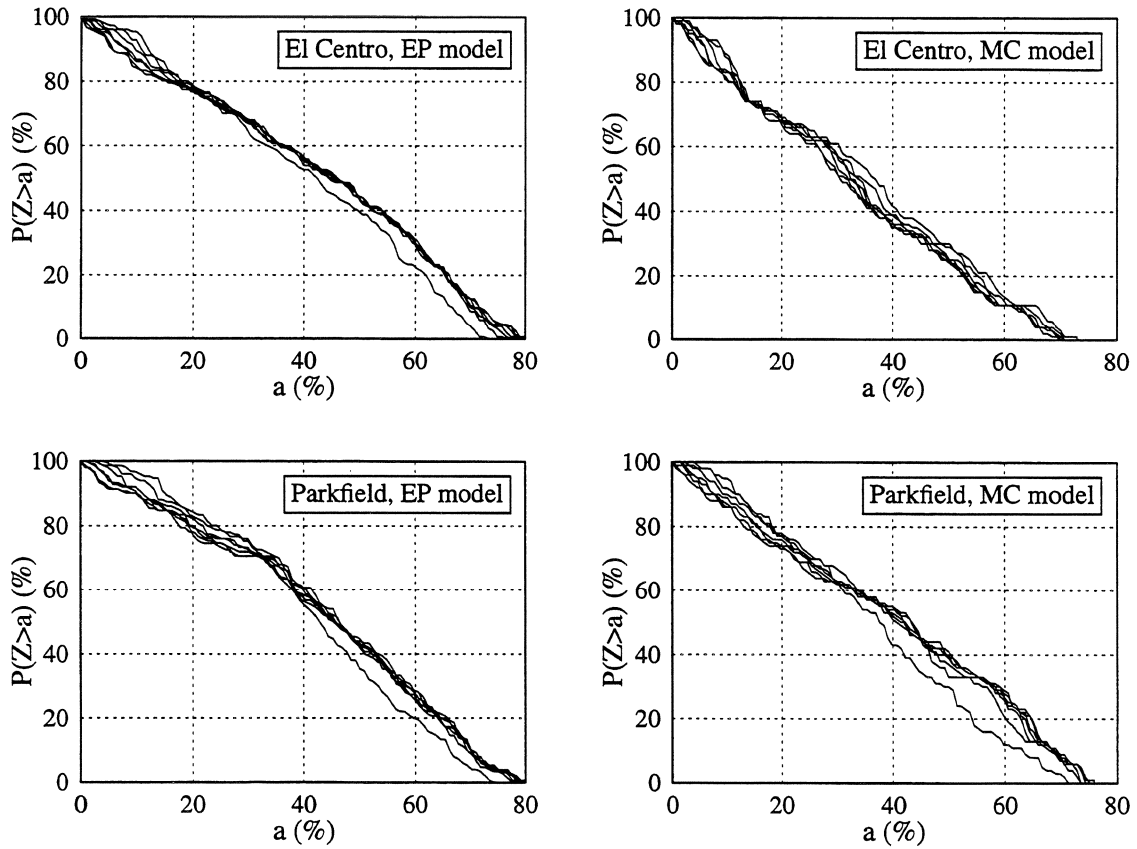
FIGURE 5-24 Probability of total time above e_a exceeding level a.

The results in Figure 5-24 indicate that there is significant probability, roughly 25% to 45% depending on the motion and the restoring force model, that $|\Theta(t)|$ will spend more than half of the motion above code eccentricity. The extreme values of Z observed tend to be higher for the elastoplastic model but not by much. Also, for both motions higher probabilities are associated with the elastoplastic model and this is more pronounced for El Centro. For instance, for $a = 50\%$ the probability $P(Z > a)$ is 40%–45% for the elastoplastic but drops to 25%–30% for the modified-Clough model.

5.2.4   Mean upcrossing rate

The mean upcrossing rate of level e_a by the absolute dynamic eccentricity, i.e., the average number of upcrossings in the unit of time, is illustrated along the height of the building in Figure 5-25. It is the only response measure employed for code evaluation that exhibits considerable variability from storey to storey. Upcrossings in the top storey are on the average about twice as frequent as in the 3rd or 4th storey. This trend combined with the almost constant mean of the total time above e_a translates into more frequent but shorter excursions for the higher storeys than for the middle storeys.

The effect of restoring force model or input motion variation is, as for the mean of Z, higher mean upcrossing rates for the elastoplastic than for the modified-Clough model and for Parkfield than for El Centro.
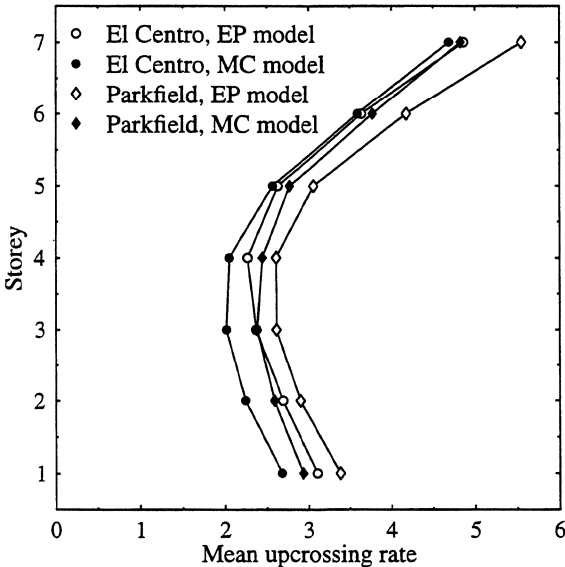
FIGURE 5-25   **Mean upcrossing rate of level** e_a **by the absolute dynamic eccentricity.**

5.2.5 Conclusions

Numerical results from the simulation study of a seven-storey regular building are used to evaluate the accidental torsion provisions in the UBC. The shear walls of this building are modeled by springs with random yield strengths. The inelastic response of this system may therefore involve torsion which is deemed accidental by the codes and is meant to be accounted for by the inclusion of accidental eccentricity in the design process.

The response measures used for the purpose of code evaluation are the dynamic eccentricity $\Theta(t)$, defined as the ratio of the dynamic storey torque to the design storey shear (given by the code), the maximum of $|\Theta(t)|$, the mean upcrossing rate of the code accidental eccentricity level $e_a = 5\%$ by $|\Theta(t)|$, and the total time $|\Theta(t)|$ spends above e_a. Numerical results for the type of building considered, i.e., a regular building with the same plan for all storeys and only minor variations of stiffness or mass from storey to storey, indicate the following:

- Most of the response measures listed above show only slight variations from one storey to another. The only exception is the mean upcrossing rate which is about twice as high for the top storey as for the middle storeys.

- The estimates of the mean of $|\Theta(t)|$ listed in Table 5-4 range from 5% to 6.7%, consistently above the code eccentricity. As is to be expected from this observation, the mean of the maximum dynamic eccentricity is very high ranging roughly from 23% to 37%.

- It is virtually certain that at some point during the motion $|\Theta(t)|$ will exceed e_a, as suggested by the probability that the total time above e_a exceed zero, shown in Figure 5-24. In fact, $|\Theta(t)|$ is expected to spend 32% to 44% of the motion duration above code eccentricity. Moreover, there is quite significant probability, roughly 10% to 30% depending on the motion and the restoring force model, that the total time of $|\Theta(t)|$ above e_a may exceed 60% of the motion duration.

- Of the two motions considered, El Centro and Parkfield, the latter appears to place somewhat higher demands on the multi-storey systems investigated. Parkfield produces dynamic eccentricity processes with larger percentage of absolute values above e_a (Figure 5-21), more frequent upcrossings of e_a, and larger fractions of the motion duration above this level. The difference between motions is more

pronounced for the modified-Clough than for the elastoplastic model.

- Use of the modified-Clough versus the elastoplastic model consistently results in lower absolute dynamic eccentricity values, less frequent upcrossings of level e_a and shorter durations of stay above e_a. Therefore, if one of these two restoring force models has to be selected for inelastic time-history analysis of a multi-storey system similar in type to the one considered in this study, the elastoplastic appears to be the conservative choice.

The above observations suggest that, for the type of building and the motions considered, the UBC accidental eccentricity of 5% may not be sufficient to account for accidental torsion caused by strength uncertainty. It should also be mentioned that the twice as high accidental eccentricity required by other codes does not appear to fare any better, as evidenced by the statistics in Table 5-4 and Figure 5-21.

5.3 Overview of code evaluation conclusions

One of the principal objectives of the present study was to evaluate whether the accidental torsion provisions in the Uniform Building Code are appropriate to account for accidental torsion caused by yield strength uncertainty.

To that purpose, a simple one-storey system was considered at first. This system consists of a rectangular slab supported by two lateral-load-resisting elements modeled as inelastic springs with random yield strengths. Next, the focus was broadened to include a realistic seven-storey building. The shear walls of this seven- by three-span frame-shear wall structure are modeled by sets of springs with random yield strengths. Both parts of the study are based on Monte Carlo simulation. Code evaluation is essentially based on a response measure referred to as dynamic eccentricity and defined as the nondimensionalized ratio of dynamic storey torsional moment to design storey shear, making it readily comparable with the accidental eccentricity in the code provisions.

Comparison of numerical results from the one- and seven-storey systems was expected to indicate which, if any, of the observations made on the simple one-storey system are still valid for the realistic seven-storey building. No quantitative agreement between numerical results is evident and it would be unrealistic to expect any given the difference in system complexity. Qualitative comparison however yields a number of similar trends, which the writers find quite encouraging. The underlying assumption in the discussion

171

that follows is that any attempt at code evaluation is limited by the systems and input motions considered. Therefore, the conclusions drawn may not apply beyond the scope of this study.

- El Centro and Parkfield, the two input motions common to both parts of the study, are representative of two groups of motions with very different characteristics. The first group is characterized by irregular accelerograms and fairly uniform energy content over a wide band of frequencies whereas the second by few pronounced acceleration pulses. The numerical results suggest that Parkfield, the motion of the second type, tends to produce larger dynamic eccentricities on a given system as result of the strength uncertainty. However, it should be mentioned that this difference in response is more evident for the one-storey than for the seven-storey systems.

- Inelastic time-history analysis may be used in the design process, in which case a restoring force model has to be selected. The issue of appropriate restoring force model does not arise in the seismic codes since inelastic response is considered only implicitly through the reduction in the base shear. Numerical results from this study consistently suggest that if the modified-Clough were the correct restoring force model but the simpler elastoplastic model was used instead, the dynamic torsional moments arising from strength uncertainty would be overestimated. The above observation would make the use of the elastoplastic model conservative in respect to the specific response measure. However, as was concluded in Sections 3 and 4, the use of the elastoplastic model is not necessarily conservative when displacements or energy dissipation are the response measures of interest.

- The accidental torsional moment prescribed by the code to account for, among other things, strength uncertainty is exceeded by the dynamic torsional moments that actually develop in the systems considered, not only for large fractions of the motion duration but by significant amounts, as well. Therefore, the UBC accidental eccentricity of 5% appears inadequate to account for accidental torsion caused by strength uncertainty. Moreover, a higher accidental eccentricity such as the 10% required by, among others, the Canadian and New Zealand codes, although unquestionably superior, may still be inadequate. However, evaluation of the 10% accidental eccentricity provision is not strictly possible since none of the systems considered was actually designed for this value.

172

SECTION 6

CONCLUSIONS

Two types of structural system, a simple one-storey structure and a realistic seven-storey building were used to evaluate the effects on seismic response and design of two aspects of system uncertainty: uncertainty in the functional form of the restoring force model and in the parameters of this model, specifically the yield strength. The restoring force model uncertainty was represented by the elastoplastic and the modified-Clough models. Of these two models, the elastoplastic does not account for stiffness degradation whereas the modified-Clough does. The yield strength was treated as a lognormally distributed random variable with mean equal to the design strength according to the Uniform Building Code (UBC) and coefficient of variation 15%. Input was deterministic consisting of three and two earthquake records, for the one- and seven-storey system, respectively. The study was based on Monte Carlo simulation.

One-storey systems. The one-storey system consists of a rigid slab supported by two lateral-load-resisting elements with random yield strengths. Other system parameters, specifically the small-vibration lateral period T and the dimensionless parameter γ used to characterize the radius of gyration, were assigned several deterministic values. The system was subjected to the strong motion portions of the El Centro, Taft, and Parkfield records scaled to various peak ground accelerations (PGA). Two levels of dependence between element yield strengths were considered: perfect correlation and independence. Torsional vibrations only occur when the element yield strengths are not perfectly correlated and the response exceeds the yield limit. The maximum displacement Y_{max}, the maximum ductility M_{max}, the dissipated energy E_{dis}, and the maximum rotation Φ_{max} were used to characterize the structural response.

Numerical results for this system show that:

- The mean of Y_{max}, M_{max}, and E_{dis}, increases monotonically with PGA.

- The mean of Y_{max} increases with the period T whereas the mean of M_{max} and E_{dis} decreases.

- Torsion results in increase in the mean of Y_{max} and M_{max}. However, the mean of E_{dis} is insensitive to variations in the mass moment of inertia of the structure as

173

well as to the uncertainty in the element yield strengths.

- The coefficients of variation of E_{dis} and Y_{max} are relatively small, whereas M_{max} and especially the maximum rotation Φ_{max} have large coefficients of variation. For example, the coefficient of variation of Φ_{max} can be as high as 88% when the coefficient of variation of the element yield strengths is 15%.

- There is significant probability for the ductility requirements of systems with strength uncertainty to exceed those of the code-designed system by a factor of two and, for certain parameter combinations, even by a factor of four.

- If the modified-Clough were the correct restoring force model, use of the elastoplastic model instead would not necessarily be conservative, because:

  - Maximum displacement can be larger for the modified-Clough than for the elastoplastic model. This tendency is strongly dependent on the input motion; it is prevalent under El Centro but rarely observed under Parkfield.

  - Energy dissipation can be lower for the modified-Clough than for the elastoplastic model, more so for higher PGA values.

Multi-storey systems. The realistic seven-storey building considered in the second part of this study is a seven- by three-span frame-shear wall structure designed according to the UBC. Each structural member was modeled by a set of inelastic springs. Yield strengths of springs employed in modeling shear walls were treated as random variables. Random yield strengths were assumed to be perfectly correlated within each wall element, i.e., a wall segment between consecutive floors, but independent from one element to another. The structure is symmetric in the elastic range but can experience torsional vibrations following yield of any of the wall springs. The structure was subjected to the El Centro record, as is, and to the Parkfield record scaled to PGA of $0.43g$.

Numerical results for the seven-storey systems indicate that:

- Torsion leads to maximum interstorey displacements Y_{max} with mean values consistently higher than the respective displacements of the deterministic symmetric system, i.e., the system resulting by the application of the code provisions. The increase is more significant for the lower storeys and can be as much as 35%.

- The coefficients of variation of Y_{max} and the total energy dissipated by the system

are relatively small, whereas the coefficient of variation of the maximum interstorey rotation can be as high as 78% when the coefficient of variation of the random yield strengths is 15%.

- Torsion results in decrease in the mean of the total energy dissipated in the first storey, the largest by far among all stories, and, consequently, in the mean of the energy dissipated by the whole system.

- The effects of torsion on the maximum displacement and on the uncertainty levels of the various response measures are similar to the ones observed for one-storey systems. However, the total energy dissipation appears to be more affected by the presence of torsion than was the case for one-storey systems.

- The conclusion reached for one-storey systems on the issue of model selection is still valid for the multi-storey systems considered. Specifically, the elastoplastic model may underestimate displacements and overestimate energy dissipation. Therefore, it is not necessarily a conservative alternative for the more realistic modified-Clough model. Once more, the effects of model uncertainty appear to be strongly dependent on the input motion.

Code evaluation. One of the principal objectives of the present study was to evaluate whether the accidental torsion provisions in the Uniform Building Code are appropriate to account for accidental torsion caused by strength uncertainty. Code evaluation was based on a response measure referred to as dynamic eccentricity and defined as the nondimensionalized ratio of dynamic storey torsional moment to design storey shear, making it readily comparable with the accidental eccentricity in the code provisions. Several aspects of the evolution of the absolute dynamic eccentricity in time were examined: its maximum value, the frequency with which it upcrosses the accidental eccentricity level, and the fraction of the motion it spends above that level.

Numerical results for the one- and multi-storey systems and the motions considered in this study lead to similar conclusions on (1) the adequacy of the code provisions and (2) the effects of restoring force model selection.

- The magnitude of dynamic torsional moments that develop in a system because of strength uncertainty depends to some extent on the input motion. El Centro and Parkfield, the two records common to both parts of the study, are representative

of two groups of motions with very different characteristics. The first group is characterized by irregular accelerograms and fairly uniform energy content over a wide band of frequencies whereas the second by few pronounced acceleration pulses. Numerical results show that Parkfield tends to produce larger dynamic eccentricities, particularly for one-storey systems with longer periods. For the type of multi-storey system considered this effect of the input motion is more pronounced for the modified-Clough than for the elastoplastic model.

- Inelastic time-history analysis may be used in design; in this case a restoring force model has to be selected but the code offers no suggestions on this matter. Numerical results from this study consistently suggest that if the modified-Clough were the correct restoring force model but the simpler elastoplastic model was used instead, the dynamic torsional moments arising from strength uncertainty would be overestimated. The above observation would make the use of the elastoplastic model conservative in respect to the specific response measure. However, as discussed earlier in this section, the use of the elastoplastic model is not necessarily conservative when displacements or energy dissipation are the response measures of interest.

- The accidental torsional moment prescribed by the code to account for, among other things, strength uncertainty is exceeded by the dynamic torsional moments that actually develop in the systems considered for large fractions of the motion duration and by significant amounts. Therefore, the UBC accidental eccentricity of 5% appears inadequate to account for accidental torsion caused by strength uncertainty. Moreover, there are indications that the twice as high accidental eccentricity of 10% required by, among others, the Canadian and New Zealand codes, may still be inadequate.

SECTION 7

REFERENCES

1. A. G. Ayala and J. A. Escobar (1991), "Respuesta Sismica de Estructuras Inelasticas con Propiedades Inciertas - Comportamiento en Torsion", *Instituto de Ingeniería, UNAM*, No 738, México.

2. Y. Bozorgnia and W. K. Tso (1986), "Inelastic Earthquake Response of Asymmetric Structures", *Journal of Structural Engineering*, Vol. 112, No. 2.

3. M. Bruneau and S. A. Mahin (1987), "Inelastic Seismic Response of Structures with Mass or Stiffness Eccentricities in Plan", Report No. UCB/EERC-87/12, Earthquake Engineering Research Center, University of California, Berkeley.

4. M. Bruneau and S. A. Mahin (1990), "Normalizing Inelastic Seismic Response of Structures having Eccentricities in Plan", *Journal of Structural Engineering*, Vol. 116, No. 12.

5. M. Bruneau and S. A. Mahin (1991), "Seismic Response of Symmetric Structures having Unbalanced Yield Strengths in Plan", *Proc. of 6th Canadian Conference on Earthquake Engineering*, Toronto, Canada.

6. CANNY-E (1995), "Three-Dimensional Nonlinear Dynamic Structural Analysis Computer Program Package", Developed by K.-N. Li, CANNY Consulatants Pte. Ltd.

7. A. M. Chandler and X. N. Duan (1991), "Evaluation of Factors Influencing the Inelastic Seismic Performance of Torsionally Asymmetric Buildings", *Earthquake Engineering and Structural Dynamics*, Vol. 20.

8. A. M. Chandler, G. L. Hutchinson, and W. Jiang (1991), "Inelastic Torsional Response of Buildings to the 1985 Mexican Earthquake: a Parametric Study", *Soil Dynamics and Earthquake Engineering*, Vol. 10, No. 10.

9. A. K. Chopra and R. K. Goel (1991), "Evaluation of Torsional Provisions in Seismic Codes", *Journal of Structural Engineering*, Vol. 117, No. 12.

10. M. De Stefano, G. Faella, and R. Ramasco (1993), "Inelastic Response and Design Criteria of Plan-Wise Asymmetric Systems", *Earthquake Engineering and Structural Dynamics*, Vol. 22.

11. M. Dolce and D. Ludovici (1992), "Torsional Effects in Buildings under Strong Earthquakes", *European Earthquake Engineering*, Vol. VI, No. 1.

12. X. N. Duan and A. M. Chandler (1993), "Inelastic Seismic Response of Code-Designed Multistorey Frame Buildings with Regular Asymmetry", *Earthquake Engineering and Structural Dynamics*, Vol. 22.

13. B. Ellingwood, T. V. Galambos, J. G. MacGregor, and C. A. Cornell (1980), "Development of a Probability Based Load Criterion for American National Standard A58, Building Code Requirements for Minimum Design Loads in Buildings and Other Structures", Report No. SP 577, National Bureau of Standards, Department of Commerce, Washington, DC.

14. J. A. Escobar and A. G. Ayala (1991), "Non-linear Seismic Response of Asymmetric Buildings with Uncertain Parameters", *Proc. of 6th International Conference on Applications of Statistics and Probability in Civil Engineering*, Vol. 1, Mexico City, Mexico.

15. ETABS (1995), "Three Dimensional Analysis of Building Systems", Version 6.0, Developed by Computers & Structures, Inc.

16. R. K. Goel and A. K. Chopra (1990), "Inelastic Earthquake Response of One-Storey, Asymmetric-Plan Systems", Report No. UCB/EERC-90/14, Earthquake Engineering Research Center, University of California, Berkeley.

17. R. K. Goel and A. K. Chopra (1990), "Inelastic Seismic Response of One-Storey, Asymmetric-Plan Systems: Effects of Stiffness and Strength Distribution", *Earthquake Engineering and Structural Dynamics*, Vol. 19.

18. R. K. Goel and A. K. Chopra (1991), "Effects of Plan Asymmetry in Inelastic Seismic Response of One-Storey Systems", *Journal of Structural Engineering*, Vol. 117, No. 5.

19. *New Zealand Standard* (1992), Standards Association of New Zealand, Wellington, New Zealand.

20. S. Otani (1981), "Hysteresis Models of Reinforced Concrete for Earthquake Response Analysis", *Journal of the Faculty of Engineering, University of Tokyo*, Vol. XXXVI, No. 2.

21. O. A. Pekau and R. Guimond (1990), "Accidental Torsion in Yielding Symmetric Structures", *Engineering Structures*, Vol. 12.

22. A. Rutenberg (1992), "Nonlinear response of asymmetric building structures and seismic codes: a state of the art review", *European Earthquake Engineering*, Anno VI, No. 2.

23. A. Rutenberg, M. Eisenberger, and G. Shohet (1992), "Inelastic Seismic Response of Code Designed Single Storey Asymmetric Structures", *Engineering Structures*, Vol. 14, No. 2.

24. A. W. Sadek and W. K. Tso (1989), "Strength Eccentricity Concept for Inelastic Analysis of Asymmetrical Structures", *Engineering Structures*, Vol. 11.

25. H. Sedarat and V. V. Bertero (1990), "Effects of Torsion on the Linear and Nonlinear Seismic Response of Structures", Report No. UCB/EERC-90/12, Earthquake Engineering Research Center, University of California, Berkeley.

26. H. Shakib and T. K. Datta (1993), "Inelastic Response of Torsionally Coupled System to an Ensemble of Nonstationary Random Ground Motion", *Engineering Structures,* Vol. 15, No. 1.

27. *Supplement to the National Building Code of Canada* (1985), Associate Committee on the National Building Code, National Research Council of Canada, Ottawa, Canada.

28. P. K. Syamal and O. A. Pekau (1985), "Dynamic Response of Bilinear Asymmetric Structures", *Earthquake Engineering and Structural Dynamics,* Vol. 13, No 4.

29. M. D. Trifunac and A. G. Brady (1975), "A Study on the Duration of Strong Earthquake Ground Motion", *Bulletin of the Seismological Society of America,* Vol. 65, No. 3.

30. W. K. Tso and Y. Bozorgnia (1986), "Effective Eccentricity for Inelastic Seismic Response of Buildings", *Earthquake Engineering and Structural Dynamics,* Vol. 14, No 3.

31. W. K. Tso and A. W. Sadek (1985), "Inelastic Seismic Response of Simple Eccentric Structures", *Earthquake Engineering and Structural Dynamics,* Vol. 13, No 2.

32. W. K. Tso and H. Ying (1990), "Additional Seismic Inelastic Deformation Caused by Structural Asymmetry", *Earthquake Engineering and Structural Dynamics,* Vol. 19.

33. W. K. Tso and H. Ying (1992), "Lateral Strength Distribution Specification to Limit Additional Inelastic Deformation of Torsionally Unbalanced Structures", *Engineering Structures,* Vol. 14, No 4.

34. W. K. Tso and T. J. Zhu (1992), "Design of Torsionally Unbalanced Structural Systems Based on Code Provisions I: Ductility Demand", *Earthquake Engineering and Structural Dynamics,* Vol. 21, No 7.

35. *Uniform Building Code, Vol. 2,* (1994), International Conference of Building Officials, Whittier, CA.

36. T. J. Zhu and W. K. Tso (1992), "Design of Torsionally Unbalanced Structural Systems Based on Code Provisions II: Strength Distribution", *Earthquake Engineering and Structural Dynamics,* Vol. 21, No 7.

179

NATIONAL CENTER FOR EARTHQUAKE ENGINEERING RESEARCH
LIST OF TECHNICAL REPORTS

The National Center for Earthquake Engineering Research (NCEER) publishes technical reports on a variety of subjects related to earthquake engineering written by authors funded through NCEER. These reports are available from both NCEER Publications and the National Technical Information Service (NTIS). Requests for reports should be directed to NCEER Publications, National Center for Earthquake Engineering Research, State University of New York at Buffalo, Red Jacket Quadrangle, Buffalo, New York 14261. Reports can also be requested through NTIS, 5285 Port Royal Road, Springfield, Virginia 22161. NTIS accession numbers are shown in parenthesis, if available.

NCEER-87-0001   "First-Year Program in Research, Education and Technology Transfer," 3/5/87, (PB88-134275, A04, MF-A01).

NCEER-87-0002   "Experimental Evaluation of Instantaneous Optimal Algorithms for Structural Control," by R.C. Lin, T.T. Soong and A.M. Reinhorn, 4/20/87, (PB88-134341, A04, MF-A01).

NCEER-87-0003   "Experimentation Using the Earthquake Simulation Facilities at University at Buffalo," by A.M. Reinhorn and R.L. Ketter, to be published.

NCEER-87-0004   "The System Characteristics and Performance of a Shaking Table," by J.S. Hwang, K.C. Chang and G.C. Lee, 6/1/87, (PB88-134259, A03, MF-A01). This report is available only through NTIS (see address given above).

NCEER-87-0005   "A Finite Element Formulation for Nonlinear Viscoplastic Material Using a Q Model," by O. Gyebi and G. Dasgupta, 11/2/87, (PB88-213764, A08, MF-A01).

NCEER-87-0006   "Symbolic Manipulation Program (SMP) - Algebraic Codes for Two and Three Dimensional Finite Element Formulations," by X. Lee and G. Dasgupta, 11/9/87, (PB88-218522, A05, MF-A01).

NCEER-87-0007   "Instantaneous Optimal Control Laws for Tall Buildings Under Seismic Excitations," by J.N. Yang, A. Akbarpour and P. Ghaemmaghami, 6/10/87, (PB88-134333, A06, MF-A01). This report is only available through NTIS (see address given above).

NCEER-87-0008   "IDARC: Inelastic Damage Analysis of Reinforced Concrete Frame - Shear-Wall Structures," by Y.J. Park, A.M. Reinhorn and S.K. Kunnath, 7/20/87, (PB88-134325, A09, MF-A01). This report is only available through NTIS (see address given above).

NCEER-87-0009   "Liquefaction Potential for New York State: A Preliminary Report on Sites in Manhattan and Buffalo," by M. Budhu, V. Vijayakumar, R.F. Giese and L. Baumgras, 8/31/87, (PB88-163704, A03, MF-A01). This report is available only through NTIS (see address given above).

NCEER-87-0010   "Vertical and Torsional Vibration of Foundations in Inhomogeneous Media," by A.S. Veletsos and K.W. Dotson, 6/1/87, (PB88-134291, A03, MF-A01). This report is only available through NTIS (see address given above).

NCEER-87-0011   "Seismic Probabilistic Risk Assessment and Seismic Margins Studies for Nuclear Power Plants," by Howard H.M. Hwang, 6/15/87, (PB88-134267, A03, MF-A01). This report is only available through NTIS (see address given above).

NCEER-87-0012   "Parametric Studies of Frequency Response of Secondary Systems Under Ground-Acceleration Excitations," by Y. Yong and Y.K. Lin, 6/10/87, (PB88-134309, A03, MF-A01). This report is only available through NTIS (see address given above).

NCEER-87-0013   "Frequency Response of Secondary Systems Under Seismic Excitation," by J.A. HoLung, J. Cai and Y.K. Lin, 7/31/87, (PB88-134317, A05, MF-A01). This report is only available through NTIS (see address given above).

NCEER-87-0014   "Modelling Earthquake Ground Motions in Seismically Active Regions Using Parametric Time Series Methods," by G.W. Ellis and A.S. Cakmak, 8/25/87, (PB88-134283, A08, MF-A01). This report is only available through NTIS (see address given above).

NCEER-87-0015   "Detection and Assessment of Seismic Structural Damage," by E. DiPasquale and A.S. Cakmak, 8/25/87, (PB88-163712, A05, MF-A01). This report is only available through NTIS (see address given above).

NCEER-87-0016   "Pipeline Experiment at Parkfield, California," by J. Isenberg and E. Richardson, 9/15/87, (PB88-163720, A03, MF-A01). This report is available only through NTIS (see address given above).

NCEER-87-0017   "Digital Simulation of Seismic Ground Motion," by M. Shinozuka, G. Deodatis and T. Harada, 8/31/87, (PB88-155197, A04, MF-A01). This report is available only through NTIS (see address given above).

NCEER-87-0018   "Practical Considerations for Structural Control: System Uncertainty, System Time Delay and Truncation of Small Control Forces," J.N. Yang and A. Akbarpour, 8/10/87, (PB88-163738, A08, MF-A01). This report is only available through NTIS (see address given above).

NCEER-87-0019   "Modal Analysis of Nonclassically Damped Structural Systems Using Canonical Transformation," by J.N. Yang, S. Sarkani and F.X. Long, 9/27/87, (PB88-187851, A04, MF-A01).

NCEER-87-0020   "A Nonstationary Solution in Random Vibration Theory," by J.R. Red-Horse and P.D. Spanos, 11/3/87, (PB88-163746, A03, MF-A01).

NCEER-87-0021   "Horizontal Impedances for Radially Inhomogeneous Viscoelastic Soil Layers," by A.S. Veletsos and K.W. Dotson, 10/15/87, (PB88-150859, A04, MF-A01).

NCEER-87-0022   "Seismic Damage Assessment of Reinforced Concrete Members," by Y.S. Chung, C. Meyer and M. Shinozuka, 10/9/87, (PB88-150867, A05, MF-A01). This report is available only through NTIS (see address given above).

NCEER-87-0023   "Active Structural Control in Civil Engineering," by T.T. Soong, 11/11/87, (PB88-187778, A03, MF-A01).

NCEER-87-0024   "Vertical and Torsional Impedances for Radially Inhomogeneous Viscoelastic Soil Layers," by K.W. Dotson and A.S. Veletsos, 12/87, (PB88-187786, A03, MF-A01).

NCEER-87-0025   "Proceedings from the Symposium on Seismic Hazards, Ground Motions, Soil-Liquefaction and Engineering Practice in Eastern North America," October 20-22, 1987, edited by K.H. Jacob, 12/87, (PB88-188115, A23, MF-A01).

NCEER-87-0026   "Report on the Whittier-Narrows, California, Earthquake of October 1, 1987," by J. Pantelic and A. Reinhorn, 11/87, (PB88-187752, A03, MF-A01). This report is available only through NTIS (see address given above).

NCEER-87-0027   "Design of a Modular Program for Transient Nonlinear Analysis of Large 3-D Building Structures," by S. Srivastav and J.F. Abel, 12/30/87, (PB88-187950, A05, MF-A01). This report is only available through NTIS (see address given above).

NCEER-87-0028   "Second-Year Program in Research, Education and Technology Transfer," 3/8/88, (PB88-219480, A04, MF-A01).

NCEER-88-0001   "Workshop on Seismic Computer Analysis and Design of Buildings With Interactive Graphics," by W. McGuire, J.F. Abel and C.H. Conley, 1/18/88, (PB88-187760, A03, MF-A01). This report is only available through NTIS (see address given above).

NCEER-88-0002   "Optimal Control of Nonlinear Flexible Structures," by J.N. Yang, F.X. Long and D. Wong, 1/22/88, (PB88-213772, A06, MF-A01).

NCEER-88-0003   "Substructuring Techniques in the Time Domain for Primary-Secondary Structural Systems," by G.D. Manolis and G. Juhn, 2/10/88, (PB88-213780, A04, MF-A01).

NCEER-88-0004   "Iterative Seismic Analysis of Primary-Secondary Systems," by A. Singhal, L.D. Lutes and P.D. Spanos, 2/23/88, (PB88-213798, A04, MF-A01).

NCEER-88-0005   "Stochastic Finite Element Expansion for Random Media," by P.D. Spanos and R. Ghanem, 3/14/88, (PB88-213806, A03, MF-A01).

NCEER-88-0006   "Combining Structural Optimization and Structural Control," by F.Y. Cheng and C.P. Pantelides, 1/10/88, (PB88-213814, A05, MF-A01).

NCEER-88-0007   "Seismic Performance Assessment of Code-Designed Structures," by H.H-M. Hwang, J-W. Jaw and H-J. Shau, 3/20/88, (PB88-219423, A04, MF-A01). This report is only available through NTIS (see address given above).

NCEER-88-0008   "Reliability Analysis of Code-Designed Structures Under Natural Hazards," by H.H-M. Hwang, H. Ushiba and M. Shinozuka, 2/29/88, (PB88-229471, A07, MF-A01). This report is only available through NTIS (see address given above).

NCEER-88-0009   "Seismic Fragility Analysis of Shear Wall Structures," by J-W Jaw and H.H-M. Hwang, 4/30/88, (PB89-102867, A04, MF-A01).

NCEER-88-0010   "Base Isolation of a Multi-Story Building Under a Harmonic Ground Motion - A Comparison of Performances of Various Systems," by F-G Fan, G. Ahmadi and I.G. Tadjbakhsh, 5/18/88, (PB89-122238, A06, MF-A01). This report is only available through NTIS (see address given above).

NCEER-88-0011   "Seismic Floor Response Spectra for a Combined System by Green's Functions," by F.M. Lavelle, L.A. Bergman and P.D. Spanos, 5/1/88, (PB89-102875, A03, MF-A01).

NCEER-88-0012   "A New Solution Technique for Randomly Excited Hysteretic Structures," by G.Q. Cai and Y.K. Lin, 5/16/88, (PB89-102883, A03, MF-A01).

NCEER-88-0013   "A Study of Radiation Damping and Soil-Structure Interaction Effects in the Centrifuge," by K. Weissman, supervised by J.H. Prevost, 5/24/88, (PB89-144703, A06, MF-A01).

NCEER-88-0014   "Parameter Identification and Implementation of a Kinematic Plasticity Model for Frictional Soils," by J.H. Prevost and D.V. Griffiths, to be published.

NCEER-88-0015   "Two- and Three- Dimensional Dynamic Finite Element Analyses of the Long Valley Dam," by D.V. Griffiths and J.H. Prevost, 6/17/88, (PB89-144711, A04, MF-A01).

NCEER-88-0016   "Damage Assessment of Reinforced Concrete Structures in Eastern United States," by A.M. Reinhorn, M.J. Seidel, S.K. Kunnath and Y.J. Park, 6/15/88, (PB89-122220, A04, MF-A01). This report is only available through NTIS (see address given above).

NCEER-88-0017   "Dynamic Compliance of Vertically Loaded Strip Foundations in Multilayered Viscoelastic Soils," by S. Ahmad and A.S.M. Israil, 6/17/88, (PB89-102891, A04, MF-A01).

NCEER-88-0018   "An Experimental Study of Seismic Structural Response With Added Viscoelastic Dampers," by R.C. Lin, Z. Liang, T.T. Soong and R.H. Zhang, 6/30/88, (PB89-122212, A05, MF-A01). This report is available only through NTIS (see address given above).

NCEER-88-0019   "Experimental Investigation of Primary - Secondary System Interaction," by G.D. Manolis, G. Juhn and A.M. Reinhorn, 5/27/88, (PB89-122204, A04, MF-A01).

NCEER-88-0020   "A Response Spectrum Approach For Analysis of Nonclassically Damped Structures," by J.N. Yang, S. Sarkani and F.X. Long, 4/22/88, (PB89-102909, A04, MF-A01).

NCEER-88-0021 "Seismic Interaction of Structures and Soils: Stochastic Approach," by A.S. Veletsos and A.M. Prasad, 7/21/88, (PB89-122196, A04, MF-A01). This report is only available through NTIS (see address given above).

NCEER-88-0022 "Identification of the Serviceability Limit State and Detection of Seismic Structural Damage," by E. DiPasquale and A.S. Cakmak, 6/15/88, (PB89-122188, A05, MF-A01). This report is available only through NTIS (see address given above).

NCEER-88-0023 "Multi-Hazard Risk Analysis: Case of a Simple Offshore Structure," by B.K. Bhartia and E.H. Vanmarcke, 7/21/88, (PB89-145213, A05, MF-A01).

NCEER-88-0024 "Automated Seismic Design of Reinforced Concrete Buildings," by Y.S. Chung, C. Meyer and M. Shinozuka, 7/5/88, (PB89-122170, A06, MF-A01). This report is available only through NTIS (see address given above).

NCEER-88-0025 "Experimental Study of Active Control of MDOF Structures Under Seismic Excitations," by L.L. Chung, R.C. Lin, T.T. Soong and A.M. Reinhorn, 7/10/88, (PB89-122600, A04, MF-A01).

NCEER-88-0026 "Earthquake Simulation Tests of a Low-Rise Metal Structure," by J.S. Hwang, K.C. Chang, G.C. Lee and R.L. Ketter, 8/1/88, (PB89-102917, A04, MF-A01).

NCEER-88-0027 "Systems Study of Urban Response and Reconstruction Due to Catastrophic Earthquakes," by F. Kozin and H.K. Zhou, 9/22/88, (PB90-162348, A04, MF-A01).

NCEER-88-0028 "Seismic Fragility Analysis of Plane Frame Structures," by H.H-M. Hwang and Y.K. Low, 7/31/88, (PB89-131445, A06, MF-A01).

NCEER-88-0029 "Response Analysis of Stochastic Structures," by A. Kardara, C. Bucher and M. Shinozuka, 9/22/88, (PB89-174429, A04, MF-A01).

NCEER-88-0030 "Nonnormal Accelerations Due to Yielding in a Primary Structure," by D.C.K. Chen and L.D. Lutes, 9/19/88, (PB89-131437, A04, MF-A01).

NCEER-88-0031 "Design Approaches for Soil-Structure Interaction," by A.S. Veletsos, A.M. Prasad and Y. Tang, 12/30/88, (PB89-174437, A03, MF-A01). This report is available only through NTIS (see address given above).

NCEER-88-0032 "A Re-evaluation of Design Spectra for Seismic Damage Control," by C.J. Turkstra and A.G. Tallin, 11/7/88, (PB89-145221, A05, MF-A01).

NCEER-88-0033 "The Behavior and Design of Noncontact Lap Splices Subjected to Repeated Inelastic Tensile Loading," by V.E. Sagan, P. Gergely and R.N. White, 12/8/88, (PB89-163737, A08, MF-A01).

NCEER-88-0034 "Seismic Response of Pile Foundations," by S.M. Mamoon, P.K. Banerjee and S. Ahmad, 11/1/88, (PB89-145239, A04, MF-A01).

NCEER-88-0035 "Modeling of R/C Building Structures With Flexible Floor Diaphragms (IDARC2)," by A.M. Reinhorn, S.K. Kunnath and N. Panahshahi, 9/7/88, (PB89-207153, A07, MF-A01).

NCEER-88-0036 "Solution of the Dam-Reservoir Interaction Problem Using a Combination of FEM, BEM with Particular Integrals, Modal Analysis, and Substructuring," by C-S. Tsai, G.C. Lee and R.L. Ketter, 12/31/88, (PB89-207146, A04, MF-A01).

NCEER-88-0037 "Optimal Placement of Actuators for Structural Control," by F.Y. Cheng and C.P. Pantelides, 8/15/88, (PB89-162846, A05, MF-A01).

NCEER-88-0038   "Teflon Bearings in Aseismic Base Isolation: Experimental Studies and Mathematical Modeling," by A. Mokha, M.C. Constantinou and A.M. Reinhorn, 12/5/88, (PB89-218457, A10, MF-A01). This report is available only through NTIS (see address given above).

NCEER-88-0039   "Seismic Behavior of Flat Slab High-Rise Buildings in the New York City Area," by P. Weidlinger and M. Ettouney, 10/15/88, (PB90-145681, A04, MF-A01).

NCEER-88-0040   "Evaluation of the Earthquake Resistance of Existing Buildings in New York City," by P. Weidlinger and M. Ettouney, 10/15/88, to be published.

NCEER-88-0041   "Small-Scale Modeling Techniques for Reinforced Concrete Structures Subjected to Seismic Loads," by W. Kim, A. El-Attar and R.N. White, 11/22/88, (PB89-189625, A05, MF-A01).

NCEER-88-0042   "Modeling Strong Ground Motion from Multiple Event Earthquakes," by G.W. Ellis and A.S. Cakmak, 10/15/88, (PB89-174445, A03, MF-A01).

NCEER-88-0043   "Nonstationary Models of Seismic Ground Acceleration," by M. Grigoriu, S.E. Ruiz and E. Rosenblueth, 7/15/88, (PB89-189617, A04, MF-A01).

NCEER-88-0044   "SARCF User's Guide: Seismic Analysis of Reinforced Concrete Frames," by Y.S. Chung, C. Meyer and M. Shinozuka, 11/9/88, (PB89-174452, A08, MF-A01).

NCEER-88-0045   "First Expert Panel Meeting on Disaster Research and Planning," edited by J. Pantelic and J. Stoyle, 9/15/88, (PB89-174460, A05, MF-A01). This report is only available through NTIS (see address given above).

NCEER-88-0046   "Preliminary Studies of the Effect of Degrading Infill Walls on the Nonlinear Seismic Response of Steel Frames," by C.Z. Chrysostomou, P. Gergely and J.F. Abel, 12/19/88, (PB89-208383, A05, MF-A01).

NCEER-88-0047   "Reinforced Concrete Frame Component Testing Facility - Design, Construction, Instrumentation and Operation," by S.P. Pessiki, C. Conley, T. Bond, P. Gergely and R.N. White, 12/16/88, (PB89-174478, A04, MF-A01).

NCEER-89-0001   "Effects of Protective Cushion and Soil Compliancy on the Response of Equipment Within a Seismically Excited Building," by J.A. HoLung, 2/16/89, (PB89-207179, A04, MF-A01).

NCEER-89-0002   "Statistical Evaluation of Response Modification Factors for Reinforced Concrete Structures," by H.H-M. Hwang and J-W. Jaw, 2/17/89, (PB89-207187, A05, MF-A01).

NCEER-89-0003   "Hysteretic Columns Under Random Excitation," by G-Q. Cai and Y.K. Lin, 1/9/89, (PB89-196513, A03, MF-A01).

NCEER-89-0004   "Experimental Study of 'Elephant Foot Bulge' Instability of Thin-Walled Metal Tanks," by Z-H. Jia and R.L. Ketter, 2/22/89, (PB89-207195, A03, MF-A01).

NCEER-89-0005   "Experiment on Performance of Buried Pipelines Across San Andreas Fault," by J. Isenberg, E. Richardson and T.D. O'Rourke, 3/10/89, (PB89-218440, A04, MF-A01). This report is available only through NTIS (see address given above).

NCEER-89-0006   "A Knowledge-Based Approach to Structural Design of Earthquake-Resistant Buildings," by M. Subramani, P. Gergely, C.H. Conley, J.F. Abel and A.H. Zaghw, 1/15/89, (PB89-218465, A06, MF-A01).

NCEER-89-0007   "Liquefaction Hazards and Their Effects on Buried Pipelines," by T.D. O'Rourke and P.A. Lane, 2/1/89, (PB89-218481, A09, MF-A01).

NCEER-89-0008   "Fundamentals of System Identification in Structural Dynamics," by H. Imai, C-B. Yun, O. Maruyama and M. Shinozuka, 1/26/89, (PB89-207211, A04, MF-A01).

NCEER-89-0009   "Effects of the 1985 Michoacan Earthquake on Water Systems and Other Buried Lifelines in Mexico," by A.G. Ayala and M.J. O'Rourke, 3/8/89, (PB89-207229, A06, MF-A01).

NCEER-89-R010   "NCEER Bibliography of Earthquake Education Materials," by K.E.K. Ross, Second Revision, 9/1/89, (PB90-125352, A05, MF-A01). This report is replaced by NCEER-92-0018.

NCEER-89-0011   "Inelastic Three-Dimensional Response Analysis of Reinforced Concrete Building Structures (IDARC-3D), Part I - Modeling," by S.K. Kunnath and A.M. Reinhorn, 4/17/89, (PB90-114612, A07, MF-A01).

NCEER-89-0012   "Recommended Modifications to ATC-14," by C.D. Poland and J.O. Malley, 4/12/89, (PB90-108648, A15, MF-A01).

NCEER-89-0013   "Repair and Strengthening of Beam-to-Column Connections Subjected to Earthquake Loading," by M. Corazao and A.J. Durrani, 2/28/89, (PB90-109885, A06, MF-A01).

NCEER-89-0014   "Program EXKAL2 for Identification of Structural Dynamic Systems," by O. Maruyama, C-B. Yun, M. Hoshiya and M. Shinozuka, 5/19/89, (PB90-109877, A09, MF-A01).

NCEER-89-0015   "Response of Frames With Bolted Semi-Rigid Connections, Part I - Experimental Study and Analytical Predictions," by P.J. DiCorso, A.M. Reinhorn, J.R. Dickerson, J.B. Radziminski and W.L. Harper, 6/1/89, to be published.

NCEER-89-0016   "ARMA Monte Carlo Simulation in Probabilistic Structural Analysis," by P.D. Spanos and M.P. Mignolet, 7/10/89, (PB90-109893, A03, MF-A01).

NCEER-89-P017   "Preliminary Proceedings from the Conference on Disaster Preparedness - The Place of Earthquake Education in Our Schools," Edited by K.E.K. Ross, 6/23/89, (PB90-108606, A03, MF-A01).

NCEER-89-0017   "Proceedings from the Conference on Disaster Preparedness - The Place of Earthquake Education in Our Schools," Edited by K.E.K. Ross, 12/31/89, (PB90-207895, A012, MF-A02). This report is available only through NTIS (see address given above).

NCEER-89-0018   "Multidimensional Models of Hysteretic Material Behavior for Vibration Analysis of Shape Memory Energy Absorbing Devices, by E.J. Graesser and F.A. Cozzarelli, 6/7/89, (PB90-164146, A04, MF-A01).

NCEER-89-0019   "Nonlinear Dynamic Analysis of Three-Dimensional Base Isolated Structures (3D-BASIS)," by S. Nagarajaiah, A.M. Reinhorn and M.C. Constantinou, 8/3/89, (PB90-161936, A06, MF-A01). This report has been replaced by NCEER-93-0011.

NCEER-89-0020   "Structural Control Considering Time-Rate of Control Forces and Control Rate Constraints," by F.Y. Cheng and C.P. Pantelides, 8/3/89, (PB90-120445, A04, MF-A01).

NCEER-89-0021   "Subsurface Conditions of Memphis and Shelby County," by K.W. Ng, T-S. Chang and H-H.M. Hwang, 7/26/89, (PB90-120437, A03, MF-A01).

NCEER-89-0022   "Seismic Wave Propagation Effects on Straight Jointed Buried Pipelines," by K. Elhmadi and M.J. O'Rourke, 8/24/89, (PB90-162322, A10, MF-A02).

NCEER-89-0023   "Workshop on Serviceability Analysis of Water Delivery Systems," edited by M. Grigoriu, 3/6/89, (PB90-127424, A03, MF-A01).

NCEER-89-0024   "Shaking Table Study of a 1/5 Scale Steel Frame Composed of Tapered Members," by K.C. Chang, J.S. Hwang and G.C. Lee, 9/18/89, (PB90-160169, A04, MF-A01).

NCEER-89-0025   "DYNA1D: A Computer Program for Nonlinear Seismic Site Response Analysis - Technical Documentation," by Jean H. Prevost, 9/14/89, (PB90-161944, A07, MF-A01). This report is available only through NTIS (see address given above).

NCEER-89-0026   "1:4 Scale Model Studies of Active Tendon Systems and Active Mass Dampers for Aseismic Protection," by A.M. Reinhorn, T.T. Soong, R.C. Lin, Y.P. Yang, Y. Fukao, H. Abe and M. Nakai, 9/15/89, (PB90-173246, A10, MF-A02).

NCEER-89-0027   "Scattering of Waves by Inclusions in a Nonhomogeneous Elastic Half Space Solved by Boundary Element Methods," by P.K. Hadley, A. Askar and A.S. Cakmak, 6/15/89, (PB90-145699, A07, MF-A01).

NCEER-89-0028   "Statistical Evaluation of Deflection Amplification Factors for Reinforced Concrete Structures," by H.H.M. Hwang, J-W. Jaw and A.L. Ch'ng, 8/31/89, (PB90-164633, A05, MF-A01).

NCEER-89-0029   "Bedrock Accelerations in Memphis Area Due to Large New Madrid Earthquakes," by H.H.M. Hwang, C.H.S. Chen and G. Yu, 11/7/89, (PB90-162330, A04, MF-A01).

NCEER-89-0030   "Seismic Behavior and Response Sensitivity of Secondary Structural Systems," by Y.Q. Chen and T.T. Soong, 10/23/89, (PB90-164658, A08, MF-A01).

NCEER-89-0031   "Random Vibration and Reliability Analysis of Primary-Secondary Structural Systems," by Y. Ibrahim, M. Grigoriu and T.T. Soong, 11/10/89, (PB90-161951, A04, MF-A01).

NCEER-89-0032   "Proceedings from the Second U.S. - Japan Workshop on Liquefaction, Large Ground Deformation and Their Effects on Lifelines, September 26-29, 1989," Edited by T.D. O'Rourke and M. Hamada, 12/1/89, (PB90-209388, A22, MF-A03).

NCEER-89-0033   "Deterministic Model for Seismic Damage Evaluation of Reinforced Concrete Structures," by J.M. Bracci, A.M. Reinhorn, J.B. Mander and S.K. Kunnath, 9/27/89, (PB91-108803, A06, MF-A01).

NCEER-89-0034   "On the Relation Between Local and Global Damage Indices," by E. DiPasquale and A.S. Cakmak, 8/15/89, (PB90-173865, A05, MF-A01).

NCEER-89-0035   "Cyclic Undrained Behavior of Nonplastic and Low Plasticity Silts," by A.J. Walker and H.E. Stewart, 7/26/89, (PB90-183518, A10, MF-A01).

NCEER-89-0036   "Liquefaction Potential of Surficial Deposits in the City of Buffalo, New York," by M. Budhu, R. Giese and L. Baumgrass, 1/17/89, (PB90-208455, A04, MF-A01).

NCEER-89-0037   "A Deterministic Assessment of Effects of Ground Motion Incoherence," by A.S. Veletsos and Y. Tang, 7/15/89, (PB90-164294, A03, MF-A01).

NCEER-89-0038   "Workshop on Ground Motion Parameters for Seismic Hazard Mapping," July 17-18, 1989, edited by R.V. Whitman, 12/1/89, (PB90-173923, A04, MF-A01).

NCEER-89-0039   "Seismic Effects on Elevated Transit Lines of the New York City Transit Authority," by C.J. Costantino, C.A. Miller and E. Heymsfield, 12/26/89, (PB90-207887, A06, MF-A01).

NCEER-89-0040   "Centrifugal Modeling of Dynamic Soil-Structure Interaction," by K. Weissman, Supervised by J.H. Prevost, 5/10/89, (PB90-207879, A07, MF-A01).

NCEER-89-0041   "Linearized Identification of Buildings With Cores for Seismic Vulnerability Assessment," by I-K. Ho and A.E. Aktan, 11/1/89, (PB90-251943, A07, MF-A01).

NCEER-90-0001   "Geotechnical and Lifeline Aspects of the October 17, 1989 Loma Prieta Earthquake in San Francisco," by T.D. O'Rourke, H.E. Stewart, F.T. Blackburn and T.S. Dickerman, 1/90, (PB90-208596, A05, MF-A01).

NCEER-90-0002   "Nonnormal Secondary Response Due to Yielding in a Primary Structure," by D.C.K. Chen and L.D. Lutes, 2/28/90, (PB90-251976, A07, MF-A01).

NCEER-90-0003   "Earthquake Education Materials for Grades K-12," by K.E.K. Ross, 4/16/90, (PB91-251984, A05, MF-A05). This report has been replaced by NCEER-92-0018.

NCEER-90-0004   "Catalog of Strong Motion Stations in Eastern North America," by R.W. Busby, 4/3/90, (PB90-251984, A05, MF-A01).

NCEER-90-0005   "NCEER Strong-Motion Data Base: A User Manual for the GeoBase Release (Version 1.0 for the Sun3)," by P. Friberg and K. Jacob, 3/31/90 (PB90-258062, A04, MF-A01).

NCEER-90-0006   "Seismic Hazard Along a Crude Oil Pipeline in the Event of an 1811-1812 Type New Madrid Earthquake," by H.H.M. Hwang and C-H.S. Chen, 4/16/90, (PB90-258054, A04, MF-A01).

NCEER-90-0007   "Site-Specific Response Spectra for Memphis Sheahan Pumping Station," by H.H.M. Hwang and C.S. Lee, 5/15/90, (PB91-108811, A05, MF-A01).

NCEER-90-0008   "Pilot Study on Seismic Vulnerability of Crude Oil Transmission Systems," by T. Ariman, R. Dobry, M. Grigoriu, F. Kozin, M. O'Rourke, T. O'Rourke and M. Shinozuka, 5/25/90, (PB91-108837, A06, MF-A01).

NCEER-90-0009   "A Program to Generate Site Dependent Time Histories: EQGEN," by G.W. Ellis, M. Srinivasan and A.S. Cakmak, 1/30/90, (PB91-108829, A04, MF-A01).

NCEER-90-0010   "Active Isolation for Seismic Protection of Operating Rooms," by M.E. Talbott, Supervised by M. Shinozuka, 6/8/9, (PB91-110205, A05, MF-A01).

NCEER-90-0011   "Program LINEARID for Identification of Linear Structural Dynamic Systems," by C-B. Yun and M. Shinozuka, 6/25/90, (PB91-110312, A08, MF-A01).

NCEER-90-0012   "Two-Dimensional Two-Phase Elasto-Plastic Seismic Response of Earth Dams," by A.N. Yiagos, Supervised by J.H. Prevost, 6/20/90, (PB91-110197, A13, MF-A02).

NCEER-90-0013   "Secondary Systems in Base-Isolated Structures: Experimental Investigation, Stochastic Response and Stochastic Sensitivity," by G.D. Manolis, G. Juhn, M.C. Constantinou and A.M. Reinhorn, 7/1/90, (PB91-110320, A08, MF-A01).

NCEER-90-0014   "Seismic Behavior of Lightly-Reinforced Concrete Column and Beam-Column Joint Details," by S.P. Pessiki, C.H. Conley, P. Gergely and R.N. White, 8/22/90, (PB91-108795, A11, MF-A02).

NCEER-90-0015   "Two Hybrid Control Systems for Building Structures Under Strong Earthquakes," by J.N. Yang and A. Danielians, 6/29/90, (PB91-125393, A04, MF-A01).

NCEER-90-0016   "Instantaneous Optimal Control with Acceleration and Velocity Feedback," by J.N. Yang and Z. Li, 6/29/90, (PB91-125401, A03, MF-A01).

NCEER-90-0017   "Reconnaissance Report on the Northern Iran Earthquake of June 21, 1990," by M. Mehrain, 10/4/90, (PB91-125377, A03, MF-A01).

NCEER-90-0018   "Evaluation of Liquefaction Potential in Memphis and Shelby County," by T.S. Chang, P.S. Tang, C.S. Lee and H. Hwang, 8/10/90, (PB91-125427, A09, MF-A01).

NCEER-90-0019   "Experimental and Analytical Study of a Combined Sliding Disc Bearing and Helical Steel Spring Isolation System," by M.C. Constantinou, A.S. Mokha and A.M. Reinhorn, 10/4/90, (PB91-125385, A06, MF-A01). This report is available only through NTIS (see address given above).

NCEER-90-0020   "Experimental Study and Analytical Prediction of Earthquake Response of a Sliding Isolation System with a Spherical Surface," by A.S. Mokha, M.C. Constantinou and A.M. Reinhorn, 10/11/90, (PB91-125419, A05, MF-A01).

NCEER-90-0021 "Dynamic Interaction Factors for Floating Pile Groups," by G. Gazetas, K. Fan, A. Kaynia and E. Kausel, 9/10/90, (PB91-170381, A05, MF-A01).

NCEER-90-0022 "Evaluation of Seismic Damage Indices for Reinforced Concrete Structures," by S. Rodriguez-Gomez and A.S. Cakmak, 9/30/90, PB91-171322, A06, MF-A01).

NCEER-90-0023 "Study of Site Response at a Selected Memphis Site," by H. Desai, S. Ahmad, E.S. Gazetas and M.R. Oh, 10/11/90, (PB91-196857, A03, MF-A01).

NCEER-90-0024 "A User's Guide to Strongmo: Version 1.0 of NCEER's Strong-Motion Data Access Tool for PCs and Terminals," by P.A. Friberg and C.A.T. Susch, 11/15/90, (PB91-171272, A03, MF-A01).

NCEER-90-0025 "A Three-Dimensional Analytical Study of Spatial Variability of Seismic Ground Motions," by L-L. Hong and A.H.-S. Ang, 10/30/90, (PB91-170399, A09, MF-A01).

NCEER-90-0026 "MUMOID User's Guide - A Program for the Identification of Modal Parameters," by S. Rodriguez-Gomez and E. DiPasquale, 9/30/90, (PB91-171298, A04, MF-A01).

NCEER-90-0027 "SARCF-II User's Guide - Seismic Analysis of Reinforced Concrete Frames," by S. Rodriguez-Gomez, Y.S. Chung and C. Meyer, 9/30/90, (PB91-171280, A05, MF-A01).

NCEER-90-0028 "Viscous Dampers: Testing, Modeling and Application in Vibration and Seismic Isolation," by N. Makris and M.C. Constantinou, 12/20/90 (PB91-190561, A06, MF-A01).

NCEER-90-0029 "Soil Effects on Earthquake Ground Motions in the Memphis Area," by H. Hwang, C.S. Lee, K.W. Ng and T.S. Chang, 8/2/90, (PB91-190751, A05, MF-A01).

NCEER-91-0001 "Proceedings from the Third Japan-U.S. Workshop on Earthquake Resistant Design of Lifeline Facilities and Countermeasures for Soil Liquefaction, December 17-19, 1990," edited by T.D. O'Rourke and M. Hamada, 2/1/91, (PB91-179259, A99, MF-A04).

NCEER-91-0002 "Physical Space Solutions of Non-Proportionally Damped Systems," by M. Tong, Z. Liang and G.C. Lee, 1/15/91, (PB91-179242, A04, MF-A01).

NCEER-91-0003 "Seismic Response of Single Piles and Pile Groups," by K. Fan and G. Gazetas, 1/10/91, (PB92-174994, A04, MF-A01).

NCEER-91-0004 "Damping of Structures: Part 1 - Theory of Complex Damping," by Z. Liang and G. Lee, 10/10/91, (PB92-197235, A12, MF-A03).

NCEER-91-0005 "3D-BASIS - Nonlinear Dynamic Analysis of Three Dimensional Base Isolated Structures: Part II," by S. Nagarajaiah, A.M. Reinhorn and M.C. Constantinou, 2/28/91, (PB91-190553, A07, MF-A01). This report has been replaced by NCEER-93-0011.

NCEER-91-0006 "A Multidimensional Hysteretic Model for Plasticity Deforming Metals in Energy Absorbing Devices," by E.J. Graesser and F.A. Cozzarelli, 4/9/91, (PB92-108364, A04, MF-A01).

NCEER-91-0007 "A Framework for Customizable Knowledge-Based Expert Systems with an Application to a KBES for Evaluating the Seismic Resistance of Existing Buildings," by E.G. Ibarra-Anaya and S.J. Fenves, 4/9/91, (PB91-210930, A08, MF-A01).

NCEER-91-0008 "Nonlinear Analysis of Steel Frames with Semi-Rigid Connections Using the Capacity Spectrum Method," by G.G. Deierlein, S-H. Hsieh, Y-J. Shen and J.F. Abel, 7/2/91, (PB92-113828, A05, MF-A01).

NCEER-91-0009 "Earthquake Education Materials for Grades K-12," by K.E.K. Ross, 4/30/91, (PB91-212142, A06, MF-A01). This report has been replaced by NCEER-92-0018.

NCEER-91-0010   "Phase Wave Velocities and Displacement Phase Differences in a Harmonically Oscillating Pile," by N. Makris and G. Gazetas, 7/8/91, (PB92-108356, A04, MF-A01).

NCEER-91-0011   "Dynamic Characteristics of a Full-Size Five-Story Steel Structure and a 2/5 Scale Model," by K.C. Chang, G.C. Yao, G.C. Lee, D.S. Hao and Y.C. Yeh," 7/2/91, (PB93-116648, A06, MF-A02).

NCEER-91-0012   "Seismic Response of a 2/5 Scale Steel Structure with Added Viscoelastic Dampers," by K.C. Chang, T.T. Soong, S-T. Oh and M.L. Lai, 5/17/91, (PB92-110816, A05, MF-A01).

NCEER-91-0013   "Earthquake Response of Retaining Walls; Full-Scale Testing and Computational Modeling," by S. Alampalli and A-W.M. Elgamal, 6/20/91, to be published.

NCEER-91-0014   "3D-BASIS-M: Nonlinear Dynamic Analysis of Multiple Building Base Isolated Structures," by P.C. Tsopelas, S. Nagarajaiah, M.C. Constantinou and A.M. Reinhorn, 5/28/91, (PB92-113885, A09, MF-A02).

NCEER-91-0015   "Evaluation of SEAOC Design Requirements for Sliding Isolated Structures," by D. Theodossiou and M.C. Constantinou, 6/10/91, (PB92-114602, A11, MF-A03).

NCEER-91-0016   "Closed-Loop Modal Testing of a 27-Story Reinforced Concrete Flat Plate-Core Building," by H.R. Somaprasad, T. Toksoy, H. Yoshiyuki and A.E. Aktan, 7/15/91, (PB92-129980, A07, MF-A02).

NCEER-91-0017   "Shake Table Test of a 1/6 Scale Two-Story Lightly Reinforced Concrete Building," by A.G. El-Attar, R.N. White and P. Gergely, 2/28/91, (PB92-222447, A06, MF-A02).

NCEER-91-0018   "Shake Table Test of a 1/8 Scale Three-Story Lightly Reinforced Concrete Building," by A.G. El-Attar, R.N. White and P. Gergely, 2/28/91, (PB93-116630, A08, MF-A02).

NCEER-91-0019   "Transfer Functions for Rigid Rectangular Foundations," by A.S. Veletsos, A.M. Prasad and W.H. Wu, 7/31/91, to be published.

NCEER-91-0020   "Hybrid Control of Seismic-Excited Nonlinear and Inelastic Structural Systems," by J.N. Yang, Z. Li and A. Danielians, 8/1/91, (PB92-143171, A06, MF-A02).

NCEER-91-0021   "The NCEER-91 Earthquake Catalog: Improved Intensity-Based Magnitudes and Recurrence Relations for U.S. Earthquakes East of New Madrid," by L. Seeber and J.G. Armbruster, 8/28/91, (PB92-176742, A06, MF-A02).

NCEER-91-0022   "Proceedings from the Implementation of Earthquake Planning and Education in Schools: The Need for Change - The Roles of the Changemakers," by K.E.K. Ross and F. Winslow, 7/23/91, (PB92-129998, A12, MF-A03).

NCEER-91-0023   "A Study of Reliability-Based Criteria for Seismic Design of Reinforced Concrete Frame Buildings," by H.H.M. Hwang and H-M. Hsu, 8/10/91, (PB92-140235, A09, MF-A02).

NCEER-91-0024   "Experimental Verification of a Number of Structural System Identification Algorithms," by R.G. Ghanem, H. Gavin and M. Shinozuka, 9/18/91, (PB92-176577, A18, MF-A04).

NCEER-91-0025   "Probabilistic Evaluation of Liquefaction Potential," by H.H.M. Hwang and C.S. Lee," 11/25/91, (PB92-143429, A05, MF-A01).

NCEER-91-0026   "Instantaneous Optimal Control for Linear, Nonlinear and Hysteretic Structures - Stable Controllers," by J.N. Yang and Z. Li, 11/15/91, (PB92-163807, A04, MF-A01).

NCEER-91-0027   "Experimental and Theoretical Study of a Sliding Isolation System for Bridges," by M.C. Constantinou, A. Kartoum, A.M. Reinhorn and P. Bradford, 11/15/91, (PB92-176973, A10, MF-A03).

NCEER-92-0001   "Case Studies of Liquefaction and Lifeline Performance During Past Earthquakes, Volume 1: Japanese Case Studies," Edited by M. Hamada and T. O'Rourke, 2/17/92, (PB92-197243, A18, MF-A04).

NCEER-92-0002   "Case Studies of Liquefaction and Lifeline Performance During Past Earthquakes, Volume 2: United States Case Studies," Edited by T. O'Rourke and M. Hamada, 2/17/92, (PB92-197250, A20, MF-A04).

NCEER-92-0003   "Issues in Earthquake Education," Edited by K. Ross, 2/3/92, (PB92-222389, A07, MF-A02).

NCEER-92-0004   "Proceedings from the First U.S. - Japan Workshop on Earthquake Protective Systems for Bridges," Edited by I.G. Buckle, 2/4/92, (PB94-142239, A99, MF-A06).

NCEER-92-0005   "Seismic Ground Motion from a Haskell-Type Source in a Multiple-Layered Half-Space," A.P. Theoharis, G. Deodatis and M. Shinozuka, 1/2/92, to be published.

NCEER-92-0006   "Proceedings from the Site Effects Workshop," Edited by R. Whitman, 2/29/92, (PB92-197201, A04, MF-A01).

NCEER-92-0007   "Engineering Evaluation of Permanent Ground Deformations Due to Seismically-Induced Liquefaction," by M.H. Baziar, R. Dobry and A-W.M. Elgamal, 3/24/92, (PB92-222421, A13, MF-A03).

NCEER-92-0008   "A Procedure for the Seismic Evaluation of Buildings in the Central and Eastern United States," by C.D. Poland and J.O. Malley, 4/2/92, (PB92-222439, A20, MF-A04).

NCEER-92-0009   "Experimental and Analytical Study of a Hybrid Isolation System Using Friction Controllable Sliding Bearings," by M.Q. Feng, S. Fujii and M. Shinozuka, 5/15/92, (PB93-150282, A06, MF-A02).

NCEER-92-0010   "Seismic Resistance of Slab-Column Connections in Existing Non-Ductile Flat-Plate Buildings," by A.J. Durrani and Y. Du, 5/18/92, (PB93-116812, A06, MF-A02).

NCEER-92-0011   "The Hysteretic and Dynamic Behavior of Brick Masonry Walls Upgraded by Ferrocement Coatings Under Cyclic Loading and Strong Simulated Ground Motion," by H. Lee and S.P. Prawel, 5/11/92, to be published.

NCEER-92-0012   "Study of Wire Rope Systems for Seismic Protection of Equipment in Buildings," by G.F. Demetriades, M.C. Constantinou and A.M. Reinhorn, 5/20/92, (PB93-116655, A08, MF-A02).

NCEER-92-0013   "Shape Memory Structural Dampers: Material Properties, Design and Seismic Testing," by P.R. Witting and F.A. Cozzarelli, 5/26/92, (PB93-116663, A05, MF-A01).

NCEER-92-0014   "Longitudinal Permanent Ground Deformation Effects on Buried Continuous Pipelines," by M.J. O'Rourke, and C. Nordberg, 6/15/92, (PB93-116671, A08, MF-A02).

NCEER-92-0015   "A Simulation Method for Stationary Gaussian Random Functions Based on the Sampling Theorem," by M. Grigoriu and S. Balopoulou, 6/11/92, (PB93-127496, A05, MF-A01).

NCEER-92-0016   "Gravity-Load-Designed Reinforced Concrete Buildings: Seismic Evaluation of Existing Construction and Detailing Strategies for Improved Seismic Resistance," by G.W. Hoffmann, S.K. Kunnath, A.M. Reinhorn and J.B. Mander, 7/15/92, (PB94-142007, A08, MF-A02).

NCEER-92-0017   "Observations on Water System and Pipeline Performance in the Limón Area of Costa Rica Due to the April 22, 1991 Earthquake," by M. O'Rourke and D. Ballantyne, 6/30/92, (PB93-126811, A06, MF-A02).

NCEER-92-0018   "Fourth Edition of Earthquake Education Materials for Grades K-12," Edited by K.E.K. Ross, 8/10/92, (PB93-114023, A07, MF-A02).

NCEER-92-0019   "Proceedings from the Fourth Japan-U.S. Workshop on Earthquake Resistant Design of Lifeline Facilities and Countermeasures for Soil Liquefaction," Edited by M. Hamada and T.D. O'Rourke, 8/12/92, (PB93-163939, A99, MF-E11).

NCEER-92-0020   "Active Bracing System: A Full Scale Implementation of Active Control," by A.M. Reinhorn, T.T. Soong, R.C. Lin, M.A. Riley, Y.P. Wang, S. Aizawa and M. Higashino, 8/14/92, (PB93-127512, A06, MF-A02).

NCEER-92-0021 "Empirical Analysis of Horizontal Ground Displacement Generated by Liquefaction-Induced Lateral Spreads," by S.F. Bartlett and T.L. Youd, 8/17/92, (PB93-188241, A06, MF-A02).

NCEER-92-0022 "IDARC Version 3.0: Inelastic Damage Analysis of Reinforced Concrete Structures," by S.K. Kunnath, A.M. Reinhorn and R.F. Lobo, 8/31/92, (PB93-227502, A07, MF-A02).

NCEER-92-0023 "A Semi-Empirical Analysis of Strong-Motion Peaks in Terms of Seismic Source, Propagation Path and Local Site Conditions, by M. Kamiyama, M.J. O'Rourke and R. Flores-Berrones, 9/9/92, (PB93-150266, A08, MF-A02).

NCEER-92-0024 "Seismic Behavior of Reinforced Concrete Frame Structures with Nonductile Details, Part I: Summary of Experimental Findings of Full Scale Beam-Column Joint Tests," by A. Beres, R.N. White and P. Gergely, 9/30/92, (PB93-227783, A05, MF-A01).

NCEER-92-0025 "Experimental Results of Repaired and Retrofitted Beam-Column Joint Tests in Lightly Reinforced Concrete Frame Buildings," by A. Beres, S. El-Borgi, R.N. White and P. Gergely, 10/29/92, (PB93-227791, A05, MF-A01).

NCEER-92-0026 "A Generalization of Optimal Control Theory: Linear and Nonlinear Structures," by J.N. Yang, Z. Li and S. Vongchavalitkul, 11/2/92, (PB93-188621, A05, MF-A01).

NCEER-92-0027 "Seismic Resistance of Reinforced Concrete Frame Structures Designed Only for Gravity Loads: Part I - Design and Properties of a One-Third Scale Model Structure," by J.M. Bracci, A.M. Reinhorn and J.B. Mander, 12/1/92, (PB94-104502, A08, MF-A02).

NCEER-92-0028 "Seismic Resistance of Reinforced Concrete Frame Structures Designed Only for Gravity Loads: Part II - Experimental Performance of Subassemblages," by L.E. Aycardi, J.B. Mander and A.M. Reinhorn, 12/1/92, (PB94-104510, A08, MF-A02).

NCEER-92-0029 "Seismic Resistance of Reinforced Concrete Frame Structures Designed Only for Gravity Loads: Part III - Experimental Performance and Analytical Study of a Structural Model," by J.M. Bracci, A.M. Reinhorn and J.B. Mander, 12/1/92, (PB93-227528, A09, MF-A01).

NCEER-92-0030 "Evaluation of Seismic Retrofit of Reinforced Concrete Frame Structures: Part I - Experimental Performance of Retrofitted Subassemblages," by D. Choudhuri, J.B. Mander and A.M. Reinhorn, 12/8/92, (PB93-198307, A07, MF-A02).

NCEER-92-0031 "Evaluation of Seismic Retrofit of Reinforced Concrete Frame Structures: Part II - Experimental Performance and Analytical Study of a Retrofitted Structural Model," by J.M. Bracci, A.M. Reinhorn and J.B. Mander, 12/8/92, (PB93-198315, A09, MF-A03).

NCEER-92-0032 "Experimental and Analytical Investigation of Seismic Response of Structures with Supplemental Fluid Viscous Dampers," by M.C. Constantinou and M.D. Symans, 12/21/92, (PB93-191435, A10, MF-A03).

NCEER-92-0033 "Reconnaissance Report on the Cairo, Egypt Earthquake of October 12, 1992," by M. Khater, 12/23/92, (PB93-188621, A03, MF-A01).

NCEER-92-0034 "Low-Level Dynamic Characteristics of Four Tall Flat-Plate Buildings in New York City," by H. Gavin, S. Yuan, J. Grossman, E. Pekelis and K. Jacob, 12/28/92, (PB93-188217, A07, MF-A02).

NCEER-93-0001 "An Experimental Study on the Seismic Performance of Brick-Infilled Steel Frames With and Without Retrofit," by J.B. Mander, B. Nair, K. Wojtkowski and J. Ma, 1/29/93, (PB93-227510, A07, MF-A02).

NCEER-93-0002 "Social Accounting for Disaster Preparedness and Recovery Planning," by S. Cole, E. Pantoja and V. Razak, 2/22/93, (PB94-142114, A12, MF-A03).

NCEER-93-0003   "Assessment of 1991 NEHRP Provisions for Nonstructural Components and Recommended Revisions," by T.T. Soong, G. Chen, Z. Wu, R-H. Zhang and M. Grigoriu, 3/1/93, (PB93-188639, A06, MF-A02).

NCEER-93-0004   "Evaluation of Static and Response Spectrum Analysis Procedures of SEAOC/UBC for Seismic Isolated Structures," by C.W. Winters and M.C. Constantinou, 3/23/93, (PB93-198299, A10, MF-A03).

NCEER-93-0005   "Earthquakes in the Northeast - Are We Ignoring the Hazard? A Workshop on Earthquake Science and Safety for Educators," edited by K.E.K. Ross, 4/2/93, (PB94-103066, A09, MF-A02).

NCEER-93-0006   "Inelastic Response of Reinforced Concrete Structures with Viscoelastic Braces," by R.F. Lobo, J.M. Bracci, K.L. Shen, A.M. Reinhorn and T.T. Soong, 4/5/93, (PB93-227486, A05, MF-A02).

NCEER-93-0007   "Seismic Testing of Installation Methods for Computers and Data Processing Equipment," by K. Kosar, T.T. Soong, K.L. Shen, J.A. HoLung and Y.K. Lin, 4/12/93, (PB93-198299, A07, MF-A02).

NCEER-93-0008   "Retrofit of Reinforced Concrete Frames Using Added Dampers," by A. Reinhorn, M. Constantinou and C. Li, to be published.

NCEER-93-0009   "Seismic Behavior and Design Guidelines for Steel Frame Structures with Added Viscoelastic Dampers," by K.C. Chang, M.L. Lai, T.T. Soong, D.S. Hao and Y.C. Yeh, 5/1/93, (PB94-141959, A07, MF-A02).

NCEER-93-0010   "Seismic Performance of Shear-Critical Reinforced Concrete Bridge Piers," by J.B. Mander, S.M. Waheed, M.T.A. Chaudhary and S.S. Chen, 5/12/93, (PB93-227494, A08, MF-A02).

NCEER-93-0011   "3D-BASIS-TABS: Computer Program for Nonlinear Dynamic Analysis of Three Dimensional Base Isolated Structures," by S. Nagarajaiah, C. Li, A.M. Reinhorn and M.C. Constantinou, 8/2/93, (PB94-141819, A09, MF-A02).

NCEER-93-0012   "Effects of Hydrocarbon Spills from an Oil Pipeline Break on Ground Water," by O.J. Helweg and H.H.M. Hwang, 8/3/93, (PB94-141942, A06, MF-A02).

NCEER-93-0013   "Simplified Procedures for Seismic Design of Nonstructural Components and Assessment of Current Code Provisions," by M.P. Singh, L.E. Suarez, E.E. Matheu and G.O. Maldonado, 8/4/93, (PB94-141827, A09, MF-A02).

NCEER-93-0014   "An Energy Approach to Seismic Analysis and Design of Secondary Systems," by G. Chen and T.T. Soong, 8/6/93, (PB94-142767, A11, MF-A03).

NCEER-93-0015   "Proceedings from School Sites: Becoming Prepared for Earthquakes - Commemorating the Third Anniversary of the Loma Prieta Earthquake," Edited by F.E. Winslow and K.E.K. Ross, 8/16/93, (PB94-154275, A16, MF-A02).

NCEER-93-0016   "Reconnaissance Report of Damage to Historic Monuments in Cairo, Egypt Following the October 12, 1992 Dahshur Earthquake," by D. Sykora, D. Look, G. Croci, E. Karaesmen and E. Karaesmen, 8/19/93, (PB94-142221, A08, MF-A02).

NCEER-93-0017   "The Island of Guam Earthquake of August 8, 1993," by S.W. Swan and S.K. Harris, 9/30/93, (PB94-141843, A04, MF-A01).

NCEER-93-0018   "Engineering Aspects of the October 12, 1992 Egyptian Earthquake," by A.W. Elgamal, M. Amer, K. Adalier and A. Abul-Fadl, 10/7/93, (PB94-141983, A05, MF-A01).

NCEER-93-0019   "Development of an Earthquake Motion Simulator and its Application in Dynamic Centrifuge Testing," by I. Krstelj, Supervised by J.H. Prevost, 10/23/93, (PB94-181773, A-10, MF-A03).

NCEER-93-0020   "NCEER-Taisei Corporation Research Program on Sliding Seismic Isolation Systems for Bridges: Experimental and Analytical Study of a Friction Pendulum System (FPS)," by M.C. Constantinou, P. Tsopelas, Y-S. Kim and S. Okamoto, 11/1/93, (PB94-142775, A08, MF-A02).

NCEER-93-0021   "Finite Element Modeling of Elastomeric Seismic Isolation Bearings," by L.J. Billings, Supervised by R. Shepherd, 11/8/93, to be published.

NCEER-93-0022   "Seismic Vulnerability of Equipment in Critical Facilities: Life-Safety and Operational Consequences," by K. Porter, G.S. Johnson, M.M. Zadeh, C. Scawthorn and S. Eder, 11/24/93, (PB94-181765, A16, MF-A03).

NCEER-93-0023   "Hokkaido Nansei-oki, Japan Earthquake of July 12, 1993, by P.I. Yanev and C.R. Scawthorn, 12/23/93, (PB94-181500, A07, MF-A01).

NCEER-94-0001   "An Evaluation of Seismic Serviceability of Water Supply Networks with Application to the San Francisco Auxiliary Water Supply System," by I. Markov, Supervised by M. Grigoriu and T. O'Rourke, 1/21/94, (PB94-204013, A07, MF-A02).

NCEER-94-0002   "NCEER-Taisei Corporation Research Program on Sliding Seismic Isolation Systems for Bridges: Experimental and Analytical Study of Systems Consisting of Sliding Bearings, Rubber Restoring Force Devices and Fluid Dampers," Volumes I and II, by P. Tsopelas, S. Okamoto, M.C. Constantinou, D. Ozaki and S. Fujii, 2/4/94, (PB94-181740, A09, MF-A02 and PB94-181757, A12, MF-A03).

NCEER-94-0003   "A Markov Model for Local and Global Damage Indices in Seismic Analysis," by S. Rahman and M. Grigoriu, 2/18/94, (PB94-206000, A12, MF-A03).

NCEER-94-0004   "Proceedings from the NCEER Workshop on Seismic Response of Masonry Infills," edited by D.P. Abrams, 3/1/94, (PB94-180783, A07, MF-A02).

NCEER-94-0005   "The Northridge, California Earthquake of January 17, 1994: General Reconnaissance Report," edited by J.D. Goltz, 3/11/94, (PB193943, A10, MF-A03).

NCEER-94-0006   "Seismic Energy Based Fatigue Damage Analysis of Bridge Columns: Part I - Evaluation of Seismic Capacity," by G.A. Chang and J.B. Mander, 3/14/94, (PB94-219185, A11, MF-A03).

NCEER-94-0007   "Seismic Isolation of Multi-Story Frame Structures Using Spherical Sliding Isolation Systems," by T.M. Al-Hussaini, V.A. Zayas and M.C. Constantinou, 3/17/94, (PB193745, A09, MF-A02).

NCEER-94-0008   "The Northridge, California Earthquake of January 17, 1994: Performance of Highway Bridges," edited by I.G. Buckle, 3/24/94, (PB94-193851, A06, MF-A02).

NCEER-94-0009   "Proceedings of the Third U.S.-Japan Workshop on Earthquake Protective Systems for Bridges," edited by I.G. Buckle and I. Friedland, 3/31/94, (PB94-195815, A99, MF-A06).

NCEER-94-0010   "3D-BASIS-ME: Computer Program for Nonlinear Dynamic Analysis of Seismically Isolated Single and Multiple Structures and Liquid Storage Tanks," by P.C. Tsopelas, M.C. Constantinou and A.M. Reinhorn, 4/12/94, (PB94-204922, A09, MF-A02).

NCEER-94-0011   "The Northridge, California Earthquake of January 17, 1994: Performance of Gas Transmission Pipelines," by T.D. O'Rourke and M.C. Palmer, 5/16/94, (PB94-204989, A05, MF-A01).

NCEER-94-0012   "Feasibility Study of Replacement Procedures and Earthquake Performance Related to Gas Transmission Pipelines," by T.D. O'Rourke and M.C. Palmer, 5/25/94, (PB94-206638, A09, MF-A02).

NCEER-94-0013   "Seismic Energy Based Fatigue Damage Analysis of Bridge Columns: Part II - Evaluation of Seismic Demand," by G.A. Chang and J.B. Mander, 6/1/94, (PB95-18106, A08, MF-A02).

NCEER-94-0014   "NCEER-Taisei Corporation Research Program on Sliding Seismic Isolation Systems for Bridges: Experimental and Analytical Study of a System Consisting of Sliding Bearings and Fluid Restoring Force/Damping Devices," by P. Tsopelas and M.C. Constantinou, 6/13/94, (PB94-219144, A10, MF-A03).

NCEER-94-0015　"Generation of Hazard-Consistent Fragility Curves for Seismic Loss Estimation Studies," by H. Hwang and J-R. Huo, 6/14/94, (PB95-181996, A09, MF-A02).

NCEER-94-0016　"Seismic Study of Building Frames with Added Energy-Absorbing Devices," by W.S. Pong, C.S. Tsai and G.C. Lee, 6/20/94, (PB94-219136, A10, A03).

NCEER-94-0017　"Sliding Mode Control for Seismic-Excited Linear and Nonlinear Civil Engineering Structures," by J. Yang, J. Wu, A. Agrawal and Z. Li, 6/21/94, (PB95-138483, A06, MF-A02).

NCEER-94-0018　"3D-BASIS-TABS Version 2.0: Computer Program for Nonlinear Dynamic Analysis of Three Dimensional Base Isolated Structures," by A.M. Reinhorn, S. Nagarajaiah, M.C. Constantinou, P. Tsopelas and R. Li, 6/22/94, (PB95-182176, A08, MF-A02).

NCEER-94-0019　"Proceedings of the International Workshop on Civil Infrastructure Systems: Application of Intelligent Systems and Advanced Materials on Bridge Systems," Edited by G.C. Lee and K.C. Chang, 7/18/94, (PB95-252474, A20, MF-A04).

NCEER-94-0020　"Study of Seismic Isolation Systems for Computer Floors," by V. Lambrou and M.C. Constantinou, 7/19/94, (PB95-138533, A10, MF-A03).

NCEER-94-0021　"Proceedings of the U.S.-Italian Workshop on Guidelines for Seismic Evaluation and Rehabilitation of Unreinforced Masonry Buildings," Edited by D.P. Abrams and G.M. Calvi, 7/20/94, (PB95-138749, A13, MF-A03).

NCEER-94-0022　"NCEER-Taisei Corporation Research Program on Sliding Seismic Isolation Systems for Bridges: Experimental and Analytical Study of a System Consisting of Lubricated PTFE Sliding Bearings and Mild Steel Dampers," by P. Tsopelas and M.C. Constantinou, 7/22/94, (PB95-182184, A08, MF-A02).

NCEER-94-0023　"Development of Reliability-Based Design Criteria for Buildings Under Seismic Load," by Y.K. Wen, H. Hwang and M. Shinozuka, 8/1/94, (PB95-211934, A08, MF-A02).

NCEER-94-0024　"Experimental Verification of Acceleration Feedback Control Strategies for an Active Tendon System," by S.J. Dyke, B.F. Spencer, Jr., P. Quast, M.K. Sain, D.C. Kaspari, Jr. and T.T. Soong, 8/29/94, (PB95-212320, A05, MF-A01).

NCEER-94-0025　"Seismic Retrofitting Manual for Highway Bridges," Edited by I.G. Buckle and I.F. Friedland, published by the Federal Highway Administration (PB95-212676, A15, MF-A03).

NCEER-94-0026　"Proceedings from the Fifth U.S.-Japan Workshop on Earthquake Resistant Design of Lifeline Facilities and Countermeasures Against Soil Liquefaction," Edited by T.D. O'Rourke and M. Hamada, 11/7/94, (PB95-220802, A99, MF-E08).

NCEER-95-0001　"Experimental and Analytical Investigation of Seismic Retrofit of Structures with Supplemental Damping: Part 1 - Fluid Viscous Damping Devices," by A.M. Reinhorn, C. Li and M.C. Constantinou, 1/3/95, (PB95-266599, A09, MF-A02).

NCEER-95-0002　"Experimental and Analytical Study of Low-Cycle Fatigue Behavior of Semi-Rigid Top-And-Seat Angle Connections," by G. Pekcan, J.B. Mander and S.S. Chen, 1/5/95, (PB95-220042, A07, MF-A02).

NCEER-95-0003　"NCEER-ATC Joint Study on Fragility of Buildings," by T. Anagnos, C. Rojahn and A.S. Kiremidjian, 1/20/95, (PB95-220026, A06, MF-A02).

NCEER-95-0004　"Nonlinear Control Algorithms for Peak Response Reduction," by Z. Wu, T.T. Soong, V. Gattulli and R.C. Lin, 2/16/95, (PB95-220349, A05, MF-A01).

NCEER-95-0005   "Pipeline Replacement Feasibility Study: A Methodology for Minimizing Seismic and Corrosion Risks to Underground Natural Gas Pipelines," by R.T. Eguchi, H.A. Seligson and D.G. Honegger, 3/2/95, (PB95-252326, A06, MF-A02).

NCEER-95-0006   "Evaluation of Seismic Performance of an 11-Story Frame Building During the 1994 Northridge Earthquake," by F. Naeim, R. DiSulio, K. Benuska, A. Reinhorn and C. Li, to be published.

NCEER-95-0007   "Prioritization of Bridges for Seismic Retrofitting," by N. Basöz and A.S. Kiremidjian, 4/24/95, (PB95-252300, A08, MF-A02).

NCEER-95-0008   "Method for Developing Motion Damage Relationships for Reinforced Concrete Frames," by A. Singhal and A.S. Kiremidjian, 5/11/95, (PB95-266607, A06, MF-A02).

NCEER-95-0009   "Experimental and Analytical Investigation of Seismic Retrofit of Structures with Supplemental Damping: Part II - Friction Devices," by C. Li and A.M. Reinhorn, 7/6/95, (PB96-128087, A11, MF-A03).

NCEER-95-0010   "Experimental Performance and Analytical Study of a Non-Ductile Reinforced Concrete Frame Structure Retrofitted with Elastomeric Spring Dampers," by G. Pekcan, J.B. Mander and S.S. Chen, 7/14/95, (PB96-137161, A08, MF-A02).

NCEER-95-0011   "Development and Experimental Study of Semi-Active Fluid Damping Devices for Seismic Protection of Structures," by M.D. Symans and M.C. Constantinou, 8/3/95, (PB96-136940, A23, MF-A04).

NCEER-95-0012   "Real-Time Structural Parameter Modification (RSPM): Development of Innervated Structures," by Z. Liang, M. Tong and G.C. Lee, 4/11/95, (PB96-137153, A06, MF-A01).

NCEER-95-0013   "Experimental and Analytical Investigation of Seismic Retrofit of Structures with Supplemental Damping: Part III - Viscous Damping Walls," by A.M. Reinhorn and C. Li, 10/1/95, (PB96-176409, A11, MF-A03).

NCEER-95-0014   "Seismic Fragility Analysis of Equipment and Structures in a Memphis Electric Substation," by J-R. Huo and H.H.M. Hwang, (PB96-128087, A09, MF-A02), 8/10/95.

NCEER-95-0015   "The Hanshin-Awaji Earthquake of January 17, 1995: Performance of Lifelines," Edited by M. Shinozuka, 11/3/95, (PB96-176383, A15, MF-A03).

NCEER-95-0016   "Highway Culvert Performance During Earthquakes," by T.L. Youd and C.J. Beckman, available as NCEER-96-0015.

NCEER-95-0017   "The Hanshin-Awaji Earthquake of January 17, 1995: Performance of Highway Bridges," Edited by I.G. Buckle, 12/1/95, to be published.

NCEER-95-0018   "Modeling of Masonry Infill Panels for Structural Analysis," by A.M. Reinhorn, A. Madan, R.E. Valles, Y. Reichmann and J.B. Mander, 12/8/95.

NCEER-95-0019   "Optimal Polynomial Control for Linear and Nonlinear Structures," by A.K. Agrawal and J.N. Yang, 12/11/95, (PB96-168737, A07, MF-A02).

NCEER-95-0020   "Retrofit of Non-Ductile Reinforced Concrete Frames Using Friction Dampers," by R.S. Rao, P. Gergely and R.N. White, 12/22/95, (PB97-133508, A10, MF-A02).

NCEER-95-0021   "Parametric Results for Seismic Response of Pile-Supported Bridge Bents," by G. Mylonakis, A. Nikolaou and G. Gazetas, 12/22/95, (PB97-100242, A12, MF-A03).

NCEER-95-0022   "Kinematic Bending Moments in Seismically Stressed Piles," by A. Nikolaou, G. Mylonakis and G. Gazetas, 12/23/95.

NCEER-96-0001   "Dynamic Response of Unreinforced Masonry Buildings with Flexible Diaphragms," by A.C. Costley and D.P. Abrams," 10/10/96.

NCEER-96-0002   "State of the Art Review: Foundations and Retaining Structures," by I. Po Lam, to be published.

NCEER-96-0003   "Ductility of Rectangular Reinforced Concrete Bridge Columns with Moderate Confinement," by N. Wehbe, M. Saiidi, D. Sanders and B. Douglas, 11/7/96, (PB97-133557, A06, MF-A02).

NCEER-96-0004   "Proceedings of the Long-Span Bridge Seismic Research Workshop," edited by I.G. Buckle and I.M. Friedland, to be published.

NCEER-96-0005   "Establish Representative Pier Types for Comprehensive Study: Eastern United States," by J. Kulicki and Z. Prucz, 5/28/96.

NCEER-96-0006   "Establish Representative Pier Types for Comprehensive Study: Western United States," by R. Imbsen, R.A. Schamber and T.A. Osterkamp, 5/28/96.

NCEER-96-0007   "Nonlinear Control Techniques for Dynamical Systems with Uncertain Parameters," by R.G. Ghanem and M.I. Bujakov, 5/27/96, (PB97-100259, A17, MF-A03).

NCEER-96-0008   "Seismic Evaluation of a 30-Year Old Non-Ductile Highway Bridge Pier and Its Retrofit," by J.B. Mander, B. Mahmoodzadegan, S. Bhadra and S.S. Chen, 5/31/96.

NCEER-96-0009   "Seismic Performance of a Model Reinforced Concrete Bridge Pier Before and After Retrofit," by J.B. Mander, J.H. Kim and C.A. Ligozio, 5/31/96.

NCEER-96-0010   "IDARC2D Version 4.0: A Computer Program for the Inelastic Damage Analysis of Buildings," by R.E. Valles, A.M. Reinhorn, S.K. Kunnath, C. Li and A. Madan, 6/3/96, (PB97-100234, A17, MF-A03).

NCEER-96-0011   "Estimation of the Economic Impact of Multiple Lifeline Disruption: Memphis Light, Gas and Water Division Case Study," by S.E. Chang, H.A. Seligson and R.T. Eguchi, 8/16/96, (PB97-133490, A11, MF-A03).

NCEER-96-0012   "Proceedings from the Sixth Japan-U.S. Workshop on Earthquake Resistant Design of Lifeline Facilities and Countermeasures Against Soil Liquefaction, Edited by M. Hamada and T. O'Rourke, 9/11/96, (PB97-133581, A99, MF-A06).

NCEER-96-0013   "Chemical Hazards, Mitigation and Preparedness in Areas of High Seismic Risk: A Methodology for Estimating the Risk of Post-Earthquake Hazardous Materials Release," by H.A. Seligson, R.T. Eguchi, K.J. Tierney and K. Richmond, 11/7/96.

NCEER-96-0014   "Response of Steel Bridge Bearings to Reversed Cyclic Loading," by J.B. Mander, D-K. Kim, S.S. Chen and G.J. Premus, 11/13/96, (PB97-140735, A12, MF-A03).

NCEER-96-0015   "Highway Culvert Performance During Past Earthquakes," by T.L. Youd and C.J. Beckman, 11/25/96, (PB97-133532, A06, MF-A01).

NCEER-97-0001   "Evaluation, Prevention and Mitigation of Pounding Effects in Building Structures," by R.E. Valles and A.M. Reinhorn, 2/20/97, (PB97-159552, A14, MF-A03).

NCEER-97-0002   "Seismic Design Criteria for Bridges and Other Highway Structures," by C. Rojahn, R. Mayes, D.G. Anderson, J. Clark, J.H. Hom, R.V. Nutt and M.J. O'Rourke, 4/30/97, (PB97-194658, A06, MF-A03).

NCEER-97-0003   "Proceedings of the U.S.-Italian Workshop on Seismic Evaluation and Retrofit," Edited by D.P. Abrams and G.M. Calvi, 3/19/97, (PB97-194666, A13, MF-A03).

NCEER-97-0004   "Investigation of Seismic Response of Buildings with Linear and Nonlinear Fluid Viscous Dampers," by A.A. Seleemah and M.C. Constantinou, 5/21/97, (PB98-109002, A15, MF-A03).

NCEER-97-0005   "Proceedings of the Workshop on Earthquake Engineering Frontiers in Transportation Facilities," edited by G.C. Lee and I.M. Friedland, 8/29/97.

NCEER-97-0006   "Cumulative Seismic Damage of Reinforced Concrete Bridge Piers," by S.K. Kunnath, A. El-Bahy, A. Taylor and W. Stone, 9/2/97, (PB98-108814, A11, MF-A03).

NCEER-97-0007   "Structural Details to Accommodate Seismic Movements of Highway Bridges and Retaining Walls," by R.A. Imbsen, R.A. Schamber, E. Thorkildsen, A. Kartoum, B.T. Martin, T.N. Rosser and J.M. Kulicki, 9/3/97.

NCEER-97-0008   "A Method for Earthquake Motion-Damage Relationships with Application to Reinforced Concrete Frames," by A. Singhal and A.S. Kiremidjian, 9/10/97, (PB98-108988, A13, MF-A03).

NCEER-97-0009   "Seismic Analysis and Design of Bridge Abutments Considering Sliding and Rotation," by K. Fishman and R. Richards, Jr., 9/15/97, (PB98-108897, A06, MF-A02).

NCEER-97-0010   "Proceedings of the FHWA/NCEER Workshop on the National Representation of Seismic Ground Motion for New and Existing Highway Facilities," edited by I.M. Friedland, M.S. Power and R.L. Mayes, 9/22/97.

NCEER-97-0011   "Seismic Analysis for Design or Retrofit of Gravity Bridge Abutments," by K.L. Fishman, R. Richards, Jr. and R.C. Divito, 10/2/97.

NCEER-97-0012   "Evaluation of Simplified Methods of Analysis for Yielding Structures," by P. Tsopelas, M.C. Constantinou, C.A. Kircher and A.S. Whittaker, 10/31/97.

NCEER-97-0013   "Seismic Design of Bridge Columns Based on Control and Repairability of Damage," by C-T. Cheng and J.B. Mander, 12/8/97.

NCEER-97-0014   "Seismic Resistance of Bridge Piers Based on Damage Avoidance Design," by J.B. Mander and C-T. Cheng, 12/10/97.

NCEER-97-0015   "Seismic Response of Nominally Symmetric Systems with Strength Uncertainty," by S. Balopoulou and M. Grigoriu, 12/23/97.